

**Catalysis By Ferrites And Cobaltites For The
Alkylation And Oxidation Of Organic Compounds**

*Thesis submitted to the
Cochin University of Science And Technology
in partial fulfillment of the
requirements for the degree of*

**Doctor of Philosophy
In
Chemistry**

In the Faculty of Science

By

Ramanathan R

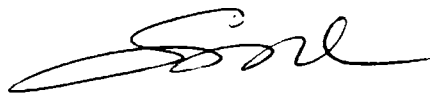
*Department of Applied Chemistry
Cochin University of Science and Technology
Kochi-682022*

December - 2006

CERTIFICATE

This is to certify that the thesis herewith is an authentic record of research work carried out by Mr.Ramanathan R under my supervision, at the Department of Applied Chemistry, in partial fulfillment of the requirements for the degree of Doctor of Philosophy of Cochin University of Science and Technology, and further that no part thereof has been presented before for any other degree.

Kochi-682022
18-12-06



Dr.S.Sugunan
(Supervising Guide)
Professor in Physical Chemistry
Department of Applied Chemistry
Cochin University of Science and Technology
Kochin-682022

DECLARATION

I here by declare that the work presented in this thesis entitled **“Catalysis By Ferrites And Cobaltites For The Alkylation And Oxidation Of Organic Compounds”** is entirely original and was carried out by me independently under the supervision of Dr.S.Sugunan, Professor in Physical Chemistry, Department of Applied Chemistry, Cochin University of Science and Technology, Kochi-22, Kerala, India, and has not been included in any other thesis submitted previously for the award of any degree.

Kochi-22
18-12-06


Ramanathan R

Acknowledgement

With extreme pleasure, I would like to express my sincere and deep sense of gratitude and obligation to my supervising guide, Prof. (Dr.) S.Sugunan, Department of Applied Chemistry, for his valuable guidance, research training, constant encouragement and timely suggestions throughout my research period. I shall ever remain grateful to him.

I am grateful to Dr.M.R.Prathapachandra Kurrup, Head, Department of Applied Chemistry and to Dr.S.Sugunan, former Head of the Department, for providing me the necessary facilities.

I take this opportunity to thank all the teaching and non-teaching staff of the Department of Applied Chemistry for their help and goodwill on all occasions. Special thanks to Dr.S.Prathapan for his valuable support and time he had spent for me in writing the organic reaction mechanisms.

I am extremely thankful to my former labmates Dr.Sanjay, Dr.Suja and Dr.Bijoy for their well-timed suggestions and encouragement during the course of this work. I feel intensely grateful to my present labmates Dr.Radhika, Maya, Binitha, Shali, Ajitha Miss, Salini, Reshmi, Bolie, Joyes Miss, George John Sir, Mery Miss, Rose Miss and Jesny for their sincere cooperation and encouragement throughout my work. Their lively company made my life in the lab much interesting. My thanks to all my friends in the Department of Applied Chemistry for their goodwill and cooperation on all occasions.

I take this opportunity to express my hearty gratitude to Dr.Radhika and Maya who has always been constantly encouraging and sincerely helping my work by their valuable and timely suggestions. I place on record here my sincere gratitude to them.

I am deeply indebted and profoundly grateful to Dr.C.G.Ramankutty, who has been my senior, for his immense assistance and valuable suggestions during the initial stages of my research work.

I remember with heart-felt thanks the help rendered by Mr.Gopimenon, Mr.Kashmiri and Mr.Jose of USIC, CUSAT and Mr.Suresh and Mr.Kumar of Chemito for their readiness to help me on occasions of technical difficulties. I extend my special thanks to my friends in STIC, CUSAT for their timely help in providing analysis results.

I remember with great pleasure the golden moments I had spend with my most dear and near friends Arun, John, Manoj, Suraj, Murugan and Jayan in the Department and in hostel. Without their company my work and life in the lab would not have been smooth. I am very grateful to them for their company and cooperation.

I am sincerely expressing my gratitude to my friends in NCL, Pune Dr.Shylesh, Prinson, Shankar, Surendran and Mr.Indraneel, IIT Chennai for their timely help in providing analysis results. Special thanks to Mr.Sreekanth for his readiness to send the literature papers. I am extremely thankful to C.P.Sebastian, Universität Münster, Germany, who has been my senior during my college studies, for providing me the necessary Mössbauer data. I remember with thanks Dr.Anas and Mr.Renjith of Süd Chemie for their help in doing the TPR analysis.

I extend my special thanks to Mr.K.P.Antony who has been my teacher, my well wisher, for his sincere encouragement throughout my work.

I would like to thank my family members for their wholehearted support and was always ready to suffer any difficulties for the completion of my Ph.D work. I owe the morel support that they extended throughout my work.

The financial support granted by DST, New Delhi is gratefully acknowledged.

Ramanathan R

PREFACE

In recent years considerable advances have been achieved in the study of the surface structure and mechanism of environmentally benign heterogeneous catalysts. Results of catalytic studies are nowadays playing a more important role in design of new industrial catalysts and catalytic processes and in optimization of existing catalytic process. Spinel ferrites are known for a long time now and have been exploited for a number of communication and defense applications.

For studying the catalytic properties of spinels, co-precipitation method is preferred over the usual ceramic methods as the former method yields homogeneous and fine particles. In the present study, we have prepared chromium and gadolinium incorporated nickel ferrites and nickel and copper cobaltites by co-precipitation method. Samples were characterized by various physico-chemical methods and a detailed study of acid-base properties were also carried out. The main objective of the work is to evaluate the catalytic activity of the systems towards industrially important reactions which include various Friedel-Crafts alkylation and oxidation reactions.

The thesis is divided into six chapters. First chapter deals with a brief introduction and literature survey on spinels, their structure and catalytic activities. Second chapter explains the materials and methods employed in the work. Third chapter presents the results and discussion regarding the characterization. Results of activity studies towards various alkylation and oxidation reactions were presented in the subsequent two chapters. Last chapter deals with the summary of the work and conclusions derived from the earlier chapters.

CONTENTS

Chapter 1	Introduction	Page No
1.1	Catalysis	1
1.2	Solid acids as catalysts	4
1.2.1	Zeolites	4
1.2.2	Heteropoly acids	5
1.2.3	Mesoporous Materials	5
1.2.4	Transition metal oxides	6
1.3	Spinels	7
1.3.1	Methods of preparation	8
1.3.2	Spinel structure	11
1.3.3	Distribution of metal ions over different sites	16
1.3.4	Factors determining cation distribution	17
1.3.5	The surface of catalytically active spinels	21
1.3.6	Spinels as catalysts	24
1.4	Acid-base properties	32
1.4.1	Surface electron donating properties	33
1.4.2	Temperature programmed desorption studies	36
1.4.3	Cyclohexanol decomposition	38
1.4.4	Cumene cracking	40
1.5	Reactions selected for present study	41
1.6	Objectives of the present work	42
	References	44

Chapter 2	Experimental	
2.1	Catalyst preparation	59
2.1.1	Materials	59
2.1.2	Preparation of different composition of spinels	59
2.2	Catalyst characterization	62
2.2.1	X-ray diffraction analysis	62
2.2.2	Energy Dispersive X-ray analysis	64
2.2.3	Scanning Electron Microscope (SEM) analysis	65
2.2.4	Diffuse Reflectance Infrared Fourier Transform (DRIFT) spectroscopy	66
2.2.5	Thermogravimetric (TG) analysis	67
2.2.6	Surface area determination (BET method)	68
2.2.7	Mössbauer spectroscopy	70
2.2.8	Acid-base properties	72
2.3	Catalytic activity studies	77
	References	79
Chapter 3	Characterization and surface properties	
3.1	Physical characterization	81
3.1.1	X-ray diffraction analysis	81
3.1.2	Diffuse Reflectance Infrared Fourier Transform (DRIFT) spectra	84
3.1.3	Thermal analysis	88
3.1.4	Scanning Electron Microgram (SEM) analysis	90
3.1.5	Energy Dispersive X-ray (EDX) analysis	90

3.1.6	Surface area and pore volume measurements	90
3.1.7	Mössbauer analysis	92
3.1.7 a	Cation distribution of spinels	99
3.2	Surface properties-acidity/basicity	99
3.2.1	TPD of ammonia	101
3.2.2	Perylene adsorption studies	107
3.2.3	IR studies of pyridine adsorbed samples	109
3.2.4	Surface electron donating properties	111
3.2.5	Cyclohexanol decomposition reaction	116
3.2.6	Cumene cracking reaction	119
	References	127
Chapter 4	Alkylation Reactions	
4.1	Phenol Methylation	133
4.1.1	Process optimization	135
4.1.1.1	Effect of methanol to phenol molar ratio	136
4.1.1.2	Effect of reaction temperature	137
4.1.1.3	Effect of flow rate	138
4.1.2	Effect of catalyst composition	139
4.1.3	Mechanism of phenol methylation	147
4.2	Phenol <i>Tert</i> Butylation	150
4.2.1	Process optimization	152
4.2.1.1	Effect of TBA to phenol molar ratio	152
4.2.1.2	Effect of reaction temperature	153
4.2.1.3	Effect of flow rate	154

4.2.2	Effect of catalyst composition	155
4.2.3	Mechanism of phenol <i>tert</i> butylation	162
4.3	Thymol Synthesis	164
4.3.1	Process optimization	166
4.3.1.1	Effect of reaction temperature	166
4.3.1.2	Effect of feed ratio	167
4.3.1.3	Effect of flow rate	168
4.3.2	Effect of catalyst composition	169
4.3.3	Mechanism of <i>m</i> -cresol isopropylation	177
4.4	Aniline Methylation	179
4.4.1	Process optimization	181
4.4.1.1	Effect of methanol to aniline molar ratio	181
4.4.1.2	Effect of reaction temperature	182
4.4.1.3	Effect of flow rate	183
4.4.2	Effect of catalyst composition	184
4.4.3	Mechanism of aniline alkylation	191
	References	193

Chapter 5 Oxidation Reactions

5.1	Cyclohexane Oxidation	201
5.1.1	Process optimization	203
5.1.1.1	Effect of reaction time	204
5.1.1.2	Effect of reaction temperature	205
5.1.1.3	Effect of solvent	205
5.1.1.4	Effect of H ₂ O ₂ to cyclohexane molar ratio	206

5.1.2	Effect of catalyst composition	207
5.1.3	Mechanism of cyclohexane oxidation	214
5.2	Benzyl Alcohol Oxidation	216
5.2.1	Process optimization	218
5.2.1.1	Effect of reaction temperature	218
5.2.1.2	Effect of solvent	219
5.2.1.3	Effect of reaction time	220
5.2.1.4	Effect of H ₂ O ₂ to benzyl alcohol molar ratio	220
5.2.2	Effect of catalyst composition	221
5.2.3	Mechanism of benzyl alcohol oxidation	228
5.3	Styrene Oxidation	230
5.3.1	Process optimization	232
5.3.1.1	Effect of reaction temperature	232
5.3.1.2	Effect of reaction time	233
5.3.1.3	Effect of solvent	234
5.3.1.4	Effect of H ₂ O ₂ to styrene molar ratio	235
5.3.2	Effect of catalyst composition	236
5.3.3	Mechanism of styrene oxidation	242
	References	245
Chapter 6	Summary and conclusions	
6.1	Summary of the work	252
6.2	Conclusions	257
6.3	Further scope of the work	260

CHAPTER 1

INTRODUCTION

1.1 Catalysis

In chemistry and biology, catalysis is the acceleration of the reaction rate of a chemical reaction by means of a substance, called catalyst that is itself not consumed by the overall reaction. Catalysts participate in reactions but are neither reactants nor products of the reaction they catalyze. The phrase *catalysis* was coined by Jöns Jakob Berzelius in 1835 who was the first to note that certain chemicals speed up a reaction. Other early chemists involved in catalysis were Alexander Mitscherlich who in 1831 referred to *contact processes* and Johann Wolfgang Döbereiner who spoke of *contact action* and whose lighter based on hydrogen and a platinum sponge became a huge commercial success in the 1820's. A good catalyst must possess both high activity and long term stability. But the most important quality is its selectivity, which reflects its ability to direct conversion of reactants in a specific way.

The specificity of a catalyst enables a chemical process to proceed more efficiently with less waste. Modern industries are learning more and more about the applications and benefits of catalysts and different ways to bring down the cost of production. Catalytic process technologies generally involve less capital investment, lower operating costs, higher purity products and reduce environmental hazards. Hence, catalysis is of crucial importance to the chemical industry. The more well defined areas of industrial catalyst are petroleum, pharmaceutical and environmental catalysis. The petroleum processing catalysts that have aroused the greatest interest and that constituted

Introduction

a major advancement when they are first introduced in the 1960s are the molecular sieves or zeolites. Catalysis is a very important process from an industrial point of view since the production of most industrially important chemicals involves catalysis. The earliest commercial processes are the Haber process for ammonia synthesis and the Fischer-Tropsch synthesis. Research into catalysis is a major field in applied science, and involves many fields of chemistry, notably in organometallic chemistry, and physics. Catalysis is important in many aspects of environmental science, from the catalytic converter in automobiles to the causes of the ozone hole. Various techniques and concepts of solid state are applied for synthesizing and modifying catalysts with required structure and chemical properties. Thus it goes without saying that the modern chemical industries cannot operate without proper study of catalysts and their specific action.

Catalysts can be either heterogeneous or homogeneous. Biocatalysis is often seen as a separate group. Heterogeneous catalysts are present in different phases from the reactants (e.g. a solid catalyst in a liquid reaction mixture), whereas homogeneous catalysts are in the same phase (e.g. a dissolved catalyst in a liquid reaction mixture). Each of the catalytic processes possesses its own advantages and disadvantages. In homogeneous catalysis the catalyst is a molecule which facilitates the reaction. The reactant(s) coordinate to the catalyst (or *vice versa*), are transformed to product(s), which are then released from the catalyst. Examples of homogeneous catalysts are H^+ (aq) which acts as a catalyst in esterification, and chlorine free radicals in the break down of ozone. Chlorine free radicals are formed by the action of ultraviolet radiation on chlorofluorocarbons (CFCs). They react with ozone forming oxygen

Chapter 1

molecules and regenerating chlorine free radicals. The synthesis of fine chemicals and pharmaceuticals generates large amount of waste, which is due in particular to the fact that most of the reactions are stoichiometric or use environmentally non-friendly homogeneous catalysts. The substitution of these polluting and corrosive homogeneous catalysts by solid catalysts, which do not possess such disadvantages, is one of the main industrial challenges. Besides the environmental improvement, heterogeneous catalysis has many technical advantages, in particular easy separation of products, easy development of continuous processes and possibility of catalyst regeneration.

In recent years, considerable advances have been achieved in the study of surface structure and mechanism of the catalytic reaction. A simple model for heterogeneous catalysis involves the catalyst providing a surface on which the reactants (or substrates) temporarily become adsorbed. Bonds in the substrate become weakened sufficiently for new bonds to be created. The bonds between the products and the catalyst are weaker, so the products are released. The nature of interaction may be chemical or physical process. The overall catalytic reaction rate depends on these physical or chemical processes or steps. Each of these steps contributes to a greater or lesser extent to the overall reaction rate.

The general steps involved in the heterogeneous catalysis are:

- ❖ External diffusion: Transfer of the reactants from the bulk fluid phase to the fluid-solid interface and external surface of the catalyst particle.
- ❖ Internal diffusion (if particle is porous): Intraparticle transfer into the catalyst particle.

- ❖ Adsorption: Physisorption and chemisorption of reactants at the surface (sites) of the catalyst particle.
- ❖ Surface reaction: Chemical reaction of adsorbed species to produce adsorbed products; this is the intrinsic or true chemical reaction step.
- ❖ Desorption: Release of adsorbed products by the catalyst.
- ❖ Internal diffusion: Transfer of products to outer surface of the catalyst particle.
- ❖ External diffusion: Transfer of products from fluid-solid interface into the reaction stream.

1.2 Solid acids as catalysts

Solid acid catalysts are appealing since the nature of acid sites is known and their chemical behavior in acid catalyzed reactions can be rationalized by means of existing theories and models. It is possible to modify the acid properties of these materials by adopting various synthesis and post synthesis routes. Solid acid catalysts in many commercial processes have proved to be more economical and often produce better quality products. Being stronger acids, they have a significantly higher catalytic activity compared to conventional acid catalysts and above all they provide clean environment.

1.2.1 Zeolites

A number of reactions that are catalyzed by acids and bases in solution are also catalyzed by solids having acidic and basic properties. The most important catalysts belonging to this class are aluminosilicates. The surface hydroxyl group of a single element, for example, silica or alumina have poor acidic behavior and are of little importance as catalysts. Binary oxides in

which the two elements are in two different oxidation states have good acidic properties and make good catalysts. The catalytic properties of zeolites depend on the pore diameter and the number and strength of acid sites.

1.2.2 Heteropoly acids

Heteropoly acids are solid acid compounds and they offer appealing characteristics as heterogeneous as well as homogeneous catalysts. Various types of heteropoly compounds are known each having its own characteristic structure. Heteropoly acids are highly acidic and the acidity of these compounds is higher than that of well known solid acid catalysts such as alumina-silica and the free acid of the heteroatom. The acid sites of heteropoly acids are found to be Brønsted type.

1.2.3 Mesoporous Materials

These materials have potential applications in the field of catalysis, mainly because of their thermal and hydrothermal stabilities and large surface areas. M41S members are of great utility as materials on which catalytically active phases such as heteropoly acids, transition metal complexes and oxides can be supported¹. It is possible to generate Brønsted acid sites on the surface of these materials and by the exchange of these protons by alkaline metal ions; one can visualize mild basicity which will be useful for base catalyzed reactions. The acidity of MCM-41 is comparable to that of amorphous silica-alumina, both in number and acid strength distribution. The mild acidity in combination with large pores has been successfully employed for reactions such as Aldol condensation¹, Friedel-Crafts alkylation^{2,3} etc. The large pores of MCM-41 combined with acidity on the walls are extensively utilized as catalysts for cracking large molecules.

1.2.4 Transition metal oxides

Transition metal oxides are technologically important materials that have found to be relevant in chemical applications. Transition metal oxides are the proficient components in catalysts employed in many reactions such as oxidation, reduction, oxidative and non-oxidative dehydrogenation, metathesis and water gas shift reaction for the production of hydrogen. Transition metal oxides are known for their redox properties and for their capacity to catalyze oxidation reactions of hydrocarbons^{4,5}. The defect in the form of non-stoichiometry for transition metal oxides or co-ordinatively unsaturated sites are important in surface chemistry, which are mainly responsible for the adsorptive and catalytic properties of transition metal oxides. Due to the formation of the defects, various cations may be differently distributed between the surface and bulk of the single as well as in the multi-component transition metal systems. When the concentration of the defects at the surface of the oxide surpasses a certain critical value, ordering of defects or formation of new bi-dimensional surface phase may occur, resulting often in a dramatic enhancement of catalytic activity and selectivity⁶⁻⁸.

Transition metal oxides possess acid-base properties. It is well known that the most active homogeneous and heterogeneous catalysts for alkane and alkene oxidation, are those based on transition metals of group 4 (Ti), 5 (V and Nb) and 6 (Mo)⁹⁻¹³. Their efficiency in oxidation reactions depends not only on their redox properties but also on their acid-base properties. Numerous work are reported to correlate the acid-base properties of mixed transition metal oxides with the catalytic activity/selectivity in selective oxidation of hydrocarbons^{14,15}.

Titania and zirconia have attracted much attention because they are found to be good supports for metals and in combination with small amount of sulphate, they will change to super acids. Hydrated Nb_2O_5 and Ta_2O_5 are making an impact for their application as unusual solid acids and showed excellent stability as a catalyst for esterification, hydrolysis and hydration reactions^{16,17}.

Transition metal oxides are efficient systems for the oxidation of CO. A number of transition metal oxide systems such as Cu-Cr-O, Cu-Al-O and Mn-Al-Mg-O have been identified to be active for over a wide range of compositions¹⁸.

1.3 Spinel

Mixed oxides having the formula AB_2O_4 are known as spinels where A and B are metal cations with charge +2 and +3 respectively. There are simple spinels and mixed spinels. Mixed metal oxides possessing spinel structure have been investigated by a number of workers as they exhibit interesting structural, electrical and magnetic properties. Mixed metal oxide materials are good alternatives to both zeolites and aluminium phenolate for many alkylation reactions. Individual metal oxides lose their catalytic activity rapidly owing to aging and formation of coke over the catalyst surface. The spinel lattice imparts extra stability to the catalyst under various reaction conditions so that these systems have sustained activities for longer periods. Spinel with B ion as Fe^{+3} are known as ferrites and those with Co^{+3} as B ion are known as cobaltites. The spinels chosen for the present study were ferrites and cobaltites. The interesting structural, electrical, magnetic and catalytic properties of these compounds are governed by their chemical

composition. So special care must be taken in the preparation stages of these compounds to get spinels with specific properties.

1.3.1 Methods of Preparation

There are various methods for the preparation of spinels leading to a wide variety of forms: thin and thick films, single crystals and poly crystalline aggregates. For the exact reproducibility of the spinel particles utmost care must be taken during the preparation stages. Minor changes in the preparation method can drastically alter their properties. Small particle size, homogeneous composition, narrow particle size distribution, high purity and dispersed particles are the ideal characteristics of spinel particles.

The oldest method of preparation of spinels is the ceramic method. The precursor compounds are oxides or carbonates of cations in the desired spinel and these are ground well by mechanical milling. But this method cannot produce fine particles and extended milling introduces significant quantities of undesired impurities and the distribution in particle size becomes extremely wide. The major drawback found for this method is the lack of homogeneity of the material prepared. Again, the high temperature (~1200K) required to complete solid state reactions leads to drastic decrease in surface area of the resulting material by sintering.

Co-precipitation is a very suitable method for the creation of homogeneous catalyst components or for the moulding of the precursors with a definite stoichiometry, which can easily be converted to the active catalyst¹⁹. This method is based on the stoichiometric mixing of aqueous solutions of chlorides, nitrates or sulphates of divalent and trivalent ions in the concentrations required for the spinel composition and their simultaneous

precipitation in the form of hydroxides by NaOH^{20,21} or NH₄OH^{22,23}. This is followed by filtration, washing and calcinations of the product to form the oxide. The morphology, the texture, the structure and size of the particles can be accurately controlled by altering the pH of the solution, temperature and nature of the reagents²⁴. By this method spinel particles with a narrow size distribution in the range 50-500 nm may be obtained with high purity. Ferrites used in catalytic applications are generally synthesized by low temperature co-precipitation methods²⁵⁻²⁷. Co-precipitation method generates Brønsted acid sites in different cationic environments in addition to the Lewis sites, which makes the catalyst active and effective for many organic transformations.

The method of precipitation from solution under hydrothermal conditions is of current interest and attractive for the direct synthesis of crystalline ceramic particles during the reaction at relatively low temperatures. It has been reported that uniform ferrite particles with controlled size, shape and stoichiometry can be produced by controlling the hydrothermal conditions. Hydrothermal reactions in general are carried out in an auto clave at temperatures between the boiling and critical points of water (100-374 °C) and at elevated pressures (up to 15 MPa). The powder synthesized by this method has excellent homogeneity and particle uniformity. It enables one to synthesize a material at a far lower temperature than those in the conventional solid state reaction methods²⁸. Further more, crystalline powders are directly prepared in the hydrothermal treatment; the need for the high temperature treatment as in the sol-gel route and in turn, the resulting aggregation and the subsequent grinding processes are eliminated²⁹. In this method the metal sulphates were dissolved in distilled water in a Teflon vessel, then desired

Introduction

amount of aqueous ammonia (28 wt %) was poured into this solution to control the pH. This mixed solution with the desired concentration was then placed in a stainless steel vessel. After sealing the vessel, it is placed in a thermostated oven, and heated at 150 to 240 °C for 5 to 50 h with constant rotation. The precipitated solid product was separated by centrifuging, washed and then dried in an oven. This hydrothermal method has been used for the synthesis of fine oxide powders and their particle size and morphology are well controlled³⁰⁻³². So far, considerable progress has been made by employing this solution technique in obtaining spinel oxides for high performance electrode materials^{33,34}.

Sol-gel techniques are receiving much attention because they can be applied to a wide variety of materials; they offer the possibility of controlling not only the size and distribution of particles, but also their shape. A broad range of spinels with any desired shape can be prepared by this technique³⁵⁻³⁷. The process involves the preparation of a sol, which is a dispersion of a solid and dispersed phase in a liquid (dispersion medium). The sol is prepared by mixing concentrated solutions containing the cations of interest with an organic solvent as dispersion medium. The sol is then destabilized by adding water, leading to the formation of a gel. This is transferred to the solid phase by high pressure heating where by the liquid containing in the gel is transformed into supercritical vapours.

Combustion synthesis is a novel method for the preparation of fine spinel particles making use of exothermic redox reaction between metal nitrate and tetraformal triazine or oxalic acid dihydrazine³⁸. In this process stoichiometric ratio of nitrates is dissolved in the minimum amount of water in

a pyrex dish; the fuel is added and is heated at 350 °C in a muffle furnace. A heating rate of 75 °C/min is used to obtain good combustion. This method can be used for Ni-Zn and Co spinels.

Spray drying technique of preparation of spinels involves precipitation from a concentrated solution of cations by solvent evaporation. To ensure that the particle remains small, the concentrated solution is atomized at high pressure into fine droplets of 100-500 µm diameter; the solvent is evaporated by an upward stream of hot gas. Several alternative methods are currently under development, as an efficient way to control the texture, composition, homogeneity and structural properties of the spinel particles³⁹⁻⁴³.

In freeze drying method, the aqueous concentrated solution is atomized into fine droplets, and is rapidly frozen by blowing into low temperature bath such as ice-acetone or liquid nitrogen. The droplets are then dried in vacuum and the anhydrous salts are calcined to produce fine powders. Ni-Zn ferrites have been obtained from freeze drying with high density and small and uniform grain size⁴⁴.

In addition to the above discussed methods, several other methods like pulsed wire discharge⁴⁵, shock wave synthesis⁴⁶ and sonochemical method⁴⁷ are also applied in spinel synthesis.

1.3.2 Spinel structure

The spinel structure was first determined by Bragg and Nishikawa⁴⁸. The unit cell of a spinel contains eight formula units and hence can be represented as 8[AB₂O₄]. The 32 oxygen ions per unit cell form a face centered cubic (fcc) lattice in which two kinds of interstitial are present. In the former the cation is surrounded by four oxygen ions located at the corners of a

Introduction

tetrahedron and in the latter by six oxygen ions located at the corners of an octahedron. These are called tetrahedral (T_d) and octahedral (O_h) sites respectively and are often represented to as A and B sites. There are 64 tetrahedral sites and 32 octahedral sites per unit cell. Of these, 8 tetrahedral holes ($1/8^{\text{th}}$ of tetrahedral interstices) and 16 octahedral interstices ($1/2$ of the octahedral interstices) are occupied by metal ions. The unit cell of an ideal spinel structure is shown in Fig. 1.1. It is convenient to divide the unit cell into eight edges of length $a/2$ to show the arrangements of the A and B sites (Fig. 1.2). The space group is $Fd3m$ (Oh^7). The oxygen atoms have four-fold coordination, formed by three B cations and A cation. The nearest neighbours of a tetrahedral site, octahedral site and oxygen anion site are shown in Fig. 1.3.

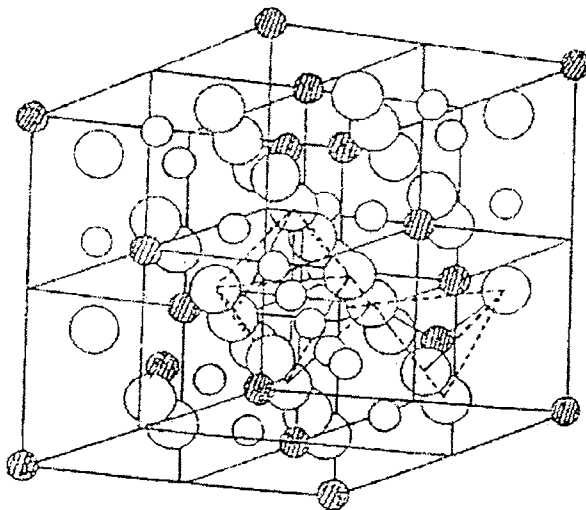


Fig. 1.1 The unit cell of an ideal spinel structure. Hatched circles indicate A cations, unhatched circles indicate B cations and large unhatched circles indicate oxygen anions.

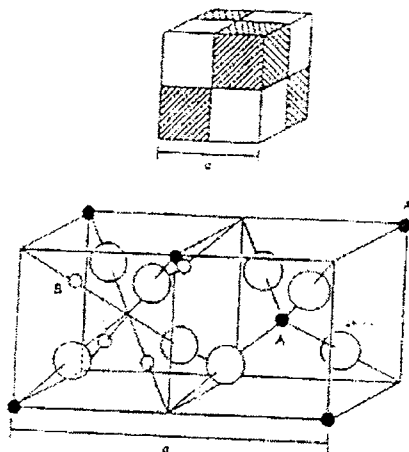


Fig.1.2 The spinel structure. The unit cell can be divided into octants; tetrahedral cations A, octahedral cations B and oxygen atoms (large circles) are shown in two octants.

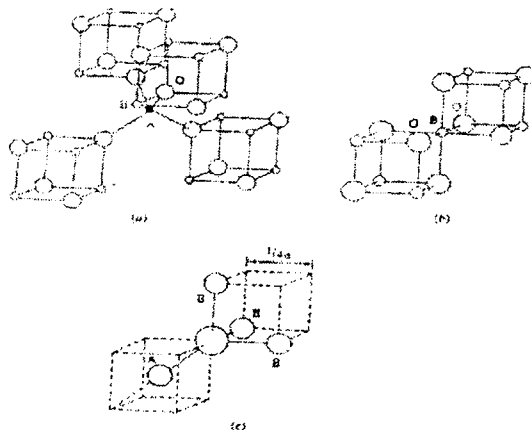


Fig.1.3 Nearest neighbours of (a) a tetrahedral site, (b) an octahedral site and (c) oxygen anion.

Introduction

The spinel structure is very flexible with respect to the cations it can incorporate; there are over 100 known compounds. In particular, the A and B cations can mix. In other words, the composition with respect to one unit cell can be

- $(A_8)(B_{16})O_{32}$, or
- $B_8(A_8B_8)O_{32} = B(AB)O_4$ in regular chemical spelling, or
- $(A_{8/3}B_{16/3})(A_{16/3}B_{32/3})O_{32}$

and so on, with the atoms in the brackets occupying the respective site at random. Few examples: Magnetite- $Fe^{3+}(Fe^{2+}Fe^{3+})O_4$; Spinel- $Mg^{2+}(Al_2^{3+})O_4$; Chromite- $Ni^{2+}(Cr_2^{3+})O_4$; Jacobsite- $Fe^{3+}(Mn^{2+}Fe^{3+})O_4$.

The ideal situation is never realized as the oxygen anions in the spinel structures are generally not located at the exact positions of the fcc sub lattice. The interstices available in an ideal close packed structure of rigid oxygen anions can incorporate only those metal ions with radius $r_{tetra} \leq 0.30 \text{ \AA}$ in tetrahedral sites and only those ions with radius, $r_{octa} \leq 0.55 \text{ \AA}$ in octahedral sites. So in order to accommodate larger cations such as Co, Cu, Mn, Mg, Ni and Zn, the lattice has to be expanded. The difference in the expansion of the octahedral and tetrahedral sites is characterized by a parameter called oxygen parameter (u). In all ideal spinels, the parameter ' u ' has a value in the neighbourhood of 0.375. But in actual spinel lattice this ideal pattern is slightly deformed, usually corresponds to $u > 0.375$. ' u ' increases because the anions in the tetrahedral sites are forced to move in the [111] direction to give space to the larger A cations. Octahedra become smaller and assume 3m symmetry.

Chapter 1

In Table 1.1, interatomic distances are given as a function of the unit cell parameter 'a' and the oxygen parameter ' u ',^{49,50}.

Table 1.1 Interatomic distances and site radii in spinels AB₂O₄, as a function of unit cell edge (a) and oxygen parameter (u)

Tetra-tetra separation A-A	$a (3/4)^{1/2}$
Tetra-octa separation A-B	$a (11/8)^{1/2}$
Octa-octa separation B-B	$a (2/4)^{1/2}$
Tetra-O separation A-O	$a [3(u-0.25)]^{1/2}$
Octa-O separation B-O	$a (3u^2-2.75 u + 43/64)^{1/2} a (5/8-u)$
O-O tetrahedral edge O-O	$a [2(2u-0.5)]^{1/2}$
O-O shared octa edge O-O	$a [2(1-2u)]^{1/2}$
O-O unshared octa edge O-O	$a [4u^2-3u + 11/16]^{1/2}$
Tetrahedral radius	$a [3(u-0.25)]^{1/2}-R_0$
Octahedral radius	$a [3u^2-2.75u + 43/64]^{1/2} -R_0 a (5/8-u)-R_0$

u is defined with unit cell origin at an A site and R_0 is the oxide ion radius.

The spinel structure is also interesting because it may contain vacancies as regular part of the crystal. For example, if magnetite is slowly oxidized by lying around a couple of billion years, or when rocks cool, Fe²⁺ will turn into Fe³⁺. If all Fe²⁺ is converted into Fe³⁺, charge balance requires a net formula of Fe_{21.67}O₃₂ per unit cell and this means that 2.33 sites must be vacant - we have what is called a defect spinel. In a way, the composition is now Fe_{21.67}Vac_{2.33}O₃₂; having lots of vacancies as an *integral part of the structure*.

1.3.3 Distribution of metal ions over different sites

Normal, inverse and random spinels

The interesting and useful electrical, magnetic and catalytic properties of the spinels are governed by the distribution of metal ions among the octahedral and tetrahedral sites of the spinel lattice. As mentioned earlier, the general formula of the spinel is AB_2O_4 , where A and B cations occupy the tetrahedral and octahedral sites respectively.

The structure and cation distribution of the spinels have been discussed by Verway and Heilman⁵¹. If A denotes a divalent cation and B a trivalent one, the cation distribution is usually indicated as $(A)[B_2]O_4$, where the square brackets indicate the octahedral site occupancy and the cation in the parenthesis are located in the tetrahedral sites. This is the so called **normal** distribution, in which the tetrahedral sites are occupied only by the A-type ions and the octahedral sites by the B-type ions. The A ions of a normal spinel occupy the 8 tetrahedral sites of the Oh^7 space group and have a point symmetry T_d . The B ions of a normal spinel occupy the 16 octahedral sites of the Oh^7 space group and have point symmetry D_{3d} . Another extreme cation distribution is, $(B)[AB]O_4$ as pointed out by Barth and Posnjak⁵². In this case the B cation occupy the tetrahedral sites and all the A cations together with the other half of the B cations occupy the octahedral sites. This type of the spinel configuration is called **inverse** spinels. Datta and Roy⁵³ and Hafner and Laves⁵⁴ have shown that there are many **intermediate** or **random** spinels which are in between the pure normal and pure inverse arrangements. They can be represented as $(A_{(1-x)}B_x)[A_xB_{(2-x)}]O_4$, where x is the degree of inversion, with a

value of zero for normal and one for the inverse distribution. This intermediate spinel structure is due to the average distribution of all the ions about all the spinel cation positions (Table 1.2).

Table 1.2 Cation distribution of some of the spinels

Spinel	Distribution
Normal	(Zn) [Fe ₂]
	(Ni) [Cr ₂]
Inverse	(Fe) [NiFe]
	(Co) [NiCo]
	(Fe) [Li _{0.5} Fe _{1.5}]
Random	(Mo _(1-x) Fe _x) [Mo _x Fe _(2-x)]
	(Mn _(1-x) Fe _x) [Mn _x Fe _(2-x)]
	(Mg _(1-x) Fe _x) [Mg _x Fe _(2-x)]

1.3.4 Factors determining cation distribution

Diverse properties of the spinel compounds are derived from the possibility of synthesis of multicomponent spinel by partial substitution of cations in position A and B of spinel structure. Among the spinels, inverse spinels have got special attention due to redox nature of the metal ions and the lack of site preference of cations, which enable them to redistribute between

Introduction

octahedral (O_h) and tetrahedral (T_d) sites during the course of catalytic transformation keeping the spinel structure intact. This accounts for the variety of reactions in which they have been used as catalysts. In these compounds the physical and chemical properties are controlled by the nature of ions, their charge and site distribution among O_h and T_d sites. It is thus of major importance to understand the factors which influence the site occupancy.

The factors that contribute to the total lattice energy in spinels are:

- i. elastic energy
- ii. electrostatic (Madelung) energy
- iii. crystal field stabilization energy
- iv. polarization effects

The elastic energy refers to the degree of distortion of the crystal structure due to the difference in ionic radii assuming that ions adopt a spherical shape. Smaller cations, with ionic radii of 0.225-0.4 Å, should occupy tetrahedral sites, while cations of radii 0.4-0.73 Å should enter octahedral sites. This distribution leads to a minimum in lattice strain. Since trivalent cations are usually smaller than divalent ions, a tendency towards the inverse arrangement would be expected.

The detailed Madelung energy calculations for spinels⁵⁵ show that this energy is dependent on the u parameter. For $u > 0.379$, the normal distribution is more stable, while for lower u values, the inverse arrangement possess a higher Madelung constant. The presence of two kinds of cation on octahedral

sites in inverse spinels leads to an additional contribution to the Madelung energy. The critical u value then becomes 0.381⁵⁶. Madelung energy is higher for the normal spinel if $u > 0.381$, and the inverse, ordered spinel is more stable for $u < 0.381$.

Romeijn⁵⁷, Adaunitz and Orgel⁵⁸ have first suggested the application of crystal field theory to understand the site preference of cations. McClare⁵⁹ has calculated the octahedral site preference energies of transition metal ions in oxide using crystal field theory and is given in Table 1.3

The data show that the systems with d^5 and d^{10} configurations have no crystal field stabilization energy and hence no site preference. The d^3 system has the highest octahedral site preference energy. The d^4 and d^9 ions can be further stabilized by Jahn-Teller distortion. In the regular O_h symmetry, octahedra of surrounding anion is elongated or compressed in the z direction to give D_{4h} symmetry, the doublet (e_g) and triplet (t_{2g}) levels split⁶⁰. The splitting of the doublet is larger. In the case of elongation, the d_z^2 orbital is stabilized compared to $d_{x^2-y^2}$ orbital. $Fe[CuFe]O_4$, $Mn[ZnMn]O_4$, and $Zn[Mn_2]O_4$ are examples of tetragonally distorted spinels.

The last factor to be discussed is polarization effects. Polarization may simply be considered as the degree of distortion of the electronic charge density around an ion. This can arise from the negligible distortion and effective removal of an electron from one ion towards its neighbour, giving rise to a purely covalent bond and a purely ionic bond respectively. With regard to the transition metal ions in spinels, only spherically symmetric ions

Introduction

Table 1.3 Crystal field stabilization energies for transition metal cations on tetrahedral and octahedral spinel sites.

Number of d electrons	Theoretical CFSE in terms of Dq		Cations	Estimated octahedral site preference energies (eV)
	Octahedral	Tetrahedral		
1	4	6	Ti ³⁺	0.33
2	8	12	V ³⁺	0.53
3	12	8	V ²⁺	1.37
4	6	4	Cr ³⁺	2.02
			Mn ³⁺	1.10
5	0	0	Cr ²⁺	0.74
			Fe ³⁺	0
6	4	6	Mn ²⁺	0
			Fe ²⁺	0.17
7	8	12	Co ³⁺	0.82
			Co ²⁺	0.09
8	12	8	Ni ²⁺	0.99
9	6	4	Cu ²⁺	0.68
10	0	0	Zn ²⁺	0

(d^5 and d^{10}) can show tendency for covalency. In this case, tetrahedral sites are preferred. Cations which show covalent affinity for tetrahedral environments are Fe^{3+} , Ga^{3+} , In^{3+} and, more strongly, Zn^{2+} and Cd^{2+} . Spinels with the former cations tend, therefore, to be inverse while those with the latter tend to be normal. When the various factors are counteracting, there can be a completely random arrangement of metal ions among the eight tetrahedral sites and sixteen octahedral sites.

1.3.5 The surface of catalytically active spinels

The surface structure and properties of spinels are of wide interest. The principle and interesting question to ask is, which plane, which coordination and which valency states are responsible for the catalytic activity and selectivity in spinels? There are many reports that the tetrahedral sites in spinels are not active⁶¹⁻⁶³. The fact that the tetrahedral sites are not active could originate from the stronger metal-oxygen bonds due to the lower valency and coordination number. Moreover, the tetrahedral sites are not accessible to the reactants⁶⁴. In the literature, usually only the low index spinels are taken into consideration when discussing the surface of spinels^{61,65-67}. Following the suggestion by Knozinger and Ratnasami⁶¹ and using their notation one can distinguish six different low-index surface planes, which are shown in Fig.1.4. From the figure it follows that A (111), C (110), E (100) and F (100) planes have both tetrahedral and octahedral sites on the surface, while B (111) and D (110) planes expose only octahedrally coordinated cations.

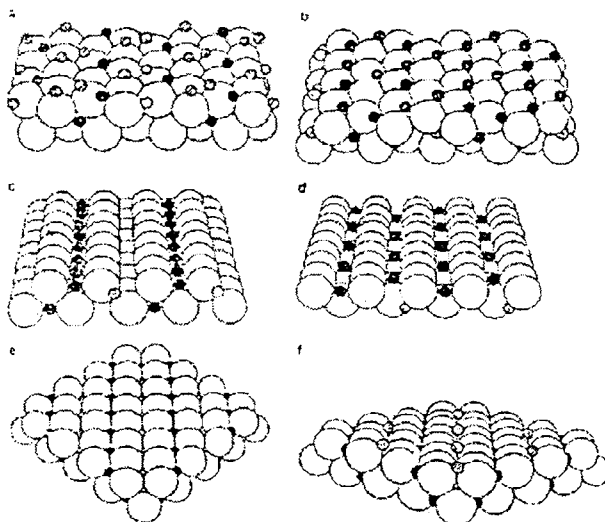


Fig.1.4 The low index planes of a normal spinel structure: (a) A (111), (b) B (111), (c) C (110), (d) D (110), (e) E (100), (f) F (100). The open spheres represent the oxygen anions, the solid spheres the octahedral cations and hatched spheres the tetrahedral cations.

According to Ziolkowski and Barbaux⁶⁵, from the theoretical calculations, the A (111) and D (110) planes are preferred in the surface, but these predictions do not form a final conclusion. Shelef and co-workers⁶⁶⁻⁶⁸ made an experimental attempt to elucidate the surface structure of spinels using the low energy ion scattering (LEIS) and they support the data that the tetrahedrally coordinated cations are not accessible for the reactant molecules.

Beaufils and Barbaux^{62,63} investigated the surface composition of normal spinel oxides by differential neutron diffraction (DND) techniques and concluded that the surface of spinel consists of a mixture of (110) and (111) planes.

By comparing the experimental results of DND with some models involving argon-oxygen distances, they observed that these planes contain only octahedral cations and oxygen anions respectively. Jacobs et al.⁶⁴ confirmed this by LEIS technique. By substitution of Mn and Co cations in different sites in the spinel structure of Mn_3O_4 and Co_3O_4 by other cations, which are not active in the selective reduction of nitrobenzene to nitrosobenzene, they studied the role of these sites in the catalytic reaction. Their results confirmed the idea that octahedral ions are almost exposed exclusively at the surface of the spinel oxide powders and only these sites participate in the reaction. The only two low-index planes of the spinel structure, which can satisfy this condition, are identified as B (111) and D (110). The absence of occupied tetrahedral sites at the surface is a more general property of spinels.

The important factors that determine the structural and magnetic properties of spinel ferrites are the cation arrangement in spinel ferrite, the radius of cations, charge and site preference energy. It is well known that the properties of non stoichiometric oxides and/or mixed oxides depend considerably on the degree of non stoichiometry^{69,70}. Recently reported examples of these unusual solids include the non stoichiometric spinel type (NSS) mixed oxides mainly employed as catalysts for hydrogenation reactions⁷¹. The specific physicochemical and catalytic properties of NSS solid

depends on the presence of excess divalent ions and/or ions with unusual coordination^{72,73} in the crystal structure.

Depending upon the nature of the metal ion occupying the B site, there are different types of spinels-ferrites (Fe in B site), cobaltites (Co in B site), manganites (Mn in B site), aluminates (Al in B site), chromites, (Cr in B site), galates (Ga in B site), gadolinites (Gd in B site) etc. Transition metal spinel oxides are an important class of compounds having large variety of electronic, magnetic and catalytic properties⁷⁴. Soft ferrites have been actively used for many kinds of magnetic devices such as transformers, induction and magnetic heads for high frequency because their electrical resistivity is higher than those of the soft magnetic alloys⁷⁵. Some spinels are super conductors with a relatively high transition temperature and some spinel ferrites exhibit magnetic properties which make them applicable in technology and industry as magnetic storage devices, microwave devices etc^{76,77}. Ultra fine ferrite particles has been extensively investigated in recent years because of their potential applications in high density magnetic recording⁷⁸, magnetic fluids⁷⁹, ferrofluid technology⁸⁰, magnetocaloric refrigeration⁸¹, magnetic resonance imaging enhancement⁸², magnetically guided drug delivery⁸³ etc.

1.3.6 Spinel as catalysts

Unlike single oxides or their mixture, the single phase spinel type binary and ternary oxides show, extra stability and exhibit interesting catalytic properties. These compounds have attracted much attention due to their remarkable transport, magnetic and electric properties. In these compounds, the properties are controlled by the nature of ions, their charge and site

distribution among the tetrahedral [T_d] and octahedral (O_h) sites. In spinel systems containing iron, Fe^{+3} ion can be easily replaced between O_h and T_d sites by stoichiometrically varying the concentration of other cations. This peculiar structural feature enables ferrospinels to withstand even extremely reducing atmospheres⁸⁴. Another important attribute to these materials, from the commercial standpoint, is that spinel structure provides high stability so that these materials can withstand extremely reducing conditions. Even if reduction of Fe^{+3} to Fe^{+2} occurs, spinel structure remains unaltered and upon reoxidation the original structure can be retained.

Spinel containing transition metal ions can act as efficient catalysts in a number of heterogeneous chemical processes such as CO oxidation⁸⁵, catalytic combustion of hydrocarbons⁸⁶ or selective oxidation and reduction of several organic molecules⁸⁷⁻⁸⁹. For these applications of metal oxides as heterogeneous catalysts, high surface area and accessible porosity are relevant properties.

Transition metal oxide or mixed oxides have now been established as inexpensive alternatives to precious metal and noble metal containing catalysts⁹⁰. Copper manganese oxide mixture based on $CuMn_2O_4$ is a long established catalyst for the removal of toxic gases and vapour since its discovery in 1920⁹¹. These catalysts are still the general choice for respiratory protection in mining industry to remove CO at near ambient temperatures. Moreover, these spinel catalysts are very effective catalysts at elevated temperatures of 200-500 °C for combustion of over 35 organic compounds and nitrogen containing compounds⁹². Transition metal oxides like hematite can be converted to spinel ferrite by adding Zn, Mg, Ni or Co to it, and can be

used for the oxidative dehydrogenation of hydrocarbons⁹³, for transformation of butane⁹⁴⁻⁹⁶ and ethyl benzene⁹⁷.

For reactions such as 1-butene oxidative dehydrogenation, the catalytic activity of a ferrite strongly depends on the cation distribution in lattice^{98,99}. For instance; MgFe_2O_4 , which has an inverted spinel structure, is having higher catalytic activity than the one of stoichiometric ZnFe_2O_4 ferrite, whose crystalline structure is not inverted¹⁰⁰. These results suggest that the distribution of iron in the tetrahedral and octahedral sites of a ferrite could determine their catalytic activity.

Spinel has been conveniently used as catalysts for a variety of industrially important reactions. They can effectively replace conventional Friedel and Crafts catalysts for many aromatic alkylation reactions, for the production of aromatic alkyl derivatives is un-economic and acid-waste makes the process non economic. The increasing demands of environmental legislation have been prompting the chemical industry to minimize or preferably eliminate waste production in chemical manufacture. Solid acid catalysts are very important alternatives to the above. The global demand of solid acid and solid base catalysts has increased considerably in recent years since such systems often give value added products with improved yield without creating major burdens on the environment. Among the various solid acid catalysts, the oxides and mixed oxides¹⁰¹⁻¹⁰³ are the best for the alkylation reactions. Although there are a number of catalysts like Th/Al oxides, Fe-Si-Mg oxides, phosphoric acid, SiO_2 , Fe_2O_3 , Cr_2O_3 , magnetite, hydrotalcite, Al_2O_3 oxides^{103,104-106}, these catalysts possess one or more of the drawbacks such as low conversion, severe operative conditions, poor selectivity due to

number of side products and lack of reproducibility. Recently Rao and co-workers established the idea of using spinels for aromatic C and/or N methylation of compounds like pyridine, aniline, phenol etc¹⁰⁷⁻¹¹¹. It is to be noted that Fe₂O₃ in combination with other oxides such as CdO, SnO₂, CeO₂, NiO, CoO, Cr₂O₃ and ZrO₂ are highly active for the alkylation reactions¹¹²⁻¹¹⁷. Diverse properties of the spinel compounds are derived from the possibility of synthesis of multi-compound spinel by partial substitution of cations in position A and B.

Spinel oxides, having cation distribution in two crystallographic environments¹¹⁸, are reported to be more active for the dehydrogenation of hydrocarbons¹¹⁹, isopropyl alcohol¹²⁰ and cyclohexanol¹²¹. Ferrites are very much effective for many of those reactions as mentioned above. The catalytic effectiveness of ferrites for many such reactions arises because of the ease with which iron can exchange its oxidation state between 2 and 3. Another important attribute of these materials, from commercial standpoint, is their stability under extremely reducing conditions, which is due to the spinel structure. Thus the reduction of Fe⁺³ to Fe⁺² takes place without altering these lattice configurations so that upon reoxidation, the original state is retained¹²². In contrast to the spinel ferrites, the catalyst Fe₂O₃ loses its activity as it is reduced to FeO and metallic iron.

Recent studies on spinels show that they can be used as supports for homogeneous catalysts¹²³. Spinel like ZnAl₂O₄ which have high thermal stability, high mechanical resistance, or inertness to water vapour make it an attractive material both as a catalyst as well as a carrier for active metal to substitute for the more traditional systems¹²³. Rhodium complexes supported

Introduction

on ZnAl_2O_4 are reported to be good catalysts for the hydroformylation and hydrogenation¹²³. Not only this, certain organic transformations can be carried out over spinels. Anisole can be transformed into other industrially important derivatives using ZnAl_2O_4 and $\text{Fe}_2\text{O}_3/\text{ZnAl}_2\text{O}_4$ ¹²³. ZnAl_2O_4 has been shown to be active for the synthesis of styrene from acetophenones¹²⁴ or for the double bond isomerization process of alkenes¹²⁵. It is also promising support for catalysts such as Pt¹²⁶ or Pt/Sn¹²⁷ (dehydrogenation process), and Cu¹²⁸ (low pressure synthesis of methanol) and in the synthesis of compounds like indenenes from indanones¹²⁹.

Spinel plays an important role in the production of fuels. Fuel production in an effective and economical route is one of the problems faced by the world today. In the last two decades, methanol decomposition into CO and H_2 is considered as a promising way to produce an effective and ecological fuel for vehicles, gas turbines and fuel cells^{130,131}. Catalysts with high activity, selectivity and stability under lower temperatures are needed but the problem is not solved enough. Recently Manova et al.¹³² reported their study on nano dimensional iron-cobalt spinel oxides as catalysts for methanol decomposition. A significant methanol conversion with H_2 and CO being the main products is registered for the above spinel just above 500-580K. The heterogeneous decomposition of H_2O_2 , though a convenient alternative to the electrolysis of water for the production and storage of O_2 gas needs a cost effective and high performance catalyst. The selectivity of the H_2O_2 decomposition catalysts has proved difficult as the suitable ones, silver oxide, Pt and Pd blacks are expensive. Among the inexpensive corrosion resistant catalysts¹³³⁻¹⁴⁰, the

binary ferros spinels seem to be potential alternatives to the noble metal catalysts. Chemical composition, crystal structure and microstructural factors have been found to contribute to the overall activity of the catalysts¹³⁷. Cobalt ferrite catalyses the decomposition of H₂O₂ to the same extent as the noble metal catalysts¹³³. Sengupta and Lahiri reported their study on manganese ferros spinel systems for H₂O₂ decomposition and these are promises to be a potential cost effective substitute for the noble metal catalysts.

The production of isobutanol and methanol from syn gas (CO and H₂) feed stream has received considerable attention recent years. Types of higher alcohol synthesis (HAS) catalysts include modified Fischer-Tropsch and methanol synthesis catalyst. These types of catalysts typically are composed of a Zn/Cr spinel structure which is promoted with Cs or K¹⁴¹⁻¹⁴⁶, and the addition of Cs usually results in better catalysts. Epling et al. reported the production of isobutyl alcohol and methanol from syngas using K and Pd promoted Zn/Cr/Mn spinel¹⁴⁷⁻¹⁴⁹.

Alkylation of benzene and substituted benzenes are attracting special attention since the products obtained from these reactions find application in a number of fields such as agrochemicals, pharmaceuticals, pesticides, herbicides, plastics, special grade paints and in the manufacture of a variety of chemicals. Conventional Friedel-Crafts catalysts can be effectively replaced by spinels. Rao et al. conducted a number of studies on the alkylation reactions of phenol, aniline etc¹⁵⁰⁻¹⁵⁶. They have employed ferros spinel based on copper and cobalt, Cu_{1-x}Co_xFe₂O₄, and showed an excellent performance towards phenol methylation both in terms of conversion and *ortho* selectivity.

Introduction

The catalytic effectiveness of these systems is due to the ability of the metallic ions to migrate between the sub lattices without altering the structure, which makes the catalyst efficient for many organic transformation reactions. These spinel oxide materials are good alternatives to both zeolites and aluminium phosphate for selective *o*-alkylation using olefins and alcohols¹⁵⁷. Many ferros spinels based on Cu, Co, Cr, Mn and Zn are proved to be highly active for the production of N-methyl aniline, N, N-dimethyl aniline, 2,6-xylenol etc. by the methylation of aniline and phenol^{155,156,158-160}. Sugunan et al. also reported the benzoilation of benzene using benzyl chloride catalyzed by ferros spinels^{161,162}.

Styrene production and styrene oxidation can be conveniently carried out by spinels. The catalytic dehydrogenation of ethyl benzene is of industrial importance in the manufacture of styrene as it is extensively used as an intermediate in the manufacture of polystyrene. Spinel such as $MgFe_2O_4$ and $ZnFe_2O_4$ are reported as highly active catalysts for the oxidation of styrene to bezaldehyde¹⁶³⁻¹⁶⁶.

The reduction of NO_x emission from automobile exhaust and removal of N_2O and CO remains a challenging problem to both academic and automobile industry. Because of the inefficiency of the conventional three way catalyst in converting NO under lean burn conditions, the selective catalytic reduction of NO with hydrocarbons is believed to be a promising alternative to eliminate NO. Recently spinels, mainly cobalt spinels are introduced for the removal of NO_x ^{167,168}. The cobalt oxide spinel Co_3O_4 is one receiving considerable interest. Yan et al. reported spinel oxide with partial replacement of Co^{2+} by Zn^{2+} in Co_3O_4 which are highly active for N_2O

decomposition into N_2 and O_2 ¹⁶⁷. Magnesium cobaltite spinels prepared by hydrothermal method shows excellent catalytic activity for N_2O decomposition¹⁶⁸.

Copper Manganese oxide mixture based on $CuMn_2O_4$ is a long established catalyst for the removal of toxic gases and vapours. These catalysts are still the general choice for respiratory protection in mining industry to remove CO at near ambient temperatures¹⁶⁹. Spinels like $NiMn_2O_4$ and $CuCo_2O_4$ show high activity in the catalytic CO oxidation¹⁷⁰.

Photocatalysis is the important field where spinels find immense application. Spinels as such or in the composite form are used for the production of H_2 and for the degradation of environmentally pollutant organic chemicals^{170,171}. Hydrogen gas is an important chemical feedstock and is highly valued as a nonpolluting renewable fuel, its production from cheap raw materials like water has been actively studied and is currently a subject of much interest. Suspension of $CuMn_2O_4$ or $ZnMn_2O_4$ in aqueous solutions containing S^{2-}/SO_3^{2-} will generate hydrogen photochemically¹⁷¹. Their narrow energy band gap and relative inertness toward photo corrosion make them attractive materials in photoelectrocatalytic systems. Solid solutions such as $Zn_{1-x}Ni_xMn_2O_4$ and $ZnFe_2O_4$ used to convert H_2S wastes to less harmful products namely polysulfides with a gain of storable form of power (hydrogen)^{172,173}. The spinel with a relatively small band gap, especially nanometer sized $ZnFe_2O_4$, is a potentially useful solar energy material for photocatalytic conversion and photochemical hydrogen production from water^{174,175}, whose advantages are to absorb visible light and to not be sensitive to photoanodic corrosion. Nanocomposites of $ZnFe_2O_4$ and TiO_2

with useful characteristics making them suitable for far reaching applications in photocatalysis. ZnFe₂O₄/TiO₂ nanocomposite is a more effective photocatalyst for the photodegradation of phenol than TiO₂ alone¹⁷⁰. Application of these nanocomposites for the photocatalytic decomposition of phenol gives an increased photocatalytic activity relative to TiO₂ only nanomaterials. These nanocomposites are promising solar energy materials for applications in photocatalysis as well as in photo electrochemical conversion.

1.4 Acid-base properties

Surface acidity and basicity investigations have received considerable attention in recent years because they can provide significant information in determining the behaviour of solid surfaces. Determination of strength of acid sites exposed on the solid surface as well as their distribution is a necessary requirement to understand the catalytic properties of acidic solids. The conversion and selectivity of a reaction are influenced not only by the nature of the acidic sites but also by their number and their strength. A variety of physico-chemical methods have been developed and widely applied to evaluate the structure and the amount of surface acid sites on catalysts, and a large variety of probe molecules have been utilized to both qualitatively ascertain in the acidity and provide a measure of the number of these acid sites. Some of the physico-chemical methods used to characterize acid sites are amine, pyridine and ammonia titrations, potentiometric titrations, spectroscopic investigations, thermal desorption and gravimetric desorption measurements. They differ from each other in their physical and chemical principles and this makes it difficult to compare the acidic results. The

temperature programmed desorption method is most promising, facilitating the direct determination of the distribution of the strength of the acidic sites. Basic sites were characterized by using electron acceptors which will accept electrons from basic sites. Cyclohexanol decomposition and cumene cracking were the test reactions suggested to get a qualitative idea about the acid-base properties. Acidity and basicity depend on the nature of the oxide and on the charge and radius of the metal ions. Other factors influencing the character of metal – oxygen bond are the co-ordination number, the filling of the d orbitals and the nature of other ligands.

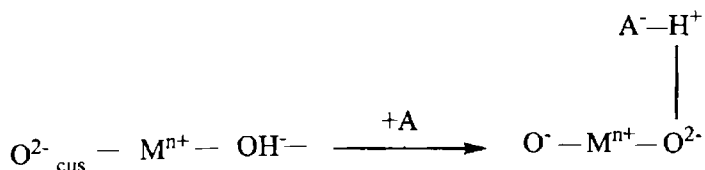
1.4.1 Surface electron donating properties

The electron donor strength of the metal oxide can be defined as the conversion power of an electron acceptor adsorbed on the surface into its anion radical¹⁷⁶. The electron donor sites are associated with surface hydroxyl groups and with defect centers involving oxide ions. Study of electron donor properties of metal oxides by the adsorption of electron acceptors of various electron affinity values has been a well established technique. The electron donor properties of alumina surface have been investigated by Flockart et al.¹⁷⁷, by the adsorption of tetracyano ethylene.

If a strong electron acceptor is adsorbed on the metal oxide, its anion radical is formed at strong as well as weak donor sites present on the surface. On the other hand, if a weak electron acceptor is adsorbed, the formation of anion radical is expected only at the strong donor sites. In the case of a very weak electron acceptor adsorption, its anion radical will not be formed even at the strongest donor sites. The electron donating capacity can be expressed as the

limiting electron affinity value at which free radical anion formation is not observed at the metal surface. Thus by comparing the limiting amount of the electron acceptor adsorbed on the catalyst surface and the electron affinity values of the respective electron acceptor used, it is possible to get an insight into the strength and distribution of the electron donor sites on the surface.

Cordishi et al.^{178,179} have correlated the electron donating sites on the surface with Lewis basicity. The donor site is proposed to be a coordinatively unsaturated oxygen ion, (O^{2-}_{cus}) associated with a nearby OH^- group, whose proton interacts with the radical anion formed giving stability. Thus Brønsted acidity stabilized the radical ion formed and the active site can be considered as acid-base pair as shown.



Surface electron donating properties have been studied by various electron acceptors such as 7,7,8,8-tetracyanoquinodimethane (TCNQ), 2,5-dichloro-*p*-benzoquinone (DCQ), *p*-dinitrobenzene (PDNB) and *m*-dinitrobenzene with electron affinity values 2.84, 2.30, 1.77 and 1.26 eV respectively¹⁸⁰. Adsorption study of 2,3,5,6-tetrachloro-*p*-benzoquinone (chloranil) with electron affinity of 2.40 eV from acidic and basic solvents on alumina and titania have been carried out by Esumi et al. and they correlated the amount of chloranil adsorbed with the acid-base interaction at the interface. By measuring the electronic spectra, esr and adsorption isotherms,

Meguro et al.¹⁸¹ have studied the adsorption of electron acceptors with electron affinity values from 1.26 to 2.84 eV on the surface of alumina. Radical concentration formed were found to be directly related to the electron affinity values of the respective electron acceptor adsorbed since the radical concentration decreased as the electron affinities of electron acceptors decreased from 2.84 to 1.77.

It was found that the calcination temperature has an effect on the electron donating property of metal oxide as shown by the studies on zirconia by Esumi et al.¹⁸². An increase of calcination temperature reduces the amount of electron acceptor adsorbed indicating the reduction of OH⁻ on the surface. Above 900 °C the amount of adsorbed species again increased due to the formation of surface oxide ions.

Solvent effects on the acid-base interactions of the electron acceptors (TCNQ and chloranil) with the metal oxides such as alumina and titania have been investigated by Esumi and co-workers^{183,184}. They observed that the amount of electron acceptors adsorbed and the concentration of anion radicals formed decreased with an increase in acid-base interaction between the electron acceptor and the organic solvents used. Using Drago equation¹⁸⁵, to understand the nature of interaction of different solvents with TCNQ, it was observed that acid-base enthalpy between TCNQ and the organic liquids increased in the order 1,4-dioxane > ethyl acetate > acetonitrile. So the electron acceptor adsorption is greatly depressed by the interaction between TCNQ and acetonitrile.

Sugunan et al. investigated the electron donor properties of rare earth oxides such as Pr₆O₁₁¹⁸⁶, CeO₂¹⁸⁷, Sm₂O₃¹⁸⁸, La₂O₃¹⁸⁹ and Nd₂O₃^{190,191} and

their mixed oxides with alumina as a function of composition and activation temperature. It was found that the number of both strong and weak donor sites is increased with increase in calcination temperature. The extent of electron transfer was characterized by magnetic measurements. During adsorption, magnetic moment decreased and reached a limiting value at the same concentration at which the limiting amount of electron acceptor was adsorbed.

1.4.2 Temperature programmed desorption studies

Temperature programmed desorption of basic molecules such as ammonia, pyridine, n-butylamine etc. is an accepted technique used to characterize the acid strength as well as acid amount on a solid catalyst surface^{192,193}. When gaseous bases are adsorbed on acid sites the one which is adsorbed on a strong acid site is more stable than the one which is adsorbed on a weak acid site and is more hard to desorb. As elevated temperatures stimulate the evacuation of adsorbed bases from the acid sites, those at weaker sites will be evacuated preferentially. Thus, the proportion of the adsorbed base evacuated at different temperatures can give a measure of acid strength. Also, the amount of gaseous base, which a solid can adsorb chemically from the gaseous state, can be taken as a measure of the amount of acid sites on its surface. The advantage of TPD method over other techniques is that it allows the study of the catalyst under conditions more or less similar to that of reaction and that the acid amount for a solid at higher temperatures (several hundred degree centigrade) can be determined.

The NH₃-TPD method is widely employed to characterize the acidity of solid catalysts^{194,195}. Ammonia is an excellent probe molecule for testing

the acidic properties of solid catalysts, because its strong basicity and small molecular size allow the determination of acidic sites of any strength and type^{194,195}. Though ammonia TPD method is unable to distinguish the type of acid sites (Lewis and Brønsted acidic sites), it gives the total acidity and acidity of solid catalyst at any temperature region. The NH₃-TPD spectra are often poorly resolved and experimental artifacts such as change in the activation treatment and curve deconvolution methods can give insights on site distribution and heat of desorption. Thus, on the basis of complementary characterization results, a fairly reliable interpretation of the NH₃-TPD pattern can be attained¹⁹⁶.

Information on the interaction of ammonia with solid acids can be generally achieved by IR spectroscopy¹⁹⁷, calorimetric¹⁹⁸ and TPD techniques. When ammonia is chemisorbed on acidic surfaces, it can interact with acidic protons, electron acceptor sites and hydrogen from neutral or weakly acidic hydroxyls¹⁹⁹. The ammonia adsorbed on a surface can be retained either by hydrogen bonding via one of its hydrogen atoms to a surface oxygen atom or oxygen of the hydroxyl group or by the transfer of protons from surface OH to ammonia²⁰⁰. These two interactions involve neighbouring anions or OH groups. The strongest interaction is the coordination to an electron deficient atom. The dissociative adsorption in the form of surface NH₂ or NH and OH is also possible. Another mode of interaction is the complete transfer of H⁺ from Brønsted sites to produce NH₄⁺.

By analyzing the TPD spectrum of ammonia it is possible to calculate the density function of activation energy for desorption of ammonia as described by Hashimoto et al.²⁰¹. Sato et al. studied the TPD of ammonia

adsorbed on cation-exchanged ZSM-5²⁰². The TPD spectrum of ammonia showed two distinct peaks for H-ZSM-5, indicating the existence of strong (a peak at 723 K) and weak (a peak at 463 K) acid sites. The heat of adsorption of a base is clearly a measure of the acid strength on a solid surface¹⁹². Tsutsumi et al. plotted differential heat of adsorption for ammonia on SiO₂-Al₂O₃ and SiO₂ against the surface coverage²⁰³. Heat of adsorption corresponding to acid strength increases with increasing alumina content in SiO₂-Al₂O₃.

Arena et al. made a characterization study of the surface acidity of solid catalysts by TPD of basic probe molecules such as ammonia, pyridine and benzene¹⁹⁶. According to them, TPD of adsorbed ammonia is a reliable method to feature the strength but not the nature (Lewis and Brønsted) of surface acid sites in solid acid catalysts. Mathematical analysis of NH₃-TPD spectra highlights the presence of weak, medium and strong acid sites on all the catalysts and also enables their quantitative estimation. A comparative evaluation of the TPD patterns of ammonia, pyridine and benzene shed light on the nature (Lewis and Brønsted) of the acid sites.

1.4.3 Cyclohexanol decomposition

Alcohol decomposition reaction has been widely studied because it is a simple model reaction to determine the functionality of an oxide catalyst, to be chosen for industrial process. Decomposition of isopropanol and cyclohexanol (CHOL) are the most widely studied reactions in this category. Alcohols are amphoteric and they interact with both acidic and basic sites. The utility of alcohol decomposition as a test reaction for acid-base property

Chapter 1

studies of metal oxides is well established^{204,205}. Dehydration of an alcohol leads to an olefine and dehydrogenation forms an aldehyde (in the case of primary alcohols) or a ketone (in the case of secondary alcohols) and hydrogen. At elevated temperatures, decomposition may involve C-C bond cleavage giving products like CO, CO₂ etc. At near ambient temperatures ether can be a major product.

Dehydration activity is linked to the acidic property and dehydrogenation activity to the combined effects of both acidic and basic properties of the catalyst. Thus dehydration activity gives the direct measure of the acidity of the system, where as the ratio of the dehydrogenation activity to the dehydration activity gives the basicity of the system. Decomposition of alcohols is one among the many classes of reactions catalyzed by oxidic spinels. Studies on the decomposition of isopropanol²⁰⁶, benzyl alcohol²⁰⁷, and CHOL²⁰⁸ by spinel oxides have been reported.

One of the most widely studied alcohol decomposition reaction for the acidity-basicity correlation is the cyclohexanol decomposition. The amphoteric nature of cyclohexanol permits its interaction with both acidic and basic sites. As a result of this, dehydration and dehydrogenation are catalyzed by the oxide systems forming cyclohexene and cyclohexanone.

Jebarathinam et al. studied the transformation of cyclohexanol to cyclohexanone over the spinel catalysts to investigate the influence of copper ions in the octahedral sites²⁰⁹. Their observation indicates that Cu⁺ at the octahedral sites is more active than Cu⁰ for the dehydrogenation of cyclohexanol. They have also studied the effect of Zn²⁺ substitution on NiFe₂O₄ for the decomposition of cyclohexanol²¹⁰. Introduction of Zn²⁺ ions

into the NiFe_2O_4 matrix has facilitated the dehydrogenation of cyclohexanol to cyclohexanone by creating strong basic sites. Joshi et al. studied the catalytic decomposition of cyclohexanol over $\text{Mg}_{1-x}\text{Zn}_x\text{Al}_2\text{O}_4$ and established correlation among transport properties, surface acidity and catalytic behaviour²¹².

According to Bezouhanava et al., decomposition of cyclohexanol is a reliable method to determine the functionality of metal oxide catalysts²¹¹. They correlated the dehydrogenation activity to the existence of basic sites originating from the lattice oxygen. Stronger acid sites are needed for dehydration of cyclohexanol compared to other secondary and tertiary alcohols like isopropyl or tertiary butyl alcohol. On stronger acid sites, formation of methyl cyclopentane, which is formed by the isomerization of cyclohexene, has been observed over alumina catalyst by Pines et al²¹³.

1.4.4 Cumene cracking

Catalytic cracking uses a solid acid catalyst and moderately high temperatures to aid the process of breaking down large hydrocarbon molecules into smaller ones. Cumene cracking reaction is generally used as a test reaction to get a qualitative idea about the Lewis and Brønsted acid sites. The cracking of alkyl aromatic compounds is a very specific reaction. Cumene is a conventional model compound for testing the catalytic acidity since it undergoes different reactions over different type of acid sites. α -methyl styrene and benzene are the major products of the reaction where as toluene, ethyl benzene and styrene are grouped into minor products.

The major reactions occurring during cumene conversion may be grouped into dealkylation (cracking) and dehydrogenation. Another possibility is the cracking of the alkyl chain to give ethyl benzene which on dehydrogenation gives styrene. Cracking of cumene to benzene is generally attributed to the action of Brönsted sites by a carbonium ion mechanism^{214,215}. Dehydrogenation of cumene yields α -methyl styrene as the major product, the formation of which has been ascribed to the Lewis acid sites²¹⁴. Boorman et al. prepared a series of catalysts containing fluoride, cobalt and molybdenum as additives to γ -alumina, both individually and in combination. The surface acidity of these systems was correlated with their reactivity for cumene conversion^{216,217}. Sohn and Jang²¹⁸ correlated the activity for cumene dealkylation with both acidity and acid strength distribution of sulphated ZrO_2 - SiO_2 catalysts.

1.5 Reactions selected for the present study

(a) Alkylation reactions

Alkylation is the transfer of an alkyl group from one molecule to another. The alkyl group may be transferred as an alkyl carbocation, a free radical or a carbanion. It is one of the most important research targets in organic chemistry. Alkylation is accomplished by using the functional groups as alkyl electrophile, alkyl nucleophile or sometimes as alkyl radical. In this work we have discussed the alkylation reactions of aniline, phenol and *m*-cresol. The alkylating agents used were methanol, *tert*-butyl alcohol and isopropyl alcohol. The reactions were conducted in vapour phase. Alkylation of aniline and phenols are

industrially outstanding reactions due to the numerous uses of the alkylated products. Alkylation of aniline gives both C-alkylated and N-alkylated products and of these, N-alkylated ones such as N-methyl aniline and N,N-dimethyl aniline are synthetically more valuable. Alkylation of phenols gives a wide range of products and among them cresols, xylenols, thymol, tertiary butyl derivatives are the most important ones. A detailed description of these reactions has been given in chapter 4.

(b) Oxidation Reactions

The activation and functionalization of paraffins is one of the world wide pursuit research directions with a high potential for the development of new catalytic process technologies. The selective oxidation of hydrocarbons, which requires activation of the relatively inert carbon-hydrogen bond, is an important commercial reaction for functionalizing hydrocarbons to yield products that are important themselves or as intermediates for other chemicals. The reactions selected for the present study were styrene oxidation, cyclohexane oxidation and benzyl alcohol oxidation using hydrogen peroxide as the oxidizing agent. The products of these reactions namely benzaldehyde, cyclohexanol and cyclohexanone have numerous applications in industry. The oxidation reactions were conducted in liquid phase. These reactions are discussed in chapter 5.

1.6 Objectives of the present work

The main objectives of the present work can be summarized as follows:

- To prepare ferrospinels and cobaltite spinels by co-precipitation method. The prepared spinels were nickel ferrites, copper cobaltites and nickel cobaltites. Ferrites were prepared by low temperature co-precipitation method where as cobaltites were prepared by high temperature co-precipitation method using NaOH.
- To improve the surface and electronic properties of spinels by incorporating various ions and by changing the stoichiometry of ions. Ferrospinels were modified by replacing iron by chromium and gadolinium. Cobaltite spinels were modified by changing the stoichiometry of nickel, copper and cobalt.
- Characterization of the prepared spinels by various methods such as XRD, DRIFT, TG, BET surface area, SEM, EDAX, Mössbauer spectroscopy etc.
- To evaluate the surface basicity using electron acceptors of various electron affinity values.
- To determine the total acidity by the temperature programmed desorption of ammonia (NH_3 -TPD) and qualitative estimation of acidity by IR studies of pyridine adsorbed samples.
- To evaluate the Lewis acidity by perylene adsorption studies.
- To study the cyclohexanol decomposition reaction and cumene cracking reaction and to correlate the results with the surface acid-base properties.
- To study the catalytic activity of the prepared spinels towards industrially important reactions which include various alkylation and oxidation reactions.

References:

- [1] A. Corma; Chem. Rev., 97 (1997) 2373.
- [2] A.Aucejo, M.C.Burjuet, A.Corma and V.Fomes; Appl. Catal., 22 (1986) 187.
- [3] E.Armengol, A.Corma, H.S.Garcia and J.Prima; J. Appl. Catal. A.,149 (1997) 411.
- [4] E.L.Pires, J.C.Magalhaes and U.Schuchardt; Appl. Catal. A: Gen., 203 (2) (2000) 231.
- [5] T.Hatori, J.Inoko and Y.Murakami; J. Catal., 42 (1976) 60.
- [6] G.K.Boreskov, Proc. Intern.Congr.Catalysis, Berlin Verlag-Chemie-Dechma and Frankfurt, Vol.3, 1984, P. 231.
- [7] J.Haber; Materials. Sci.Forum., 25 (1988) 17.
- [8] J.Haber; (Eds, H.f.Barry and P.C.W.Mitchel), Proc.4th Intern.Conf.Chemistry and uses of Molebdenum, golden, CO, Climax Molebdenum Co., AnnArbor, 1982, P.395.
- [9] R.A.Sheldon, in: B. Cornils, W.A.Hermann (Eds), Applied Homogeneous Catalysis with Organomettalic compounds, Vol.1, VCH, Weinheim, 1996, p.411.
- [10] F.Maspero and U.Romano, European patent 0,190,609 (1980).
- [11] T.Tatsumi, M.Yako, M.Nakamuro, Y.Yahura and H.Tominaga; J. Mol. Catal. A.,78 (1993) L 41.
- [12] J.S.Reddy and A.Sayari; J. Chem. Soc. Chem. Commun., 23 (1995).
- [13] H.Arzuomanian, G.Agrifoglio, H.Krentzien and M.Capparelli; New. J. Chem., 20 (1996) 699.
- [14] M.Ai and S.Susuki; J. Catal., 30 (1973) 362.

-
- [15] Yu. Belokopytov, K.M.Kholyavalenko and M.Y.A.Rubanic, *Kin. I Ktaliz*, 14 (1973) 1280.
- [16] Z.Chen, T.Iizuka and K.Tanabe; *Chem. Lett.*, (1994) 1085.
- [17] T.Iizuka, K.Ogasawara and K.Tanabe; *Bull. Chem. Soc. Jpn.*, 56 (1983) 2927.
- [18] G.Xanthopoulou and G.Vekinis; *Appl. Catal.*, 19 (1998) 37.
- [19] T.Takoda; *Proc.3rd Inter.Conf. on Ferrites, Japan* (Eds, H.Watanabe, S.Iida and M.Suginoto), Centre for Academic Publications, Tokyo, Japan, 1980, P.3-8.
- [20] T.Takoda and M.Kiyama; *Proc.3rd Inter.Conf. on Ferrites, Japan* (Eds;Y.Hoshino,S.Iida and M.Sugimoto), University of Tokyo Press, Tokyo, 1970.P.69-71.
- [21] D.G.Wikham; *Inorg. Synt.*, 9 (1967) 152.
- [22] M.Mohammadpour Amini and L.Torkian; *Materials Letters.*, 57 (2002) 639.
- [23] Gui-Qin Yang, Bing Han, Zheng-Tao Sun, Le-Mei Yan, Xiu-Yu Wang; *Dyes and Pigments.*, 55 (2002) 9.
- [24] C.Marcilly; *Rev. Tnst. Fr. Pet.*, 39 (1984) 189.
- [25] K.Sreekumar, T.Mathew, R.Rajagopal, R.Vetrivel and B.S.Rao; *Catal. Lett.*,65 (2000) 99.
- [26] K.Sreekumar, T.Mathew, S.P.Mirajkar, S.Sugunan and B.S.Rao; *Appl. Catal.A.*,201 (2000) L1.
- [27] B.S.Rao, K.Sreekumar and T.M.Jyothi; *Indian Patent 2702/98* (1998).
- [28] M.Yoshimura; *J. Mater. Res.*, 13 (1998) 769.
- [29] K.Byrappa and M.Yoshimura, *Handbook of Hydrothermal*
-

Introduction

-
- Technology: A Technology for Crystal Growth and Materials processing, William Andrew Publishing, LCC Norwich, 2001.
- [30] W.J.Dawson; *Am. Ceram. Soc. Bull.*, 67 (1988)1673.
- [31] M.Hirano and E.Kato; *J. Mater. Sci. Lett.*, 79 (1996) 777.
- [32] M.Hirano and E.Kato; *J. Am. Ceram. Soc.*, 82 (1996) 736.
- [33] Q.Feng, H.Kanoh and Y.Miyai; *Chem. Mater.*, 7 (1995) 1226.
- [34] T.Kanasaku, K.Amezawa and N.Yamamoto; *J. Jpn. Soc. Powder, Powder Metall.*, 45 (1998) 758.
- [35] I.J.Mccolm and N.J.Clerk; “ Forming, Shaping and Working of High Performance Ceramics”, Blackie, Glasgow, (1988) 1.
- [36] X.Fan and E.Matijevic; *J. Am. Cer. Soc.*, 71 (1988), C-60.
- [37] K.G.Brooks and V.R.W.Mmarakoon; *J. Am. Cer. Soc.*, 74 (1991) 851.
- [38] K.Suresh, N.R.S.Kumar and K.C.Patil; *Adv. Mater.*, 3(1991) 148.
- [39] K.Matsumota, K.Yamaguchi and T.Fujii; *J. Appl. Phys.*, 69 (1991) 5912.
- [40] W.A.Kaczmarek, B.W.Ninham and A.Calka; *J. Appl. Phys.*, 70 (1991) 5909.
- [41] H.K.Xu, C.M.Sorenson, K.J.Klabunde and G.C.Hadjipanayia; *J. Mat. Res.*, 7 (1992) 712.
- [42] G.C.Jain, B.K.Das and R.Autar; *Ind. J. Pur. Appl. Phys.*, 14 (1976) 796.
- [43] M.J.Rothner; *J. de Phy.*, 38 (1977) 311.
- [44] F.J.Schnettler and D.W.Johnson; *Proc.Inter.Conf.on Ferrites*, (Eds., Y.Hoshino, S.Iida and M.Sugimoto), University of Tokyo Press, Tokyo, Japan, 1970, P. 121-124.
- [45] Y.Kinemuchi, K.Ishizaka, H.Suematsu, W.Jiang and K.Yatsui; *Thin*
-

- Solid Films., 407 (2002) 109.
- [46] J.Liu, H.He, X.Jin, Z.Hao and Z.Hu; Mater. Res. Bull., 36 (2001) 2357.
- [47] P.Jeevanandam, Yu.Koltypin and A.Gedanken; Mater. Sci. Eng. B., 90 (2002) 125.
- [48] W.H.Bragg; Philosophical Magazine, 30 (1915) 305.
- [49] R.J.Hill, J.R.Craig and G.V.Gibbs; Phys. Chem. Miner., 4 (1979) 317.
- [50] H.Jagodzinski; "Crystallographic Aspects of Non-Stoichiometry of Spinels", (Eds., A.Rabenau), North-Holland, Amsterdam, P.131.
- [51] E.J.W.Verwey and E.C.Heilmann; J. Chem. Phys., 15 (1947) 174.
- [52] T.F.W.Barth and E.Posnjak; Z.Krist., 84 (1952) 325.
- [53] R.K.Datta and K.Roy; Nature, 191 (1961) 169.
- [54] S.Hafner and F.Laves; Z.Krist., 115 (1961) 321.
- [55] E.J.W.Verwey, F.de Boer and J.A.van Santen; J. Chem. Phys., 16 (1948) 1091.
- [56] F.de Boer, J.H.van Santen and E.J.W.Verwey; J. Chem. Phys., 18 (1950) 1032.
- [57] F.C.Romeijn; Phil. Res., 8 (1953) 304.
- [58] J.D.Dunitz and L.E.Orgel; Phy. Chem. Solids., 3 (1957) 318.
- [59] D.S.McClare; Phys. Chem. Solids., 3 (1957) 311.
- [60] G.Blasse; Philips. Res. Repts. Supplement, 3 (1964) 40.
- [61] H.Knozinger and P.Ratnasami; Catal. Rev-Sci. Eng., 17 (1979) 31.
- [62] J.P.Beaufils and Y.Barboux; J. Chem. Phys., 78 (1981) 347.
- [63] J.P.Beaufils and Y.Barboux; J. Appl. Crystallogr., 15 (1982) 301.
- [64] J.P.Jacobs, A.Maltha, J.G.H.Reinjes, J.Drimal, V.Ponec and H.H.Brongersma; J. Catal., 147 (1994) 294.

Introduction

- [65] J.Ziolkowski and Y.Barbaux; *J. Mol. Catal.*, 67 (1991) 199.
- [66] B.C.Lippens and J.J.Steggerda; (Eds., B.G.Linsen), "Physical and Chemical Aspects of Adsorbents and Catalysts", Academic Press, New York, 1970, P. 171.
- [67] H.C.Yao and M.Shelef; *J. Phys. Chem.*, 78 (1974) 2490.
- [68] M.Shelef, M.A.Z.Wheeler and H.C.Yao; *Surf.Sci.*, 47 (1975) 697.
- [69] R.J.D.Tilley, *Defect Crystal chemistry and its Applications*, Blackie, London, 1987.
- [70] G.Centi, F.Trifiro and A.Vaccari; *Chim. Ind. (Milan)*, 71 (1989) 5.
- [71] F.Trifiro and A.Vaccari in R.K.Grasselli and A.W.Sleigh (Eds.), *Structure Activity & Selectivity Relationship in Heterogeneous Catalysis*, Elsevier, Amsterdam, 1991, P.157.
- [72] M.Di Conca, A.Riva, F.Trifiro, A.Vaccari, G.Del Picro, V.Fattore and F.Picolini in *Proc. 8th Int.congress on Ctalysis, Vol.2, DECHEMA, Frankfurt am Main, 1984, P.173.*
- [73] J.M.Correa Bueno, M.Gazzano, M.Goncalves Coelno and A.Vaccari; *Appl. Catal. A: Gen.*, 103 (1993) 69.
- [74] R.S.Rennard and W.C.Khel; *J. Catal.*, 21 (1971) 282.
- [75] S.Manjura Hoque, Md.Amanullah Choudhury and Md.Fakhrul Islam; *J. Magn. Magn. Mater.*, 251 (2002) 292.
- [76] M.H.Kryder; *MRS Bull.*, 21(9) (1996) 17.
- [77] A.Vassiliev and A.Lagrange, *IEEE Trans.Magn.Mag.*, 2 (1966) 707.
- [78] M.P.Sharrook, *IEEE Trans. Magn.*, 25 (1989) 4374.
- [79] J.Popplewell and L.Sakhnini; *J. Magn. Magn. Mater.*, 149 (1995) 72.
- [80] K.Raj, B.Moskowitz and R.Casciari; *J. Magn. Magn. Mater.*, 149

- (1996) 174.
- [81] R.D.McMichael, R.D.Shull, L.J.Swartzendruber and C.H.Bennett, *J. Magn. Magn. Mater.*, 111 (1992) 29.
- [82] D.G.Mitchell; *J. Magn. Reson. Imaging.*, 7 (1997) 1.
- [83] U.Hafezi, W.Schutt, J.Teller and M.Zborowski (Eds.), *Scientific and Clinical Application on Magnetic Carriers*, Plenum, New York, 1997.
- [84] B.Viswanathan: in *Ferrite Materials-Science and Technology*, Edited by B.Viswanathan and V.R.K.Murthy, P.8. Springer-Verlah and Narosha Publishing house, Narosa, N.Delhi, Madras 1990.
- [85] J.Ghose and K.S.R.C.Murthy; *J. Catal.*, 162 (1996) 359.
- [86] N.Guilhaume and M.Primet; *J. Chem. Soc. Farady. Trans.*, 90 (1994) 1541.
- [87] B.L.Yang, D.S.Chen and S.B.Lee; *Appl. Catal.*, 70 (1991) 161.
- [88] J.P.Jacobs, A.Maltha, J.G.H.Reinjes, J.Drimal, V.Pones and H.H.Brongersma; *J. Catal.*, 147 (1994) 294.
- [89] J.Sloczynski, D.Jachewicz, K.Weislo and L.Gengembre; *J. Catal.*, 187 (1999) 410.
- [90] M.Flytzani-Stephanopoulos; *MRS Bull.*, (2001) 885.
- [91] A.B.Lamb, W.C.Brag and J-C.Frazer; *J. Ind. Eng. Chem.*, 12 (1920).
- [92] L.S.Puckhaber, H.Cheung, D.L.Cocke and A.Clearfield; *Solid State Ionics.*, 32/33 (1989) 206.
- [93] H.H.Kung; *Ind. Eng. Chem. Prod. Res. Dec.* 25 (1986) 171.
- [94] B.J.Liaw, D.S.Cheng and B.L.Yang; *J. Catal.*, 118 (1989) 312.
- [95] B.L.Yang, F.Hong and H.H.Kung; *J. Phy. Chem.*, 88 (1984) 2531.
- [96] B.L.Yang, M.C.Kung and H.H.Kung; *J. Catal.*, 89 (1984) 172.
-

Introduction

-
- [97] F.Hong, B.L.Yang, L.H.Schwartz and H.H.Kung; *J. Phy. Chem.*, 88 (1984) 2525.
- [98] H.H.Kung, M.C.Kung and B.L.Yang; *J. Catal.*, 69 (1989) 506.
- [99] B.L.Yang, D.S.Cheng and S.B.Lee; *Appl. Catal.*, 70 (1991) 161.
- [100] J.A.Toledo-Antonio, N.Nava, M.Martinex and X.Bokhimi; *Appl. Catal. A: Gen.*, 234 (2002) 137.
- [101] S.Sato, R.Takahashi, T.Sodesawa, K.Matsumoto and Y.Kamimura; *J. Catal.*, 184 (1999) 180.
- [102] T.Kotanigawa, M.Yamamoto, K.Shimokawa and Y.Yoshida; *Bull. Chem. Jpn.*, 44 (1971) 1961.
- [103] M.Inove and S.Emoto; *Chem. Pharm. Bull.*, 20 (1972) 232.
- [104] Z.P.Aleksandrova; *J. Gen. Chem. (U.S.S.R)*.12 (1942) 522.
- [105] A.G.Bayer, EP 102 493, 1983.
- [106] S.Velu and C.S.Swamy; *Res. Chem. Intermed.*, 26 (2000) 295.
- [107] K.Sreekumar, T.Mathew, R.Rajagopal, R.Vetrivel and B.S.Rao; *Catal. Lett.*, 65 (2000) 99.
- [108] K.Sreekumar, T.Mathew, S.P.Mirajkar, S.Sugunan and B.S.Rao; *Appl. Catal. A.*, 201 (2000) L1.
- [109] K.Sreekumar, T.Mathew, B.M. Devassay, R.Rajagopal, R.Vetrivel and B.S.Rao; *Appl. Catal. A.*, 205 (2001) 11.
- [110] K.Sreekumar, T.M.Jyothi, T.Mathew, M.B.Talawar, S.Sugunan and B.S.Rao; *J. Mol. Catal. A.*, 159 (2000) 327.
- [111] B.S.Rao, K. Sreekumar and T.M.Jyothi; *Indian Patent 2707/98* (1998).
- [112] H.Grabowska, J.Jablonski, W.Mista and J.Wrzyszcz; *Res. Chem. Intermed.*, 22 (1996) 53.
-

Chapter 1

- [113] M.Misono and N.Nojiri; *Appl. Catal.*, 64 (1990) 1.
- [114] B.E.Leach, US Patent 4227024 (1980).
- [115] T.Kotanigawa, M.Yamamoto, K.Shimakowa and Y.Yoshisha;
Bull. Chem. Soc. Jpn., 44 (1871) 1961.
- [116] T.Kotanigawa and K.Shimakowa; *Bull. Chem. Soc. Jpn.*, 47 (1974)
1535.
- [117] T.Kotanigawa; *Bull. Chem. Soc. Jpn.*, 47 (1974) 950.
- [118] E.J.W.Verwey and E.C.Herlman; *J. Chem. Phys.*, 15 (1947) 174.
- [119] H.H.Kung and M.C.Kung; *J. Phy. Chem.*, 84 (1980) 383.
- [120] K.Balasubramanian and V.Krishnaswami; *Indian J. Chem.*, 21A (1982)
813.
- [121] W.S.Chen, M.D.Lee and J.F.Lee; *Appl. Catal.*, 83 (1992) 201.
- [122] C.S.Narasimhan and C.S.Swamy; *Appl. Catal.*, 2 (1982) 315.
- [123] J.Wrzyszcz, M.Zawadzki, Anna M.Trzeciak and Jozef J.Ziolkowski;
J. Mol. Catal. A: Chem., 189 (2002) 203.
- [124] R.Roesky, J.Weiguny, H.Bestgen and U.Dingerdissen; *Appl. Catal. A:
Gen.*, 176 (1999) 213.
- [125] M.B.Welch, US Patent 4692430 (1986).
- [126] G.Aguilar-Rios, M.A.Valenzuela, H.Armendariz, P.Salas,
J.M.Dominguez, D.R.Acosta and I.Schifter; *Appl. Catal. A: Gen.*, 90
(1992) 25.
- [127] H.Miura and T.Itoh; *React. Kinet. Catal. Lett.*, 66 (1999) 189.
- [128] A.Kiennemann, H.Idriaa, J.P.Hindermann, J.C.Lavalley, A.Vallet,
P.Chaumette and ph. Courty; *Appl. Catal. A. Gen.*, 59 (1990) 165.
- [129] J.S.Reddy, R.Kumar and P.Ratnasamy; *Appl. Catal.*, 58 (1999) L1.

Introduction

- [130] L.Petterson and K.Sjostrom; *Combust. Sci. Technol.*, 80 (1991) 265.
- [131] J.Agrell, B.Lindstrem, L.J.Petterson and S.Jaras; *Catal. Today*, 16 (2002) 67.
- [132] E.Manova, T.Tsoncheva, D.Paneva, I.Mitov, K.Tenchev and L.Petrov; *Appl. Catal. A: Gen.*, 277 (2004) 119.
- [133] Cota HM.Katan, J.Chin M and Schoenweis.F; *J. Natur London*, 203 (1964) 1281.
- [134] Schumb WC, Satterfield CN and Wentworth RL, *Hydrogen peroxide* (Reinhold, New York) 1955.
- [135] Ahuja L.D, Rajeshwer.D and Nagpal K.C, in proceedings of 7th National Symposium on Advances in Catalysis-Science and Technology, Baroda, India, Jan.1985, Edited by TSR Prasada Rao (Weily Eastern Ltd, New Delhi) 1985, pp 563-572.
- [136] Prasad SVS and Sitakar Rao, in proceedings of 7th National symposium on Advances in Catalysis-Science and Technology, Baroda, India, Jan. 1985, Edited by TSR Prasada Rao (Weily Eastern Ltd, New Delhi) 1985, p.241-248.
- [137] Goldstein JR and Tseunh ACC; *J. Catal.*, 32 (1974) 452.
- [138] Onuchukwu AI; *J. Chem. Soc. Faraday. Trans I*, 80 (1984) 1447.
- [139] Onuchukwu AI and Zuru AB; *Mater. Chem. Phys.*, 15 (1986) 131.
- [140] Lahiri P and Sengupta SK; *Can. J. Chem.*, 69 (1991) 33.
- [141] P.Forzatti, E.Tronconi and I.Pasquon; *Catal. Rev. Sci. Eng.*, 33 (1991) 109.
- [142] A.Riva, F.Trifiro, A.Vaccari, G.Busca, L.Mintchev, D.Sanfilippo and W.Mazzanti; *J. Chem. Soc. Farady. Trans I*, 83 (1987) 2213.
-

Chapter 1

- [143] A.Beretta, E.Tronconi, P.Forzatti, I.Pasquon, E.Micheli, L.Tagliabue and G.B.Antonelli; *Ind. Eng. Chem. Res.*, 35 (1991) 2144.
- [144] A.Beretta, Q.Sun, R.G.Herman and K.Klier; *J. Chem. Soc. Chem. Commun.*, (1995) 2525.
- [145] W.S.Epling, G.B.Hoflund and D.M.Minahan; *J. Catal.*, 169 (1997) 438.
- [146] W.S.Epling, G.B.Hoflund and D.M.Minahan; *J. Catal.*, 172 (1997) 13.
- [147] W.S.Epling, G.B.Hoflund and D.M.Minahan; *Appl. Catal. A: Gen.*, 183 (1999) 335.
- [148] W.S.Epling, G.B.Hoflund and D.M.Minahan; *Catal. Lett.*, 50 (1998) 199.
- [149] W.S.Epling, G.B.Hoflund and D.M.Minahan; *Catal. Lett.*, 62 (1999) 169.
- [150] T.Mathew, M.Vijayraj, Shivanand Pai, Balakrishna B.Tope, S.G.Hegde, B.S.Rao and C.S.Gopinath; *J. Catal.*, 227 (2004) 175.
- [151] T.Mathew, N.R.Shiju, V.V.Bakade, B.S.Rao and C.S.Gopinath; *Catal. Lett.*, 94 (3-4) (2004) 223.
- [152] T.Mathew, B.S.Rao and C.S.Gopinath ; *J. Catal.*, 222 (2004) 107.
- [153] T.Mathew, S.Shylesh, B.M.Devassy, M.Vijayraj, C.V.V.Satyanarayana, B.S.Rao and C.S.Gopinath; *Appl. Catal. A: Gen.*, 273 (1-2) (2004) 35.
- [154] T.Mathew, S.Shylesh, S.N.Reddy, C.P.Sebastian, S.K.Date, B.S.Rao and S.D.Kulakrni; *Catal. Lett.*, 93 (3-4) (2004) 155.
- [155] K.Sreekumar, T.Jyothi, C.G.Ramankutty, B.S.Rao and S.Sugunan; *React. Kinet. Catal. Lett.*, 70 (1) (2000) 161.
- [156] K.Sreekumar, T.Mathew, S.P.Mirajkar, S.Sugunan and B.S.Rao; *Appl.*
-

- Catal. A: Gen., 201 (2000) L1-L8.
- [157] H.Fiege, Ullmann's Encyclopedia of Industrial Chemistry, Federal Republic of Germany, A.G.Bayer, Leverkusen, A19, p.324.
- [158] K.Sreekumar and S.Sugunan; Appl. Catal. A: Gen., 230 (2002) 245.
- [159] K.Nishamol, K.S.Rahna and S.Sugunan; J. Mol. Catal. A: Chem., 209 (2003) 89.
- [160] K.Sreekumar and S.Sugunan; J. Mol. Catal. A: Chem., 185 (2002) 259.
- [161] K.Nishamol, K.S.Rahna and S.Sugunan; React. Kinet. Catal. Lett., 81 (2) (2004) 229.
- [162] C.G.Ramankutty and S.Sugunan; Appl. Catal. A: Gen., 218 (2001) 39.
- [163] T.Mathew, S.Malwadkar, Shivanand Pai, N.Saharanappa, C.P.Sebastian, C.V.V.Satyanarayana and V.V.Bokade; Catal. Lett., 91 (3-4) (2003) 217.
- [164] Ning Ma, Yinghong Yue, Weiming Hua and Zi Gao; Appl. Catal. A: Gen., 251 (2003) 39.
- [165] Dehanjan Guin, Babitha Barowati and Sunkara V.Manorama; J. Mol. Catal. A: Chem., 242 (2005) 26.
- [166] N.John Jebarathinam, M.Eswaramoorthy and V.Krishnaswamy; Appl. Catal. A: Gen., 145 (1996) 57.
- [167] Liang Yan, Tong Ren, Xiaolai Wang, Qiang Gao, Dong Ji and Jishoan Suo; Catal. Commun., 4 (2003) 505.
- [168] U.Chellam, Z.P.Xu and H.C.Zeng; Chem. Mater., 12 (2000) 650.
- [169] S.Paldey, S.Gedevanishvili, W.Zhang and F.Rasouli; Appl. Catal. B: Environ., 56 (2005) 241.
- [170] G.Fortunato, H.R.Oswald and A.Reller; J. Mater. Chem., 11 (2001)

- 905.
- [171] Y.Bessekhouad and M.Tari; *Inter.J. Hydrogen Energy*, 27 (2002) 357.
- [172] Gautier JL, Brenet JB, Fuentealba F. *C R Acad Paris* 1984; 305 (II): 957.
- [173] Lu G and Li S; *Inter. J. Hydrogen Energy*, 17 (1992) 767.
- [174] Z.H.Yuan, W.You, J.H.Jia and L.D.Zhang; *Chin. Phy. Lett.*, 15 (1998) 535.
- [175] L.G.J.De Harrt and G.Blasse; *J. Electrochem. Soc.*, 132 (1985) 2933.
- [176] K.Esumi and K.Meguro; *J.Colloid and Interface Sci.*, 66 (1) (1978) 192.
- [177] B.D.Flockart, I.R.Leith and R.C.Pink; *Trans. Farady Soc.*, 65 (1969) 54.
- [178] D.Cordischi, V.Indovina and A.Cimino; *J. Chem. Soc. Farady I*, 70 (1974) 2189.
- [179] D.Cordischi, V.Indovina and A.Cimino; *J. Chem. Soc. Farady. Trans.*, 72 (10) (1976) 2341.
- [180] K.Esumi and K.Meguro; *J.Colloid and Interface Sci.*, 66 (1) (1978) 192.
- [181] K.Megoru and K.Esumi; *J.Colloid and Interface Sci.*, 59 (1) (1977) 93.
- [182] K.Esumi and K.Meguro; *Bull. Chem. Soc. Jpn.*, 55 (1982) 315.
- [183] K.Esumi, K.Miyata and K.Meguro; *Chem. Soc. Jpn.*, 58 (1985) 3524.
- [184] K.Esumi, K.Miyata, F.Waki and K.Meguro; *Bull. Chem. Soc. Jpn.*, 59 (1986) 3363.
- [185] R.S.Drago, L.B.Parr and C.S.Chambelain; *J. Am. Chem. Soc.*, 99 (1977) 3203.

Introduction

- [186] S.Sugunan, G.D.Devika Rani and P.A.Unnikrishnan;
J. Mater. Sci. Technol., 10 (1994) 425.
- [187] S.Sugunan and J.M.Jalaja; Collect. Czech. Chem. Commun., 59 (1994)
2605.
- [188] S.Sugunan and J.J.Malayan; J. Adhesion Sci. Technol., 9 1 (1995) 73.
- [189] S.Sugunan and K.B.Sherly; Ind. J. Chem., 32 A (1993) 689.
- [190] S.Sugunan and G.D.Devika Rani; Ind. J. Chem., 32 A (1993) 993.
- [191] S.Sugunan and G.D.Devika Rani; J. Mater. Sci., 29 (1993) 4811.
- [192] K.Tanabe; "Solid Acids and Bases-Their Catalytic Properties",
Kodansha, Tokyo, Academic Press, New York, 1970.
- [193] K.Tanabe, M.Misono, Y.Ono and H.Hattori; "Solid acids and bases",
Kodansha-Elsevier, Yokyo, 1989.
- [194] W.E.Farneth and R.J.Gorte; Chem. Rev., 95 (1995) 615.
- [195] H.G.Karge and V.Dondur; J. Phys. Chem., 94 (1990) 765.
- [196] F.Arena, R.Dario and A.Parmaliana; Appl. Catal., 170 (1998) 127.
- [197] N.Y.Topsoc, K.Pederson and E.G.Derouane; J. Catal., 70 (1981) 41.
- [198] S.B.Sharma, B.I.Meyers, D.T.Chen and J.A.Dunesie; Appl. Catal., 102
(1993) 253.
- [199] J.Kijenski and A.Baiker; Catal. Today, 5 (1989) 1.
- [200] A.Auroux and A.Antonella, J. Phys. Chem., 94 (1990) 6371.
- [201] K.Hashimoto, T.Masuda and Y.Mori; Proc.7th Inter.Zeolite Conf.,
(Eds., Y.Murakami et al.) Kodansha, Tokyo and Elsevier, Amsterdam,
1986, p.503.
- [202] H.Sato, N.Ishii, K.Hirose and S.Nakamura, Proc. 7th Inter.Zeolite
Conf., (Eds., Y.Murakami et al.) Kodansha, Tokyo and Elsevier,

- Amsterdam, 1986, p.755.
- [203] T.Tsutsumi, S.Haigiwara and H.Takahashi; Bull.Chem.Soc.Jpn., 48 (1975) 3576
- [204] M.Ai; J. Catal., 50 (1977) 291.
- [205] M.Ai and S.Susuki; J. Catal., 30 (1973) 362.
- [206] C.S.Narasimhan and C.S.Swamy, Appl. Catal., 2 (1982) 315.
- [207] G.R.Dube and V.S.Darshane; J. Chem. Soc. Faraday. Trans., 88 (9) (1992) 1299.
- [208] M.V.Joshi, S.G.Oak and V.S.Darshane, in: N.M.Gupta, D.K.Chakrabarthy (Eds.), Catalysis: Modern Trends, Narosha, New Delhi, 1995, p.275.
- [209] N.J.Jebarathinam and V.Krishnaswamy; "Catalysis: Modern Trends", (Eds., N.M.Guptha and D.K.Chakrabarthy) 1995, Narosha Publishing House, New Delhi, India.
- [210] N.J.Jebarathinam and V.Krishnaswamy; "Catalysis" Present and Future", (Eds., P.Kantha Rao and B.S.Benwal), Publication and Information Directorate, New Delhi, P.288.
- [211] C.Bezouhanava and M.A.Al-Zihari; Catal. Lett., 11 (1991) 245.
- [212] M.V.Joshi, S.G.Oak and V.S.Darshane; "Catalysis: Modern Trends" (Eds., N.M.Guptha and D.K.Chakrabarthy) 1995, Narosha Publishing House, New Delhi, India.
- [213] H.Pines and C.N.Pillai; J. Am. Chem. Soc., 82 (1960) 2401.
- [214] A.Corma and B.W.Wojciechowski; Catal. Rev. Sci. Eng., 24 (1982) 1.
- [215] J.W.Ward; J.Catal., 9 (1967) 225.
- [216] P.M.Boorman, R.A.Kydd, Z.Sarbak and A.Somogyvari; J. Catal., 96
-

(1985) 115.

[217] P.M.Boorman, R.A.Kydd, and A.Somogyvari; *J. Catal.*, 100 (1986) 287.

[218] J.R.Sohn and H.J.Jang; *J. Mol. Catal.*, 64 (1991) 349.

This chapter gives a detailed description of the catalyst preparation and pretreatment conditions, materials used, the techniques used to characterize the catalysts, the experimental set up and measures used for the catalytic activity study.

2.1 Catalyst preparation

The catalytic activity strongly depends on the methods of preparation and pretreatment conditions apart from the reaction parameters. Small variations in the preparation conditions radically alter the performance of the catalyst. So intense care must be taken during the selection of materials and preparation of the systems.

2.1.1 Materials

Analar grade $\text{Gd}(\text{NO}_3)_2 \cdot 6\text{H}_2\text{O}$, $\text{Fe}(\text{NO}_3)_3 \cdot 9\text{H}_2\text{O}$, $\text{Cr}(\text{NO}_3)_3 \cdot 9\text{H}_2\text{O}$, $\text{Co}(\text{NO}_3)_2 \cdot 6\text{H}_2\text{O}$, $\text{Ni}(\text{NO}_3)_2 \cdot 6\text{H}_2\text{O}$, $\text{Cu}(\text{NO}_3)_2 \cdot 3\text{H}_2\text{O}$, and NaOH from Merck were used as such without further purification.

2.1.2 Preparation of different composition of spinels

Chromium and gadolinium incorporated nickel ferrites of formula $\text{NiCr}_x\text{Fe}_{2-x}\text{O}_4$ and $\text{NiGd}_x\text{Fe}_{2-x}\text{O}_4$ ($x = 0-2$), nickel cobaltites, $\text{Ni}_x\text{Co}_{3-x}\text{O}_4$ ($x = 0.5-1.5$) and copper cobaltites, $\text{Cu}_x\text{Co}_{3-x}\text{O}_4$ ($x = 0.5, 1.0$) were prepared for the present work. Their compositions with labels are given in table (Table 2.1.1).

Experimental

Table 2.1.1 Catalyst composition and labelling of different series of ferrites and cobaltites.

x	Catalyst composition	Catalyst labelling
NiCr _x Fe _{2-x} O ₄ series		
0.0	NiFe ₂ O ₄	NF
0.4	NiCr _{.4} Fe _{1.6} O ₄	NCrF 1
0.8	NiCr _{.8} Fe _{1.2} O ₄	NCrF 2
1.2	NiCr _{1.2} Fe _{.8} O ₄	NCrF 3
1.6	NiCr _{1.6} Fe _{.4} O ₄	NCrF 4
2.0	NiCr ₂ O ₄	NCr
NiGd _x Fe _{2-x} O ₄ series		
0.4	NiGd _{.4} Fe _{1.6} O ₄	NGF 1
0.8	NiGd _{.8} Fe _{1.2} O ₄	NGF2
1.2	NiGd _{1.2} Fe _{.8} O ₄	NGF 3
1.6	NiGd _{1.6} Fe _{.4} O ₄	NGF 4
2.0	NiGd ₂ O ₄	NG
Cobaltite series		
0.5	Ni ₅ Co _{2.5} O ₄	NC .5
1.0	NiCo ₂ O ₄	NC 1
1.5	Ni _{1.5} Co _{1.5} O ₄	NC 1.5
0.5	Cu ₅ Co _{2.5} O ₄	CC .5
1.0	CuCo ₂ O ₄	CC 1

Chapter 2

For the synthesis of all compositions of chromium and gadolinium containing nickel ferrites, low temperature co-precipitation method reported by Date et al.¹ was adopted. The co-precipitation method is preferred over the usual ceramic method as the spinels prepared by former route provide chemically homogeneous and fine particles. And between the usual co-precipitation routes, viz. oxalate and hydroxide, the latter is preferred for achieving higher surface areas. The present study, accordingly employed hydroxide route co-precipitation method for the synthesis of the systems. Metals were precipitated as their hydroxides from their nitrate solutions using sodium hydroxide as the precipitant alkali.

Solutions of the metal nitrates in the required stoichiometric ratios were prepared and mixed and rapidly added to the 5.3M NaOH solutions with vigorous stirring. Due to the exothermic nature of the precipitation reaction, the temperature of the slurry rose to 45 °C. The pH of the final slurry was carefully adjusted to 9 for chromium containing systems and to 14 for gadolinium containing systems. The precipitate was kept overnight for ageing and then washed several times with double distilled water until free from nitrate ions and alkali. It was filtered, dried in an air oven at 120 °C for 24 h and were calcined at 650 °C for 8 h to achieve complete spinel phase formation.

Different compositions of the cobaltite spinels were prepared by the high temperature co-precipitation route as reported by Ferreira et al.². The nitrates were weighed in the adequate molar ratios, dissolved in distilled water and poured into a hot hydroxide solution at 77 °C-97 °C, keeping a constant vigorous stirring. The solution pH was confirmed to be higher than 12. Black precipitates were formed and the solution was heated at 77 °C for 1 h. After

Experimental

repeated filtering and washing with boiling distilled water the precipitate was dried on a sand bath at 197 °C for 12 h. The materials were powdered and calcined at 650 °C for 8 h. The dried materials were powdered and sieved below 75 µm mesh.

2.2 Catalyst characterization

All the prepared catalysts were characterized by different physico-chemical techniques viz. X-ray diffraction (XRD), energy dispersive x-ray (EDX) analysis, scanning electron microscopy (SEM), surface area measurements (BET), thermogravimetric analysis (TG/DTA), DRIFT spectroscopy, Mössbauer spectroscopy and acidity-basicity determination by various methods such as electron acceptor adsorption studies, temperature programmed desorption of ammonia, perylene adsorption studies and IR studies of pyridine adsorbed samples. Test reactions conducted to obtain a qualitative idea regarding acid-base properties were cyclohexanol decomposition and cumene cracking reactions. A brief discussion of the various methods adopted is presented below.

2.2.1 X-Ray Diffraction analysis

XRD is the one of the widely used and versatile techniques for the qualitative and quantitative analysis of the solid phases³. Diffraction from microcrystalline and amorphous powder can be studied by this technique. Compared to the three dimensional location of each reflection in a single crystal diffraction experiment, the powder diffraction pattern can give only one dimensional data due to the rotational projection of the randomly oriented

Chapter 2

reciprocal lattices. Powder XRD is a long-range order technique sensitive to the basic periodic structure of a solid sample. The purity of the substance, transition to different phases, allotropic transformation, lattice constants and presence of foreign atoms in the crystal lattice can also be recognized by this technique. The XRD method involves the interaction between the monochromatic X-rays (like Cu K_{α} or Mo K_{α}) with family of planes (identified by a system of Miller Indices, hkl) in the polycrystalline material. A fixed wavelength is chosen for the incident radiation and the Bragg's peaks are identified as a function of scattering angle 2θ . The interplanar distances (d spacing) are calculated from the Bragg's equation,

$$n\lambda = 2d \sin \theta,$$

Where λ is the X-ray wavelength and n is an integer called order of reflection.

The mean crystallite size of a material can also be determined from the broadening of an X-ray diffraction peak, which is inversely proportional to crystallite size and this can be achieved by following the Scherrer method using the formula,

$$t = 0.9\lambda / \beta \cos \theta$$

which derived from Bragg's equation. 't' is the thickness of the crystal and β = FWHM (half the width of the peak with maximum intensity).

One can calculate the crystallinity with respect to a standard material by determining the integrated area under the peaks between a set 2θ limits in the sample (A_S) and compared with the area obtained for a standard or reference material (A_R) in the same 2θ limits [% crystallinity = $(A_S \times 100) / A_R$]. Research workers have set their own ways of measuring crystallinity for relative comparison, for example, doing integration of the

Experimental

peaks by gravitation methods or integrating the area of several strong peaks in the region $2\theta_1$ - $2\theta_2$ and dividing it by the total area in the same $2\theta_1$ - $2\theta_2$ region or routinely taking the intensity of the strongest peak as a faster route to know the crystallinity of the sample. Quantifying the number of phases and their concentration is invariably done using the comprehensive libraries (ASTM and JCPDS or PDF indices) of available characteristic d spacing and intensities of previously studied solids.

One cannot detect an impurity phase of less than 2-3 % when a XRD profile is scanned for routine analysis. If there is an impurity phase detected on fast scanning, one has to do a slow step scanning for sufficiently long time to maximize the detection of minority or impurity phases by accumulation of intensity counts and refine the profile if necessary for phase quantification. The quantitative analysis can also be done by Rietveld refinement method, which requires the knowledge of the crystal structure of all the phases present in the mixture.

The XRD patterns of the catalyst samples were taken using Philips diffractometer (PW 1710). Ni filtered Cu K_{α} radiation ($\lambda = 1.5404 \text{ \AA}$) and a movable detector, which measures the intensity of diffracted radiation as a function of 2θ are the main parts of the instrument.

2.2.2 Energy dispersive X-ray analysis

The chemical compositions of catalysts were determined using energy dispersive X-ray analyzer (EDX). This technique is used in conjunction with SEM. An electron beam strikes the surface of a conducting sample. The energy of the beam is typically in the range 10-20 K eV. This causes X-rays to

be emitted from the point of the material. The energy of the X-rays emitted depends on the material under examination. The X-rays are generated in a region about 2 microns in depth. By moving the electron beam across the material an image of each element in the sample can be acquired. The detector used in EDX is the Lithium drifted Silicon detector. This detector must be operated at liquid nitrogen temperature. When an X-ray strikes the detector, it will generate a photoelectron within the body of the Si, as this photoelectron travels through the Si, it generates electron-hole pairs. The electrons and holes are attracted to the opposite ends of the detector with the aid of a strong electric field. The size of the current pulse generated depends on the number of electron-hole pairs created, which in turn depends on the energy of the incoming X-ray. Thus, an X-ray spectrum can be acquired giving information on the elemental composition of the material under examination. The Si - Li detector is often protected by a Beryllium window. The absorption of the soft X-ray by Be precludes the detection of elements below an atomic number of 11 (Na). In windowless systems, element with atomic number as 4 (Be) have been detected, but the problems involved get progressively worse as the atomic number is reduced⁴. The chemical compositions of catalysts were obtained from Stereoscan 440 Cambridge, UK energy dispersive X-ray analyzer used in conjunction with SEM.

2.2.3 Scanning electron microscope (SEM) analysis

Scanning electron microscopy (SEM) is based on the strong interaction of electrons with matter and appreciable scattering by quite small atomic clusters. Electrons can be conveniently deflected and focused by

electric or magnetic fields so that magnified real-space images can be formed in addition to simple diffraction patterns. This property of electron beam is used in SEM analysis. In SEM, the electron optics act before the specimen is reached to convert the beam into a fine probe, which can be as small as 100 Å in diameter at the specimen surface⁵. The technique is of high interest in catalysis because of its high special resolution. However, a serious drawback is that the results need not be really representative of the whole sample. This can be overcome by making many analyses at different locations of the sample particles and for many catalyst particles.

SEM analysis of the sample was done using Stereoscan 440 Cambridge, U.K scanning electron microscope.

2.2.4 Diffuse Reflectance Infrared Fourier Transform (DRIFT) spectroscopy

Infrared spectroscopy (IR) is widely used in the field of characterization of heterogeneous catalysts. Identification of the structural features of the catalysts itself; adsorbed and dispersed species and their structure, metal-metal interaction, reaction intermediates on the catalyst surface etc. are some of the important information obtained from infrared spectral studies. The introduction of Diffuse Reflectance Infrared Fourier Transform (DRIFT) spectroscopy^{6,7} has improved the application of infrared spectroscopy by giving valuable informations which are inherent in a mid-IR (4000-200 cm⁻¹) spectrum. The diffuse reflectance spectrum of a dilute sample of 'infinite depth' (i.e., up to 3 mm) is usually calculated with reference to the diffuse reflectance of the pure diluents to yield the reflectance, $R_{i\bar{\lambda}}$. $R_{i\bar{\lambda}}$ is

related to the concentration of the sample, c , by the Kubelka-Munk (K-M) equation⁸:

$$f(R_{i\bar{\lambda}}) = (1 - R_{i\bar{\lambda}})^2 / 2R_{i\bar{\lambda}} = 2.303ac/s$$

Where 'a' is the absorptivity and 's' is the scattering coefficient. The scattering coefficient depends on both particle size and degree of sample packing; thus the K-M function can be used for accurate quantitative analysis, provided the particle size and packing method are strictly controlled. For good diffuse reflectors plots of the K-M function, $f(R_{i\bar{\lambda}})$, are analogous to absorbance plots for transmission spectra. Care must be taken in applying the K-M equation when $R_{i\bar{\lambda}}$ is much less than about 30 % since deviations from linearity can occur when the sample concentration is high. Diluting ensures deeper penetration of the incident beam, thus increasing the contribution to the spectrum of the transmission and internal reflection component.

The technique of diffuse reflection spectroscopy has been used successfully in many fields as an adjunct to better-known spectroscopic methods, and is often useful where traditional techniques fail. In spinels the metal cations are distributed in two different crystallographic environments and the spinel phase formation can be well assigned by the appearance of two IR bands^{9,10}. Usually these two IR bands are hidden in ordinary FTIR spectroscopy. The infrared spectra of the prepared samples were recorded by a DR-IR (Shimadzu, model 8300) in the range 400-1400 cm^{-1} .

2.2.5 Thermogravimetric (TG) analysis

Thermogravimetric analysis is used in catalyst characterization procedure as an important tool to provide valuable information regarding

Experimental

drying ranges, hydration, decomposition temperature, stability limits, etc. In thermogravimetry, the weight of a sample is recorded over a period of time while its temperature is being raised linearly. A thermogram is obtained by plotting weight of a sample (on ordinate) against temperature (on abscissa). The horizontal region of the thermogram indicates the thermal stability of the sample, while weight loss is indicated by the curved portions. DTG is the first derivative plot of the TG curve from which a better understanding of the weight loss can be obtained from the dip in the curve.

Thermogravimetric analysis of the samples were carried out using Perkin Elmer Pyris Diamond thermogravimetric/differential thermal analyzer by heating the samples at a rate of 20 °C /min from room temperature to 1100 °C in nitrogen atmosphere.

2.2.6 Surface area determination (BET method)

The Brunauer, Emmett and Teller (BET) method¹¹ has been adopted as a standard procedure for surface area determination. BET method is ideally suited for the determination of surface areas of finely divided solids. By the introduction of a number of simplifying assumptions, the BET theory extends Langmuir model to multilayer adsorption. In the BET theory it is assumed that the solid surface possesses uniform, localized sites and the adsorption at one site does not affect adsorption at neighbouring sites. It is further assumed that the adsorption is multiplayer and the heat of adsorption of the second and the subsequent layers are identical and is equal to the liquefaction of the adsorbate. The BET equation can be represented as,

$$\frac{P}{v(p_0-p)} = \frac{1}{Cv_m} + \frac{(C-1)P}{Cv_m p_0}$$

Here, C = a constant for a given system at a given temperature and is related to the heat of adsorption, v = volume adsorbed at equilibrium pressure p , v_m = volume of the adsorbate necessary to form a monolayer on the surface and p_0 = saturation vapour pressure of the adsorbate.

The BET equation demands a linear relation between $p/[v(p_0-p)]$ and p/p_0 , where slope = $C-1/Cv_m$ and y intercept = $1/Cv_m$. From the slope and y -intercept, v_m can be calculated. The specific surface area of the sample is then calculated using the relation,

$$\text{Surface area (m}^2\text{g}^{-1}\text{)} = \frac{v_m N_0 a_m}{22414 \times \text{weight of the catalyst}}$$

Where a_m = average area occupied by the nitrogen molecule (1.62 \AA^2) and N_0 = Avagadro number.

Although in principle any gas or vapour may be chosen as the adsorbate, the usual choice is nitrogen as it is inexpensive, easily obtained, inert towards most of the solids and is able to penetrate even the finest pores. Occasionally, however, as in the case of iron catalysts, nitrogen may chemisorb on the solid even at low temperatures and may therefore, be preferable to use a more inert gas like argon. For determination of low surface areas, low-pressure techniques have to be employed and for these, krypton is the usual adsorbate.

Experimental

Micrometrics Gemini analyzer was used to determine the surface area with nitrogen as adsorbate. The preactivated samples were degassed at 200 °C under nitrogen flow for 2 h and then brought to 77 K using liquid nitrogen.

2.2.7 Mössbauer spectroscopy

Mössbauer spectroscopy is a versatile technique to yield better understanding of the oxidation state, phase transition, magnetic properties and electronic environment of the Mössbauer active elements in the catalysts and of the particle size of the samples. Mössbauer spectroscopy is based on Mössbauer effect, which is the recoil-free emission of γ - radiation from a solid radioactive material¹². This radiation can be absorbed by stationary atoms, and is best observed in isotopes, which have long-lived low-lying excited nuclear energy states.

A transmission Mössbauer spectrometer is very simple, and typically consists of a γ -ray source, the absorber (sample) and a detector. The γ -ray source is excited ^{57}Fe nuclei, produced by the decay of ^{57}Co isotope. Approximately 90 % of the ^{57}Fe nuclear excited state decays through the intermediate level to produce 14.4 K eV gamma radiation. These gamma photons can then be absorbed by ^{57}Fe in a sample. The source is moved relative to the absorber, shifting the energy spectrum due to the Doppler effect. The spectrum is plotted as percent transmission versus source velocity (energy).

The interpretation of the Mössbauer spectrum is mainly done through the analysis of Mössbauer parameters such as isomer shift (δ), center shift (CS), quadrupole splitting (ΔE_Q), Hyperfine magnetic field (H) and line width

(I). All these parameters are expressed in velocity units, mm/s except for hyperfine magnetic field, which is expressed in Tesla.

The isomer shift (δ) is the energy difference between source and absorber nuclei resulting from the effects including differences in valence state, spin state and coordination of the absorber atoms¹³. Experimentally one observes a single line shifted from a reference zero point by an isomer shift plus the second order Doppler shift (SOD), a small thermal shift due to atomic vibration. The contribution from SOD is similar in most standard materials, so for the purpose of comparison the isomer shift is always taken to be equal to the center shift.

The quadrupole splitting (ΔE_Q) is the splitting of energy levels caused by the interaction between the nuclear quadrupolar moment and an electric field gradient (EFG) at the nucleus. It depends on the valence and spin state of the absorber atoms as well as the coordination and degree of distortion of the crystallographic site. Experimentally one observes a doublet with components of equal intensity and line width in the ideal random absorber case. The quadrupole splitting is given by the energy separation between the components.

The interaction of the nuclear dipole moment of the nucleus and a hyperfine magnetic field causes a splitting of the nuclear energy levels, resulting in six peaks for ⁵⁷Fe spectra in the simplest case. For an ideal random absorber with no quadrupole interaction the line width of the peaks is equal with intensity ratio, 3:2:1:1:2:3. The separation of peak 1 and 6 is proportional to the magnitude of the hyperfine magnetic field.

Experimental

The line width is expressed in full width at half maximum of the peak height (FWHM). The peaks are broadened beyond the natural line width by effects due to equipment (vibrational, thermal and electronic problems), the source (self-absorption resulting from decay) and the sample (thickness broadening, next nearest neighbour effects and dynamic processes such as relaxation).

A continuous flow cryostat was applied to record ^{57}Fe Mössbauer spectra at room temperature. The chemical isomer shifts are related to α -iron. The source of radiation used is commercial $^{57}\text{Co/Rh}$ -foil.

2.2.8 Acid-base property studies

Acid-base properties of the solid catalysts play decisive role in determining the catalytic activity and selectivity. Independent methods adopted for the thorough understanding of the acid-base properties of prepared spinels are temperature programmed desorption of ammonia, IR studies of pyridine adsorbed samples, perylene adsorption studies, electron donating property studies and test reactions such as decomposition of cyclohexanol and cracking of cumene.

(a) Temperature programmed desorption (TPD) of ammonia

The NH_3 -TPD method is widely employed in characterizing the acidity of solid catalysts. This is an easy method used to find out the total acidity as well as acid strength distribution.

The pellets were prepared from the sample (about 0.5 g) using a pelletiser and activated at $500\text{ }^\circ\text{C}$ for 2 h. The accurately weighed pellets were

placed in a home built stainless steel reactor of internal diameter 1 cm and length 15 cm kept in a cylindrical furnace. The temperature of the reactor is maintained using a temperature controller and the temperature was measured by an Al-Cr thermocouple kept inside the furnace. The sample was degassed at 300 °C using a flow of nitrogen for half an hour. It was then allowed to cool to room temperature and a definite amount of ammonia is injected into the reactor and allowed to adsorb uniformly over the catalyst surface. The physisorbed ammonia was flushed out using a flow of nitrogen gas. Under a controlled temperature programme, the amount of chemisorbed ammonia leached out -up to a temperature of 600 °C- was trapped into H₂SO₄ solution (0.025 N) and ammonia desorbed was determined by back titration with NaOH solution (0.025 N).

$$\text{Amount of ammonia desorbed} = \frac{\Delta V \times N_{\text{NaOH}} \times 5}{\text{Weight of the sample}}$$

Where ΔV is the difference in titre values of NaOH between blank H₂SO₄ and the ammonia trapped H₂SO₄ at each temperature.

(b) Electron donating property study

Adsorption of electron acceptors has been investigated to study and characterize the electron donating property of the systems. The following electron acceptors were used.

7,7,8,8-tetracyanoquinodimethane (TCNQ) [Merck – Schuchardt] was purified by repeated crystallization from acetonitrile¹⁴, 2,3,5,6-tetra-chloro-4-benzoquinone (chloranil) [Sisco Research Laboratories PVT. Ltd.] was

Experimental

crystallized from benzene before use¹⁵. Chloroform was used as the solvent for the crystallization of *p*-dinitrobenzene (PDNB)¹⁶. SQ grade acetonitrile [Qualigens Fine Chemicals] was purified by passing through silica gel for drying followed by distillation with P₂O₅ and the fraction between 79-82 °C was collected.

The following procedure was adopted for adsorption studies. The catalyst samples were activated at 500 °C for 2 h prior to each experiment. The adsorption study was carried out over 0.5 g catalyst placed in a 25 ml cylindrical glass tube fitted with a mercury sealed stirrer. 10 ml of solution of an electron acceptor in acetonitrile was then admitted to the catalyst. Stirring was continued for 4 h in a mechanically driven stirrer at room temperature and atmospheric pressure. The amount of electron acceptor adsorbed was determined from the difference in concentration of the electron acceptor in solution before and after adsorption, which was measured by means of a Shimadzu UV-VIS spectrophotometer. The λ_{\max} of electron acceptors in acetonitrile is 393.5 nm for TCNQ, 288 nm for chloranil and 262 nm for PDNB. The amount of electron acceptors adsorbed increases with increase in the concentration of the solution containing electron acceptors. This increasing trend continues up to a particular concentration and thereafter the amount adsorbed decreased with increase in concentration. This value is called the limiting amount.

(c) Perylene adsorption studies

Adsorption studies using perylene as electron donor gives information regarding the Lewis acidity in the presence of Brønsted acidity¹⁷. The

principle is based on the ability of the catalyst surface acid sites (electron deficient centres) to accept electron from an electron donor, like perylene to form a charge transfer complex. The amount of the adsorbed species can be measured by spectroscopic means¹⁸. Perylene has an electron affinity of 1.17 eV¹⁹, which accounts for the ease with which it can form cation radical in liquid solutions. The adsorption of the molecule on the metal oxide leads to the reduction of the molecule and implies the presence of sufficiently stronger electron acceptor sites (Lewis acid sites) on the catalyst surface²⁰.

In this method, the adsorption experiment was carried out in a 50 ml U- shaped tube taking 10 ml each of freshly prepared perylene in benzene solution and stirring it with a weighed amount of the catalyst for 4 h. After 4 h, the contents were filtered and the absorbance of the filtrate was measured at a particular wavelength. For all the cases, the sorption experiments were performed in the adsorbate concentration range where Beer-Lambert's law is valid. Since perylene is getting adsorbed on the catalyst surface, its concentration will be less in the solution after adsorption. The amount of perylene adsorbed was determined by measuring the absorbance of the solution before and after adsorption. The amount of perylene adsorbed increases with concentration of perylene solution. This increasing trend continues up to a particular perylene concentration and thereafter the amount of perylene adsorbed decreases with increase in concentration. This constant value is called the limiting amount, which corresponds to the surface one electron accepting capacity or Lewis acidity.

The chemical interaction between the adsorbate and the sample may be determined by the Langmuir adsorption isotherm,

Experimental

$$C/X = 1/BX_m + C/X_m.$$

Where, C is the concentration of perylene solution, B, a constant and X_m is the limiting amount of perylene adsorbed, which corresponds to the theoretical amount of the adsorbate required to cover all the active sites for the base adsorption.

All the absorbance measurements were done in a UV-VIS spectrometer (Shimadzu UV- 160 A) at a λ_{max} 439 nm using 10 nm quartz cell.

(d) IR studies of pyridine adsorbed samples

Qualitative estimation of acidity can be obtained by analyzing IR spectrum of pyridine adsorbed samples. There are three modes by which pyridine can be retained on the surface of oxides. (1) Interaction of the N lone pair electron and H atom of the OH group, (2) transfer of a proton from a surface OH group to the pyridine forming a pyridinium ion (Brönsted acidity) and (3) pyridine coordination to an electron deficient metal atom (Lewis acidity). Important pyridine ring modes occur at approximately 1606, 1573, 1485 and 1446 cm^{-1} termed ν_{8a} , ν_{8b} , ν_{19a} and ν_{19b} respectively^{21,22}. IR bands, ν_{8a} and ν_{19b} , are due to Lewis acid sites. Band due to pyridinium ion will be at $\sim 1540 \text{ cm}^{-1}$ ^{23,24}. The preactivated samples were kept in a desiccator saturated with pyridine vapour for 24 h. Then IR spectra were taken in the DRIFT mode by a DR-IR (Shimadzu, model 8300) in the range 1400-1800 cm^{-1} .

(e) Vapour-phase cumene cracking and cyclohexanol decomposition reactions

Vapour-phase cumene cracking and cyclohexanol decomposition reactions are test reactions suggested for identifying the acid-base properties of a catalyst. Cumene cracking reaction differentiates Lewis and Brønsted acidity of a catalyst where as cyclohexanol decomposition reaction gives idea about total acidity and basicity of a catalyst.

The reactions were performed in a fixed bed, vertical, down-flow quartz reactor (2 cm ID and 30 cm length) inside a double zone furnace. 0.5 g of the catalyst activated at the required temperature was placed inside the reactor immobilized using glass wool. Reactants were fed into the reactor using a syringe pump. The reactions were performed at optimized conditions. Product analysis was done by gas chromatography. The Chemitto 1000 GC was equipped with a FID detector and a capillary column. N₂ was used as the carrier gas. The identification of products was carried out by comparison of their retention times to the standards.

2.3 Catalytic activity studies

The reaction studied for the present work can be put under two categories as liquid-phase reactions and vapour-phase reactions. Under the liquid phase reactions, oxidation reactions of styrene, cyclohexane and benzyl alcohol and under vapour phase reactions, alkylation reactions of aniline and phenols were carried out.

(a) Liquid-phase reactions

For the liquid-phase reactions, the reagents in the required molar ratio were taken in a 50 ml double-necked round bottom flask fitted with water

Experimental

condenser and guard tube. The reactions were carried out in an oil bath using 0.1 g of the catalyst (activated at 500 °C for 2 h) and the temperature of the reaction was controlled using a dimmerstat. Using a magnetic stirrer, the uniform stirring of the reaction mixture was attained. The reaction mixture was analyzed by gas chromatography (Chemitto 1000 GC, FID detector, N₂ carrier gas, capillary column) and product identification was done by comparing the retention times with standards.

(b) Vapour-phase reactions

The vapour-phase reactions were performed in a fixed bed, vertical, down-flow quartz reactor of 2 cm ID and 30 cm length placed inside a double-zone furnace and at atmospheric pressure. 0.5 g of the catalyst activated at 500 °C for 2 h is positioned at the center of the reactor in such a way that the catalyst is sandwiched between the layers of inert silica beads. The upper portion of the reactor served as a vaporizer cum pre-heater. The temperature measurements were done using a temperature controller and a Cr-Al thermocouple. A home built syringe pump fed the liquid reactant mixture. The products of the reaction were collected downstream from the reactor in a receiver connected through a cold water-circulating condenser. The products were collected at various time intervals and were analyzed by GC (Chemitto 1000 GC, FID detector, N₂ carrier gas, appropriate columns) and the products were identified by comparing the retention times with standards.

References:

- [1] P.S.Anilkumar, J.JShortri, S.D.Kulkarni, C.E.Deshpande and S.K.Date; *Matt. Lett.*, (1996) 293.
- [2] T.A.S.Ferreira, J.C.Waerenborgh, M.H.R.M.Mendonca, M.R.Nones and F.M.Costa; *Sol. State Sciences*, 5 (2003) 383.
- [3] C.Whiston; "X-ray methods", (Eds., F.E.Prichard), ACOL. Tmames Polytech., London, 1991
- [4] J.Matta, D.Courcot, E.Abi-Aad and A.Aboukais; *Chem. Mater.*, 14 (2002) 411.
- [5] A.Howie; "Characterisation of Catalysts", (Eds., J.M.Thoams and R.M.Lambert), John Wiley, New York, 1980, p.114.
- [6] M.P.Fuller and P.G.Griffiths; *Anal. Chem.*, 58 (1978) 1906.
- [7] J.P.Blitz; "Modern Techniques in Applied Molecular Spectroscopy", (Eds., F.M.Mirabella), John Wiley, New York, 1998, p.213.
- [8] P.Kubelka and F.Munk; *Z. Tech. Phys.*, 12 (1931) 593.
- [9] R.D.Waldron; *Phy. Rev.*, 99 (1955) 1727.
- [10] W.B.White and B.A.DeAngelis; *Spectrochemica Acta*, 23A (1967) 985.
- [11] S.Braunauer, P.H.Emmett and E.Teller; *J. Am. Chem. Soc.*, 60 (1938) 309.
- [12] C.N.Banwell and E.M.McCash; "Fundamentals of Molecular Spectroscopy", 4th Edn., Tata McGraw-Hill Publishing Company Ltd., New Delhi, 1995.
- [13] R.C.Burns and T.C.Solberg; "Spectroscopic Characterization of Minerals and their Surfaces", (Eds., L.M.Coyne, S.W.S. McKeever

Experimental

- and D.F.Blake), ACS symposium series, American Chemical Society, Washington DC, 1990, p. 262-283.
- [14] D.S.Acker and W.R.Hertler; J. Am. Chem. Soc., 84 (1962) 3370.
- [15] L.F.Fiesser and M.Fiesser; "Reagents for Organic Synthesis", John Wiley, New York, 1967, p.125.
- [16] B.S.Furness, A.J.Hannaford, V.Roger, P.W.G.Smith and A.R.Tatchel; "Vogel's Text Book of Practical Organic Chemistry", 4th Edn., ELBS, London, 1978, P.708.
- [17] H.Dzisko; Proc. Inter.Cong.Catal., Amsterdam (1964) 19.
- [18] K.Shibata, T.Kiyoura, J.Kitagawa, T.Sumiyoshi and K.Tanabe; Bull. Chem. Soc. Jpn., 46 (1973).
- [19] S.Sugunan and Anto Paul; Ind. J. Chem., 36A (1997) 1068.
- [20] M.Shimokawabe, H.Asakawa and N.Takezawa; Appl. Catal., 59 (1990) 45.
- [21] M.A.Aramendia, V.Borau, I.M.Garcia, C.Jimenez, A.Marians, J.M.Marinas, A.Porras and F.J.Urbano; Appl. Catal., 184 (1999) 115.
- [22] C.Morterra, A.Chiorino, G.Ghiotti and E.Garrone, J. Chem. Soc. Farady Trans., 1 75 (1979) 271.
- [23] S.Ghorpade, V.S.Darshane and S.G.Dixit; Appl. Catal. A., 166 (1998) 135.
- [24] G.Busca; Catal. Today, 41 (1998) 191.

3.1 Physical characterization

The various physical methods used for characterizing the prepared spinels were XRD, DRIFT, SEM, EDAX, BET surface area measurement, TG/DTA etc. Mössbauer analysis was performed for iron containing samples.

3.1.1 X-ray diffraction analysis

Every crystalline substance has a unique X-ray pattern because the line position depends on unit cell size, and the line intensity depends on the type of the atoms present and their arrangement in the crystal¹. X-ray diffraction patterns of the samples packed in a glass holder were recorded at room temperature with Ni filtered Cu K α radiation in a Philips diffractometer (PW 1710). X-ray diffraction patterns of the prepared spinels were shown in Fig. 3.1.1-3.1.3.

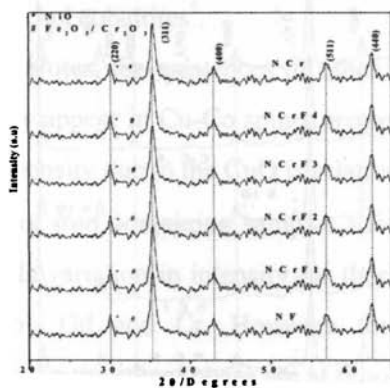


Fig.3.1.1 XRD pattern for chromium containing nickel ferrites.

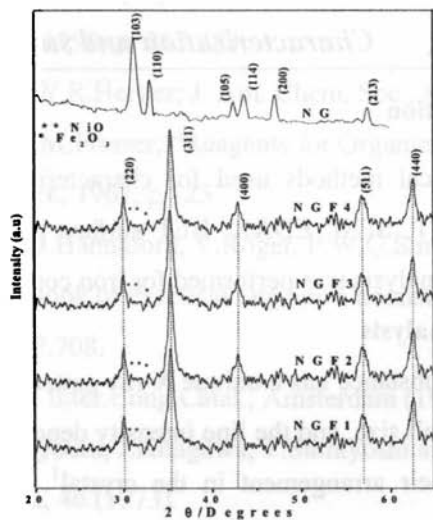


Fig.3.1.2 XRD pattern for gadolinium containing nickel ferrites.

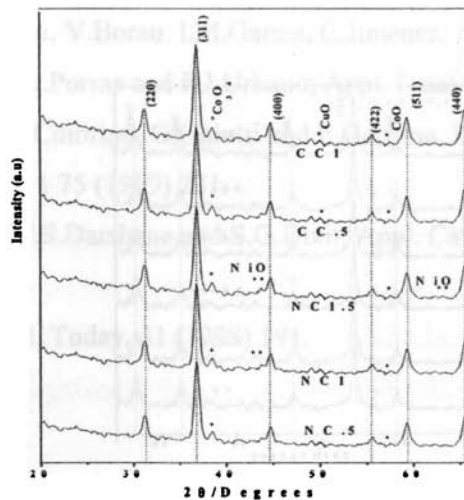


Fig.3.1.3 XRD pattern for cobaltites.

The XRD results were compared with JCPDS data and all the prepared samples were found to contain the spinel phase. The XRD pattern contains all the peaks due to spinel phase at characteristic 2θ values. In addition to the spinel phase, the pattern contains peaks due to individual oxides. The XRD pattern indicates the fine particle nature of the spinels formed by coprecipitation method. The theoretical (from JCPDS card data) and experimental d_{hkl} values for simple spinels NF, NCr, NG, NC and CC are presented in table 3.1.1. It can be seen that the experimental data are well coordinated with the theoretical data. For nickel cobaltites, the intensity due to NiO peak increases as x increases. The presence of NiO agrees with previous reports^{2,3} which indicates that while a single phase exists only from pure Co_3O_4 up to the NiCo_2O_4 composition, beyond NiCo_2O_4 nickel oxide, NiO is also formed. De Faris et al. reported that the nickel cobalt oxide prepared at 400 °C shows additional NiO formation when the nominal Ni content exceeds the stoichiometric amount corresponding to NiCo_2O_4 ⁴. Marco et al. reported the presence of CoO for nickel cobaltites⁵.

For copper cobaltites, the existences of other phases such as CuO and Co_3O_4 , which generally appear in Cu-Co spinel preparations, were detected by XRD analysis⁶. The intensity due to the CuO is relatively low.

XRD patterns of iron containing samples show peaks due to $\alpha\text{-Fe}_2\text{O}_3$ and NiO. No noticeable variation in intensity for these peaks is observed with replacement of Fe by Gd and Cr. However for nickel gadolinite, the characteristic peaks due to the spinel phase are at those positions such that they merge with those for NiO. So whether NiO is present as impure phase is not detectable.

The average crystallite size of the spinels is determined from the Scherrer equation:

$$t = 0.9\lambda/\beta \cos\theta,$$

where t = average crystallite size,

λ = wavelength of the X-ray used,

θ = glancing angle and

β = FWHM (half width of the peak with maximum intensity)

The crystallite sizes of the different spinel series are presented in table 3.1.2.

3.1.2 DRIFT spectra

IR studies in the diffuse reflectance mode were carried out to understand the band positions attributed to the lattice sites. Since, in spinels metal ions are distributed in two different crystallographic environments, the spinel phase formation can very well be assigned by the appearance of two IR bands. DRIFT spectra of the calcined samples were taken in the 400-1000 cm^{-1} wave number region. The spectra typically show two strong bands ν_1 and ν_2 around 700 cm^{-1} and 500 cm^{-1} respectively. The DRIFT spectra of representative spinels are shown in Fig.3.1.4 and 3.1.5. For ferrites, the high frequency band appeared at around 700 cm^{-1} and low frequency band at around 460 cm^{-1} . For cobaltite spinels the typical bands appeared at around 590 cm^{-1} and 680 cm^{-1} . Generally, the spectrum for cobaltites shows two absorption bands in the region 660-650 cm^{-1} and 560-550 cm^{-1} corresponding to the metal-oxygen stretching vibrations which are characteristics of cobaltites⁷. However reports show that there may be shift in the positions of these characteristic bands^{8,9}. For NC 1.5, which is having high nickel content, the

Chapter 3

Table 3.1.1 Experimental and theoretical XRD data for simple spinels.

Sample	JCPDS data		Experimental data		hkl
	I/I ₀	d _{hkl}	I/I ₀	d _{hkl}	
NiFe ₂ O ₄	33	2.948	33	2.947	220
	100	2.514	100	2.513	311
	22	2.084	21	2.085	400
	28	1.605	27	1.604	511
NiCr ₂ O ₄	30	2.930	30	2.929	220
	100	2.500	100	2.500	311
	35	2.070	35	2.069	400
	60	1.600	60	1.594	511
NiGd ₂ O ₄	100	2.848	100	2.847	103
	70	2.729	69	2.729	110
	35	2.068	35	2.067	114
	40	1.599	40	1.597	200
NiCo ₂ O ₄	25	2.871	25	2.872	220
	100	2.448	100	2.449	311
	10	2.344	10	2.343	222
	25	2.031	25	2.030	400
CuCo ₂ O ₄	25	2.852	25	2.851	220
	100	2.432	100	2.431	311
	20	2.312	20	2.313	222
	31	1.551	31	1.552	511

peak at around 585 cm⁻¹ can be attributed to cobalt oxide or nickel oxide¹⁰.

Characterization and surface properties

Table 3.1.2 Crystallite size of different spinels.

Catalyst	Crystallite size (nm)
NF	8.82
NCrF 1	8.76
NCrF 2	8.75
NCrF 3	8.74
NCrF 4	8.76
NCr	8.84
NGF 1	8.83
NGF2	8.82
NGF 3	8.81
NGF 4	8.79
NG	8.77
NC .5	8.82
NC 1	8.81
NC 1.5	8.79
CC .5	8.84
CC 1	8.82

According to Waldern et al.¹¹ and White et al.¹², the high frequency band is due to the stretching vibration of the tetrahedral M-O bond and the low frequency band is due to the vibration of the octahedral M-O bond. In spinel lattice, every oxygen anion is bonded to three octahedral and one tetrahedral cation as shown in Fig.3.1.6. The three octahedral bonds are perpendicular to

each other and provide an isotropic force field in the three directions if the tetrahedral bond was absent. The tetrahedral cation M_T introduces a supplementary force in a preferential direction along the M_T -O bond. This is responsible for the ν_1 mode in which the oxygen is forced to oscillate along the M_T -O bond, and thus appears as a stretching vibration of the tetrahedral group. Vibration of this group corresponds to the higher restoring force and thus is assigned to the high-frequency absorption band. If we consider an oxygen vibration at right angles with the preceding one, the restoring force due to the tetrahedral cation M_T will be negligible. This leads to ν_2 modes, which may be considered as a stretching vibration of the octahedral bond. Thus the appearance of IR bands at expected positions confirms the formation of spinel phase.

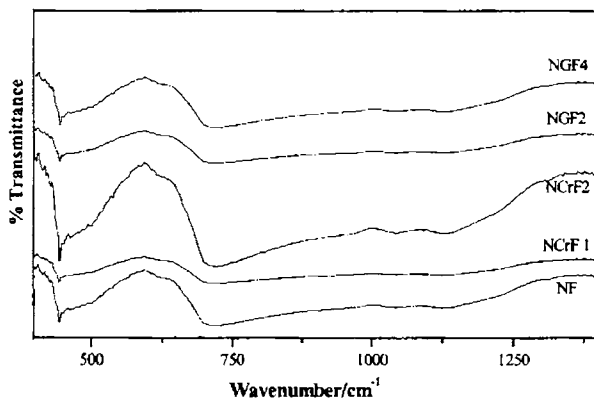


Fig.3.1.4 DRIFT spectra of some representative ferrites.

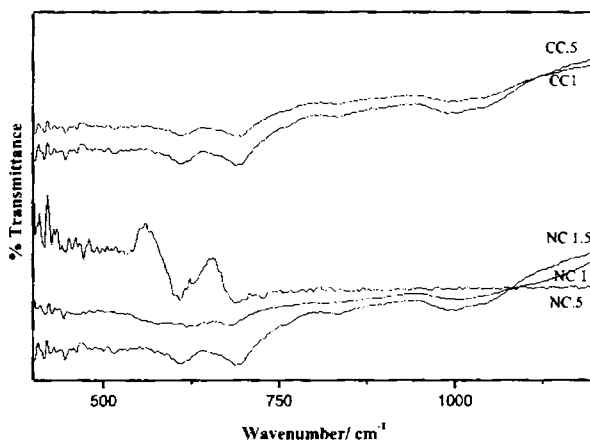


Fig.3.1.5 DRIFT spectra of cobaltites.

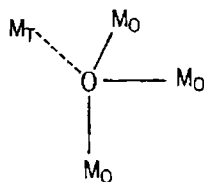


Fig. 3.1.6 The nearest neighbours of oxygen anion in the spinel lattice. M_T: tetrahedral cation and M_O: octahedral cation.

3.1.3. Thermal analysis

TG/DTA curves for NF, NCr, NG, NC.5, NC1, CC.5 and CC1 are given in Fig.3.1.7 and 3.1.8. For nickel ferrite, initial weight loss is due to loss of water. Weight loss due to removal of nitrate ion has been observed at around 300 °C. After that there is no detectable weight loss observed which indicates

the high thermal stability of the sample. TG pattern for nickel gadolinite shows no major weight loss after 350 °C which shows its high thermal stability.

For nickel chromite, the TG pattern is almost similar to that of nickel ferrite except that chromite shows a third weight loss in the range 600-700 °C. The first two weight losses can be attributed to the loss of water and nitrate ion. The third weight loss represents the decomposition of chromite into individual oxides¹³.

Thermal studies of cobaltites show that they are thermally not stable. At higher temperatures the samples show weight loss and this can be attributed to the decomposition to the individual oxides, oxygen and cobalt enriched spinel phase¹⁴.

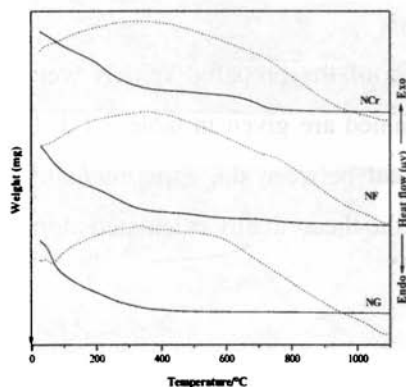


Fig.3.1.7 TG/DTA pattern for NG, NF and NCr.

Solid curve-TG, dotted curve-DTA

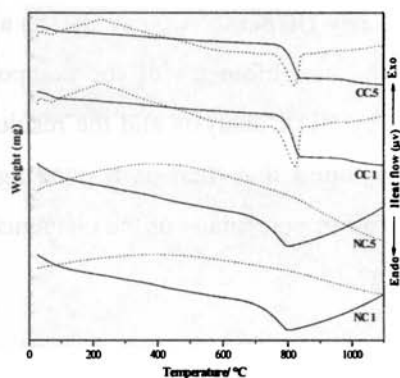


Fig.3.1.8 TG/DTA pattern for cobaltites.

3.1.4 Scanning Electron Microgram (SEM) analysis

Scanning electron micrograms of representative samples are shown in Fig.3.1.9. The successive replacement of iron by chromium has little effect on the morphology of the samples. Samples containing both iron and chromium are having block like structure with well-defined edges where as morphology of NiCr_2O_4 is different from the rest of the samples. Unlike in the case of chromium containing samples, gadolinium is found to have an effect on the morphology of NiFe_2O_4 . Replacement of iron by gadolinium gradually disappears the edges and the morphology of NiGd_2O_4 particles is entirely different from that of NiFe_2O_4 . Cobaltite spinel particles exist as bulk spheres. Copper cobaltites are bigger in size than nickel cobaltites.

3.1.5 Energy Dispersive X-ray (EDX) analysis

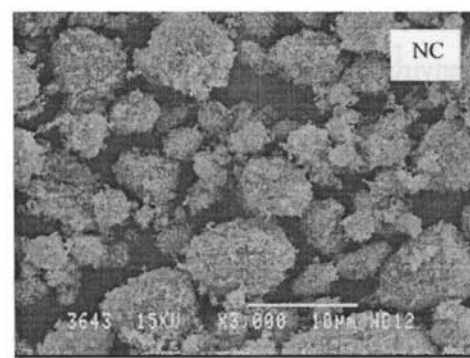
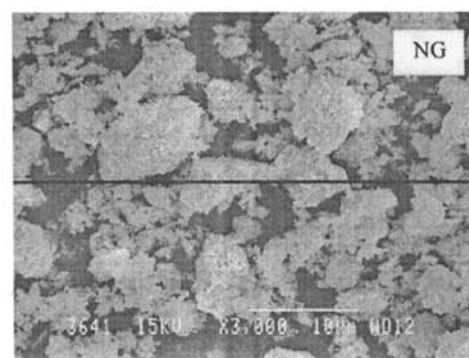
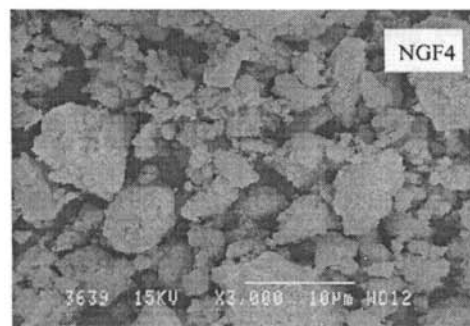
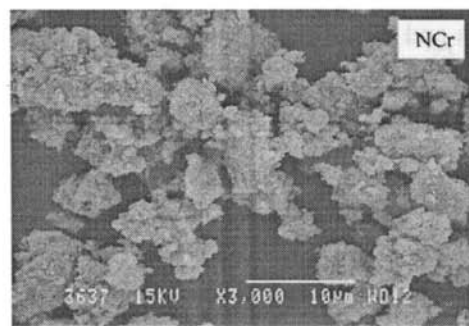
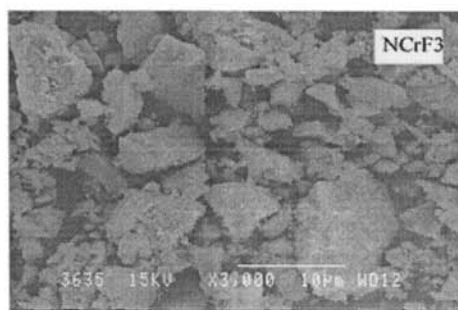
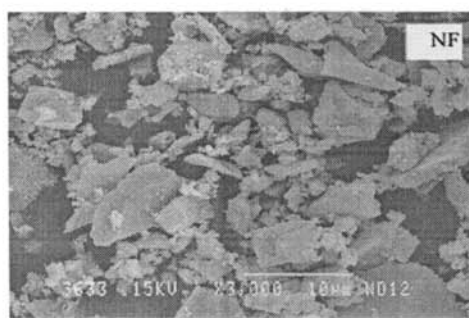
The stoichiometry of the compositions of the prepared spinels were checked by EDX analysis and the results obtained are given in table 3.1.3. It has been found that there is a good agreement between the experimentally obtained atom percentage of the elements and the theoretically calculated atom percentage.

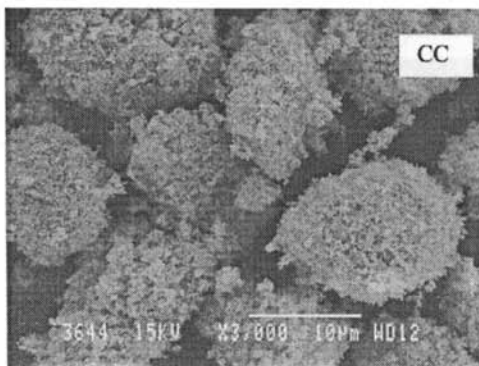
3.1.6. Surface area and pore volume measurements

The BET and Langmuir surface areas and total pore volume of the prepared spinel systems were measured by nitrogen adsorption at liquid nitrogen temperature. The data are presented in table 3.1.4. Replacing iron by chromium increases the surface area up to NCrF_3 and incorporation of more than 60 % chromium decreased the surface area. Gradual replacement of iron

Chapter 3

Fig. 3.1.9 SEM pictures of some of the representative spinels.





by gadolinium increased the surface area and nickel gadolinite is having more surface area in that series. In cobaltite series, copper cobaltites are having lower surface area than nickel cobaltites.

3.1.7 Mössbauer analysis

In catalysis, Mössbauer spectroscopy is generally employed for the characterization of catalysts. This technique gives a better understanding of the oxidation state¹⁵⁻¹⁷, phase transitions¹⁸, magnetic properties¹⁹, and electronic environments of the Mössbauer active elements. Mössbauer spectra of nickel ferrite along with chromium and gadolinium containing samples are shown in Fig. 3.1.10 and the corresponding Mössbauer data are presented in table 3.1.5. For NGF4, Mössbauer data are not presented because at higher gadolinium content it is really difficult to record the Mössbauer data due to the high absorption of γ -rays by the heavy gadolinium atom. At room temperature the spectrum of nickel ferrite shows two signals corresponding to two sites, with both sites magnetically split showing sextets. When iron is substituted by chromium, the magnetic hyperfine interaction is lost and the spectra for chrom-

Chapter 3

Table 3.1.3 EDX data for spinels.

Catalyst	Atom %					
	Ni	Fe	Cr	Gd	Cu	Co
NF	32.84	67.16	-	-	-	-
NCrF 1	28.63	54.63	16.74	-	-	-
NCrF 2	33.34	37.00	29.58	-	-	-
NCrF 3	30.76	26.73	42.51	-	-	-
NCrF 4	31.49	12.50	56.00	-	-	-
NCr	27.18	-	72.82	-	-	-
NGF 1	29.28	57.17	-	13.55	-	-
NGF2	36.77	36.72	-	26.5	-	-
NGF 3	33.37	26.49	-	40.13	-	-
NGF 4	31.73	16.37	-	52.00	-	-
NG	32.31	-	-	66.41	-	-
NC .5	15.34	-	-	-	-	84.66
NC 1	33.59	-	-	-	-	66.41
NC 1.5	50.59	-	-	-	-	49.41
CC .5	-	-	-	-	19.11	80.89
CC 1	-	-	-	-	35.23	64.77

ium containing samples are characterized by quadrupole splitting pattern in the range 0.44-0.50 mm/s. Upon incorporation of chromium, there is no hyperfine Zeeman splitting and only paramagnetic doublet exists. The doublet observed in chromium containing samples can arise from iron in ultra dispersed ferrite

Characterization and surface properties

Table.3.1.4 Surface areas and pore volume of the spinels.

Catalyst	Surface area (m ² /g)		Pore volume (cc/g)
	BET	Langmuir	
NF	34.0	52.0	0.1400
NCrF 1	85.3	128.0	0.1532
NCrF 2	104.8	157.0	0.1621
NCrF 3	116.5	176.0	0.1688
NCrF 4	82.6	124.7	0.1484
NCr	7.0	11.0	0.0190
NGF 1	17.0	25.0	0.0409
NGF2	29.0	43.5	0.0793
NGF 3	34.6	51.0	0.1044
NGF 4	42.0	62.5	0.1122
NG	60.4	89.0	0.1646
NC .5	29.6	44.3	0.0528
NC 1	38.0	58.0	0.0659
NC 1.5	40.0	60.0	0.0824
CC .5	9.0	13.5	0.0151
CC 1	13.0	19.0	0.0254

particles exhibiting superparamagnetic (SPM) behaviour²⁰⁻²². Mössbauer spectra of gadolinium containing samples (except NGF4) show not only considerable doublets from the quadrupole splitting, but also detectable sextets from the magnetic splitting. The appearance of doublets from the quadruple

splitting of ^{57}Fe nucleus can be attributed to SPM relaxation effect²². Mössbauer spectra for NGF4 contains only singlet with no splitting pattern. Koznetsov et al.²³ have studied the Mössbauer spectrum of lithium ferrite with partial substitution of iron by chromium. They also obtained a central singlet component with chromium substitution for iron coexisting with the sextet and observed only singlets at higher chromium content. In our case, the appearance of singlet for NGF4 can be attributed to inhomogeneous substitution by gadolinium leading to some of the iron atoms becoming isolated from the majority of exchanged-coupled iron atoms as explained by Koznetsov et al.²³. This result in paramagnetic behaviour in the case of individual atom, or superparamagnetic behaviour in the case of clusters, either of which can give rise to a singlet in the spectra.

In Mössbauer spectroscopy if the two sites are equally coordinated, we cannot differentiate the sites. This is a huge drawback in Mössbauer analysis. Mössbauer spectra of a partially inverse or completely inverse spinel with iron at both T_d and O_h sites would be the resultant of two quadrupole split spectra due to two reasons: (i) In the Mössbauer spectra of cubic spinels, in which either Fe^{2+} or Fe^{3+} ions are present at the O_h sites only, show a quadrupole splitting due to the trigonal field at the O_h sites in the spinel structure, and (ii) the Mössbauer spectrum of an inverse cubic spinel containing Fe^{3+} ions at the T_d sites only, also shows a quadrupole splitting due to the electric field gradient produced by the asymmetric charge distribution on the twelve O_h neighbours of each T_d site. If the value of electric field gradient at the T_d site is different from that of the O_h site, the quadrupole splitting of the two component spectra will be different. In such cases, it may be possible to

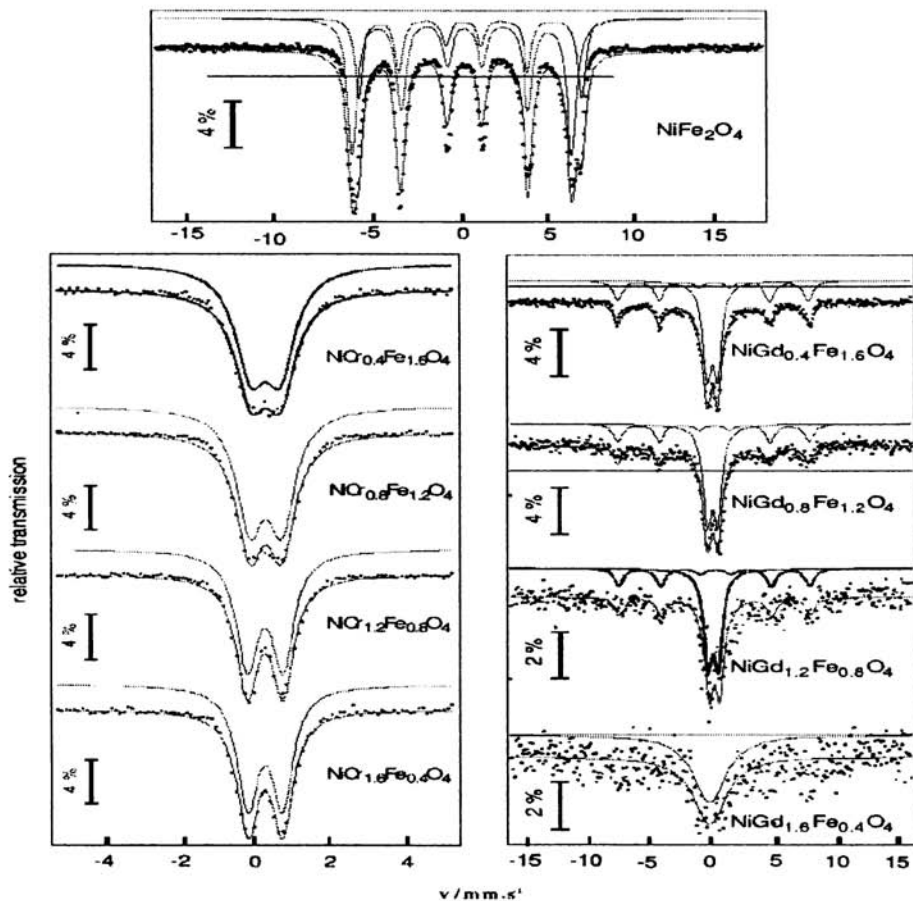


Fig.3.1.10 Mössbauer spectra of iron containing samples.

resolve the Mössbauer spectra of an inverse spinel into two separate quadrupole split spectra. Unfortunately here we could not able to resolve the spectra of chromium containing samples into two quadrupole splitting due to the same electric field gradient.

Chapter 3

Table 3.1.5 Mössbauer parameters of ferrites.

Catalyst	Fe site*	δ (mm/s)	ΔE_Q (mm/s)	Γ (mm/s)	B_{hf} (T)	Fe %
NF	1	0.15(9)	-0.15(3)	0.58(3)	35.22(6)	52
	2	0.33(7)	0.35(6)	0.46(3)	35.00(3)	49
NCrF 1	1	0.12(8)	0.44(3)	0.54(7)	---	100
NCrF 2	1	0.18(1)	0.47(2)	0.48(3)	---	100
NCrF 3	1	0.18(1)	0.53(2)	0.39(3)	---	100
NCrF 4	1	0.18(7)	0.52(2)	0.38(4)	---	100
NGF 1	1	0.24(1)	-0.87(6)	0.85(4)	---	57
	2	0.34(5)	-0.16(9)	0.91(2)	0.49(5)	43
NGF2	1	0.26(2)	-0.84(1)	0.78(4)	---	54
	2	0.34(3)	-0.18(3)	0.84(1)	0.40(3)	46
NGF 3	1	0.24(4)	-0.81(7)	0.72(1)	---	47
	2	0.35(7)	-0.15(5)	0.79(7)	0.34(1)	53
NGF 4	---	---	---	---	---	---

* 1-T_d site, 2-O_h site, values in parenthesis: statistical error in the last digit.

The isomer shift (δ) values were found out with respect to the metallic iron (⁵⁷Fe). Mössbauer isomer shift range for Fe³⁺ is within 0.2-0.5 mm/s²⁴. The IS values for gadolinium containing samples are in accordance with this. But chromium containing samples showing values less than 0.2 mm/s. Many authors have been reported IS value less than 0.2 for Fe³⁺ ion^{23,25-27}. As explained earlier, due to the same electric field gradient, the Mössbauer signals for chromium containing samples could not be resolved and hence we got IS

values for one site only. IS values for chromium containing samples show that substitution of iron by chromium is found to have an effect on the s electron density of Fe^{3+} ion. For gadolinium containing samples, the observed IS values show an insignificant change with increase in concentration of gadolinium ions. It implies that the s electron charge density of Fe^{3+} ion is not influenced by the increased gadolinium concentration. It is known that the IS value for O_h site is more than that for T_d site. In spinel ferrites, the bond separation $\text{Fe}^{3+}\text{-O}^{2-}$ is larger for O_h sites as compared to that for T_d sites due to which the overlapping of orbital of Fe^{3+} ions is small at O_h sites and thus a larger IS at O_h site is expected²⁸⁻³⁰.

The quadrupole splitting (ΔE_Q) exhibited by ^{57}Fe reflected the asymmetry of the electric field gradient (EFG) experienced by Fe^{3+} ions in the systems. For Fe^{2+} ion, the EFG at ^{57}Fe nucleus may be due to the nonspherical distribution of 3d electrons ($t_{2g}^4 e_g^2$). However, Fe^{3+} ion possesses half filled 3d configuration ($t_{2g}^3 e_g^2$), the EFG arises from the neighbouring ions. For pure nickel ferrite, the ΔE_Q values indicate that, there is more asymmetry at the O_h site compared to T_d site. Incorporation of chromium is found to create more and more asymmetry. For gadolinium containing samples, the ΔE_Q values show that there is more asymmetry at the T_d site as compared to O_h site.

The Mössbauer line widths are a measure of the chemical disorder around the Mössbauer nucleus. The line width is broadened compared to the natural line width of ^{57}Fe ($\Gamma \sim 0.2$ mm/s), this may be due to the asymmetrical arrangement of the Fe atom.

Only samples that split magnetically (exchange of magnetic flux from the magnetic nuclei) will give a B_{hf} value. The chromium containing samples

are magnetically not splitting. That is why no B_{hf} values for these systems. In the gadolinium containing samples, only one site is magnetically splitting, that is why only one site is showing B_{hf} value.

3.1.7a. Cation distribution of spinels

In chromium containing systems, chromium preferably goes to O_h site because the crystal field effects are favourable²³. Here we suppose that both T_d and O_h sites are equally occupied by Fe^{3+} ions since we could not resolve the Mössbauer peaks into two due to same electric field. As reported by many authors, for chromium containing nickel ferrites, Ni^{2+} ion is shifted from O_h site to T_d site only after $x = 1^{31-33}$. Incorporation of gadolinium has a different effect. Gadolinium preferentially goes to O_h site due to the larger size of Gd^{3+} ion (1.08\AA)³⁴. According to Said³⁵, gadolinium incorporated nickel ferrites have a partially inverse structure. Gadolinium substitution for iron leads to replacement of Fe^{3+} ions from T_d site to O_h site which agrees with previous reports³⁸. Nickel cobaltite is inverse and copper cobaltite is partially inverse as reported earlier^{36,37}. Based on these, the expected cation distribution for the prepared spinels is presented in table 3.1.6.

3.2 Surface properties-acidity/basicity

A series of active site with different strengths are distributed over solid catalysts. These distributions are closely related to catalytic activity and selectivity. In order to design catalysts with high activity and selectivity, the properties of active sites should be accurately measured. The strength of the sites exposed on the surface and their distribution depend strongly up on the

Characterization and surface properties

Table 3.1.6 Cation distribution of spinels.

Catalyst	Tetrahedral site	Octahedral site
NF	$\text{Fe}^{+3}_{1.04}$	$\text{Fe}^{+3}_{0.96}, \text{Ni}^{+2}$
NCrF 1	$\text{Fe}^{+3}_{0.8}$	$\text{Fe}^{+3}_{0.8}, \text{Cr}^{+3}_{0.4}, \text{Ni}^{+2}$
NCrF 2	$\text{Fe}^{+3}_{0.6}$	$\text{Fe}^{+3}_{0.6}, \text{Cr}^{+3}_{0.8}, \text{Ni}^{+2}$
NCrF 3	$\text{Fe}^{+3}_{0.4}, \text{Ni}^{+2}_{0.6}$	$\text{Fe}^{+3}_{0.4}, \text{Cr}^{+3}_{1.2}, \text{Ni}^{+2}_{0.4}$
NCrF 4	$\text{Fe}^{+3}_{0.2}, \text{Ni}^{+2}_{0.8}$	$\text{Fe}^{+3}_{0.2}, \text{Cr}^{+3}_{1.6}, \text{Ni}^{+2}_{0.2}$
NCr	Ni^{+2}	Cr^{+3}_2
NGF 1	$\text{Fe}^{+3}_{0.91}, \text{Ni}^{+2}_{0.5}$	$\text{Fe}^{+3}_{0.69}, \text{Gd}^{+3}_{0.4}, \text{Ni}^{+2}_{0.5}$
NGF2	$\text{Fe}^{+3}_{0.65}, \text{Ni}^{+2}_{0.5}$	$\text{Fe}^{+3}_{0.55}, \text{Gd}^{+3}_{0.8}, \text{Ni}^{+2}_{0.5}$
NGF 3	$\text{Fe}^{+3}_{0.376}, \text{Ni}^{+2}_{0.5}$	$\text{Fe}^{+3}_{0.42}, \text{Gd}^{+3}_{1.2}, \text{Ni}^{+2}_{0.5}$
NGF 4	Ni^{+2}	$\text{Fe}^{+3}_{0.4}, \text{Gd}^{+3}_{1.6}$
NG	Ni^{+2}	Gd^{+3}_2
NC .5	$\text{Co}^{+3}_{1.25}$	$\text{Ni}^{+2}_{0.5}, \text{Co}^{+3}_{1.25}$
NC 1	Co^{+3}	$\text{Ni}^{+2}, \text{Co}^{+3}$
NC 1.5	$\text{Co}^{+3}_{0.75}$	$\text{Ni}^{+2}_{1.5}, \text{Co}^{+3}_{0.75}$
CC .5	$\text{Co}^{+3}_{0.75}, \text{Cu}^{+2}_{0.2}$	$\text{Cu}^{+2}_{0.3}, \text{Co}^{+3}_{1.75}$
CC 1	$\text{Co}^{+3}_{0.6}, \text{Cu}^{+2}_{0.4}$	$\text{Cu}^{+2}_{0.6}, \text{Co}^{+3}_{1.4}$

catalytic composition. According to many authors^{39,40}, whatever be the type of spinel, the octahedral sites are exposed almost exclusively at the catalyst surface of the spinel oxides and so the catalytic performance is greatly dependent on the composition of the octahedral sites. Hence the relative acid-base properties of the cations present in the octahedral sites are relevant in determining the acidity and basicity of the systems.

Different methods used to study acid-base properties of prepared spinels were (i) TPD of ammonia, (ii) perylene adsorption studies, (iii) IR studies of pyridine adsorbed samples, (iv) surface electron donating property study by using various electron acceptors and (v) vapour phase cumene cracking and cyclohexanol decomposition reactions.

3.2.1 TPD of ammonia

The ammonia TPD method is a quantitative method, which is easy and rapid, widely is employed in characterizing the acidity of solid catalysts. Ammonia TPD detects total acidity (Lewis and Brønsted). The method permits to identify the strength, the number and type of active sites that are available on the catalyst surface. The method consists of desorbing a previously adsorbed gas such as ammonia by a linear temperature rate.

Ammonia is used frequently as a probe molecule because of its small molecular size, stability and strong basic strength. Owing to the smaller size and strong basicity, ammonia can get adsorbed on acid sites of any strength and type. In solid catalysts, the acidity is due to the exposed cations (Lewis type) and surface OH groups (Brønsted type). Different modes of adsorption of ammonia on the catalyst surface are shown in Fig.3.2.1. These modes comprise

Characterization and surface properties

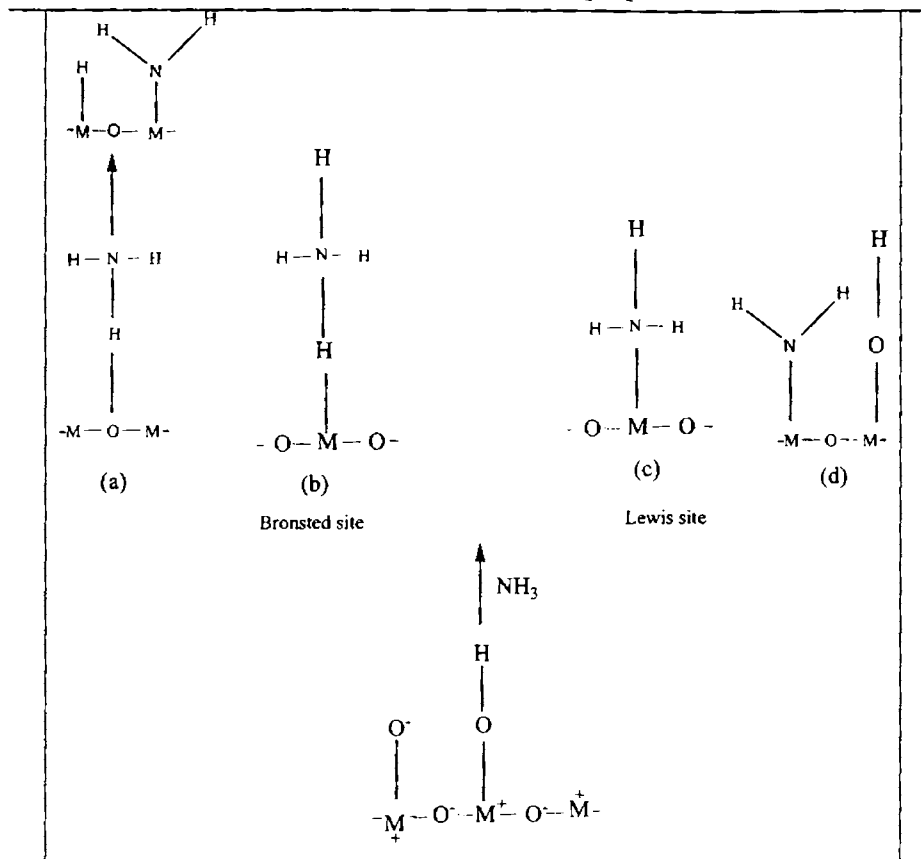


Fig.3.2.1 Different modes of adsorption of ammonia on oxide surface.

adsorption at Brønsted and Lewis acidic sites. The coordination of ammonia to Lewis sites is stronger than that at Brønsted sites.

Ammonia TPD studies were done in the temperature range RT-600 °C. A definite amount of ammonia is injected into the sample in the reactor and allowed to adsorb over the catalyst surface in a uniform manner. Then nitrogen is passed for 30 minutes to remove the weakly adsorbed ammonia. The

ammonia desorbed in the range RT-600 °C is divided into three different temperature ranges such as RT-200, 201-400 and 401-600 assigned as weak, medium and strong acid sites respectively. Conclusions derived for the different spinels are presented in the following sections.

(a) $\text{NiCr}_x\text{Fe}_{2-x}\text{O}_4$ ($x = 0-2$) series

The acidity in the weak, medium and strong regions for the chromium containing nickel ferrites is shown in table 3.2.1.

Table 3.2.1 NH_3 -TPD values for chromium containing nickel ferrites.

Catalyst	Acidity (mmol/g)			
	Weak (RT-200 °C)	Medium (201-400 °C)	Strong (401-600 °C)	Total (RT-600 °C)
NF	0.112	0.037	0.013	0.162
NCrF 1	0.270	0.120	0.016	0.406
NCrF 2	0.306	0.136	0.018	0.460
NCrF 3	0.350	0.154	0.029	0.533
NCrF 4	0.161	0.081	0.014	0.256
NCr	0.132	0.052	0.013	0.197

It can be seen from the above table that the progressive addition of chromium into pure nickel ferrite increases the total acidity up to 60 % chromium addition and thereafter decreases. The total acidity values for NCrF4 and NCr are much lower than NCrF2 and NCrF3. Incorporation of chromium up to 60 % increases the acid strength in the weak, medium and strong regions.

The increase in the weak and medium sites is more pronounced than in strong sites. NH₃-TPD method lacks in discriminating the type of acid sites (Lewis and Brønsted). However, it is generally accepted that evacuation of ammonia adsorbed at 400 °C removes most of the Brønsted acid sites⁴¹. Again, it is implied that the coordinatively bonded ammonia on the strong Lewis acid sites can be desorbed only at higher temperatures and the acidity in the strong region can be due to strong Lewis acid sites. The acidity in the weak + medium regions is due to the Brønsted and weak Lewis acid sites.

From the cation distribution data (Table 3.1.6), it can be seen that the concentration of iron at the octahedral site is decreasing with chromium incorporation and Ni²⁺ goes to tetrahedral site only when x = 1.2. As x increases, the concentration of Cr³⁺ ion at the octahedral site increases gradually and the concentration of Ni²⁺ ion at the octahedral site decreases only after x = 0.8. NCrF₃ is having maximum acidity in the series and it is supposed that a moderate concentration of Cr³⁺ and Ni²⁺ ions may be responsible for the high acidic behaviour of NCrF₃.

(b) NiGd_xFe_{2-x}O₄ (x = 0-2) series

The acidity values obtained for the gadolinium containing nickel ferrites in the weak, medium and strong regions are shown in table 3.2.2.

Incorporation of gadolinium increases the acidic strength and complete replacement of iron by gadolinium resulted in drastic increase in acidity. Not only this, the distribution of acid sites in the weak, medium and strong regions increases gradually with progressive substitution by gadolinium. For systems having higher gadolinium content, the strength of acid sites in weak, medium

Chapter 3

and strong regions shown a large increase and this resulted in increase of total acidity considerably.

Table 3.2.2 NH₃-TPD values for gadolinium containing nickel ferrites.

Catalyst	Acidity (mmol/g)			
	Weak (RT-200 °C)	Medium (201-400 °C)	Strong (401-600 °C)	Total (RT-600 °C)
NF	0.112	0.037	0.013	0.162
NGF 1	0.124	0.039	0.032	0.195
NGF2	0.243	0.115	0.078	0.436
NGF 3	0.263	0.120	0.080	0.463
NGF 4	0.285	0.167	0.141	0.593
NG	0.503	0.310	0.281	1.094

Cation distribution data show that up to NGF3, the percentage of Ni²⁺ at the octahedral site does not change and after that it completely goes to tetrahedral site. But total acidity goes on increasing from NF to NG. So it is supposed that Ni²⁺ ion has no effect on the total acidity. Hence it is the concentration of other ions (Fe³⁺ and Gd³⁺) which determines the acidity. The total concentration of Fe³⁺ and Gd³⁺ at the octahedral site increases with incorporation of gadolinium and acidity increases in the same order. Although the concentration of ions in NGF4 and NG are same, NG contains more Gd³⁺ ions which may be creating strong acid centers and hence more acidic.

(c) Cobaltite series

For cobaltites, the distribution of acid sites in weak, medium and strong

Characterization and surface properties

regions is presented in table 3.2.3.

Table 3.2.3 NH₃-TPD values for cobaltites.

Catalyst	Acidity (mmol/g)			
	Weak (RT-200 °C)	Medium (201-400 °C)	Strong (401-600 °C)	Total (RT-600 °C)
NC .5	0.163	0.068	0.054	0.285
NC 1	0.196	0.086	0.013	0.295
NC 1.5	0.206	0.082	0.055	0.343
CC .5	0.221	0.083	0.055	0.359
CC 1	0.230	0.085	0.059	0.374

Copper cobaltites are more acidic than nickel cobaltites. In nickel cobaltite series, the total acidity increases as the percentage of nickel increases. Although the acidic strength in the weak and medium acid site increases with increase in percentage of nickel, the variation in strong region does not follow the order. For copper cobaltites, no prominent increase in acid strength has been observed with increase in copper content.

According to the cation distribution data, as the percentage of Ni²⁺ increases in nickel cobaltites, concentration of Ni²⁺ ions at the octahedral site increases. So it is believed that the increased concentration of Ni²⁺ at the O_h site may be responsible for the increased acidity in that series. Presence of more copper in Cu_xCo_{3-x}O₄ (x = 0.5, 1) increases the total acidity slightly. There is not much pronounced increase in the weak, medium and strong acid regions compared to other series. The concentration of octahedral Cu²⁺ is more in CCl. So it is the increase in concentration of Cu²⁺ ions at the O_h site that

may be responsible for the increased acidity of CCl compared to CC.5.

3.2.2 Perylene adsorption studies

The base adsorption method and amine titration help to establish only the total acidity of the systems. Neither of these methods allows the quantitative determination of Lewis acidity of the surface. Lewis acidity, in the presence of Brönsted acid sites, can be quantitatively obtained by utilizing the ability of the catalyst surface to accept a single electron. The polyaromatic compounds which are generally used in the studies of one electron acceptor properties of solids are perylene, pyrene, chysene and phenothiazine.

When an acidic surface is exposed to electron donor molecules, these molecules get adsorbed on the catalyst surface by the donation of an electron. Hence the amount of surface sites, which act as electron acceptors, can be obtained by measuring the amount of adsorbed molecules. The quantitative measurement of donor molecules that are adsorbed on the one electron accepting sites indirectly determines the amount of electron deficient sites i.e., the Lewis acid sites.

In the present study, activated catalyst systems were stirred with a solution of perylene in benzene at room temperature; in the course of stirring perylene gets adsorbed on the solid surface, leading to colour change of the solution. Perylene readily donates electron to the Lewis acid site and gets adsorbed on the solid surface. Thus, after adsorption, the concentration of perylene in the solution was considerably reduced. The decrease in the amount of perylene in the solution can be obtained by measuring the absorbance of the solution before and after adsorption. The amount of perylene adsorbed

Characterization and surface properties

increases with concentration of perylene solution. This increasing trend continues up to a particular perylene concentration and thereafter the amount of perylene adsorbed decreased with increase in concentration. This constant value is called the limiting amount, which corresponds to the surface one electron accepting capacity or Lewis acidity.

The data for perylene adsorption studies of the prepared systems are given in table 3.2.4.

Table 3.2.4 Perylene adsorption study.

Catalyst	Limiting amount of perylene adsorbed (10^{-6} mol/g)	Catalyst	Limiting amount of perylene adsorbed (10^{-6} mol/g)
NF	8.31	NGF 3	11.50
NCrF 1	10.27	NGF 4	12.74
NCrF 2	11.32	NG	15.32
NCrF 3	12.25	NC .5	8.67
NCrF 4	9.59	NC 1	9.22
NCr	8.63	NC 1.5	9.87
NGF 1	8.56	CC .5	10.00
NGF2	9.87	CC 1	10.15

For chromium containing nickel ferrites, the limiting amount of perylene adsorbed shows a regular gradation up to NCrF3 and thereafter decreases for samples containing higher chromium content, where as incorporation of gadolinium into nickel ferrite gradually increases the Lewis

character with increase in percentage of gadolinium and nickel gadolinite possesses more Lewis acidic character than nickel ferrite. In the case of cobaltites, increase in percentage of nickel and copper in the respective cobaltites is found to increasing the Lewis acidity.

The perylene adsorption results are observed to be proportional to the variation of total acidity obtained from the ammonia TPD studies. Aramendia et al.⁴², using temperature programmed desorption mass spectrometry (TPD-MS) techniques with pyridine, 2,6-dimethyl pyridine and CO₂ as probe molecules, showed that the effect of calcination temperature on acidity of metal oxide surfaces was to reduce the number of Brönsted acid sites and to leave only the Lewis type sites among the strongest acid sites. Thus at higher calcination temperature, most of the Brönsted acid sites would have disappeared, and at the same time, the strength and number of Lewis acid sites per unit area would have increased due to creation of surface defects and more coordinatively unsaturated cations. Hence in the case of the prepared spinels it is believed that the major contribution towards total acidity comes from Lewis sites.

3.2.3 IR studies of pyridine adsorbed samples

Adsorption of pyridine has been investigated with the intention of characterizing the active acidic species present on the spinel phase. The spinel samples were subjected to pyridine vapour adsorption at room temperature for 24 h and then IR spectra were taken in the DRIFT mode in the range 1400-1800 cm⁻¹. The spectra of some of the representative samples are shown in Fig.3.2.2 and 3.2.3.

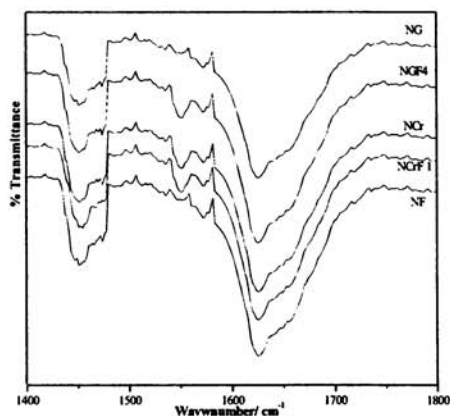


Fig.3.2.2 IR spectra of pyridine adsorbed ferrites, gadolinite and chromite.

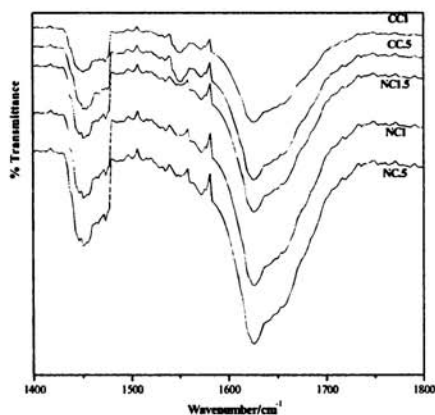


Fig.3.2.3 IR spectra of pyridine adsorbed cobaltites.

Important pyridine ring modes occur at approximately 1606, 1573, 1485 and 1446 cm⁻¹ termed ν_{8a} , ν_{8b} , ν_{19a} and ν_{19b} respectively^{43,44}. According to Kline and Turkevich⁴³, ν_{8a} and ν_{19a} are symmetric ring vibrations and ν_{8b} and ν_{19b} are asymmetric ring vibrations to the two-fold rotational axis. The 8a and 19b are very sensitive with regard to the nature of intermolecular interactions via nitrogen lone pair electrons⁴⁵. There are three modes by which pyridine can be retained on the surface of oxides⁴⁶: (1) interaction of the N lone pair electron and H atom of the OH group, (2) transfer of a proton from a surface OH group to the pyridine forming a pyridinium ion (Brønsted acidity) and (3) pyridine coordination to an electron deficient metal atom (Lewis acidity). The ν_{8a} and ν_{19b} , whose positions depend up on the strength of the

adsorbing Lewis site, are taken as a measure of Lewis acid strength.

From the figures, predominant IR bands, ν_{8a} and ν_{19b} confirm that the major contribution of acidity is due to Lewis acid sites. Among the above four vibration modes, ν_{8a} is very sensitive with respect to the oxidation state, coordination symmetry and cationic environment⁴⁷. Hence it is suggested that these species are bound to terminal OH groups via hydrogen bonding. The band centered at $\sim 1540\text{ cm}^{-1}$ is attributed to pyridinium ion (Brönsted acidity). The small band at around 1480 cm^{-1} (ν_{19a}) involves both Lewis and Brönsted acid sites⁴⁸.

3.2.4 Surface electron donating properties

The utility of electron acceptor adsorption for the study of the electron donor property of the catalyst surface has been well established. Electron donor strength of a surface is defined as the conversion power of an adsorbed electron acceptor into its anion radical. It can be expressed as the limiting electron affinity value at which free radical formation is not observed. The limiting amount of electron acceptors adsorbed on the catalyst surface depends on nature of the donor sites and also on the electron affinity of the electron acceptors used. Thus, by a comparison between the limiting concentration of electron acceptors adsorbed and the electron affinity values of the respective electron acceptors, information regarding the strength and distribution of the electron donor sites can be obtained.

The electron acceptors selected for the study were tetracyanoquinodimethane (TCNQ), 2,3,5,6-tetra-chloro-4-benzoquinone (chloranil) and *p*-dinitrobenzene (PDNB) with electron affinity values 2.84,

2.40 and 1.77 eV respectively. The adsorption experiments were done after activating the samples at 500 °C for 2 h. Acetonitrile was used as the solvent for the adsorption studies. The amount of electron acceptors adsorbed increases with increase in concentration of solution containing electron acceptors. This increasing trend continues up to a particular concentration and thereafter the amount of adsorbed decreases with increase in concentration. This constant value is called the limiting amount. The limiting amount of TCNQ gives a measure of total amount of basic sites whereas limiting amount of chloranil signifies the measure of moderate and strong basic sites. The difference between the limiting amounts of TCNQ and chloranil represents a measure of weaker basic sites. Negligible adsorption of PDNB in all systems indicated the absence of very strong basic sites. The results obtained for the different spinel series are discussed below.

(a) $\text{NiCr}_x\text{Fe}_{2-x}\text{O}_4$ ($x = 0-2$) series

The limiting amounts of TCNQ and chloranil adsorbed for chromium containing nickel ferrites are shown in table 3.2.5.

Nickel ferrite is found to be more basic. Substitution of iron by chromium is found to be decreasing the basic character of the systems. Replacement of iron by more than 60 % chromium increases the basic character which shows that higher chromium content creates more basic sites but the basic strength is lower than pure nickel ferrite. The weak basic sites are represented by the difference in the limiting amounts of TCNQ and chloranil. Variation in limiting amounts of TCNQ and chloranil adsorbed follows the same trend.

Table 3.2.5 Limiting amount of electron acceptors adsorbed for chromium incorporated nickel ferrites.

Catalyst	Limiting amount adsorbed (10^{-4} mmol $l^{-1}g^{-1}$)		
	TCNQ	Chloranil	TCNQ-chloranil
NF	25.71	8.23	17.48
NCrF 1	18.12	7.12	11.00
NCrF 2	16.28	6.28	10.00
NCrF 3	12.13	5.42	6.71
NCrF 4	21.22	7.79	13.43
NCr	22.56	7.21	15.35

Pure nickel ferrite contains maximum concentration of Fe^{3+} ion at the octahedral site as compared to other chromium containing samples. For chromium containing systems, concentration of Fe^{3+} ions at octahedral site is less than that for pure nickel ferrite. Presence of more Fe^{3+} ions at the exposed octahedral site can be attributed to the high basic character of pure nickel ferrite. In the rest of the series, up to NCrF3, it is the ratio Ni^{2+}/Cr^{3+} at the O_h site which is found to control the basic character. From NCrF3, the role of Cr^{3+} becomes dominant in determining the basic character. Basicity increases from NCrF3, neglecting the role of Ni^{2+} ion. Although this is the case, basic strength of rest of the samples are less than that of pure nickel ferrite and this is due to the diminished concentration of Fe^{3+} ions at the octahedral site in the rest of the series.

Characterization and surface properties

(b) $\text{NiGd}_x\text{Fe}_{2-x}\text{O}_4$ ($x = 0-2$) series

Limiting amounts of TCNQ and chloranil adsorbed for gadolinium containing nickel ferrites are shown in table 3.2.6.

Table 3.2.6 Limiting amount of electron acceptors adsorbed for gadolinium incorporated nickel ferrites.

Catalyst	Limiting amount adsorbed ($10^{-4} \text{ mmol l}^{-1} \text{ g}^{-1}$)		
	TCNQ	Chloranil	TCNQ-chloranil
NF	25.71	8.23	17.48
NGF 1	22.89	8.19	14.7
NGF2	18.29	8.02	10.22
NGF 3	14.11	7.76	6.35
NGF 4	12.21	6.52	5.69
NG	11.19	6.32	4.87

Incorporation of gadolinium into nickel ferrite is found to decreasing the basic strength of the systems in all regions. Nickel ferrite is the more basic and nickel gadolinite is less basic.

Concentration of Fe^{3+} ions at the O_h site is less for gadolinium containing systems as compared to pure nickel ferrite. As the concentration of Gd^{3+} ion increases, basic character decreases. Here the concentration of Ni^{2+} ions at the octahedral site does not changes up to NGF3 so it is supposed that Ni^{2+} ion has no involvement in determining the basic strength. It is the ratio $\text{Fe}^{3+}/\text{Gd}^{3+}$ at the O_h site which is found to control the basic strength. Since this ratio is decreasing with gadolinium content, basicity also decreases.

(c) Cobaltite series

The limiting amount of TCNQ and chloranil adsorbed for cobaltite series are shown in table 3.2.7.

Table 3.2.7 Limiting amount of electron acceptors adsorbed for cobaltites.

Catalyst	Limiting amount adsorbed (10^{-4} mmol l^{-1} g^{-1})		
	TCNQ	Chloranil	TCNQ-chloranil
NC .5	22.23	9.13	13.10
NC 1	20.19	9.06	11.13
NC 1.5	19.22	8.32	10.90
CC .5	16.80	8.25	8.55
CC 1	16.44	8.12	8.32

In nickel cobaltite series, NC.5 and in copper cobaltite series, CC.5 are found to be more basic. Incorporation of more Ni^{2+} into nickel cobaltite is found to decreasing the basic character both in strong and weak regions. Nickel cobaltites are inverse in nature i.e., Ni^{2+} ion occupies octahedral site. Incorporation of more and more nickel causes more Ni^{2+} ions to occupy octahedral sites and basicity decreases. Here it is the ratio Co^{3+}/Ni^{2+} at the O_h site which is controlling the basic strength. For copper cobaltite series, incorporation of more Cu^{2+} ions decreases the basicity. Here also Co^{3+} ion has dominant role in determining the basicity. System having high Co^{3+}/Cu^{2+} ratio at the O_h site is more basic.

3.2.5 Cyclohexanol decomposition reaction

The functionality of an oxide catalyst can be determined by cyclohexanol decomposition reaction⁴⁹⁻⁵¹. The surface acid-base and redox properties of a catalyst are related to the selectivity of the products^{52,53}. Spinel oxides contain both acidic and basic sites and the amphoteric nature of the cyclohexanol permits their interaction with acidic and basic sites. The formation of cyclohexene by dehydration is linked to the acidic property and the dehydrogenation leading to the formation of cyclohexanone is linked to the combined effects of both acidic and basic properties⁵⁴. A proposed mechanism⁵¹ for the decomposition of cyclohexanol is depicted in Fig.3.2.4.

Besides cyclohexene and cyclohexanone, phenol, benzene, cyclohexane and methylcyclopentane are also reported to form during this reaction⁴⁹. Cyclohexanol decomposition reaction was performed over different spinels in vapour-phase at 250 °C for a time period of 2 h and the products were analyzed by GC fitted with FID (column-carbovax, N₂ carrier gas) by comparing the retention times with standards. Cyclohexene and cyclohexanone were the observed reaction products. The data for cyclohexanol decomposition reaction is shown in table 3.2.8.

(a) NiCr_xFe_{2-x}O₄ (x = 0-2) series

The percentage conversion of cyclohexanol was increased with incorporation of chromium. Higher percentage of chromium is found to decreasing the cyclohexanol conversion. Cyclohexene selectivity follows the same trend as that of cyclohexanol conversion. No such variation was observed for cyclohexanone selectivity. Variation of cyclohexene selectivity is parallel to the variation of acidity values obtained from the NH₃-TPD studies.

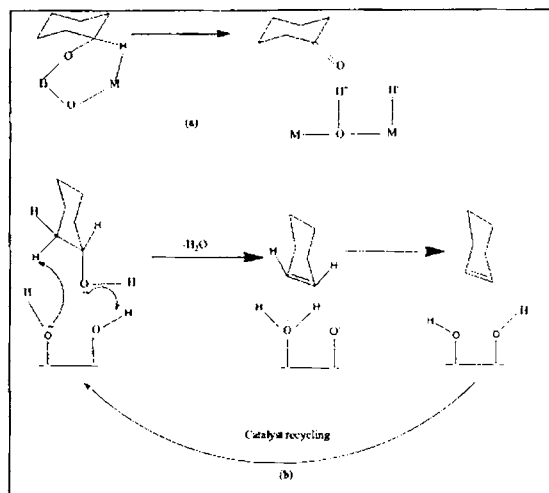


Fig.3.2.4 Mechanism (a) dehydrogenation and (b) dehydration of cyclohexanol on oxide surface.

Replacing iron by chromium is found to increase the acid strength of pure nickel ferrite, but after NCrF_3 , the total acidity decreases. Nickel chromite is more acidic than nickel ferrite which is evident from the low cyclohexene selectivity for nickel ferrite. Only nickel ferrite shows high dehydrogenation activity producing cyclohexanone which is attributed to its high basic strength in that series. Incorporation of chromium up to NCrF_3 creates strong acidic centers and after that acidic strength decreases. A moderate concentration of Cr^{3+} and Ni^{2+} may be responsible for the higher activity of NCrF_3 .

(b) $\text{NiGd}_x\text{Fe}_{2-x}\text{O}_4$ ($x = 0-2$) series

Characterization and surface properties

Table 3.2.8 Reaction data for cyclohexanol decomposition.

Catalyst	Cyclohexanol conversion (%)	Selectivity (%)	
		Cyclohexene	Cyclohexanone
NF	43.9	71.4	28.6
NCrF 1	85.3	89.5	9.4
NCrF 2	89.9	91.4	6.9
NCrF 3	90.8	94.4	5.2
NCrF 4	88.2	83.1	6.5
NCr	80.3	80.5	3.8
NGF 1	90.3	81.2	10.5
NGF2	92.4	92.5	6.7
NGF 3	94.0	93.6	5.3
NGF 4	94.5	94.0	5.6
NG	95.0	99.0	1.0
NC .5	86.9	90.3	1.0
NC 1	91.3	92.5	--
NC 1.5	100	94.6	--
CC .5	89.8	96.3	2.6
CC 1	93.2	97.4	2.3

Temperature-250 °C, flow rate-4 mlh⁻¹, TOS- 2 h, catalyst-0.5 g.

Both cyclohexanol conversion and cyclohexene selectivity are increasing with increase in the percentage of gadolinium. Substitution of gadolinium for iron is found to increase the acidity in the weak, medium and strong regions (from NH₃-TPD) and this gradation is clearly reflected in their activity, and

selectivity towards cyclohexene, which is believed to be formed by action of acid sites. Gadolinium, on replacement of iron, enters into the octahedral site and is responsible for the enhancement of acidity. Entry of Gd^{3+} ions into the more exposed octahedral site might have created strong acidic centers. The dehydration activity, which is a measure of acidic strength, is gradually increasing with the incorporation of Gd^{3+} ions at the octahedral site.

(c) Cobaltite series

For cobaltite series, the selectivity towards cyclohexene is found to be directly proportional to the variation of acidic strength. From NH_3 -TPD studies it was found that copper cobaltites are more acidic than nickel cobaltites. Incorporation of more Ni^{2+} or Cu^{2+} ions into the cobaltites is found to increasing the acidic strength and this is clearly reflected in the selectivity towards cyclohexene.

In the case of nickel cobaltite series, increase in percentage of Ni^{2+} increases the acidic strength in the weak and medium region. Cyclohexene selectivity is in parallel with this result. It is supposed that the weak and medium acid sites are involved in catalyzing the cyclohexanol decomposition reaction. Many authors^{55,42}, during their investigation of different organic test reactions over acid-base catalysts, have concluded that weak to medium acid sites were responsible for dehydration. Fig.3.2.5 and 3.2.6 shows correlation diagram of cyclohexene selectivity with weak+medium acidity.

3.2.6 Cumene cracking reaction

Cumene cracking reaction was chosen as a test reaction for acidity

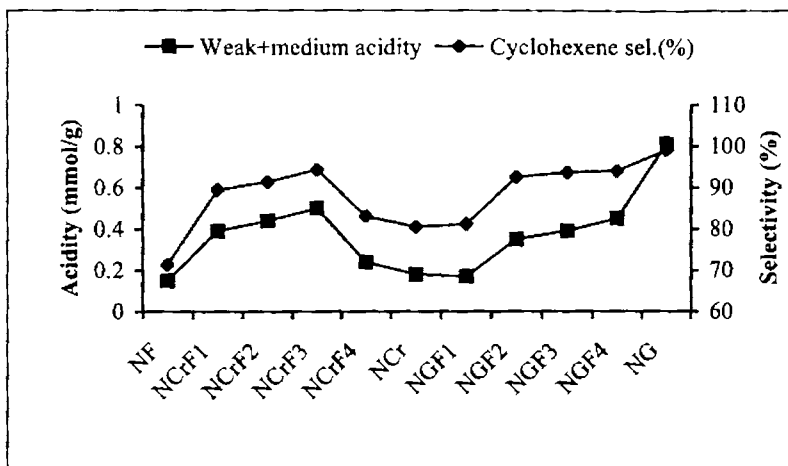


Fig.3.2.5 Weak+medium acidity Vs cyclohexene selectivity for ferrites.

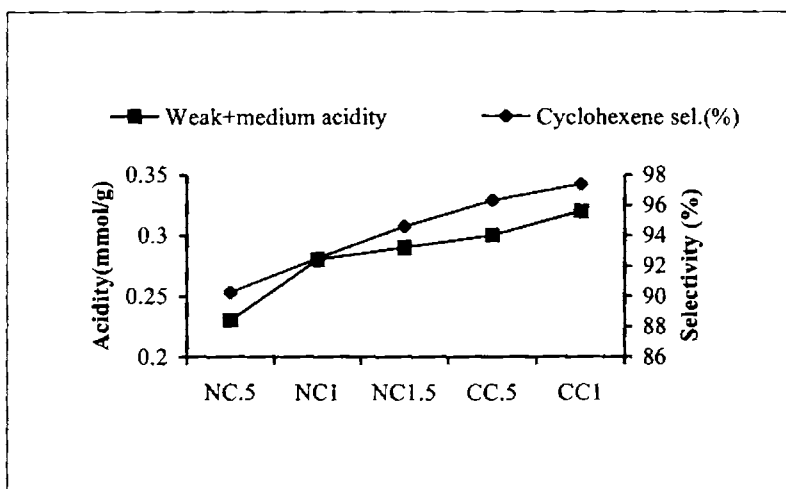


Fig.3.2.6 Weak+medium acidity Vs cyclohexene selectivity for cobaltites.

Chapter 3

where the cumene conversion and the relative product selectivity could be correlated with the surface acidic properties. In vapour phase cumene cracking, α -methyl styrene and benzene were obtained as the major products while ethyl benzene, toluene and styrene were appeared in minor quantities. Cumene cracking was carried out in vapour phase at 350 °C at a flow rate of 4 mlh⁻¹ and with a time on stream 2 h. In the present case the various cracking products such as, toluene, styrene and ethyl benzene were considered together while calculating the selectivities. Cumene conversion and product selectivities over different spinel systems are shown in table 3.2.9.

Selectivities for various products furnished in the table indicates that dehydrogenation of cumene to α -methyl styrene is the predominant reaction. For chromium containing nickel ferrites, substitution of iron by chromium leads to an enhancement in catalytic activity towards cumene conversion compared to pure nickel ferrite. Cumene conversion and selectivity towards α -methyl styrene increases up to NiCrF₃ and then decreases. Replacing Fe³⁺ by Gd³⁺ has a different effect on the cracking of cumene. Both cumene conversion as well as α -methyl styrene selectivity increases gradually upon iron substitution by gadolinium.

In cobaltite series, copper cobaltites show little enhanced activity compared to nickel cobaltites. For both the cobaltites, the activity is found to be very much dependent on the percentage of Ni²⁺ and Cu²⁺ in their series. An increase in percentage of Ni²⁺ and Cu²⁺ ions in nickel and copper cobaltites leads to more cumene conversion and more α -methyl styrene selectivity.

Cumene cracking reaction is known to be catalyzed by strong or moderate acid sites^{56,57}. Major reactions occurring during cumene conversion

Characterization and surface properties

Table 3.2.9 Reaction data for cumene cracking reaction.

Catalyst	Cumene conversion (%)	Selectivity (%)		
		α -methyl styrene	Benzene	Others
NF	14.4	83.4	10.9	5.7
NCrF 1	17.2	92.4	4.5	3.1
NCrF 2	25.2	93.3	3.2	3.5
NCrF 3	26.0	95.5	2.2	2.3
NCrF 4	21.7	89.1	5.9	5.0
NCr	12.0	84.7	11.9	3.4
NGF 1	17.5	85.8	4.2	10.0
NGF2	21.2	86.5	12.5	1.0
NGF 3	26.1	87.5	10.5	2.0
NGF 4	27.9	90.1	9.9	--
NG	28.1	94.6	5.4	--
NC .5	20.2	80.8	10.1	9.1
NC 1	21.4	90.1	5.8	4.1
NC 1.5	23.9	91.5	6.6	1.9
CC .5	23.95	88.4	10.3	1.3
CC 1	24.2	93.3	5.6	1.2

Temperature-350 °C, flow rate-4 mlh⁻¹, TOS-2 h, catalyst-0.5 g.

may be grouped into dealkylation (cracking) and dehydrogenation. Cracking of cumene is generally attributed to the action of Brönsted acid sites by a carbonium ion mechanism while dehydrogenation of cumene yields α -methyl

styrene as the major product, the formation of which has been ascribed to the Lewis acid sites⁵⁸⁻⁶⁰. The selectivity towards dehydrogenated products may be thus related to the Lewis acidity of the systems and the generation of cracking products with the Brönsted acidity of the systems. Boorman et al. prepared a series of catalysts containing fluoride, cobalt and molybdenum as additives to γ -alumina, both individually and in combination and the surface acidity of these systems was correlated with their reactivity for cumene conversion^{61,62}. Sohn et al.⁶³ correlated the activity for cumene dealkylation with both acidity and acid strength distribution of sulphated ZrO_2 - SiO_2 catalysts.

In our case, the cumene conversion seemed to dependent on the total amount of acid sites. Pure nickel ferrite is less active compared to chromium and gadolinium containing systems and the gradation in activity is seem to be parallel to the variation in total acidity obtained from NH_3 -TPD studies. Similar is the case for cobaltite series. The trend in α -methyl styrene selectivity can be very well correlated with the trend in the limiting values obtained for perylene adsorption studies i.e., Lewis acidity.

The correlation between the limiting amount of perylene from the adsorption studies and the dehydrogenation selectivity is presented in Fig.3.2.7 and 3.2.8. The figure gives a proportional relationship between the two, supporting the fact that Lewis sites are responsible for the dehydrogenation. Comparing the percentage cumene conversion with total acidity of the systems from NH_3 -TPD studies, we can conclude that the cumene conversion is related to the total acidity of the systems (Fig.3.2.9 and 3.2.10).

Regarding the mechanism of cumene cracking reaction, many authors have proposed different mechanisms. Corma et al. reported that dealkylation of

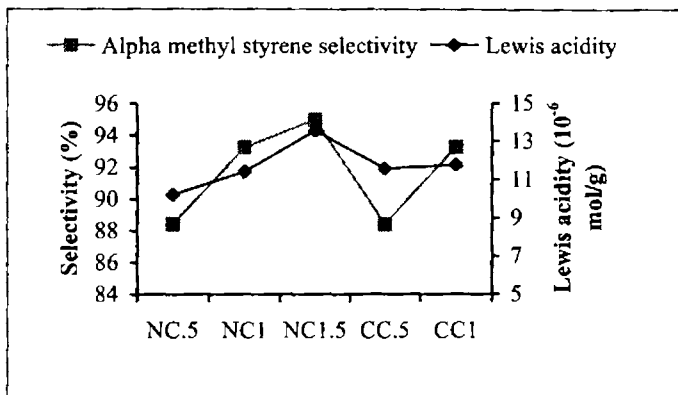


Fig.3.2.7 Lewis acidity Vs α -methyl styrene selectivity for cobaltites.

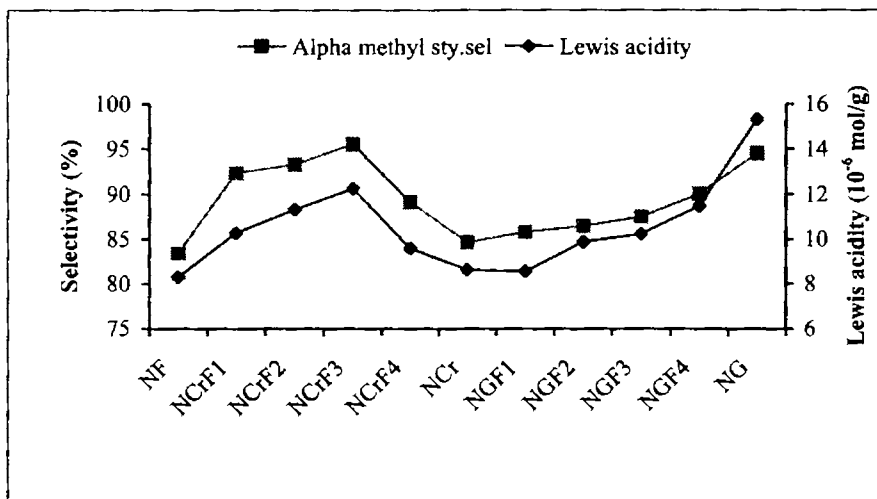


Fig.3.2.8 Lewis acidity Vs α -methyl styrene selectivity for ferrites.

cumene requires the presence of a small number of Brønsted acid sites, which are capable of formation of a σ -complex with the ipso form of the cumene molecule⁶⁴. Bautista et al. have proposed a different mechanism^{65,66}. These

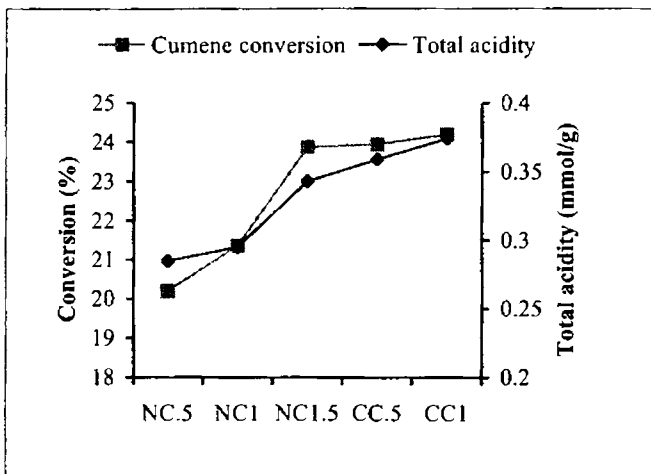


Fig.3.2.9 Cumene conversion Vs total acidity for cobaltites.

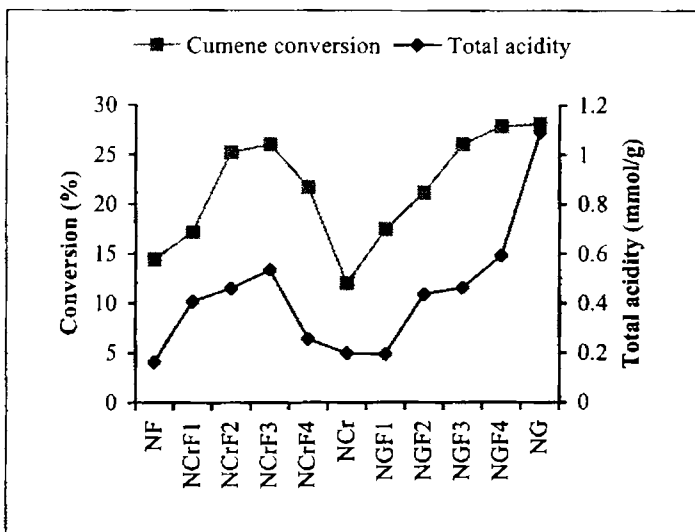


Fig.3.2.10 Cumene conversion Vs total acidity for ferrites.

authors assume that the Brønsted acid sites take part in the protonation of the cumene molecule which yields a π -complex of the aromatic ring and subsequently this complex is transformed to a σ -complex.

A Friedel-Crafts mechanism involving initial protonation of aromatic ring followed by the cleavage of the ring side chain bond, is generally accepted for the cumene dealkylation over acidic catalysts⁶⁷. Cracking of cumene to benzene is generally attributed to the action of Brønsted sites by a carbocation mechanism while dehydrogenation of cumene leading to α -methyl styrene, the formation of which has been ascribed to the Lewis acid sites. A plausible mechanism of cumene conversion reaction is represented in Fig. 3.2.11.

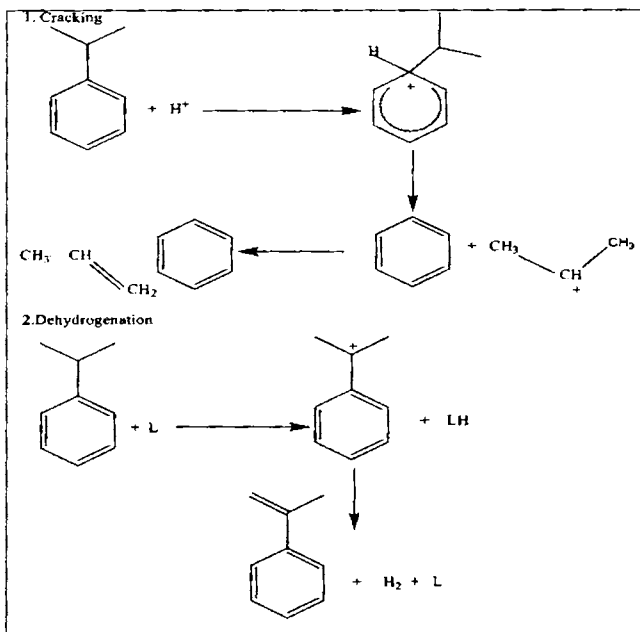


Fig.3.2.11 Mechanism of cumene conversion reaction.

References:

- [1] C.Whiston; "X-ray Methods", (Eds., F.E.Prichard), ACOL, Thames Polytech., London, 1991.
- [2] W.J.King and A.C.C.Tseung, *Electrochim. Acta.*, 19 (1974) 485.
- [3] Yu.E.Roginskaya, O.V.Moozova, E.N.Lubnin, Yu.E.Ulitina, G.V.Lopukhova and S.Trasatti, *Langmuir*, 13 (1997) 4621.
- [4] L.A.De Faria, M.Prestat, J.F.Koenig, P.Chartier and S.Trasatti, *Electrochim. Acta.*, 44 (1998) 1481.
- [5] J.F.Marco, J.R.Gancedo, J.Ortiz and J.L.Gautier; *Appl. Sur. Sci.*, 227 (2004) 175.
- [6] H.G.El-Shobaky; *Appl. Catal. A: Gen.*, 278 (2004) 1.
- [7] K.C.Patil; *Bull. Mater. Sci.*, 16 (1993) 533.
- [8] H.Guan, C.Shao, Y.Liu, Na Yu and X.Yang; *Solid State Commun.*, 131 (2004) 107.
- [9] L.Zhou, J.Xu, H.Miao, F.Wang and X.Li; *Appl. Catal. A: Gen.*, 292 (2005) 223.
- [10] B.Lefez, P.Nkeng, J.Lopitiaux and G.Poillerat; *Mater. Res. Bull.*, 31 (10) (1996) 1263.
- [11] R.D.Wardron; *Phys. Rev.*, 99 (1955) 1727.
- [12] W.B.White and B.A.De Angelis; *Spectrochim. Acta A.*, 23 (1967) 985.
- [13] R.Rajeev, K.A.Devi, A.Abraham, K.Krishnan, T.E.Krishnan, K.N.Ninan and C.G.R.Nair; *Thermochimica Acta.*, 254 (1995) 235.
- [14] K.Petrov, T.Karmanevo, S.Angelev and D.Mahadjiev; *Mater. Res. Bull.*, 18 (1983) 637.
- [15] G.Amthaner and G.R.Rossman; *Phys. Chem. Minerals.*, 11 (1984) 37.

- [16] G.M.Bancroft and R.G.Burns; *Geochim. Cosmochim. Acta.*, 31 (1967) 2219.
- [17] R.G.Burns; *Ann. Rev. Earth Planet. Sci.*, 9 (1981) 345.
- [18] S.J.Campell; *Astr. J. Phys.*, 37 (1984) 429.
- [19] J.M.D.Coey; “Chemical Applications of Mössbauer Spectroscopy”, (Eds., G.L.Long), Plenum Press, New York, 1 (1984) 443.
- [20] Y.Shi, J.Ding and H.Yin; *J. Alloys Compd.*, 308 (2000) 290.
- [21] Y.Ahn, E.J.Choi, S.Kim and H.N.Ok; *Mater. Lett.*, 50 (2001) 47.
- [22] Y.G.Ma, M.Z.Jin, M.L.Liu, G.Chen, Y.Sui, Y.Tian, G.J.Zhang and Y.Q.Jia; *Mater. Chem. Phys.*, 65 (2000) 79.
- [23] M.V.Kuznetsov, Q.A.Pankhurst and I.P.Parkin; *J. Phys. D: Appl. Phys.*, 31 (1998) 2886.
- [24] E.V.A.Ebsworth, D.W.H.Rankin and S.Cradock; “Structural Methods in Inorganic Chemistry”, ELBS/Blackwell Scientific Publications, Great Britain, 1987, p.287.
- [25] L.C.A.Olievira, J.D.Fabris, R.R.V.A.Rios, W.N.Mussel and R.M.Lago; *Appl. Catal. A: Gen.*, 259 (2004) 253.
- [26] T.Moyo, J.Z.Msomi and K.Bharuth-Ram, *Hyperfine interactions.*, 136/137 (2001) 579.
- [27] H.M.widatallah, C.Johnson, F.Bery and M.Pekala; *Sol. State Commun.*, 120 (2001) 171.
- [28] N.N.Greenwood and T.C.Gibb, “Mössbauer Spectroscopy”, Chapman and Hall, London, 1971, p.259.
- [29] K.H.Rao, S.B.Raju, R.G.Mendiratta and J.P.Eymery; *Sol. State Commun.*, 45 (1983) 919.

- [30] R.E.Watson and A.J.Freeman; *Phys. Rev.*, 123 (1961) 2027.
- [31] A.K.Ghatage and S.A.Patil; *Sol. State Commun.*, 98 (10) (1996) 885.
- [32] M.Lenglet, A.D'huysser and C.K.Jorgensen; *Inorganica Chimica Acta.*, 133 (1987) 61.
- [33] A.M.Gismelseed and A.A.Yousif; *Physica B.*, 370 (2005) 215.
- [34] E.E.Sileo and S.F.Jacob; *Physica B.*, 354 (2004) 241.
- [35] M.Z.Said; *Mater. Lett.*, 34 (1998) 305.
- [36] J.-G.Kim, D.L.Pugmire, D.Bottaglia and M.A.Langell; *Appl. Sur. Sci.*, 165 (2000) 70.
- [37] J.L.Gautier, E.Trollund, E.Rios, P.Nkeng and G.Poillerat; *J.Electrochemical Chemistry.*, 428 (1997) 47.
- [38] K.Vijayakumar and D.Ravinder; *Mat. Lett.*, 52 (2002) 166.
- [39] H.Knozinger and P.Ratnaswami; *Catal. Rev.-Sci.Eng.*, 17 (1979) 31.
- [40] J.P.Beaufils and Y.Barboux; *J. Chem. Phys.*, 78 (1981) 347.
- [41] A.Aurox and A.Gervasini; *J. Phys. Chem.*, 94 (1990) 6371.
- [42] M.A.Aramendia, V.Borau, I.M.Garcia, C.Jimenez, A.Marinas, J.M.Marinas, A.Porras and F.J.Urbano; *Appl. Catal.*, 184 (1999) 115.
- [43] C.H.Kline and J.Turkevich; *J. Chem. Phys.*, 12 (1944) 300.
- [44] C.Morterra, A.Chiorino, G.Ghiotti and E.Garrone; *J. Chem. Soc. Faraday Trans.1* 75 (1979) 271.
- [45] H.Knozinger; *Adv. Catal.*, 25 (1976) 184.
- [46] G.Busca; *Catal. Today*, 27 (1996) 323.
- [47] G.Busca; *Catal. Today*, 41 (1998) 191.
- [48] S.P.Ghorpade, V.S.Darshane and S.G.Dixit; *Appl. Catal. A: Gen.*, 166 (1998) 135.

- [49] N.J.Jebarathinam and V.Krishnaswamy; "Catalysis: Present and Future" (Eds., P.Kanta Rao and R.S.Beniwai), Wiely Eastern Ltd., New Delhi, 1995, p.354.
- [50] M.V.Joshi, S.G.Oak and V.S.Darshane; "Catalysis: Modern Trends"; (Eds., N.M.Gupta and D.K.Chakrabarthy), Narosha Publishing house, New Delhi, 1995, p.275.
- [51] C.P.Bezouhanova and M.A.Al-Zihari; Catal. Lett., 11 (1991) 245.
- [52] K.Tanabe, M.Misono, I.Ono and N.Hattori; Stud. Surf. Sci. Catal., 51 (1989).
- [53] J.M.Winterbottom; "Catalysis", Royal Soc. Chem., 4 (1981) 141.
- [54] M.Ai; Bull. Chem. Soc. Jpn., 50 (10) (1997) 2579.
- [55] C.G.Ramankutty, S.Sugunan, B.Thomas; J. Mol. Catal. A: Chem., 187 (2002) 105.
- [56] Y-Y.Huang, B-Y.Zhao and Y-C.Xie; Appl. Catal. A: Gen., 171 (1998) 65.
- [57] S.J.Decanio, J.R.Sohn, P.O.Pauel and J.H.Lunsford; J. Catal., 101 (1986) 132.
- [58] A.Corma and B.W.Wojciechowski; Catal. Roy. Sci. Eng., 24 (1982) 1.
- [59] J.W.Ward; J. Catal., 9 (1967) 225.
- [60] W.Przystajko, R.Fieddorow and I.G.Dalla Lana; Appl. Catal., 15 (1985) 265.
- [61] P.M.Boorman, R.A.Kydd, Z.Sarbak and A.Somogyvari; J. Catal., 96 (1985) 115.
- [62] P.M.Boorman, R.A.Kydd, Z.Sarbak and A.Somogyvari; J. Catal., 100 (1986) 287.

Chapter 3

- [63] J.R.Sohn and H.J.Jang; *J. Mol. Catal.*, 64 (1991) 349.
- [64] A.Corma, J.L.G.Fiero, R.Montanana and F.Thomas; *J. Mol. Catal.*, 30 (1985) 361.
- [65] F.M.Bautista, J.M.Campelo, A.Garcia, D.Leina, J.M.Marinas, A.A.Romero, J.A.Navio and M.Macias; *J. Catal.*, 145 (1994) 107.
- [66] F.M.Bautista, J.M.Campelo, A.Garcia, D.Leina, J.M.Marinas and A.A.Romero; *Appl. Catal.*, 104 (1993) 109.
- [67] N.Y.Chen, W.W.Kaeding and F.H.Dwyer; *J. Am. Chem. Soc.*, 101 (1979) 6783.

Chapter 4

Alkylation Reactions

Alkylation is the transfer of an alkyl group from one molecule to another. The alkyl group may be transferred as an alkyl carbocation, a free radical or a carbanion. It is one of the most important research targets in organic chemistry. Alkylation is accomplished by using the functional groups as alkyl electrophile, alkyl nucleophile or sometimes as alkyl radical. This chapter presents Friedel-Crafts vapour phase alkylations of aniline, phenol and *m*-cresol. The Friedel-Crafts reaction is of wide scope, principally for introducing carbon substituents into an aromatic ring. Friedel-Crafts alkylation attaches an alkyl group, using an alkyl halide, alcohol or olefine. The choice of the reagent and catalyst is normally dictated by the reactivity of the aromatic substrate. Activated benzene rings require milder electrophiles to bring about the reaction, while deactivated benzene rings need more vigorous reagent/catalyst combinations. The reaction is an aromatic electrophilic substitution, the attacking electrophile being generated by the interaction of the reagent with the acid catalyst.

The chapter is divided into four sections. The first two sections deals with the methylation and *tert* butylation of phenol. Third chapter deals about the thymol synthesis i.e., isopropylation of *m*-cresol. Alkylation of aniline using methanol as the alkylating agent is presented in the last section. Influence of various reaction parameters such as feed ratio, temperature, flow rate etc. were investigated. An attempt has been made to correlate the activity of the catalysts with their acid-base properties.

4.1 Phenol Methylation

Alkyl phenols are industrially important compounds, used either directly or as chemical intermediates in the manufacture of pesticides, herbicides, plastics and a variety of chemicals¹. *O*-cresol is used in the synthesis of herbicides. 2,6-xyleneol is a monomer in the manufacture of polyphenylene oxide (PPO) and special grade paints. So the choice of a suitable catalyst and the proper operating condition is of primary importance in determining the industrial convenience of the process. A schematic representation of the various reaction pathways of phenol alkylation using methanol as the alkylating agent is presented in Fig 4.1.1.

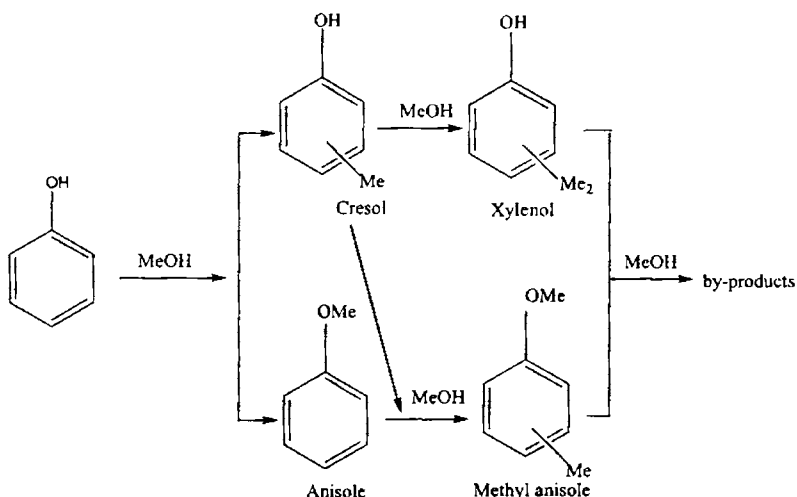


Fig.4.1.1 Reaction scheme for phenol alkylation using methanol.

Several types of solid acid/base catalysts based on zeolites, oxides and hydrotalcite like materials have been examined for this reaction^{2,9}. However,

low life time, very high reaction temperature or poor product selectivity make such systems less attractive to chemical industries. Frequently, due to coke formation, catalysts deactivate with time. The commercial process for the synthesis of *o*-cresol and 2,6-xylend is mainly based on magnesium oxide and supported vanadium iron mixed oxide¹⁰. Generally, the oxide catalysts show better selectivity than zeolites and it was pointed out that Brönsted acid sites are responsible for coke formation².

Mixed metal oxide materials are good alternative to both zeolites and aluminium phenolate for selective *ortho* alkylation using olefins/alcohols since undesired *para* alkylated products can be brought down considerably¹. Among the various oxides, transition metal oxides based on iron oxide in combination with other oxides such as CdO, SnO₂, CeO₂, NiO, CaO, Cr₂O₃, and ZrO₂ show high selectivity to *ortho* methylation^{1,11-18}. Alkylation agents, such as C₁-C₄ alcohols, various olefines, and dimethyl carbonate are widely employed for alkylation. The reaction is sensitive to the acidic and basic properties of the catalysts, the mol ratio of the reactants and the type of the alkylating agent. These studies revealed that there is always a competition between O - and C - alkylation and that acid-base properties of the catalysts played an important role in the product selectivity. Kotanigowa and co-workers^{12,17,18} studied the adsorption behaviour of phenol and methanol on a ZnO – Fe₂O₃ system and highlighted the importance of acid-base sites for the selective *ortho* methylation.

Recently, spinel oxides are widely used to catalyse these types of reactions. Thomas Mathew et al. have successfully employed low temperature co-precipitation method for the synthesis of Cu_{1-x}Co_xFe₂O₄ catalyst system and

these catalysts are found to be highly active towards *ortho* methylation of phenol¹⁹⁻²¹. Sreekumar and Sugunan have prepared ferrosphenel based on Zn, Co and Ni and studied the phenol methylation reaction^{22,23}. They have concluded that acidity of catalyst plays the decisive role in determining the catalyst activity.

To improve the catalyst performance of ferrites, modifying cations can be introduced into the structure. In these alkylation processes, the activity is mainly attributed to the presence of Lewis acid sites, as deactivation occurs on Brönsted sites^{2,24}.

This section gives detailed discussion on vapour phase phenol alkylation reaction with methanol as the alkylating agent over the prepared spinels. *O*-Cresol and 2,6-xyleneol were the important products formed. *O*-alkylation leading to anisole was observed in negligible amount. A description of process optimization such as effect of reaction temperature, effect of flow rate, effect of methanol to phenol molar ratio is also included in this section.

4.1.1 Process Optimization

The vapour phase alkylation of phenol using methanol was carried out in a vertical flow type reactor of 2 cm ID and 30 cm length, kept in a cylindrical furnace mounted vertically and at atmospheric pressure. 0.5 g of the catalyst activated at 500 °C for 2 h was placed in the middle of the reactor and packed with silica beads. The temperature of the reactor was maintained by means of a thermo couple. A pre-mixed phenol-methanol solution was introduced at the top of the reactor by means of a syringe pump. The products were analyzed by gas chromatography (Chemitto GC 1000, FID, SE 30

column-2 m length, N₂ carrier gas). Product identification was done by comparing the retention times with standards.

4.1.1.1 Effect of methanol to phenol molar ratio

In order to choose an optimum feed mix ratio, a series of reactions were performed over NCrF₄ with several methanol to phenol molar ratios at a temperature of 350 °C. C-alkylated products such as *o*-cresol and 2,6-xyleneol were the major reaction products observed. Anisole is obtained only in negligible amounts (< 0.5 %). Variation in phenol conversion and product selectivities with change in methanol to phenol molar ratio is presented in the following figure (Fig.4.1.2).

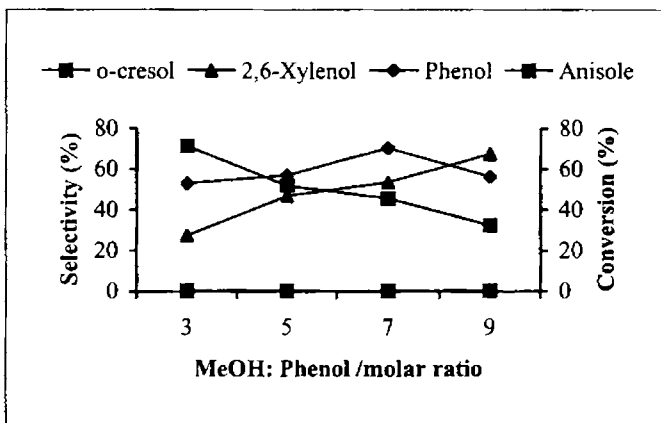


Fig.4.1.2 Effect of MeOH to phenol molar ratio on phenol methylation.

Temperature-350 °C, flow rate – 4 mlh⁻¹, time-2 h, catalyst-NCrF₄.

At lower methanol to phenol molar ratios, phenol conversion was less and a progressive increase was observed up to a molar ratio of 7 and then decreased. Amount of *o*-alkylated product, anisole remained more or less

constant through out the molar ratios studied. Selectivity towards *o*-cresol was maximum at lower methanol to phenol molar ratio and decreases at higher molar ratios; where as the selectivity for 2,6-xylenol follows the reverse trend. *o*-cresol and 2,6-xylenol showed a combined selectivity of greater than 96 %. Since maximum phenol conversion was observed for a methanol to phenol molar ratio of 7, this feed mix ratio was selected for further studies.

4.1.1.2 Effect of reaction temperature

Phenol methylation was carried out over NCrF₄ in the temperature range 300-450 °C at a methanol to phenol molar ratio of 7. Phenol conversion and product selectivities at different temperatures were shown in Fig. 4.1.3.

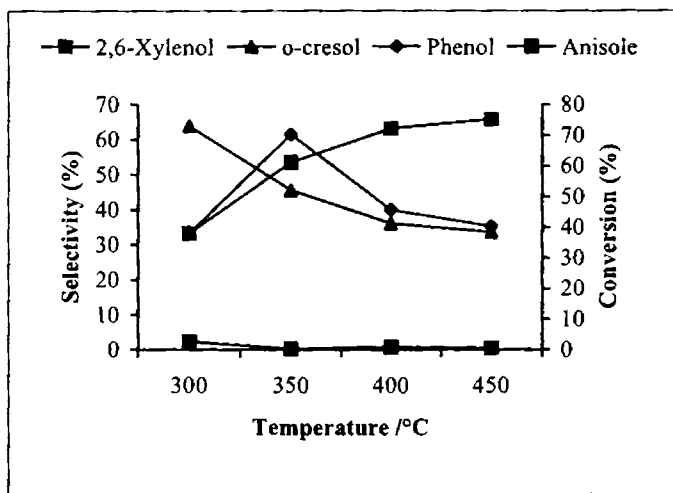


Fig. 4.1.3 Effect of temperature on phenol methylation.

MeOH:p - 7:1, flow rate - 4 mlh⁻¹, time-2 h, catalyst-NCrF₄.

Phenol conversion increased with rise in temperature up to 350 °C. At

temperatures higher than 350 °C, phenol conversion showed a drastic decrease. Temperature did not show any marked influence on *o*-alkylation and anisole obtained less than 3 % through out the temperature region studied. The reaction mainly yields *ortho* methylated products, with total *ortho* selectivity greater than 97 %. With increase in temperature, the rate of consecutive methylation of *o*-cresol to 2,6-xyleneol is increased; maximum yield of 2,6-xyleneol was observed at 450 °C. Since maximum phenol conversion obtained at 350 °C and thereafter decreased, the reaction temperature of 350 °C was selected for further studies.

4.1.1.3 Effect of flow rate

The effect of flow rate on phenol conversion and product selectivity at 350 °C over NCrF4 at a methanol/phenol molar ratio of 7 is shown in Fig. 4.1.4.

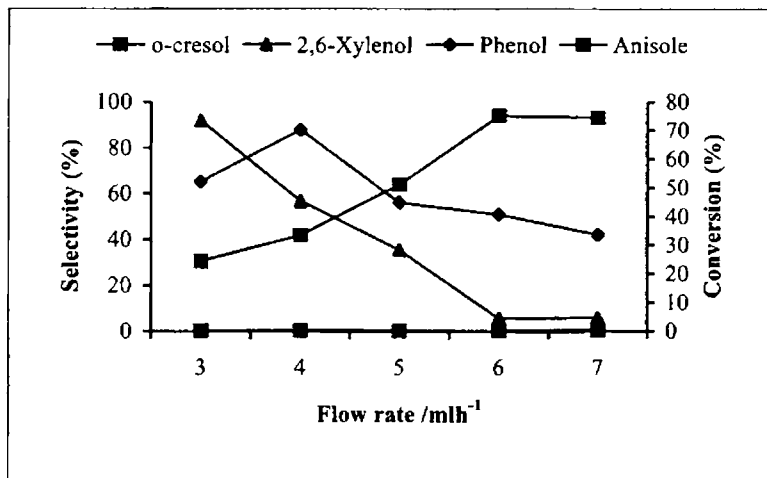


Fig.4.1.4 Effect of flow rate on phenol methylation.

Temperature- 350 °C, MeOH:p-7:1, time-2 h, catalyst-NCrF4.

The reaction shows a maximum phenol conversion at a flow rate of 4 mlh^{-1} . Phenol conversion decreased drastically at higher flow rates. At higher flow rates, the residence time of the reactant molecules over the catalyst surface is less compared to the lower flow rates resulting in lower phenol conversions. At lower contact time, *o*-cresol was observed as a major product with negligible amount of 2,6-xylenol. Higher contact time resulted in an increase in the formation of 2,6-xylenol, and this was allied with a resultant decrease in *o*-cresol yield. This is an indication of the consecutive methylation of *o*-cresol over the catalyst surface at higher contact time. Anisole concentration virtually remained unaffected with space velocity variations.

4.1.2 Effect of catalyst composition

Phenol methylation was carried out over the different spinel systems at a temperature of $350 \text{ }^\circ\text{C}$ and a methanol to phenol molar ratio of 7. A flow rate of 4 mlh^{-1} was used. C-alkylation was found to be predominant over O-alkylation.

(a) $\text{NiCr}_x\text{Fe}_{2-x}\text{O}_4$ ($x = 0$ to 2) series

A series of experiments were performed over the chromium containing nickel ferrites. The phenol conversion and product selectivities were shown in table 4.1.1.

Replacement of iron by chromium is found to be increasing the activity of the systems towards phenol methylation. Phenol conversion increases with chromium content up to NCrF_3 and decreases there after. Replacement of iron by 60 % chromium results in maximum activity with a phenol conversion of 93.9 %. Presence of chromium is also favourable for the production of more

Table 4.1.1 Alkylation of phenol with methanol over $\text{NiCr}_x\text{Fe}_{2-x}\text{O}_4$ type systems.

Catalyst	Phenol conversion (%)	Selectivity (%)		
		<i>o</i> -cresol	2,6-xyleneol	Anisole
NF	57.4	57.8	39.8	2.4
NCrF 1	75.3	53.5	45.5	1.0
NCrF 2	78.1	43.8	55.3	0.9
NCrF 3	93.9	13.6	86.3	0.1
NCrF 4	63.9	30.8	66.7	2.5
NCr	60.2	32.8	67.0	0.2

Temperature-350 °C, flow rate-4 mlh⁻¹, MeOH:phenol-7:1, time-2 h.

and more 2,6-xyleneol, where as for *o*-cresol, a reverse trend was observed. Both phenol conversion and selectivity towards 2,6-xyleneol varies in similar manner. Anisole is formed only in negligible amounts.

Since phenol is a polar molecule, even very weak basic sites can easily remove a H⁺ from phenolic O-H bond forming phenolate ion. The phenolate ion then co-ordinate with the acidic site of the catalyst. Therefore in phenol alkylation, it is the acidity rather than basicity that controls the catalytic activity.

The trend in which phenol conversion varies is in accordance with the variation of acid-base properties of the systems on incorporation of chromium into nickel ferrite. Replacing iron by chromium is found to increasing the total acidity of the systems as revealed from the ammonia TPD studies. The result

Alkylation Reactions

of cyclohexanol decomposition reaction enlightens evidence to this trend where we observed maximum cyclohexene selectivity for NCrF₃, which is having maximum acidity in that series. The limiting concentration values of electron acceptors adsorbed are very low for NCrF₃ which show that it is least basic, The acid-base properties of NCrF series along with the phenol conversion are presented in table 4.1.2.

Table 4.1.2 Acid-base properties and phenol conversion of NiCr_xFe_{2-x}O₄ type systems.

Catalyst	Dehydration activity (%) (Cyclohexene sel.)	Total acidity (mmol g ⁻¹)	Limiting amount (10 ⁻⁴ mmol l ⁻¹ g ⁻¹)		Phenol conversion (%)
			TCNQ	Chloranil	
NF	71.4	0.162	25.71	8.23	57.4
NCrF 1	89.5	0.406	18.12	7.12	75.3
NCrF 2	91.4	0.460	16.28	6.28	78.1
NCrF 3	94.4	0.533	12.13	5.42	93.9
NCrF 4	83.1	0.256	21.22	7.79	63.9
NCr	80.5	0.197	22.56	7.21	60.2

In spinel catalysis, the distribution of cations in octahedral and tetrahedral sites is playing an important role in determining the catalytic activity. Due to the lower co-ordination number of the tetrahedral cations, the attractive force for a single tetrahedral M-O bond will be strong. Since each octahedral cation is surrounded by more number of anions, the octahedral M-O bond will be weaker, and hence will be more polar. Additionally, using low

energy ion scattering (LEIS), a technique that is sensitive to the outer most atomic layer, Jacobs et al.²⁵ revealed that spinel surface sites are mainly octahedral and hence the octahedral cations are mainly exposed on the surface. In the case of chromium containing nickel ferrites, chromium occupies O_h site, where as iron equally occupies O_h and T_d site. Ni^{2+} goes to T_d site only after $x = 0.8$. Systems having low x values are rich in Ni^{2+} where as those having high x values are rich in Cr^{+3} ions at the O_h site. In this series, it is the ratio, Cr^{+3}/Ni^{2+} which is controlling the catalytic activity. Extreme systems are having too high or too low concentration of Cr^{+3} or Ni^{2+} . $NiCrF_3$ is more active and it is supposed that, it is the moderate concentration of Cr^{+3} and Ni^{2+} ions at the O_h site that is responsible for it's high activity.

(b) $NiGd_xFe_{2-x}O_4$ ($x = 0$ to 2) series

Results obtained for the NGF systems were tabulated in table 4.1.3.

Table 4.1.3 Phenol alkylation over $NiGd_xFe_{2-x}O_4$ type systems.

Catalyst	Phenol conversion (%)	Selectivity (%)		
		<i>o</i> -cresol	2,6-xyleneol	Anisole
NF	57.4	57.8	39.8	2.4
NGF 1	65.5	66.8	31.1	2.1
NGF2	75.3	80.3	16.4	3.3
NGF 3	82.0	96.3	2.2	1.5
NGF 4	88.5	100	--	--
NG	93.5	100	--	--

Temperature-350 °C, flow rate-4 mlh⁻¹, MeOH:phenol-7:1, time-2 h.

Successive incorporation of gadolinium into nickel ferrite has a positive effect on phenol methylation. Phenol conversion increases with gradual incorporation of gadolinium and nickel gadolinite shows a maximum phenol conversion of 93.5 %. Here, the mono alkylated product- *o*-cresol is the predominant product. Systems having higher percentage of gadolinium are selectively forming *o*-cresol. Formation of anisole is observed only in few systems.

Here also, acidity of the systems is found to be the decisive factor in determining the catalytic activity. Replacement of iron by gadolinium has increased the acidity of systems and maximum acidity in that series has been obtained by the complete replacement of iron by gadolinium. This trend in acidity is clearly reflected in the phenol conversion.

Ammonia TPD studies show that the total acidity increases with gadolinium incorporation. Cyclohexanol decomposition reaction provides evidence for this trend in acidity. Selectivity towards cyclohexene, which is believed to be form by the action of acid sites, increases with gadolinium content. The limiting amount of electron acceptors adsorbed showed a decrease with gadolinium content. Acid-base properties along with phenol conversion for gadolinium containing nickel ferrites are presented in table 4.1.4.

Although phenol alkylation is essentially an acid-base reaction, the acidity of the catalysts has a decisive role in determining the activity.

In the case of NGF series, gadolinium preferably enters to the O_h site. Ni^{2+} is shifted to T_d site only after $x = 1.2$. After $x = 1.2$, the systems are having no Ni^{2+} ions at the O_h site. But phenol conversion is tending to increase with x . Hence it is supposed that Ni^{2+} ion has very little effect in catalyzing the

Chapter 4

Table 4.1.4 Acid-base properties and phenol conversion for NiGd_xFe_{2-x}O₄ systems.

Catalyst	Dehydration activity (%) (Cyclohexene sel.)	Total acidity (mmolg ⁻¹)	Limiting amount (10 ⁻⁴ mmol l ⁻¹ g ⁻¹)		Phenol conversion (%)
			TCNQ	Chloranil	
NF	71.4	0.162	25.71	8.23	57.4
NGF 1	81.2	0.195	22.89	8.19	65.5
NGF2	92.5	0.436	18.29	8.02	75.3
NGF 3	93.6	0.463	14.11	7.76	82.0
NGF 4	94.0	0.593	12.21	6.52	88.5
NG	99.0	1.094	11.19	6.32	93.5

reaction. It is the concentration of other ions present at the octahedral site which is determining the activity. The total concentration of trivalent ions present at the O_h site goes on increasing with gadolinium incorporation and activity increases in the same order. NG is more active than NGF4 and this may be due to the fact that more Gd³⁺ ions in NG might have created strong acidic centers for NG.

(c) Cobaltite series

The results of phenol methylation carried out over nickel cobaltites and copper cobaltites are shown in table 4.1.5.

Cobaltites having copper showed a high phenol conversion than those having nickel. With in nickel cobaltites, the phenol conversion was found to

Alkylation Reactions

Table 4.1.5 Phenol alkylation over cobaltites.

Catalyst	Phenol conversion (%)	Selectivity (%)		
		<i>o</i> -cresol	2,6-xyleneol	Anisole
NC .5	58.3	59.2	39.0	1.8
NC 1	61.4	57.8	39.8	2.4
NC 1.5	73.3	44.4	48.5	7.1
CC .5	80.5	39.2	58.7	2.1
CC 1	86.2	36.1	62.5	1.4

Temperature-350 °C, flow rate-4 mlh⁻¹, MeOH:phenol-7:1, time-2 h.

increase with increase in the percentage of divalent ion (nickel) in the series. Similar is the case for copper cobaltites. CCl, which is having more copper, is more active than CC.5. *o*-cresol and 2,6-xyleneol were the major products formed.

Comparing the variation in total acidity with the phenol conversion, it is revealed that the variation in activity of the systems is in accordance with the variation in acidity of the systems. Copper cobaltites are more acidic than nickel cobaltites and accordingly copper cobaltites are showing more phenol conversion. Result of cyclohexanol decomposition reaction show that more cyclohexene is formed by CCl, which is having more acidity. Limiting values of electron acceptors adsorbed shows a reverse trend of variation in acidity. Acidic-base properties along with phenol conversion for cobaltites are shown in table 4.1.6.

Incorporation of more divalent ion (nickel) into nickel cobaltite series

Cochin University of Science and Technology

Chapter 4

Table 4.1.6 Acid-base properties and phenol conversion for cobaltites.

Catalyst	Dehydration activity (%) (Cyclohexene sel.)	Total acidity (mmolg ⁻¹)	Limiting amount (10 ⁻⁴ mmol l ⁻¹ g ⁻¹)		Phenol conversion (%)
			TCNQ	Chloranil	
NC .5	90.3	0.285	22.23	9.13	58.3
NC 1	92.5	0.295	20.19	9.06	61.4
NC 1.5	94.6	0.343	19.22	8.32	73.3
CC .5	96.3	0.359	16.80	8.25	80.5
CC 1	97.4	0.374	16.44	8.12	86.2

creates more acidic centers. Similar is the case for the copper cobaltite series. But the acidic strength of nickel cobaltites is less than that for copper cobaltites and hence nickel cobaltites are less active towards phenol methylation compared to copper cobaltites.

For nickel cobaltite series, more and more Ni²⁺ ions are going to O_h site as we increase the percentage of nickel. Here it is supposed that Ni²⁺/Co³⁺ ratio which determines the catalytic activity. NC1.5, which is having high Ni²⁺/Co³⁺ ratio is more active in that series. For copper cobaltites, the system having high Cu²⁺/Co³⁺ ratio at the O_h site (CC1) is more active since it is this ratio which is supposed to control the activity.

Effect of time on stream

The spinels were checked for catalytic stability by noting the phenol conversion for a period of 9 h. The reaction is carried out at 350 °C, with a

methanol to phenol mol ratio of 7. Product analysis was done at regular intervals and the results are presented in Fig.4.1.5. All the systems showed excellent catalytic stability.

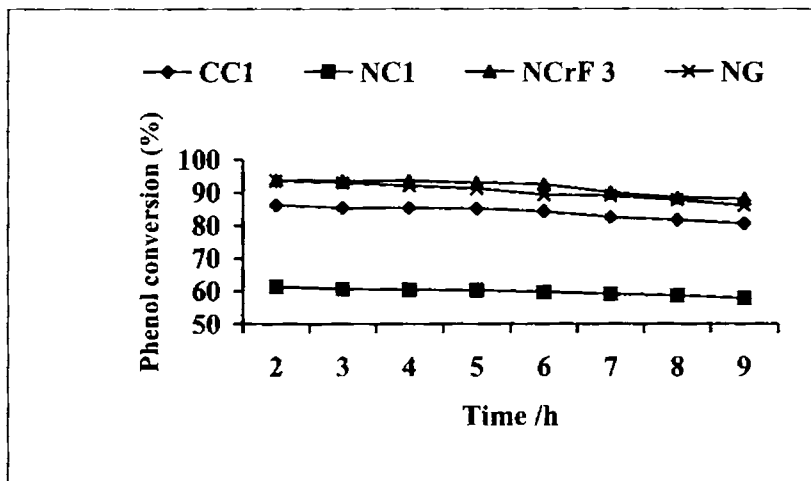


Fig.4.1.5 Effect of time on stream on phenol methylation.

Temperature-350 °C, flow rate-4 mlh⁻¹, MeOH:phenol-7:1.

4.1.3 Mechanism of phenol methylation

Both acidic and basic characters of the spinels vary with composition and therefore the variation of acid-base properties with composition is an important factor in explaining the catalytic effectiveness of the present systems. Surface acid-base property of the catalyst is a very strong influencing factor. All the spinel systems are highly selective towards *ortho* alkylation. As reported by Tanabe and Nishizaki²⁶, the Brönsted acid sites strongly interact with the aromatic ring. Such interaction make the phenol molecules orient

parallel to the catalyst surface (Fig.4.1.6) and therefore the *o* and *p* positions of the ring will become equally accessible for the incoming group leading to poor selectivity for *ortho* alkylation.

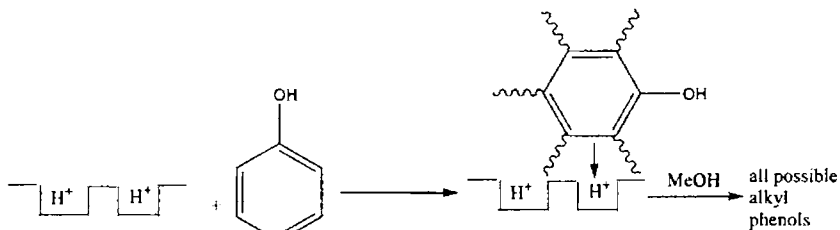


Fig.4.1.6 Parallel orientation of aromatic ring on the catalyst surface.

However for the studied catalysts, the total *ortho* selectivity was above 96 %. This observation strongly rejects the possibility of a parallel orientation of the phenol molecule over the catalyst surface. High *ortho* selectivity can be explained by assuming vertical orientation of adsorbed phenol on Lewis acid sites, as postulated for γ -alumina surface by Klemm et al.²⁷. The mechanism is shown in Fig.4.1.7, according to which the phenolate ion is adsorbed on the Lewis acid site and the hydrogen ion is bound to the basic site. This proton site activates methanol to produce a carbonium ion. It has been reported that methylation of phenol is initiated by the protonation of methanol with the aid of a Lewis acid-base pair¹⁸ and the protonated methanol attacks the *ortho* position of phenol to form the *ortho* methylated products. Protons released from phenol are quite mobile and are capable of protonating CH_3OH molecules leading to $\text{CH}_3^{\delta+}$ cations²⁸. Thus the methanol molecule is directed to adsorb on H^+ released from phenol for methylation and hence the active centers for *ortho* methylation is likely to be an acid-base pair site. Phenol itself is highly

Alkylation Reactions

polar and even very weak basic sites can easily bound with an H^+ ion from the phenol O-H bond. Moreover, phenoxide ion is resonance stabilized. Therefore a sufficiently strong acidic site is desirable for strongly interacting with the phenoxide ion. In other words, in the case of phenol alkylation, it is the acidity rather than the basicity which controls the catalytic activity.

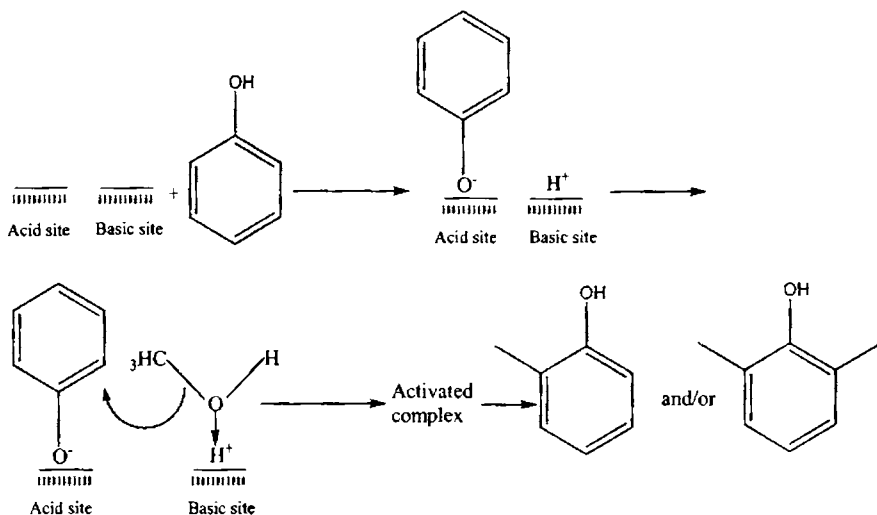


Fig.4.1.7 Reaction mechanism of phenol methylation.

4.2 Phenol *Tert* Butylation

Alkyl phenols are very valuable industrial chemicals; among which *t*-butylated phenols find many applications. 2-*t*BP is an intermediate for pesticides, fragrances and other products where as 4-*t*BP is used to make phosphate esters, fragrances and oil field chemicals. 2,4-*dt*BP is an intermediate for antioxidants and 2,6-*dt*BP is used as an antioxidant intermediate and in pharmaceuticals. Tertiary butylation of phenol is a typical Friedel-Crafts alkylation and can be catalyzed by acid sites. Various catalysts reported for tertiary butylation of phenol include Cr₂O₃, ion exchange resins, ZnO₂, sulfated zirconia, aluminium hydrotalcites, molecular sieves and zeolites including mordenite, SAPO-11, HY, H β , AlMCM-41 and FeMCM-41¹⁻¹³.

Tert butylated phenols are generally prepared by reacting phenol with pure isobutylene gas or C₄ fraction of naphtha, by using a liquid acid catalyst, giving wide product distribution. Both C- and O- alkylation are possible depending on reaction conditions such as temperature, source of isobutylene and type of catalyst. It is advantageous to generate isobutylene in situ, amongst which cracking of methyl *tert* butyl ether and dehydration of *tert* butyl ether are attractive¹⁴⁻¹⁶. Alkylation of phenol with tertiary butyl alcohol (TBA) was carried out by simultaneously employing near-critical water as the reaction solvent and catalyst to get *ortho* and *para* substituted compounds^{17,18}.

Kui Zhang et al.¹⁹ have conducted alkylation of phenol with TBA catalyzed by large pore zeolites and they arrived at the conclusion that the distribution of acid sites in the weak, medium and strong regions are responsible for the production of various isomers. Recently spinels are found to be highly active toward many aromatic alkylation reactions such as phenol

alkylation, aniline methylation, and pyridine methylation. Thomas Mathew et al.²⁰ have studied, in detail, the phenol *tert* butylation over $\text{Cu}_{1-x}\text{Co}_x\text{Fe}_2\text{O}_4$. They found good correlation between activity, in terms of phenol conversion and selectivity of various products for this reaction, and the acid base properties of the catalysts. Schematic representation of phenol *tert* butylation is shown in Fig.4.2.1.

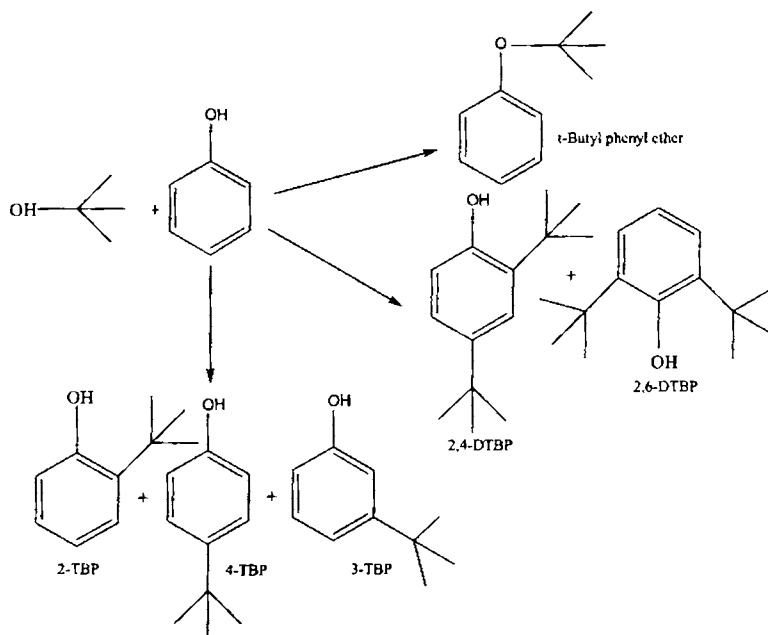


Fig.4.2.1 Reaction scheme for phenol *tert* butylation.

This section contains the study of phenol *tert* butylation reaction using TBA over different ferrites and cobaltites. Various reaction parameters were optimized and an attempt has been made to correlate the catalytic activity with acid-base properties.

4.2.1 Process optimization

Vapour phase reactions were carried out in an experimental set up as described earlier. Reaction products were collected at definite intervals and analyzed by gas chromatography.

4.2.1.1 Effect of TBA to phenol molar ratio

A series of reactions were performed over NCrF₂ at different TBA to phenol molar ratios at a temperature of 200 °C. The results obtained were shown in Fig.4.2.2.

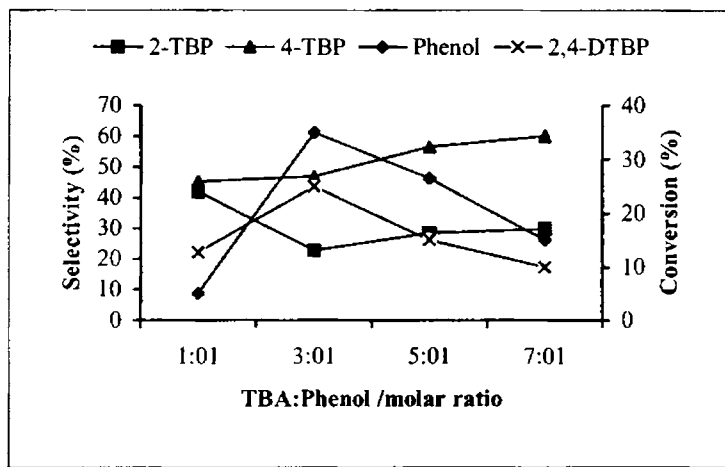


Fig.4.2.2 Effect of feed ratio on phenol *tert* butylation.

Flow rate- 4 mlh⁻¹, temperature-200 °C, time-2 h, catalyst-NCrF₂.

Main products of tertiary butylation of phenol are 2-tBP, 4-tBP and 2,4-dtBP. Maximum phenol conversion was obtained at a molar ratio of 3 and thereafter phenol conversion decreases. It was found that more TBA in the feed mix improves the selectivity of the *p*-isomer. Selectivity towards the *o*-isomer

first decreases considerably and then increased slightly. 2,4-dtBP is obtained in the reverse order as that of the *o*-isomer.

4.2.1.2 Effect of reaction temperature

Results obtained for the reaction carried out at different temperatures over NCrF₂ is shown in Fig.4.2.3.

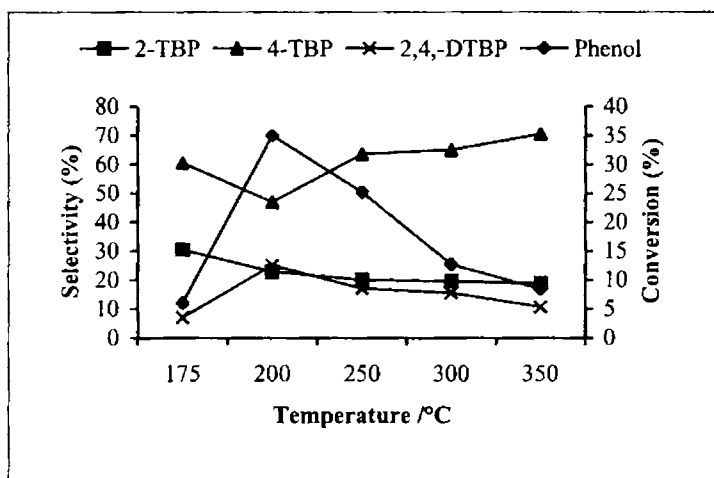


Fig.4.2.3. Effect of temperature on phenol *tert* butylation.

Flow rate-4 mlh⁻¹, TBA: phenol -3:1, time-2 h, catalyst-NCrF₂.

The reaction is found to be very much susceptible to the rise in temperature. When temperature is increased from 175 °C to 200 °C, phenol conversion showed a drastic increase from 6 % to 35 %. At higher temperatures, phenol conversion decreases sharply. Rise in temperature, first decreases the selectivity for 2-tBP and then remain almost constant i.e., higher temperatures have no significant effect on the selectivity for 2-tBP. But high

temperature is found to be favorable for 4-tBP formation even though it showed a decrease in selectivity at the initial stage. Selectivity for 2,4-dtBP reaches maximum at 200 °C. Reaction temperature of 200 °C is selected for the further studies.

4.2.1.3 Effect of flow rate

Phenol *tert* butylation has been carried out at various flow rates from 3 to 6 mlh⁻¹ in order to find out the influence of contact time on the reaction. The result of the studies carried out at 200 °C and a TBA: phenol molar ratio of 3:1 over NCrF2 is shown in Fig.4.2.4.

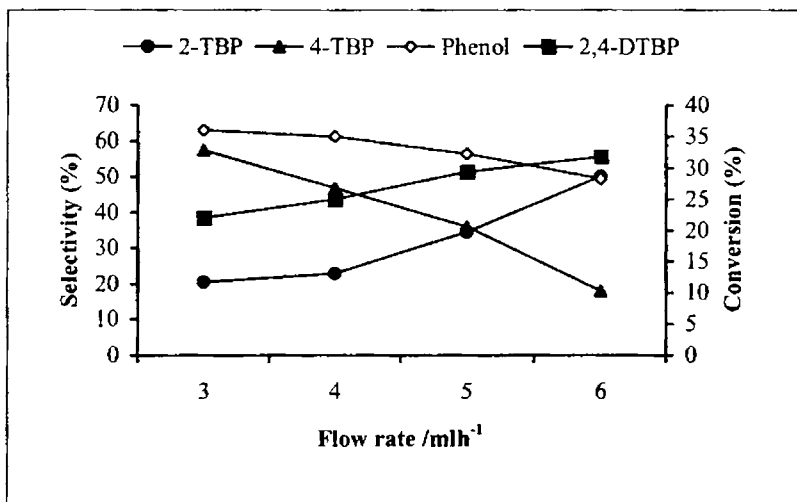


Fig.4.2.4 Effect of flow rate on phenol *tert* butylation.

Temperature- 200 °C, TBA:phenol-3:1,time-2 h, catalyst-NCrF2.

Phenol conversion decreased after the flow rate of 4 mlh⁻¹. 2-tBP is the preferred product at shorter contact time. As contact time increased, selectivity

for the *p*-isomer increased. The dialkylated derivative also shows the similar trend as that of *o*-isomer.

4.2.2 Effect of catalyst composition

(a) NiCr_xFe_{2-x}O₄ (x=0 to 2) series

Phenol conversion and selectivities of various products obtained for chromium incorporated nickel ferrites is shown in the table 4.2.1.

Table 4.2.1 Phenol *tert* butylation over NiCr_xFe_{2-x}O₄ series.

Catalyst	Phenol conversion (%)	Selectivity (%)		
		2-tbp	4-tbp	2,4-dtbp
NF	16.3	49.2	34.8	16.0
NCrF 1	31.3	52.3	35.6	12.1
NCrF 2	35.0	23.9	48.7	27.4
NCrF 3	37.0	23.5	68.6	7.9
NCrF 4	20.2	38.8	42.1	19.1
NCr	18.5	28.0	44.3	27.7

Temperature-200 °C, TBA:phenol - 3:1, flow rate- 4 mlh⁻¹, time- 2 h.

A trend similar to phenol methylation reaction is observed here also. Phenol conversion increases with chromium content in the system up to NCrF3. Further increase of chromium is found to decreasing the activity. Eventhough, the end compositions are more active than pure nickel ferrite. Up to NCrF2, the *o*-isomer- 2-tBP- is the preferred product. Selectivity for *p*-isomer increases only after that.

Chapter 4

The total acidity, obtained from ammonia TPD studies, cyclohexene selectivity (from cyclohexanol decomposition reaction) and basic properties for chromium containing nickel ferrites is shown in table 4.2.2.

Table 4.2.2 Acid-base properties and phenol conversion for $\text{NiCr}_x\text{Fe}_{2-x}\text{O}_4$ series.

Catalyst	Dehydration activity (%) (Cyclohexene sel.)	Total acidity (mmol g^{-1})	Limiting amount ($10^{-4} \text{ mmol l}^{-1} \text{ g}^{-1}$)		Phenol conversion (%)
			TCNQ	Chloranil	
NF	71.4	0.162	25.71	8.23	16.3
NCrF 1	89.5	0.406	18.12	7.12	31.3
NCrF 2	91.4	0.460	16.28	6.28	35.0
NCrF 3	94.4	0.533	12.13	5.42	37.0
NCrF 4	83.1	0.256	21.22	7.79	20.2
NCr	80.5	0.197	22.56	7.21	18.5

A simple comparison of phenol conversion and acid-base properties demonstrates that, the acid-base properties of the systems have considerable influence on product selectivity and phenol conversion. The variation of phenol conversion is in accordance with the variation of total acidity of the systems.

Substitution of iron by chromium up to 60 % is found to be increasing the acidity of the systems and then decreases. This trend is clearly reflected in their selectivity towards cyclohexene. NCrF3, which is more acidic in this series, shows a maximum phenol conversion of 39 %. NCrF2 and NCrF3 are

having high acidic values in this series. They are showing high selectivity towards *p*-isomer. Not only the phenol conversion but the *p*-isomer selectivity is also found to be directly related to the acidity variation.

Substitution of iron by chromium leads Cr^{+3} ions to occupy more exposed O_h site and Ni^{2+} ion shifts to T_d only after $x = 0.8$. As in the case of phenol methylation, here also it is the ratio $\text{Cr}^{+3}/\text{Ni}^{2+}$ which is found to control the catalytic activity. Extreme systems are having too high or too low concentrations of Cr^{3+} or Ni^{2+} and they are less active than NCrF_3 . So it is supposed that it is the moderate concentration of Cr^{+3} and Ni^{2+} ions at the O_h site which is responsible for the high activity of NCrF_3 .

(b) $\text{NiGd}_x\text{Fe}_{2-x}\text{O}_4$ ($x= 0$ to 2) series

The results obtained for phenol *tert* butylation reaction for gadolinium incorporated nickel ferrites is shown in table 4.2.3.

Table 4.2.3 Phenol *tert* butylation over $\text{NiGd}_x\text{Fe}_{2-x}\text{O}_4$ series.

Catalyst	Phenol conversion (%)	Selectivity (%)		
		2-tbp	4-tbp	2,4-dtbp
NF	16.3	49.2	34.8	16.0
NGF 1	20.3	53.4	34.6	12.0
NGF2	34.4	44.7	37.3	18.0
NGF 3	35.0	37.2	48.5	14.3
NGF 4	37.2	25.3	62.7	12.0
NG	39.0	25.2	67.3	7.5

Temperature-200 °C, TBA:phenol - 3:1, flow rate- 4 mlh⁻¹, time- 2 h.

It was observed that the substitution of iron by gadolinium has profound effect on the catalytic activity of nickel ferrite. Incorporation of gadolinium into nickel ferrite has increased the phenol conversion considerably. Phenol conversion reaches a maximum value with complete replacement of iron by gadolinium. Not only the phenol conversion but the selectivity towards *o*- and *p*-isomers also shows a regular gradation with increase in concentration of gadolinium. Selectivity for 4-tBP follows the same trend as that of phenol conversion i.e., increases with increase in x , whereas 2-tBP is preferably formed over systems containing more iron. Up to NGF2, 2-tBP is the preferred product and only after that the selectivity for *p*-isomer increases. No such gradation was observed for the selectivity of 2,4-dtBP.

Phenol tertiary butylation is a Friedel-Crafts alkylation reaction and the activity of catalysts is found to be closely related to the variation of acidic strength of the catalyst. The acid-base properties together with phenol conversion are shown in table 4.2.4.

Successive incorporation of gadolinium has improved the acidity of the systems. Improvement of cyclohexene selectivity is in accordance with this. Phenol conversion increases with incorporation of gadolinium and this variation is parallel to the variation in acidic strength. It is found that the acid-base properties of the systems have considerable influence on product selectivity. Improved acidity helps in the formation of 4-tBP. On the other hand, the selectivity of 2-tBP is lowest on the systems with strong acidity.

Substitution of iron by gadolinium favors more and more Fe^{+3} ions to come into O_h site. Concentration of Ni^{2+} ions at the O_h site does not change up to NGF3 and hence it does not seem to play any role in deciding the catalytic

Alkylation Reactions

Table 4.2.4 Acid-base properties and phenol conversion for NiGd_xFe_{2-x}O₄ series.

Catalyst	Dehydration activity (%) (Cyclohexene sel.)	Total acidity (mmolg ⁻¹)	Limiting amount (10 ⁻⁴ mmol l ⁻¹ g ⁻¹)		Phenol conversion (%)
			TCNQ	Chloranil	
NF	71.4	0.162	25.71	8.23	16.3
NGF 1	81.2	0.195	22.89	8.19	20.3
NGF2	92.5	0.436	18.29	8.02	34.4
NGF 3	93.6	0.463	14.11	7.76	35.0
NGF 4	94.0	0.593	12.21	6.52	37.2
NG	99.0	1.094	11.19	6.32	39.0

activity. It is the concentration of Fe⁺³ and Gd⁺³ ions present at the O_h site which determines the activity. The higher activity of NG as compared to NGF4 may be due to the fact NG is having strong acidic centers compared to NGF4, that may be created by the improved concentration of gadolinium as revealed from ammonia TPD studies.

(c) Cobaltite series

A series of experiments were performed over cobaltite spinels. The results obtained were given in table 4.2.5.

In nickel cobaltite series, the activity is found to be increasing with increase in nickel content. Copper cobaltites also showed an improved phenol conversion with increase in copper content. More over, copper cobaltites are

Chapter 4

Table 4.2.5 Phenol *tert* butylation over cobaltites.

Catalyst	Phenol conversion (%)	Selectivity (%)		
		2-tbp	4-tbp	2,4-dtbp
NC .5	21.3	26.3	60.2	13.5
NC 1	23.8	24.1	64.3	11.6
NC 1.5	26.2	23.1	66.4	10.5
CC .5	28.5	23.0	67.7	9.3
CC 1	30.6	20.2	69.7	10.1

Temperature-200 °C, TBA:phenol - 3:1, flow rate- 4 mlh⁻¹, time-2 h.

more active than nickel cobaltites. All the cobaltites preferably formed *p*-isomer as the major product.

The relationship between acid-base properties and the activity of the catalysts can be understood by comparing the variations of acid-base properties with phenol conversion and product selectivities. Acid-base properties along with phenol conversion for cobaltites are shown in table 4.2.6.

Improved acidity is found to increase the catalytic activity. From the table it is clear that copper cobaltites are more acidic than nickel cobaltites. This higher acidic behaviour of copper cobaltites can be clearly seen in their activity towards the tertiary butylation of phenol. Not only phenol conversion, the selectivity for *p*-isomer also follows the same trend which shows that an increase in acidic strength of cobaltites has resulted in the improved selectivity towards 4-tBP. On the other hand, selectivities for 2-tBP and 2,4-dtBP are lower on systems with strong acidity.

In nickel cobaltites, since Ni²⁺ ion occupies O_h site; as the percentage

Alkylation Reactions

Table 4.2.6 Acid-base properties and phenol conversion for cobaltites.

Catalyst	Dehydration activity (%) (Cyclohexene sel.)	Total acidity (mmolg ⁻¹)	Limiting amount (10 ⁻⁴ mmol l ⁻¹ g ⁻¹)		Phenol conversion (%)
			TCNQ	Chloranil	
NC .5	90.3	0.285	22.23	9.13	21.3
NC 1	92.5	0.295	20.19	9.06	23.8
NC 1.5	94.6	0.343	19.22	8.32	26.2
CC .5	96.3	0.359	16.80	8.25	28.5
CC 1	97.4	0.374	16.44	8.12	30.6

of nickel is increased, more and more nickel enters into the more exposed O_h site. Improved concentration of Ni²⁺ ions at the O_h site might have created strong acid sites. It is the ratio Ni²⁺/Co³⁺ which is supposed to be determining the catalytic activity. As this ratio increases with increase in concentration of nickel, the activity also increases. For copper cobaltites, an increment in Cu²⁺ ion concentration at the O_h site may be responsible for the improved acidity. Here Cu²⁺/Co³⁺ ratio determines the catalytic activity.

Effect of time on stream

The systems were checked for catalytic stability for the phenol *tert* butylation by observing the catalytic performance for a period of 9 h. The reaction was performed at 200 °C at a TBA to phenol molar ratio of 3. Product analysis was done at regular intervals and the results are presented in Fig.4.2.5. Copper cobaltite sample has shown little deactivation after a period of 6 h.

Other systems showed excellent catalytic stability by maintaining the phenol conversion.

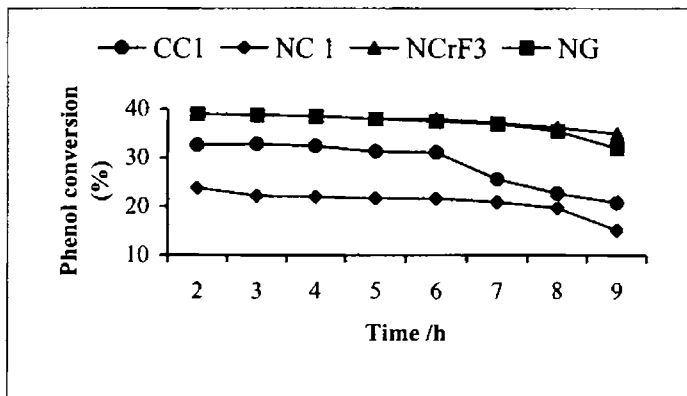


Fig.4.2.5 Effect of time on stream on phenol *tert* butylation.
Temperatre-200 °C, TBA:phenol = 3:1, flow rate- 4 mlh⁻¹.

4.2.3 Mechanism of phenol *tert* butylation

Tert-butylation of phenol has been carried out using TBA. In the presence of an acid catalyst, TBA gets dehydrated into isobutylene and water²¹. Phenol is adsorbed as phenolate ion by dissociative adsorption on an acid-base site. Simultaneously protonation of isobutene occurs by the H⁺ ion from the above process to form *t*-butyl cation²⁰ which in turn attacks phenoxide ion either from the adsorbed or from the gaseous state. If carbocation attacks preferably from the adsorbed state, 2-*t*BP will be the selective product²⁰. However in our case, the high selectivity of *p*-isomer shows the probable attack of carbocation from the gaseous phase. We observed an increment in the selectivity of 4-*t*BP with improvement in acidity of the systems. It is in agreement that strong acid sites favour the formation of 4-*t*BP as in zeolites¹⁰.

Alkylation Reactions

However the requirement for strong acid sites for 2,4-dtBP on the above mentioned material is contrary to the present results. The mono *tert*-butylated phenols are more active than phenol, subsequent *t*-butylation occurs only where there is less steric hindrance. Steric hindrance of the *t*-butyl group prevents the further attack of carbocation at the *o*-position of already formed 2-tBP, supported by the fact that no second *ortho* *t*-butylated product (2,6-dtBP) was observed. Schematic representation of the above proposed mechanism is shown in Fig.4.2.6.

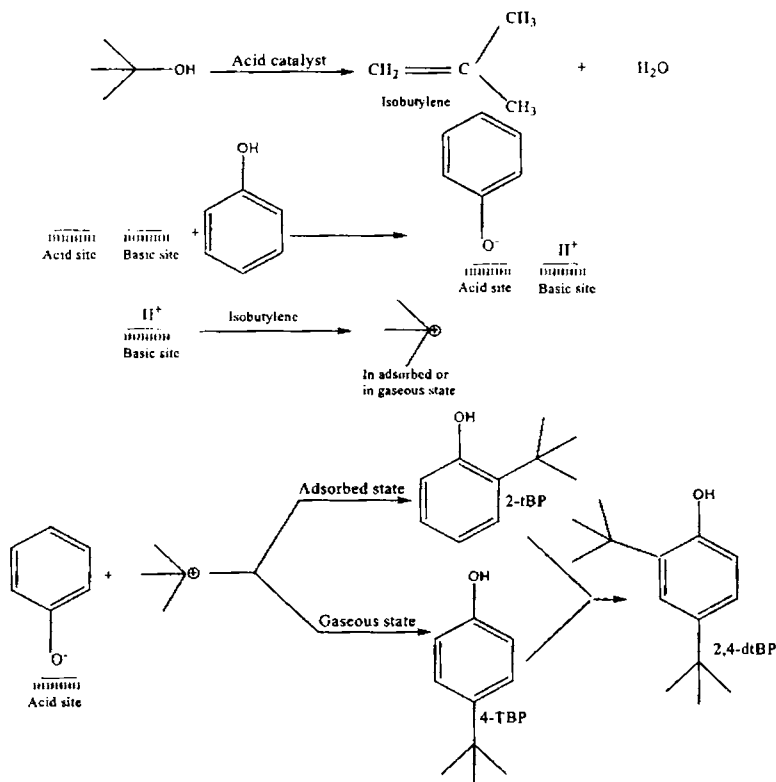


Fig.4.2.6 Mechanism of phenol *tert* butylation reaction.

4.3 Thymol Synthesis

Thymol is 2-isopropyl-5-methyl phenol. Natural thymol is extracted from the oil of thyme and mint. It has antiseptic properties, antimicrobial activity on bacteria involved in upper respiratory tract infections¹, inhibitory activity against *Escherichia coli* and *salmonella typhimurium*² and on oral bacteria^{3,4}.

In an industrial process employed by Bayer, thymol is obtained by liquid phase isopropylation of *m*-cresol in the presence of activated alumina at 633 K and at a pressure of 50 bar⁵. It is already known to prepare thymol by liquid phase alkylation of *m*-cresol with isopropylene over acid catalyst⁶, by the gas phase alkylation of *m*-cresol with propylene in the presence of supported metal sulphates⁷, wide and medium - pored zeolites⁸, and γ -Al₂O₃^{9,10}. Isopropyl alcohol (IPA) can also be used as an alkylating agent for *m*-cresol isopropylation.

The results of alkylation of *m*-cresol with isopropanol in the presence of Mg-Al hydrotalcites were published by Velu and Sivakumar¹¹. They reported that during their studies both O- and C- isopropylation was observed, as the main reaction product thymol was obtained with selectivity up to 79.9 % for 36.4 % *m*-cresol conversion.

Gbrabowska et al. have developed an oxide catalyst that contains Fe, Cr, Si and K, which is active in the alkylation of *meta*- and *para*- cresols by isopropyl alcohol¹²⁻¹⁵, giving in the case of *meta*-cresol up to 59 % selectivity to thymol. In the case of *para*-cresol it is possible to obtain thymol with selectivity 57 % at conversion of raw material up to 66 %.

Gbrabowska et al.¹⁶ have also studied the thymol synthesis catalyzed by spinels. The authors used as catalysts two zinc aluminates, prepared from different precursors by hydrothermal method. In the presence of $ZnAl_2O_4$ obtained from basic aluminium chloride and hydrated zinc acetate, nearly 90 % selectivity towards thymol was obtained. Umamahesvari studied isopropylation of *m*-cresol in the presence of mesoporous Al-MCM-41 molecular sieves¹⁷. During the reaction *m*-cresol conversion reached 35 % with 100 % thymol selectivity. Shanmugapriya et al. used isopropyl acetate as alkylating agent to produce thymol in the presence of Al-MCM-41 molecular sieves¹⁸.

It has been reported that $Al(OC_6H_5)_3$ and $ZnCl_2-HCl$ ^{9,19} have been used as catalysts in the liquid phase isopropylation of *m*-cresol. Y and β zeolites, ZSM-5, erionite and mordenite⁸, and supported metal sulfates⁹ were used in the vapour phase for such reactions. Synthetic silica-alumina and large-pore Y-type catalysts have yielded isothymol through isomerization and transalkylation reaction²⁰.

This section includes a detailed study of isopropylation of *m*-cresol using IPA by optimizing various reaction parameters. The reaction has been studied using the prepared ferrites and cobaltites under optimized conditions and an attempt has been made to correlate the catalytic activity with acidic properties. Thymol and isothymol were the major reaction products obtained. No ether formation was observed. According to Taylor and Ludlum²¹, isothymol formation may be due to the different configuration of aromatic ring on the catalyst surface. Reaction scheme for the *m*-cresol isopropylation is given in Fig.4.3.1.

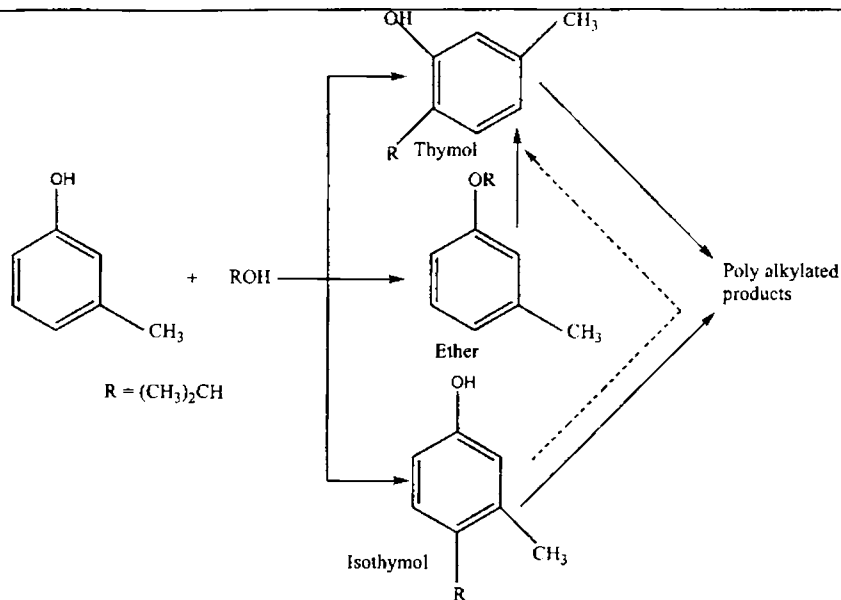


Fig.4.3.1 Reaction scheme for isopropylation of *m*-cresol.

4.3.1 Process optimization

Various reaction parameters such as temperature, reactant molar ratio, flow rate etc. were optimized. These are discussed below.

4.3.1.1 Effect of reaction temperature

A series of reactions were carried out over the catalyst NCrF_4 in the temperature range 220-300 °C at a flow rate of 4 mlh⁻¹. The feed mix ratio was *m*-cresol:IPA:H₂O = 1 : 7 : 1. Water was added to the reactant mixture to prolong the activity of the catalyst during the reaction of alkylation²⁶. The results obtained were shown in Fig.4.3.2.

m-cresol conversion was found to be very much susceptible to the rise in temperature. A steady rise in *m*-cresol conversion was obtained with increase in temperature up to 260 °C and then decreased. In the temperature range studied, thymol was found to be the major product. Thymol selectivity increases with increase in temperature and reaches maximum at 300 °C with a corresponding decrease in isothymol selectivity. However at lower temperatures, more unwanted products were formed. These may contain higher alkylated phenols¹⁶. Even though thymol selectivity increases largely after 260 °C, *m*-cresol conversion drops sharply. So 260 °C was chosen as the optimum temperature for further studies.

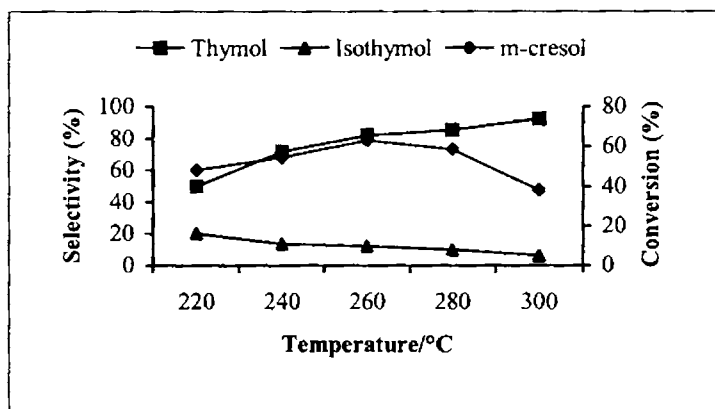


Fig.4.3.2 Effect of temperature on thymol synthesis.

Flow rate-4 mlh⁻¹, *m*-cresol: IPA:H₂O-1:7:1, time-2 h, catalyst-NCrF4.

4.3.1.2 Effect of feed ratio

Feed mix ratio was optimized by conducting the reaction at 260 °C at different feed ratios and at a flow rate of 4 mlh⁻¹ over NCrF4. The results obtained were shown in Fig.4.3.3.

m-cresol conversion was found to be increased with increase in percentage of IPA in the feed mix. We found an increase in *m*-cresol conversion up to a feed ratio of 1:7:1 and then remained almost constant. The selectivities of other products were unaffected by the change in feed mix ratio. Thymol is the major product.

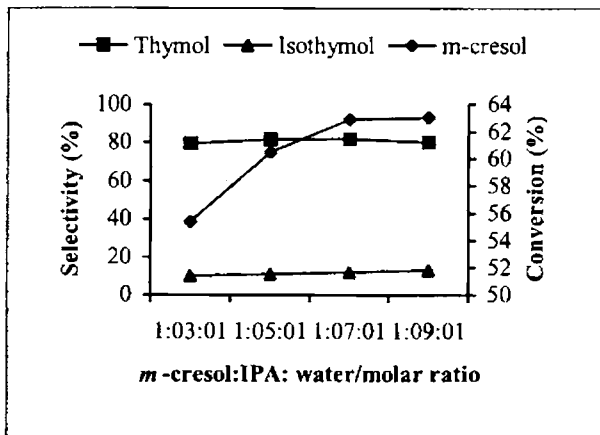


Fig.4.3.3. Effect of reactant mol ratio on thymol synthesis.

Temperature-260 °C, flow rate-4 mlh⁻¹, time-2 h, catalyst-NCrF4.

4.3.1.3 Effect of flow rate

Isopropylation of *m*-cresol was carried out at different flow rates from 3 to 6 mlh⁻¹ over NCrF4 at a temperature of 260 °C and a feed mix ratio of *m*-cresol:IPA:H₂O = 1:7:1. *m*-cresol conversion and product selectivities were shown in Fig.4.3.4.

Maximum *m*-cresol conversion was obtained at higher contact time. As flow rate increases, *m*-cresol conversion showed a sharp decrease. Selectivities of products were also found to be depending upon the contact time. At higher contact time, more impurities were formed. Thymol is the major product

obtained and its selectivity is found to be increasing with increase in flow rate with corresponding decrease in isothymol selectivity. Although the *m*-cresol conversion was decreased from 80 % to 63 % when flow rate is increased from 3 to 4 mlh⁻¹, thymol selectivity was found to be much improved. The flow rate of 4 mlh⁻¹ was selected for further studies.

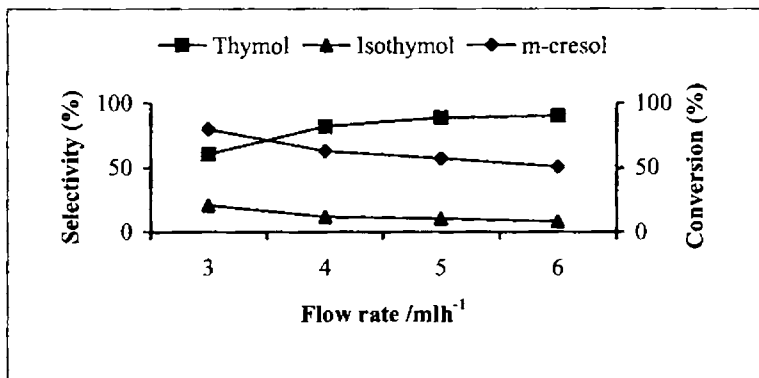


Fig.4.3.4 Effect of flow rate on thymol synthesis.

Temperature-260°C, *m*-cresol:IPA:H₂O-1:7:1,time-2 h, catalyst-NCrF₄.

4.3.2 Effect of catalyst composition

(a) NiCr_xFe_{2-x}O₄ (x = 0-2) series

Thymol synthesis was carried out over chromium incorporated nickel ferrites under optimized conditions. The results are tabulated in table 4.3.1.

Replacing iron by chromium is found to improving the catalytic activity of nickel ferrite up to a certain level and then decreases. Nickel ferrite is the least active towards isopropylation of *m*-cresol. Substitution of iron by chromium drastically increases the *m*-cresol conversion. The trend continued up to NCrF₃ and then showed a decrease. Nickel chromite is more active than nickel ferrite. The selectivities of products were also found to be very much

susceptible to the substitution by chromium. Percentage of impurities was found to be more at initial stages but at higher percentages of chromium, impurities were minimized and thymol selectivity improved.

Table 4.3.1 Thymol synthesis over NiCr_xFe_{2-x}O₄ series.

Catalyst	<i>m</i> -cresol conversion (%)	Selectivity (%)		
		Thymol	Isothymol	Others
NF	33.5	28.2	32.4	39.4
NCrF 1	68.2	47.6	22.5	29.9
NCrF 2	76.7	50.4	18.6	31.0
NCrF 3	81.8	92.3	5.2	2.5
NCrF 4	62.9	82.0	12.0	6.0
NCr	53.1	75.0	11.5	13.5

Temperature-260 °C, flow rate- 4 mlh⁻¹, *mc*:IPA:H₂O-1:7:1, time-2 h.

m-cresol conversion and product selectivities are found to be proportional to the variation of acid-base properties upon incorporation of chromium. Acid-base properties together with *m*-cresol conversion are shown in table 4.3.2.

The table clearly shows that the activity of the systems varies in accordance with the variation in acidity. Substitution by chromium improved the acidic strength up to NCrF3 and then decreased. NCrF3 has showed maximum *m*-cresol conversion and thymol selectivity. Cyclohexene selectivity obtained from cyclohexanol decomposition reaction provides evidence for this.

Alkylation Reactions

Table 4.3.2 Acid-base properties together with *m*-cresol conversion for NiCr_xFe_{2-x}O₄ series.

Catalyst	Dehydration activity (%) (Cyclohexene sel.)	Total acidity (mmolg ⁻¹)	Limiting amount (10 ⁻⁴ mmol l ⁻¹ g ⁻¹)		<i>m</i> -Cresol conversion (%)
			TCNQ	Chloranil	
NF	71.4	0.162	25.71	8.23	33.5
NCrF 1	89.5	0.406	18.12	7.12	68.2
NCrF 2	91.4	0.460	16.28	6.28	76.7
NCrF 3	94.4	0.533	12.13	5.42	81.8
NCrF 4	83.1	0.256	21.22	7.79	62.9
NCr	80.5	0.197	22.56	7.21	53.1

The acid-base character on the catalyst surface is due predominantly to octahedral cations. So it seems that the distribution of cations between O_h and T_d site is also important in determining the catalytic activity. Chromium preferably enters to O_h site on substitution, and Ni²⁺ ion shifts to T_d site after x = 0.8. The ratio Cr³⁺/Ni²⁺ is found to controlling the catalytic activity. Systems with high and low x values are having too high or too low concentration of Cr³⁺ or Ni²⁺ ions at the O_h site and they are less active than NCrF3. The moderate concentration of Cr³⁺ and Ni²⁺ at the O_h site may be responsible for the high activity of NCrF3 and hence it shows maximum *m*-cresol conversion and thymol selectivity.

(b) NiGd_xFe_{2-x}O₄ (x = 0 to 2) series

m-cresol conversion and product selectivities for the isopropylation of *m*-cresol over gadolinium containing nickel ferrites are shown in table 4.2.3.

Table 4.2.3 Thymol synthesis over NiGd_xFe_{2-x}O₄ systems.

Catalyst	<i>m</i> -cresol conversion (%)	Selectivity (%)		
		Thymol	Isothymol	Others
NF	33.5	28.2	32.4	39.4
NGF 1	69.2	61.2	23.4	15.4
NGF2	72.2	75.2	22.1	2.7
NGF 3	82.1	90.3	4.0	5.7
NGF 4	86.7	91.5	4.8	3.7
NG	88.2	92.0	5.2	2.8

Temperature-260 °C, flow rate-4 mlh⁻¹, *mc*:IPA:H₂O-1:7:1, time-2 h.

Substitution of iron by gadolinium has a profound effect on the activity of nickel ferrite. Incorporation of 20 % of gadolinium into nickel ferrite increased the *m*-cresol conversion from 33.5 % to 69 %. *m*-cresol conversion is then found to increasing with gadolinium content and nickel gadolinite is more active in that series. Systems with higher gadolinium content are showing more selectivity towards thymol. NGF3, NGF4 and NG have showed a thymol selectivity of greater than 90 %.

Replacing iron by gadolinium improves the acidic strength of nickel ferrite gradually with corresponding decreases in the basic strength. This variation in acid-base properties is clearly reflected in their activity. Acid-base

Alkylation Reactions

properties together with *m*-cresol conversion for NiGd_xFe_{2-x}O₄ series are shown in table 4.2.4.

Table 4.2.4 Acid-base properties and *m*-cresol conversion for NiGd_xFe_{2-x}O₄ systems.

Catalyst	Dehydration activity (%) (Cyclohexene sel.)	Total acidity (mmolg ⁻¹)	Limiting amount (10 ⁻⁴ mmol l ⁻¹ g ⁻¹)		<i>m</i> -cresol conversion (%)
			TCNQ	Chloranil	
NF	71.4	0.162	25.71	8.23	33.5
NGF 1	81.2	0.195	22.89	8.19	69.2
NGF2	92.5	0.436	18.29	8.02	72.2
NGF 3	93.6	0.463	14.11	7.76	82.1
NGF 4	94.0	0.593	12.21	6.52	86.7
NG	99.0	1.094	11.19	6.32	88.2

Systems with more acidic strength are more active and more selective towards thymol. Those which are more acidic forms more cyclohexene from the decomposition of cyclohexanol. Basic character is found to be decreasing with the substitution of iron by gadolinium. Activity of gadolinium containing nickel ferrites is related to the variation of acid-base properties which clearly show that the catalytic activity in vapour phase alkylation reaction very much depend upon the strength and variation of acidic and basic sites.

In the case of gadolinium containing nickel ferrites, Gd³⁺ ion preferably enters into the O_h site due to its larger ionic radius. Mössbauer data show that

Chapter 4

incorporation of gadolinium improves the percentage of Fe^{3+} ions at the O_h site; and the concentration of Ni^{2+} ion is not changing up to $x = 1.2$. So it is supposed that it is the Gd^{3+} ions at the O_h site together with increased concentration of Fe^{3+} ions would be responsible for the increased acidity and activity with increase in gadolinium content. Since the concentration Ni^{2+} ions at the O_h site is not changing up to $x = 1.2$, it is reasonable to suggest that it is not involved in deciding the catalytic activity. It is the concentration of other ions present at the O_h site which is found to control the catalytic activity.

(c) Cobaltite series

Table 4.2.5 shows the results of isopropylation of *m*-cresol carried out over different cobaltite spinels under optimized conditions.

Table 4.2.5 Thymol synthesis over cobaltites.

Catalyst	<i>m</i> -cresol conversion (%)	Selectivity (%)		
		Thymol	Isothymol	Others
NC .5	59.5	80.2	10.3	9.5
NC 1	62.4	84.5	10.8	4.7
NC 1.5	67.2	86.2	11.2	2.6
CC .5	72.5	89.0	8.7	2.3
CC 1	74.4	89.9	6.6	3.5

Temperature-260 °C, flow rate-4 mlh⁻¹, *mc*:IPA:H₂O-1:7:1, time-2 h.

Of the two series of cobaltites studied, copper cobaltites are found to be more active than nickel cobaltites. Increase in concentration of nickel in nickel

cobaltites has improved the activity of the systems towards the *m*-cresol isopropylation. At higher percentage of nickel, *m*-cresol conversion increases to a maximum value of 67.2 %. Thymol is observed as the major product. Thymol selectivity also increases in accordance with the increase in concentration of nickel. The high activity of copper cobaltites compared to nickel cobaltites is not only reflected in *m*-cresol conversion, but in thymol selectivity also. Both CC.5 and CC1 are forming thymol more selectively than nickel cobaltites. But selectivity towards thymol remains almost constant even with change in concentration of copper in copper cobaltites. Isothymol is the second major product observed.

Comparing the variation in acid-base properties of cobaltites with their activity, it is revealed that the activities of the systems much depend up on the acid-bade properties. *M*-cresol conversion, together with acid-base properties for the cobaltite series are shown in table 4.2.6.

Table 4.2.6 Acid-base properties and *m*-cresol conversion for cobaltites.

Catalyst	Dehydration activity (%) (Cyclohexene sel.)	Total acidity (mmolg ⁻¹)	Limiting amount (10 ⁻⁴ mmol l ⁻¹ g ⁻¹)		<i>m</i> -cresol conversion (%)
			TCNQ	Chloranil	
NC .5	90.3	0.285	22.23	9.13	59.5
NC 1	92.5	0.295	20.19	9.06	62.4
NC 1.5	94.6	0.343	19.22	8.32	67.2
CC .5	96.3	0.359	16.80	8.25	72.5
CC 1	97.4	0.374	16.44	8.12	74.4

It is clear from the table that the activity of the systems or the *m*-cresol conversion varies in parallel to the variation in acidic strength of the catalysts. As strong acid sites are created, it results in the removal of basic sites. Since copper cobaltites are more acidic than nickel cobaltites, the former is showing an improved catalytic activity. Evidence for the higher acidity of copper cobaltites comes from the cyclohexanol decomposition reaction. Copper cobaltites are more selectively forming cyclohexene compared to nickel cobaltites, which is believed to be formed by the action of acid sites.

It is well known that, for spinels, the cations present at the O_h sites are preferentially exposed at the surface of the catalyst. The acid-base properties are determined predominantly by the O_h cations and they play the crucial role in determining the catalytic activity. Although nickel cobaltites contains Ni^{2+} and Co^{3+} ions at the O_h site, it is the ratio Ni^{2+}/Co^{3+} which is found to play the role in determining the catalytic activity. Since Ni^{2+} preferably occupies O_h site, the ratio Ni^{2+}/Co^{3+} at the O_h site increases as the concentration of Ni^{2+} increased. Hence, as the concentration of Ni^{2+} increases, the improved catalytic activity can be attributed to the increased Ni^{2+}/Co^{3+} ratio at the O_h site. For copper cobaltites, system having high Cu^{2+}/Co^{3+} ratio at the O_h site has more activity. It is supposed that for CC1, as more Cu^{2+} ions enter into the O_h site, stronger acid sites would have been created and these sites are involved in improving the catalytic activity.

Effect of time on stream

Effect of time on stream for thymol synthesis was studied over the spinels and the results are depicted in Fig.4.3.5. The reaction was studied for a

period of 9 h. Product mixture was analyzed by GC at regular intervals. Spinels containing cobalt showed little deactivation after 7 h where as the other systems showed no considerable decrease in *m*-cresol conversion showing the better catalytic performance of the systems for a long period.

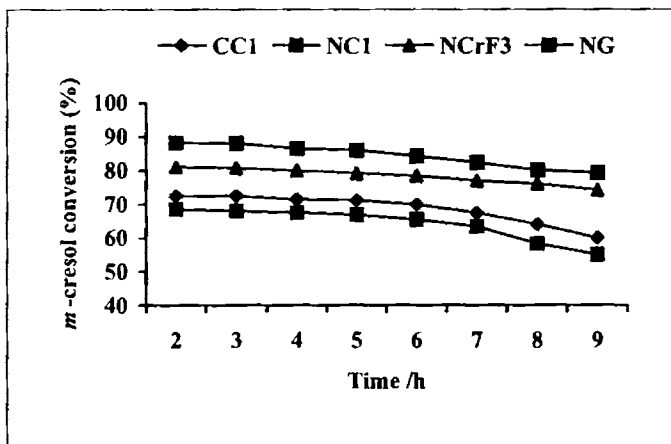


Fig. 4.3.5 Effect of time on stream for isopropylation of *m*-cresol.

Temp.-260 °C, flow rate-4 mlh⁻¹, *m*-cresol:IPA:H₂O-1:7:1, time-2 h.

4.3.3 Mechanism of *m*-cresol isopropylation

Alkylation of phenols, just like other aromatic compounds, follows the Friedel-Craft mechanism. For spinels, the observed catalytic activity is mainly attributed to acid-base properties²²⁻²⁵. Grabowska et al.¹⁶ have carried out the vapour phase thymol synthesis using ZnAl₂O₄ spinels and they have explained the activity in terms of Lewis acid sites and comparatively weaker basic sites. The prepared catalysts are having acidity mainly due to Lewis acid sites which is confirmed from IR studies of pyridine adsorbed samples. Predominant IR

bands at 1606 and 1446 cm^{-1} confirm that the major contribution towards acidity is due to Lewis acid sites for all the compositions. Based on their study of vapour-phase isopropylation of *m*-cresol over sol-gel prepared alumina, Grabowska et al.²⁶ have proposed a mechanism similar to Friedel-Craft reaction. The reaction takes place via the formation of a nucleophile and an electrophile. The cresol will adsorb on the surface of the catalyst resulting in the formation of a reactive phenoxide ion. IPA is co-adsorbed with cresol and results in isopropoxide formation. Under the influence of acidic sites of the catalyst, the C-O bond of the isopropoxide is strongly polarized and electrons are shifted towards the oxygen atom. In the extreme case, 2-propyl carbocation is formed. The isopropoxide which is an electrophile then reacts with the nearest nucleophilic phenoxide, when the C-C bond is formed and C-O bond of the isopropoxide is broken. Attack of the electrophilic isopropyl moiety at the *ortho* position leads to the formation of thymol. The schematic representation of the above proposed mechanism is shown in Fig. 4.3.6.

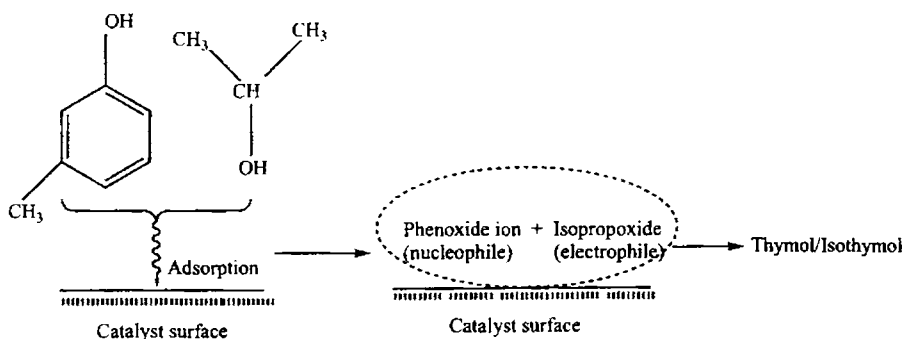


Fig.4.3.6. Schematic representation of *m*-cresol isopropylation.

4.4 Aniline Methylation

Methylation of aniline is industrially important owing to the wide uses of various substituted anilines like N-methyl aniline (NMA), N,N-dimethylaniline (NNDMA), toluidines and xyloidines. The C-alkylated products are formed through the intramolecular transformations of N-alkylated products.

Alumino phosphate based molecular sieves are found to be good options for aniline alkylation reaction with high selectivity to N-alkylated products. Prasad and Rao¹ have studied the alkylation of aniline using methanol over $\text{AlPO}_4\text{-5}$ catalyst and observed the formation of NMA at lower temperature, which is subsequently converted to NNDMA, which itself isomerizes to N-methyl toluidine as the temperature is increased. Isomerization occurs largely by the carbocation mechanism, as demonstrated by studying the reaction of NNDMA.

Weak and moderate acid sites are sufficient for N-alkylation whereas strong acid sites are mandatory for C-alkylation². Investigations by Sreekumar et al. on the alkylation of aniline with methanol over ferrospinels containing zinc and cobalt showed that the systems possessing low cobalt content are highly active and selective for N-monomethylation of aniline^{3,11}. Many of the reports available in the literature reveal the dependence of aniline alkylation on acid-base properties of the catalysts⁴⁻⁷; the type and strength of acidic and basic sites have been an area under discussion. Though the small amount of basic sites in zeolites exhibit more activity in the methylation of aniline, an excessive amount of basicity might cover the active sites and deactivate the catalyst⁵⁻⁸. According to Narayan and Deshpande^{9,10}, a combination of Brønsted and

Lewis acid sites on the catalyst surface is more favourable for aniline alkylation. Sreekumar et al. have studied the aniline alkylation by methanol using zinc ferrite containing cobalt and have concluded that the basicity of the catalyst surface played a dominating role on the adsorption and activation of aniline to give NMA¹².

A wide variety of metal orthophosphates have been employed as catalysts for aniline alkylation. Aramendia et al.¹³ tested various magnesium orthophosphates with different structures and acid-base properties as catalysts for aniline methylation. They observed that the catalysts were selectively forming N-methylaniline with methanol as they yield no C-alkylated product. Also the magnesium pyrophosphates were found to be more active than magnesium orthophosphates.

Schematic representation of aniline alkylation using methanol as the alkylating agent is shown in Fig.4.4.1.

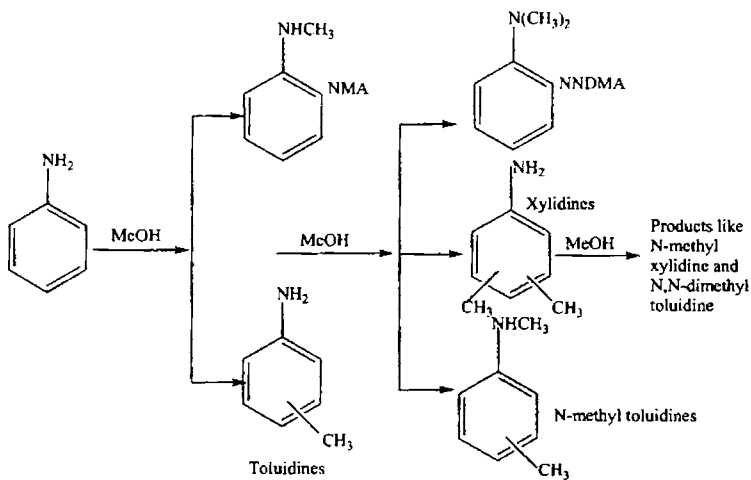


Fig.4.4.1 Reaction scheme for aniline alkylation using methanol.

The vapour-phase aniline alkylation using methanol as the alkylating agent was done over the prepared catalysts. We observed that all the catalysts were highly active for the reaction. Ferrites showed more selectivity towards NMA as compared to cobaltite series.

4.4.1 Process optimization

4.4.1.1 Effect of methanol to aniline molar ratio

Aniline conversion and product selectivities for aniline alkylation at different methanol to aniline molar ratios at 350 °C, and a space velocity of 4 mlh⁻¹ studied over NC.5 is shown in Fig.4.4.2.

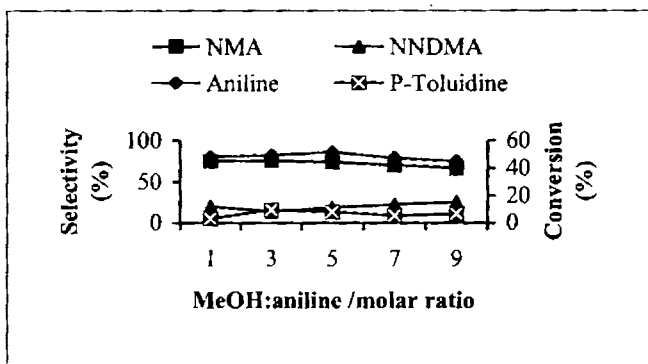


Fig.4.4.2 Effect of feed ratio on aniline methylation.

Temperature-350 °C, flow rate-4 mlh⁻¹, time-2 h, catalyst-NC.5.

The major reaction product is NMA. After a methanol to aniline molar ratio of 5, there observed a decrease in selectivity for NMA with corresponding increase in the selectivity for NNDMA. This suggests that higher methanol to aniline molar ratios favour the consecutive methylation of NMA. The C-alkylated product, *p*-toluidine was formed only in smaller amount. Maximum aniline conversion was obtained for a molar ratio of 5. Excess of

methanol beyond the molar ratio of 5 lowered the aniline conversion because the alcohol probably may undergo side reactions leading to the formation of coke. Therefore methanol to aniline molar ratio of 5 was selected as the optimum feed mix ratio in the subsequent experiments.

4.4.1.2 Effect of reaction temperature

A series of aniline alkylation reactions were performed in the temperature range 300-500 °C over NC.5. Fig.4.4.3 shows the influence of reaction temperature on aniline conversion and product selectivities.

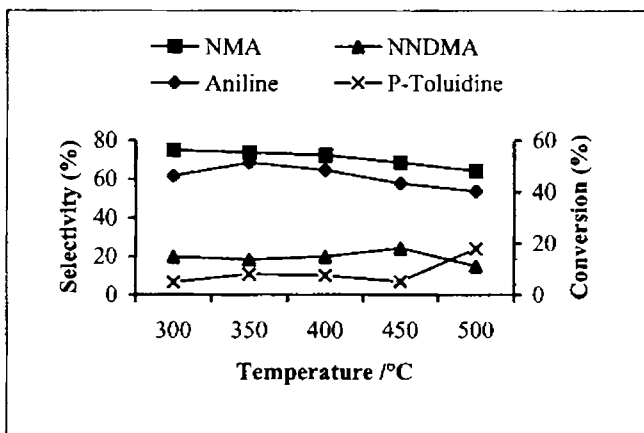


Fig.4.4.3 Effect of reaction temperature on aniline methylation.

Flow rate- 4 mlh⁻¹, MeOH: aniline-5, time-2 h, catalyst- NC.5.

It has been seen that temperature has a marked influence on aniline conversion and product selectivity. At all temperatures, NMA was observed to be the main product. Rise of temperature is found to decrease the selectivity of NMA. At higher temperatures, NNDMA is formed by the methylation of NMA. This reduced the NMA selectivity and increased the NNDMA

selectivity. Ring alkylation leading to *p*-toluidine was increased at higher temperatures. According to Prasad and Rao¹ the C-alkylated products are formed by the isomerization of N, N-dialkylated product at high temperature. Maximum aniline conversion was observed at 350 °C, and further increase in temperature rather reduced the aniline conversion, which may be due to the coke deposition in the high temperature range. Another possible reason for the reduced conversion is that methanol decomposition to C-oxides will be larger at higher temperature. The results indicate that the optimum temperature is 350 °C for high aniline conversion and high NMA selectivity.

4.4.1.3 Effect of flow rate

Fig.4.4.4 shows the influence of flow rate on aniline methylation carried out over NC.5 at 350 °C and a methanol to aniline molar ratio of 5.

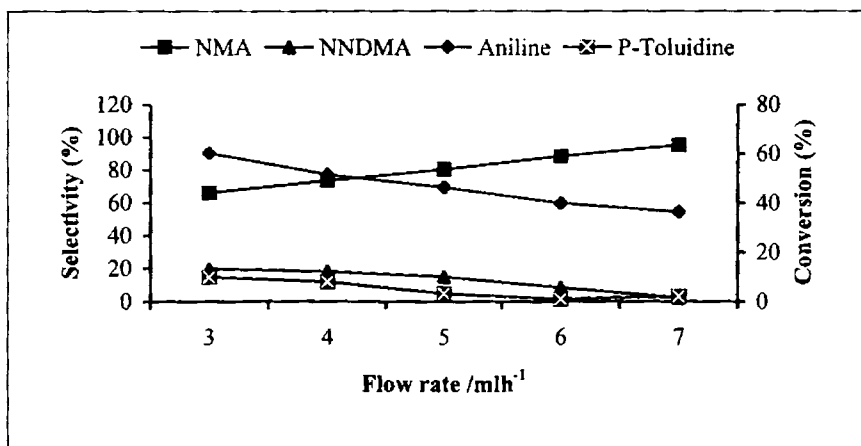


Fig.4.4.4 Influence of flow rate on aniline methylation.

Temperature-350 °C, MeOH:aniline-5, time-2 h, catalyst-NC.5.

At lower contact time (higher flow rate) the reactants gets less time to spend on the catalyst surface which will result in a decrease in aniline conversion and decrease in selectivity for higher alkylated products of aniline. A similar trend was reported by Yuvraj et al. over zeolites Y and β ¹⁴. With increase in flow rate, aniline conversion decreased dramatically. At higher flow rates, mono alkylated products were selectively formed and selectivity for NNDMA was reduced. Selectivity towards the C-alkylated product, *p*-toluidine was also reduced at higher flow rate. An optimum flow rate of 4 mlh⁻¹ was chosen for further studies.

4.4.2 Effect of catalyst composition

(a) NiCr_xFe_{2-x}O₄ (x = 0-2) series

Percentage aniline conversion and selectivities of various products obtained for chromium containing nickel ferrites were shown in table 4.4.1.

Pure nickel ferrite shows a maximum aniline conversion and maximum selectivity towards NMA. Incorporation of chromium is found to decrease the activity of the systems towards aniline methylation. But systems having higher chromium content show little enhanced activity as compared to those having low chromium content. NMA is the preferred product obtained in all the cases. No C-alkylated products were observed in this case. The products coming under 'others' include benzene, toluene etc. Since aniline itself is a strong base, the basicity of the catalyst surface plays a dominating role in determining the catalytic activity^{12,15}. The basic character of the systems varies with progressive substitution of iron by chromium. The limiting values of different electron acceptors adsorbed gives evidence for this variation. Incorporation of

Alkylation Reactions

Table 4.4.1 Aniline methylation over NiCr_xFe_{2-x}O₄ series.

Catalyst	Aniline conversion (%)	Selectivity (%)			
		NMA	NNDMA	<i>p</i> -toluidine	Others
NF	65.3	99.5	0.5	--	--
NCrF 1	59.5	99.0	0.6	--	0.4
NCrF 2	57.8	88.2	8.2	--	3.6
NCrF 3	50.0	88.6	7.3	--	4.1
NCrF 4	63.1	84.2	6.9	--	8.9
NCr	63.8	84.0	11.0	--	5.0

Temperature-350 °C, MeOH:aniline-5, flow rate-4 mlh⁻¹, time-2 h.

chromium is found to decrease the basic strength up to NCrF3 and then increases. Nickel ferrite is the system having more basic strength. The acid-base properties together with aniline conversion for the series are given in table 4.4.2.

From the table it is clear that, the way in which aniline conversion varies with increasing the chromium content in the system is in the parallel order in which the basic strength varies. Nickel ferrite is having maximum value for the electron acceptors adsorbed showing its high basic character. High activity towards aniline methylation has been shown by nickel ferrite. Although aniline alkylation is an acid-base catalyzed reaction, we cannot exclude the importance of cation distribution of ions at various sites in determining the catalytic activity. From the cation distribution data it is clear that, NF is having more Fe⁺³ ions at O_h site. Concentration of Fe⁺³ ions at O_h

Table 4.4.2 Acid-base properties and aniline conversion for NiCr_xFe_{2-x}O₄ series.

Catalyst	Total acidity (mmol g ⁻¹)	Limiting amount (10 ⁻⁴ mmol l ⁻¹ g ⁻¹)		Aniline conversion (%)
		TCNQ	Chloranil	
NF	0.162	25.71	8.23	65.3
NCrF 1	0.406	18.12	7.12	59.5
NCrF 2	0.460	16.28	6.28	57.8
NCrF 3	0.533	12.13	5.42	50.0
NCrF 4	0.256	21.22	7.79	63.1
NCr	0.197	22.56	7.21	63.8

site is decreased by the incorporation of Cr⁺³ ions. Systems other than NF are less active towards aniline methylation compared to pure NF. This may be due to the high basic character of NF created by the presence of more Fe⁺³ ions at the O_h site and for chromium containing systems basic strength is decreasing due to low concentration of Fe³⁺ ions at the O_h site. However, systems having higher chromium content are showing little enhancement in basic strength. In chromium containing systems, it is the Ni²⁺/Cr³⁺ ratio which is supposed to be determining the catalytic activity. Even though this is the case, the extreme systems (x = 1.8 and 2) are more active than other mixed systems. This may be due to the higher chromium content in these systems which may be creating strong basic centers. The increase in the limiting values of electron acceptors adsorbed is the evidence for that.

(b) NiGd_xFe_{2-x}O₄ (x=0 to 2) series

The results of aniline methylation reaction for NGF series are shown in table 4.4.3.

Table 4.4.3 Aniline methylation over NiGd_xFe_{2-x}O₄ series.

Catalyst	Aniline conversion (%)	Selectivity (%)			
		NMA	NNDMA	<i>p</i> -toluidine	Others
NF	65.3	99.5	0.5	--	--
NGF 1	64.0	98.0	2.0	--	--
NGF2	63.5	87.7	10.0	1.0	1.3
NGF 3	60.3	85.2	12.3	1.1	1.4
NGF 4	59.2	84.8	12.7	1.2	1.3
NG	58.0	84.0	11.8	0.9	3.3

Temperature-350 °C, MeOH:aniline-5, flow rate-4 mlh⁻¹, time-2 h.

Substitution of iron by gadolinium is found to decrease the activity of the systems towards methylation of aniline. Aniline conversion gradually decreases with progressive incorporation of gadolinium. Nickel ferrite is found to be most active towards the reaction. NMA is found to be the predominant product. More dimethyl derivatives are obtained in the present case. Unlike in chromium containing series, here detectable amount of *p*-toluidine is also formed. The formation of *p*-toluidine is reasonable according to the previous reports^{5,6}, according to which strong acid sites are mandatory for ring alkylation. Incorporation of gadolinium in to nickel ferrite creates more strong acid sites as compared to chromium containing systems.

Chapter 4

As already stated, basicity of the catalyst plays crucial rule in the catalytic activity. The basic strength of pure nickel ferrite is decreased by gadolinium incorporation. Limiting values of electron acceptors adsorbed show a gradual decrease with gadolinium incorporation. Aniline conversion gradually decreases from pure nickel ferrite and this gradation is in accordance with the variation of basic strength. Incorporation of gadolinium has improved the acid strength of the systems by creating more acid sites. Simultaneously this would have been resulted in the removal of basic centers. Acid-base properties and percentage aniline conversion for gadolinium containing nickel ferrites were shown in table 4.4.4.

Table.4.4.4 Acid-base properties and aniline conversion for $\text{NiGd}_x\text{Fe}_{2-x}\text{O}_4$ series.

Catalyst	Total acidity (mmol g^{-1})	Limiting amount ($10^{-4} \text{ mmol l}^{-1} \text{ g}^{-1}$)		Aniline conversion (%)
		TCNQ	Chloranil	
NF	0.162	25.71	8.23	65.3
NGF 1	0.195	22.89	8.19	64.0
NGF2	0.436	18.29	8.02	63.5
NGF 3	0.463	14.11	7.76	60.3
NGF 4	0.593	12.21	6.52	59.2
NG	1.094	11.19	6.32	58.0

According to the cation distribution data, systems containing both gadolinium and iron are having Gd^{3+} and Fe^{3+} ions at the O_h site and Ni^{2+} goes to T_d site only when $x = 1.6$, i.e., concentration of Ni^{2+} ion at the O_h site is not

changing up to $x = 1.2$. Therefore it is supposed that Ni^{2+} ion has no role in determining the catalytic activity; it is the Fe^{3+}/Gd^{3+} ratio which determine the variation in catalytic activity. Since this ratio decreases upon gadolinium incorporation, aniline conversion also decreases.

(c) Cobaltite series

Aniline conversion and selectivities of various products for the cobaltite series are shown in table 4.4.5.

Table 4.4.5 Aniline alkylation over cobaltites.

Catalyst	Aniline conversion (%)	Selectivity (%)			
		NMA	NNDMA	<i>p</i> -toluidine	Others
NC .5	63.5	70.2	17.4	1.2	11.2
NC 1	61.8	69.8	20.5	1.0	8.7
NC 1.5	59.2	68.0	27.2	1.4	3.4
CC .5	54.6	83.2	14.3	2.5	--
CC 1	52.3	82.5	15.0	2.5	--

Temperature-350 °C, MeOH:aniline-5, flow rate-4 mlh⁻¹, time-2 h.

Cobaltites are less active towards aniline methylation as compared to ferrites. With in the cobaltite series nickel cobaltites are more active than copper cobaltites. Low nickel content is found to be favorable for the aniline alkylation. NC.5 is more active than the other two. Similar is the case for copper cobaltites; the system having low copper content is more active. Nickel

Chapter 4

cobaltites formed more dialkyl derivative as compared to copper cobaltites. Formation of C-alkylated product, *p*-toluidine, is also observed.

The variation in activity of cobaltites is in accordance with the variation in basic strength. Incorporation of more and more nickel and copper into cobaltites has diminished the basic character. Nickel cobaltites are found to be more basic than copper cobaltites. The acid-base properties along with aniline conversion for cobaltites are shown in table 4.4.6.

Table 4.4.6. Acid-base properties and aniline conversion for cobaltites.

Catalyst	Total acidity (mmol g ⁻¹)	Limiting amount (10 ⁻⁴ mmol l ⁻¹ g ⁻¹)		Aniline conversion (%)
		TCNQ	Chloranil	
NC .5	0.285	22.23	9.13	63.5
NC 1	0.295	20.19	9.06	61.8
NC 1.5	0.343	19.22	8.32	59.2
CC .5	0.359	16.80	8.25	54.6
CC 1	0.374	16.44	8.12	52.3

From the cation distribution data, in nickel cobaltites, Ni²⁺ occupies O_h site, and for copper cobaltites, Cu²⁺ ions occupies T_d and O_h site. For nickel cobaltites, it is the ratio Co³⁺/Ni²⁺ which determines the activity. NC.5 is having high Co³⁺/Ni²⁺ ratio and hence more active in that series. In the case of copper cobaltites the one which is having high Co³⁺/Cu²⁺ ratio at O_h site is highly active towards aniline alkylation than the other.

Effect of time on stream

Some of the representative spinels were studied for the catalyst stability by running the reaction for a period of 9 h under optimized conditions. Activity was checked at regular intervals. The studied spinels were found to maintain their activity. No considerable decrease in aniline conversion was observed for ferrite where as cobaltites showed little deactivation after 7 h. Effect of time on stream is shown in Fig.4.4.5.

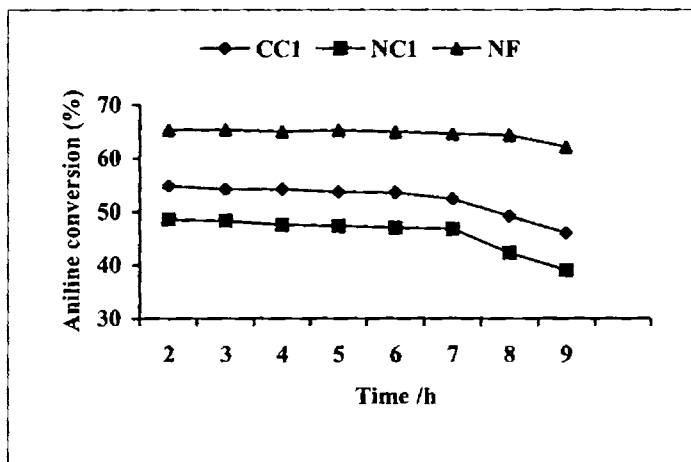


Fig.4.4.5 Effect of time on stream on aniline methylation.
Temperature-350 °C, MeOH:aniline-5, flow rate-4 mlh⁻¹.

4.4.3 Mechanism of aniline alkylation

The reaction mechanism for N-mono methylation of aniline is shown in Fig.4.4.6. This scheme involves adsorption of methanol and aniline on the surface, using acid-base centers in each case. This results in O-H and N-H bond polarization of methanol and aniline respectively and followed by a

methyl group migration from the co-ordinated methanol to the nitrogen atom of aniline which leads to NMA¹². Since aniline itself is a strong base, even weak Lewis acid sites on the catalyst surface can effectively co-ordinate with aniline. If acidity is sufficiently high, the interaction of aniline and the co-ordinate site will be sufficiently strong. This leads to deamination of aniline leading to the formation of benzene and toluene. In the case of aniline methylation, since aniline itself is a strong base, the basicity of the catalyst surface plays a dominating role on the adsorption and activation of aniline to give NMA¹².

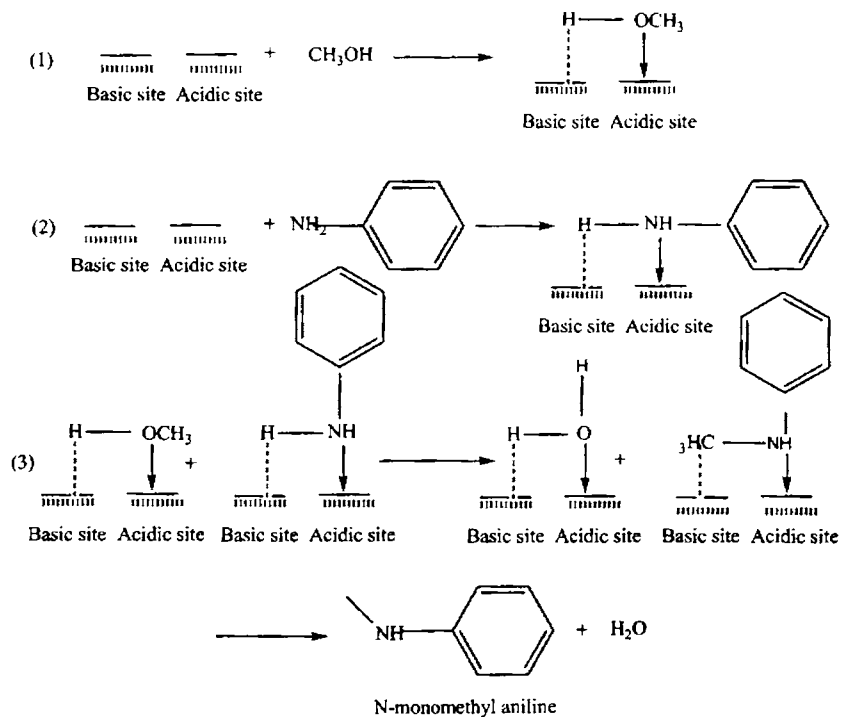


Fig.4.4.6 Mechanism of aniline alkylation using methanol as alkylating agent.

References:

Phenol methylation

- [1] R.Fieze, Ullmann's Encyclopedia of Industrial Chemistry: Federal Republic of Germany, A.G.Bayer, Leverkusen, A 19, p. 324.
- [2] E.Santhacesaria, D.Grasso, D.Galosa and S.Carra; Appl. Catal., 64 (1990) 83.
- [3] F.Nozaki and I.Kimura; Bull. Chem. Soc. Jpn., 50 (1977) 614.
- [4] K.Li, I.Wang and K.Chang; Ind. Eng. Chem. Res., 32 (1993) 1007.
- [5] M.C.Samoloda, E.Grgoriadov, Z. Kiprarissides and I.A.Vasalos; J. Catal., 152 (1995) 52.
- [6] C.Bezouhanova and M.A.Al. Zahari; Appl. Catal., 83 (1992) 45.
- [7] S.Sato, K.Koisumi and F.Nozaki; Appl. Catal. A., 133 (1995) L7.
- [8] S.Velu and C.S.Swami; Appl. Catal. A., 162 (1997) 81.
- [9] S.Namba, T.Yoshima, Ttba and N.Hara; Stud. Surf. Sci. Catal., 5 (1980) 105.
- [10] R.Dowbwnko, in: J.I. Kroschwitz, M.Houl-Grant (Eds.), Kirk-Othmer Encyclopedia of Chemical Technology, Vol.2, 4th Edition, 1999, p.106.
- [11] M.Inoue and S.Enomoto; Chem. Parm. Bull., 20 (1972) 232.
- [12] T.Kotanigowa, M.Yamamoto, K.Shimakowa and Y.Yoshida; Bull. Chem. Soc. Jpn., 44 (1971) 1961.
- [13] V.Venkatrao, K.V.R.Chary, V.Durgakumari and S.Narayan; Appl. Catal., 61 (1990) 89.
- [14] H.Grabowska, J.Jablonski, W.Mista and J.Wrzyszcz; Res. Chem. Intermed., 22 (1996) 53.

- [15] M.Misono and N.Nojiri., *Appl. Catal.*, 64 (1990) 1.
- [16] B.E.Leach, US Patent 4227024 (1980).
- [17] T.Kotanigawa and K.Shimakowa; *Bull. Chem. Soc. Jpn.*, 47 (1974) 1535.
- [18] T.Kotanigawa; *Bull. Chem. Soc. Jpn.*, 47 (1974) 950.
- [19] B.S.Rao, K.Sreekumar and T.M.Jyothi; Indian Patent 2707/98 (1998).
- [20] K.Lazar, T.Mathew, Z.Koppany, J.Megyeri, V.Samuel, S.P.Mirajkar, B.S.Rao and L.Guczi; *Phys. Chem. Chem. Phys.*, 4 (2002) 3530.
- [21] T.Mathew, N.R.Shiju, K.Sreekumar, B.S.Rao and C.S.Gopinath; *J. Catal.*, 210 (2002) 405.
- [22] K.Sreekumar and S.Sugunan; *J. Mol. Catal. A. Chem.*, 185 (2002) 259.
- [23] K.Sreekumar and S.Sugunan; *Appl.Catal. A. Gen.*, 230 (2002) 245.
- [24] E.Santacesaria, D.Grasso, D.Gelosa and S.Carra; *Appl. Catal.*, 64 (1990) 83.
- [25] J.P.Jacobs, A.Maltha, J.R.H.Reintjes, T.Drimal, V.Ponec and H.H.Brogersma; *J. Catal.*, 147 (1994) 294.
- [26] K.Tanabe, T.Nishizaki, in: F.C.Tompkins (Eds.), *Proceedings of the Sixth International Congress on Catalysis*, The Chemical Society, London, 1997.
- [27] L.H.Klemm, C.E.Klopfenstein and J.Shabtai; *J. Org. Chem.*, 35 (1970) 1069.
- [28] T.Mathew, M.Vijayraj, S.Pai, B.B.Tope, S.G.Hegde, B.S.Rao and C.S.Gopinath; *J. Catal.*, 227 (2004) 175.

Phenol tert butylation

- [1] M.Inoue and S.Emoto; *Chem. Pharm. Bull.*, 20 (1972) 232.
- [2] S.Velu and C.S.Swami; *Res. Chem. Intermed.*, 26 (2000) 295.
- [3] A.Sakthivel, N.Saritha and P.Selvam; *Catal. Lett.*, 72 (2001) 225.
- [4] K.G.Chandra and M.M.Sharma; *Catal. Lett.*, 19 (1993) 309.
- [5] R.A.Rajadhyakasha and D.D.Chawdhari; *Ind. Eng. Chem. Res.*, 26 (1987) 1276.
- [6] S.K.Badamali, S.Sakthivel and P.Selvam; *Catal. Lett.*, 65 (2000) 291.
- [7] K.Zhang, H.Zhang, G.Xu, S.Xiang, D.Xu, S.Liu and H.Li; *Appl. Catal. A.*, 207 (2001) 183.
- [8] S.K.Badamali, S.Sakthivel and P.Selvam; *Catal. Today.*, 63 (2000) 291.
- [9] S.Subramanian, M.Mitra, C.V.V.Satyanarayana and D.K.Chakrabarthy; *Appl. Catal. A.*, 159 (1997) 229.
- [10] K.Zhang, C.Huang, S.Xiang, S.Liu, D.Xu and H.Li; *Appl. Catal. A.*, 166 (1998) 89.
- [11] A.H.Padmasri, V.D.Kumari and P.K.Rao; *Stud.Surf.Sci.Catal.*, 113 (1998) 563.
- [12] J.W.Yoo, C.W.Lee, B.Wang and S.E.Park; *Res.Chem.Intermed.*, 27 (2001) 561.
- [13] M.Naga, T.Yoda and M.Kodomari; *J.Catal.*, 201 (2001) 105.
- [14] F.Cunill, J.Tejero and J.F.Izquierdo; *Appl.Catal.*, 34 (1987) 341.
- [15] J.Tajero, F.Cunill and S.Manzano; *Appl.Catal.*, 38 (1988) 327.
- [16] G.D.Yadav; *Bull. Catal. Soc. India.*, 15 (1998) 21.
- [17] K.Chandler, F.Deng, A.K.Dillow, C.L.Liotta and C.A.Eckert; *Ind. Eng.*

- Chem. Res., 36 (1997) 5175.
- [18] X.Xu, M.J.Antal Jr and D.G.M.Anderson; *Ind. Eng. Chem. Res.*, 36 (1997) 23.
- [19] K.Zhang, H.Zhang, G.Xu, S.Xiang, D.Xu, S.Liu and H.Li; *Appl. Catal. A. Gen.*, 207 (2001) 183.
- [20] T.Mathew, B.S.Rao and C.S.Gopinath; *J. Catal.*, 222 (2004) 107.
- [21] G.D.Yadav and N.S.Doshi; *Appl. Catal. A. Gen.*, 236 (2002) 129.

Thymol synthesis

- [1] N.Dirdy, L.Dubereuil and M.Pinkas; *Pharmazie.*, 48 (1993) 301.
- [2] I.M.Helander, H.L.Alakomi, K.Latva-Kala, T.Mattila-Sandholm, I.Pol, E.J.Smid, L.G.M.gorris and A.von Wright; *J. Agric. Food. Chem.*, 46 (1998) 3590.
- [3] S.Shapiro; *Oral Microbiol. Immun.*, 11 (1996) 350.
- [4] M.G.Botelho; *Microbios.*, 103 (2000) 31.
- [5] H.-G.Franc and J.W.Stadelhofer; *Industrial Aromatic Chemistry*, Springer, Berlin, Heidelberg, 1988, p. 168.
- [6] T.Yamanaka; *Bull. Chem. Soc. Jpn.*, 49 (1976) 2669.
- [7] M.Nitta, K.Yamaguchi and K.Aomura; *Bull. Chem. Soc. Jpn.*, 47 (1974) 2897.
- [8] P.Wimmer, H.-G.Buysch and L.Puppe; *US Patent 5030770* (1991).
- [9] M.Nitta, K.Aomura and K.Yamaguchi; *Bull. Chem. Soc. Jpn.*, 47 (1974) 2360.
- [10] W.Biedermann, H.Kollor and K.Wedemeyer; *US Patent 4086283*, 1978.
- [11] S.Velu and S.Sivakumar; *Res. Chem. Intermed.*, 24 (1998) 657.

- [12] H.Grabowska and J.Wrzyszcz; *Res. Chem. Intermed.*, 27 (2001) 281.
- [13] H.Grabowska, W.Kaczmarczyk and J.Wrzyszcz; *Appl. Catal.*, 47 (1989) 351.
- [14] J.Wrzyszcz and H.Grabowska; *Polish. J. Chem. Technol.*, 1 (1999) 50.
- [15] H.Grabowska, J.Wrzyszcz and C.S.Joshi; *Res. Chem. Intermed.*, 25 (1999) 425.
- [16] H.Grabowska, W.Mista, J.Trawczynski, J.Wrzyszcz and M.Zawadzki; *Appl. Catal. A. Gen.*, 220 (2001) 207.
- [17] V.Umamaheswari, M.Palanichami and V.Murugesan; *J. Catal.*, 210 (2002) 367.
- [18] K.Shanmugapriya, M.Palanichami, B.Arabindoo and V.Murugesan; *J. Catal.*, 224 (2004) 347.
- [19] R.Stroh, R.Seydel, W.Hahn, in: W.Forest (Eds.), *Newer Methods of Preparative Organic Chemistry*, Vol. 2, Academic Press, New York, 1963, p.337.
- [20] A.Kelvin, K.Wedemeyer and Bayer DE-OS 224 2628 (1972).
- [21] D.R.Taylor and K.H.Ludlum, *J. Phys. Chem.*, 76 (1972) 2882.
- [22] T.Mathew, M.Vijayraj, S.Pai, B.B.Tope, S.G.Hegde, B.S.Rao and C.S.Gopinath; *J. Catal.*, 227 (2004) 175.
- [23] K.Sreekumar and S.Sugunan; *Appl. Catal. A. Gen.*, 230 (2002) 245.
- [24] K.Sreekumar, T.Mathew, S.P.Mirajkar, S.Sugunan and B.S.Rao; *Appl. Catal. A. Gen.*, 210 (2000) L1-L8.
- [25] T.Mathew, B.S.Rao and C.S.Gopinath; *J. Catal.*, 222 (2004) 107.
- [26] H.Grabowska, L.Syper and M.Zawadzki; *Appl. Catal. A. Gen.*, 277

(2004) 91.

Aniline methylation

- [1] S.Prasad and B.S.Rao; *J. Mol. Catal.*, 62 (1990) 12.
- [2] S.P.Elangovan, C.Kannan, B.Arabindoo and V.Murugesan; *Appl. Catal.*, 174 (1998) 213.
- [3] K.Sreekumar, T.M.Jyothi, B.P.Kiran, B.S.Rao and S.Sugunan; *J. Mol. Catal. A. Chem.*, 159 (2) (2000) 327.
- [4] F.M.Bautista, J.M.Campdo, A.Garcla, D.Luna, J.M.Marrinas, A.Romero and M.R.Urbano; *J. Catal.*, 172 (1997) 103.
- [5] S.I.Woo, J.K.Lee, S.B.Hong, Y.K.Park and Y.S.Un; *Stud. Surf. Sci. Catal.*, 49 (1989) 1095.
- [6] Y.K.Park, K.Y.Park and S.I.Woo; *Catal. Lett.*, 26 (1994) 169.
- [7] P.Y.Chen, M.C.Chen, H.Y.Chu, N.S.Chang and T.K.Chuang; *Stud. Surf. Sci. Catal.*, 28 (1986) 739.
- [8] K.G.Lone and O.V.Kiktyanin; *Stud. Surf. Sci. Catal.*, 49 (1989) 1073.
- [9] S.Narayan and K.Deshpande; *J. Mol. Catal.*, 104 (1995) 109.
- [10] S.Narayan and K.Deshpande; *Appl. Catal. A.*, 135 (1996) 125.
- [11] K.Sreekumar, T.Raja, B.P.Kiran, S.Sugunan and B.S.Rao; *Appl. Catal. A.*, 182 (1999) 327.
- [12] K.Sreekumar and S.Sugunan; *Appl. Catal. A. Gen.*, 230 (2002) 245.
- [13] M.A.Aramendia, V.Borau, C.Jimenez and F.J.Romero; *Appl. Catal.*, 183 (1999) 73.
- [14] S.Yuvaraj and M.Palanichami; "Catalysis: Modern Trends" (Eds., N.M.Gupta and D.K.Chakrabarthy) Narosa Publishing House, New

Delhi, India, 1995.

- [15] K.Sreekumar, T.Mathew, S.P.Mirajkar, S.Sugunan and B.S.Rao; Appl. Catal. A. Gen., 201 (2000) L1-L8.

Catalytic oxidation is widely employed in the manufacture of bulk chemicals from aromatics and more recently, as an environmentally attractive method for the production of fine chemicals. The oxidation of organic substrates represents one of the most important industrial chemical reactions, explaining the significant efforts invested in the research and development of new heterogeneous catalysts with increased activities and selectivities in these type reactions. As known, the scope of partial oxidation is wide, ranging from the large-scale production of commodities to the synthesis of minute amounts of pharmaceuticals and fine chemicals. Compared with other chemical processes the oxidation process is complex and difficult to be controlled or to be stopped at a certain stage. For these reason the selective oxidation is an attractive field of research. Mixed oxides containing transition metal oxides are becoming popular in heterogeneously catalyzed oxygen transfer reactions in the liquid phase using hydroperoxides. The use of hydrogen peroxides in the oxidation of organic molecules is a mojour goal, both in academic and in industry, because of the environmental acceptability of this oxidant, which depends mainly on the nature of its by-product, water. This chapter has been divided into three sections-oxidation reactions of cyclohexane, benzyl alcohol and styrene. The oxidation products of these reactions are important in fine chemical industry, pharmaceuticals etc. Oxidation reactions were carried out in liquid phase using hydrogen peroxide as oxidant. Effect of change in catalyst composition on oxidation behaviour has been discussed thoroughly.

5.1 Cyclohexane Oxidation

The activation and functionalization of paraffins is one of the world wide pursuit research directions with a high potential for the development of new catalytic process technologies. The selective oxidation of hydrocarbons, which requires activation of the relatively inert carbon-hydrogen bond, is an important commercial reaction for functionalizing hydrocarbons to yield products that are important themselves or as intermediates for other chemicals. The oxidation of cyclohexane into cyclohexanol and cyclohexanone is of considerable importance in the chemical industry for producing nylon-6 polymers and is performed industrially in the liquid phase by using homogeneous catalysts and air as an oxidant. Most of the current process still uses “sacrificial” oxidants like nitric acid, hydrogen peroxide and alkyl hydroperoxides, which may have low energy efficiency and selectivity as well as generate environmentally hazardous waste and by-products¹. Alternatively, cyclohexane can be oxidized to cyclohexene, which can be further converted to valuable products. Many research efforts are focused in the last time to find new and selective catalysts²⁻⁵.

Transition metal ions such as Co^{3+} , Mn^{3+} and Fe^{3+} substituted aluminophosphates and MeAPO-n are promising catalysts for the selective oxidation of cyclohexane with molecular oxygen due to both the highly dispersed redox active centers and the unique shape- selectivity in the metal incorporated aluminophosphates⁶. Although the catalytic activity of transition metal ions is reported to be normally low in homogeneous systems while an enhanced activity is observed when they are heterogenised onto a solid support⁷. Several work have been published for the oxidation of cyclohexane

in the presence of compressed CO₂⁸⁻¹⁰, which indicated that it is advantageous to conduct the reaction in supercritical CO₂.

However rare earth metal oxides are known for their strong redox properties and for their ability to catalyze the oxidation of several hydrocarbons under rigorous conditions¹¹⁻¹². Oxidation of cyclohexane to cyclohexanol and cyclohexanone catalyzed by SmCl₃ and EuCl₃ have been reported^{13,14}.

Transition metals based on groups 4 (Ti), 5 (V and Nb) and 6 (Mo) are well known amongst the most active homogeneous and heterogeneous catalysts for alkene and alkane oxidation¹⁵⁻¹⁹. Transition metal oxides have been extensively studied for the cyclohexane oxidation reaction. Baiker²⁰ has studied cyclohexane oxidation reaction in the presence of silica-based mixed oxides prepared by sol-gel route and the resulting metallosilicates have shown a good activity. More recently, Schuchardt et al.²¹⁻²⁴ have oxidized cyclohexane with *tert*-butyl hydroperoxide (TBHP) using M_xO_y-SiO₂ catalysts (M = Cu, Cr, Ce) prepared by sol-gel route. Gekhman et al.²⁵ have studied the oxidation of cyclohexane with H₂O₂/AcOH in the presence of vanadium (V) complex catalyst. The results showed a good conversion, reaching up to 40 % while the reaction product is the ol-one (cyclohexanol-cyclohexanone) mixture. Bellifa et al.²⁶ have studied the cyclohexane oxidation catalyzed by 20 wt % V₂O₅-TiO₂ mixed oxide and they obtained an approximate 8 % conversion into cyclohexanol and 76 % selectivity.

MCM-41 molecular sieves have been tried extensively for the cyclohexane oxidation reaction. Selvam et al. used systems with (Cr) MCM-41²⁷ and (Fe) MCM-41²⁸ as catalysts and obtained excellent results for the

Oxidation Reactions

selective oxidation of cyclohexane. More recently, Qian et al. reported on the oxidation of cyclohexane with Au/ZSM-5²⁹ and Au/MCM-41³⁰ as catalysts and oxygen as an oxidant in a solvent-free system. The results indicated that Au-ZSM-5 and Au-MCM-41 are very efficient catalysts for the oxidation of cyclohexane. Incorporation of transition metal ions into the lattice can lead to stable isolated and well defined redox active catalytic sites³¹⁻³³. Pires et al. have demonstrated that REYs are active catalysts for the oxidation of cyclohexane with TBHP. Rare earth exchanged zeolite Y with Si:Al ratios of 2.6, 12.5 and 28 are active catalysts for the liquid phase oxidation of cyclohexane³⁴. Reaction scheme for cyclohexane oxidation is given in Fig. 5.1.1.

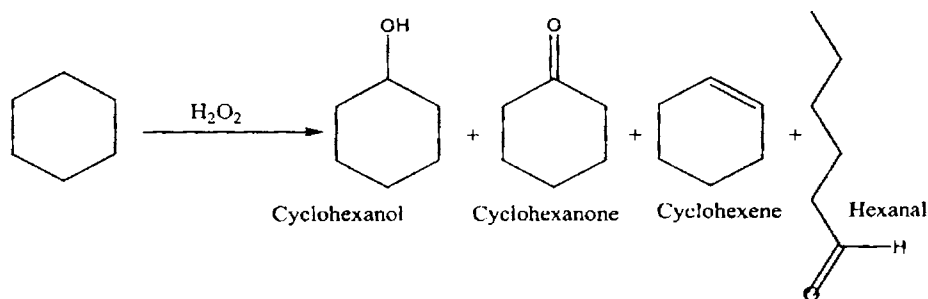


Fig.5.1.1 Reaction scheme for cyclohexane oxidation.

This section contains a detailed investigation of cyclohexane oxidation using H₂O₂ as oxidant. The prepared systems were tried for the reaction under optimized conditions. Cyclohexanol, cyclohexanone and cyclohexene were the main products obtained.

5.1.1 Process optimization

Reaction parameters such as time, temperature, effect of solvent,

reactant molar ratio etc. were optimized by using 0.1 g of catalyst.

5.1.1.1 Effect of reaction time

Cyclohexane oxidation was studied over the catalyst NF for a period of 12 h. The results obtained are shown in Fig.5.1.2.

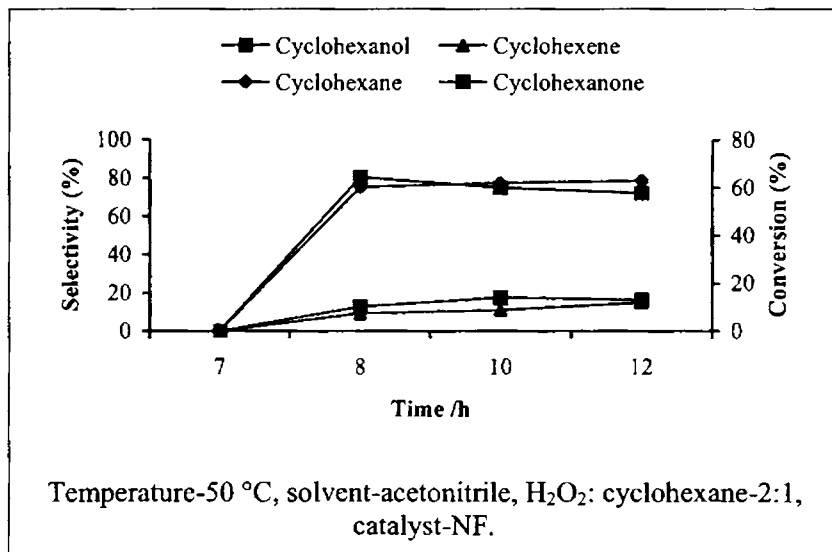


Fig.5.1.2 Effect of reaction time on cyclohexane oxidation.

Up to 7 h, there was found very little or no reaction. After 8th h, there observed a drastic increase in conversion of cyclohexane up to 60 %. Cyclohexanol was the main product obtained initially. As time proceeds, the selectivity towards 'ol' was decreased where as that of 'one' and 'ene' were increased. After 10 h, no pronounced increase in cyclohexane conversion was observed. A reaction time of 8 h is selected for further studies.

5.1.1.2 Effect of reaction temperature

Effect of variation in reaction temperature on cyclohexane oxidation reaction carried over the catalyst NF is shown in Fig.5.1.3.

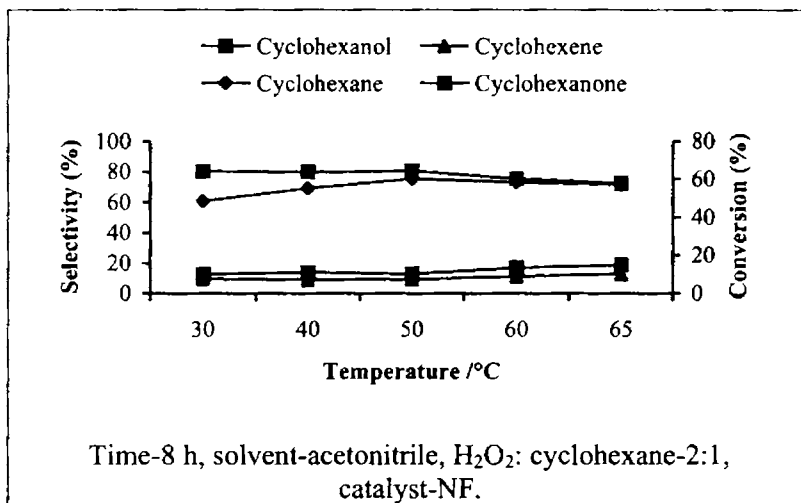


Fig.5.1.3 Effect of temperature on cyclohexane oxidation.

Cyclohexane oxidation was studied over a range of temperatures from 30 °C to 65 °C. Rise in temperature is found to be favourable for the reaction up to 50 °C and cyclohexane conversion is found to be decreasing slightly after 50 °C. At higher temperatures, selectivity towards 'ol' decreases. A reaction temperature of 50 °C is selected for further studies.

5.1.1.3 Effect of solvent

Effect of solvent on cyclohexane oxidation is shown in Fig.5.1.4.

The reaction was studied using protic and aprotic solvents. Aprotic solvents were found to be favourable for cyclohexane oxidation. Although no detectable variation in cyclohexane conversion was observed when the

reaction was carried out in acetonitrile and acetone, the 'ol' selectivity was better in acetonitrile. Cyclohexanone is the second main product obtained. Acetonitrile is selected as solvent for further studies.

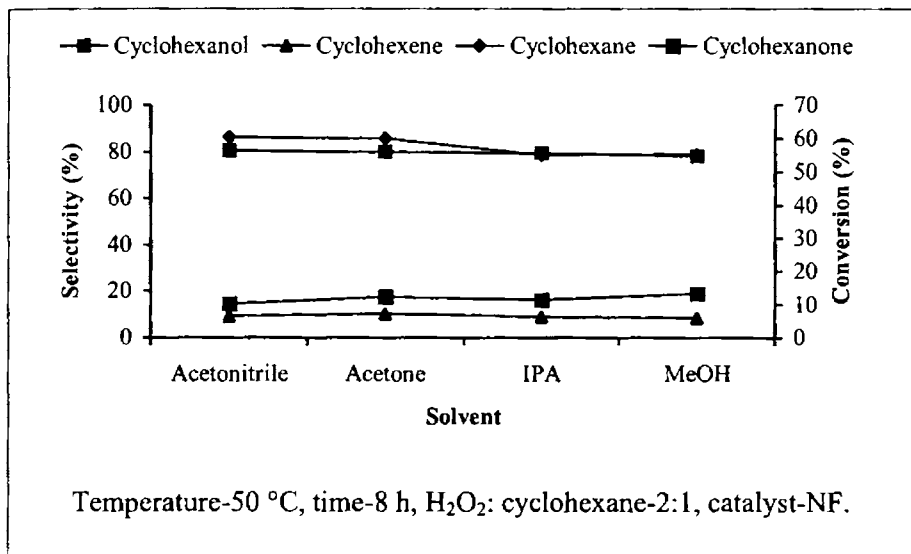


Fig.5.1.4 Effect of solvent on cyclohexane oxidation.

5.1.1.4 Effect of H₂O₂ to cyclohexane molar ratio

Cyclohexane oxidation was performed at different H₂O₂: cyclohexane molar ratios using NF catalyst. Fig.5.1.5 shows the response of the reaction towards the variation in reactant molar ratio.

More H₂O₂ in the reaction mixture is found to be favourable for the reaction. At higher percentage of cyclohexane, low conversion was observed. Initially, an increase in the percentage of cyclohexane favored the formation of 'ol' and decreases thereafter. At higher percentage of cyclohexane, selectivity towards 'one' was improved. H₂O₂: cyclohexane molar ratio of 2:1 was selected for the further studies.

Oxidation Reactions

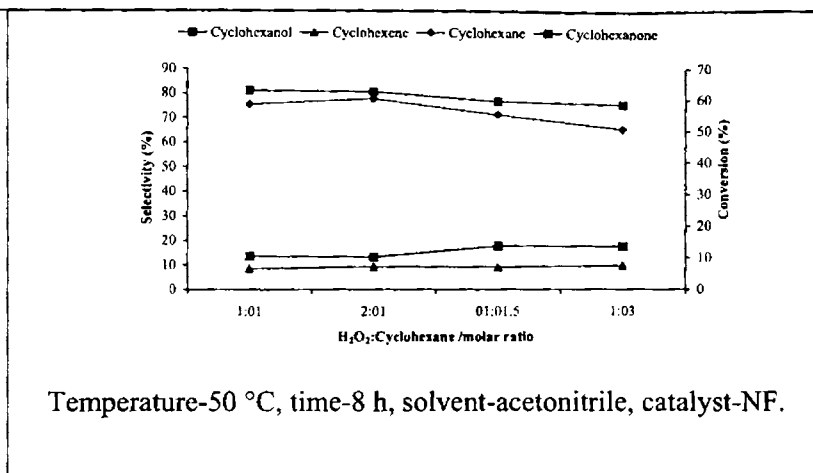


Fig.5.1.5 Effect of reactant molar ratio on cyclohexane oxidation.

5.1.2 Effect of catalyst composition

(a) $\text{NiCr}_x\text{Fe}_{2-x}\text{O}_4$ ($x = 0-2$) series

The results obtained for chromium containing nickel ferrites for the cyclohexane oxidation reaction carried out under optimized conditions are given in table 5.1.1.

Table 5.1.1 Cyclohexane oxidation over chromium containing nickel ferrites.

Catalyst	Cyclohexane con. (%)	Selectivity (%)		
		Cyclohexanol	Cyclohexene	Cyclohexanone
NF	50.3	80.5	9.3	10.2
NCrF 1	63.1	81.2	9.5	9.3
NCrF 2	64.8	81.6	9.5	8.9
NCrF 3	65.8	82.1	7.4	10.5
NCrF 4	66.5	80.2	9.8	10.0
NCr	51.7	80.0	7.6	11.4

Time-8 h, temperature-50 °C, H_2O_2 : cyclohexane-2:1, solvent-acetonitrile.

Substitution of iron by chromium is found to have profound effect on the oxidation of cyclohexane. Incorporation of 20 % chromium has increased the cyclohexane conversion by 13 %. This increase in conversion has been continued up to NCrF_4 . Nickel chromite is less active as compared to mixed systems but it is more active than nickel ferrite. More than 80 % of the products were cyclohexanol. Not much variation in cyclohexanol selectivity was observed with chromium incorporation. NCrF_3 showed a maximum cyclohexanol selectivity of 82 %.

(b) $\text{NiGd}_x\text{Fe}_{2-x}\text{O}_4$ ($x = 0-2$) series

Table 5.1.2 shows the results obtained for cyclohexane oxidation carried over gadolinium incorporated nickel ferrites.

Table 5.1.2 Cyclohexane oxidation over gadolinium containing nickel ferrites.

Catalyst	Cyclohexane con. (%)	Selectivity (%)		
		Cyclohexanol	Cyclohexene	Cyclohexanone
NF	50.3	80.5	9.3	10.2
NGF 1	62.3	80.5	9.7	9.8
NGF2	66.2	82.1	7.7	10.2
NGF 3	68.8	82.7	7.4	9.9
NGF 4	72.0	83.1	6.4	10.5
NG	53.2	84.2	4.8	11.0

Time-8 h, temperature-50 °C, H_2O_2 : cyclohexane-2:1, solvent-acetonitrile.

Incorporation of gadolinium into nickel ferrite has much improved the activity as compared to chromium containing series. Cyclohexane conversion

Oxidation Reactions

increased with increase in percentage of gadolinium. Mixed spinels i.e., those containing both iron and gadolinium are more active than pure systems. Although nickel gadolinite is little more active than nickel ferrite, its activity is much lower as compared to systems containing both iron and gadolinium. Incorporation of gadolinium has improved the 'ol' selectivity. Nickel gadolinite is more selective towards 'ol'. At higher percentages of gadolinium, the selectivity towards 'one' also improved by little.

(c) Cobaltite series

The results obtained for cobaltite series is given in table 5.1.3.

Table 5.1.3 Cyclohexane oxidation over cobaltites.

Catalyst	Cyclohexane con. (%)	Selectivity (%)		
		Cyclohexanol	Cyclohexene	Cyclohexanone
NC .5	55.5	82.3	6.5	11.2
NC 1	70.3	82.5	6.2	11.3
NC 1.5	73.4	84.2	3.6	12.2
CC .5	70.3	83.1	6.4	10.5
CC 1	72.3	82.8	7.0	10.2

Time-8 h, temperature-50 °C, H₂O₂: cyclohexane-2:1, solvent-acetonitrile.

For nickel cobaltites, increase in percentage of nickel is found to be favourable the reaction; systems having more nickel (divalent ion) are more active. Similar is the case for copper cobaltites. CC1, which is having more copper, is more active than CC.5.

In heterogeneous catalysis system, the activity of catalyst depends on the number of actual active sites available for the chemical reaction to take

place. The activity of spinels depends on the distribution of cations among the octahedral and tetrahedral sites. Moreover, it was established that the octahedral sites are exclusively exposed at the surface of the spinel crystallites and thus the catalytic activity is mainly due to the octahedral cations^{35,36}. Many authors have reported that the octahedral ions present in the spinel crystal lattice were responsible for the activity towards oxidation reactions^{37,38}. For chromium containing systems, the activity is found to be increasing with increase in chromium content. Chromium preferably occupies O_h site on substitution for iron. Even though the concentration of nickel at the octahedral site decreases after $x = 0.8$ (table 3.1.6), the activity of the catalysts increases with increase in chromium content which shows that Ni^{2+} ion has no role in determining the activity. It is the concentration of trivalent ions present at the octahedral site, which determines the activity. $NiCrF_4$ is having more trivalent ion concentration at the octahedral site and has maximum activity. Nickel chromite is less active than systems containing both iron and chromium, which shows that even though the incorporation of chromium enhances the activity, the presence of iron is also important for the performance of the catalyst. The result indicates that although the presence of chromium ions is more favorable for the reaction than iron ions, the reaction requires the presence of iron also even though if it is present in minimum concentration, which is confirmed from the diminished activity of pure nickel chromite which does not contain iron.

The trend in activity of the catalysts with substitution of iron by chromium can also be explained in terms of the reducibility of the catalysts. The behaviour of these oxide systems towards the oxidation of hydrocarbons

Oxidation Reactions

can be very well correlated with their reducibility, which can be found from the H₂-TPR study. Systems which show high oxidation behaviour can be easily reduced with hydrogen or the reduction temperature will be less. The low reduction temperature in the TPR experiments confirms the availability of lattice oxygen³⁹. We have investigated the reduction behaviour upon chromium incorporation and the results follows the order-NF (510 °C) > NCrF₂ (424 °C) > NCrF₄ (367 °C) < NCr (509 °C), where the values in the parenthesis indicates the reduction temperature obtained from the TPR experiment. These results indicate that the reduction temperature of pure nickel ferrite can be minimized by the incorporation of chromium; accordingly they showed an increased activity towards the oxidation reaction. Comparing the reducibility with the oxidation behaviour, it follows that the sequence of increasing activity clearly follows the sequence of increasing reducibility of the systems.

Similar effect is found to play in the case of gadolinium containing systems. When iron is replaced by gadolinium, gadolinium preferably occupies the octahedral site. Since the concentration of Ni²⁺ ions remains unchanged up to x = 1.2, and activity increases with increase in gadolinium content, it is supposed that the catalytic activity is mainly determined by the iron and gadolinium ions. Activity is found to be increasing with increase in the trivalent ion concentration at the octahedral site. Here also pure nickel gadolinite, which does not contain iron, is less active than mixed systems having both iron and gadolinium which once again enlightens to the fact that although in minimum amount, presence of Fe³⁺ ions is found to be beneficial for improving the catalytic activity.

Replacing iron by gadolinium has improved the activity of the systems towards the oxidation of cyclohexane. The reduction temperature, obtained from the TPR studies is found to be gradually decreasing with incorporation of gadolinium- NF (510 °C) > NGF3 (368 °C) > NGF4 (359 °C) < NG (483 °C). But reduction temperature of nickel gadolinite is higher than mixed systems. This shows that systems containing both gadolinium and iron can be easily reduced compared to pure systems. This increased reducibility upon gadolinium incorporation is clearly reflected in their activity towards the oxidation reaction. In other words the oxidation capacity has been improved by the incorporation of gadolinium into nickel ferrite. The lower reducibility of NG has reduced its activity compared to mixed systems.

As far as the cobaltite series is considered, nickel cobaltites are more active than copper cobaltites. The high activity of nickel cobaltites can be correlated with their high reducibility as compared to copper cobaltites. The reduction temperature obtained from TPR experiment for nickel cobaltites is lower than that for copper cobaltites; NC1 (331 °C) > NC1.5 (306 °C), CC.5 (456 °C) > CC1 (434 °C). Within the nickel cobaltites, the activity is increasing with increase in concentration of nickel. Since nickel cobaltites have an inverse structure, nickel occupies octahedral site. As we increase the concentration of nickel, more and more nickel goes to the exposed octahedral site. Hence here it is supposed that it is the increase in concentration of Ni²⁺ ions at the octahedral site which is responsible for the improved catalytic activity of nickel cobaltites. A similar effect is found to play in the case of copper cobaltites. CC1 is having more Cu²⁺ ions at O_h site. An increase in

Oxidation Reactions

concentration of Cu^{2+} ions at the octahedral site is supposed to be a responsible factor for the high oxidation activity of CC1 as compared to CC.5.

Catalyst reusability

Reusability studies of catalysts were studied by recycling the reaction using the same catalysts. After the reaction, the catalyst was separated from the reaction mixture by filtration and was washed with acetone to remove the organic contents. The catalyst was then dried, activated and again used for the same reaction under same reaction conditions. The results obtained were presented in table 5.1.4.

Table 5.1.4 Catalyst reusability study for cyclohexane oxidation reaction.

Catalyst	1 cycle		2 cycle		3 cycle	
	*ANE con. (%)	**CHOL sel. (%)	ANE con. (%)	CHOL sel. (%)	ANE con. (%)	CHOL sel. (%)
NCrF4	65.2	82.1	63.2	79.3	60.1	76.5
NGF4	72.8	84.2	72.9	84.0	70.5	82.5
NCI	70.3	82.5	69.5	82.8	66.4	81.0
CC1	72.0	82.0	71.0	83.2	67.8	80.1

* Cyclohexane, ** Cyclohexanol

The catalysts were found to lose their activity after 2nd cycle. For cobaltites, activity diminished considerably in the 3rd cycle. Decrease in cyclohexanol selectivity has also been observed for certain systems. The loss in activity may be due to leaching effect where by active ions leach out during the reaction.

5.1.3 Mechanism of cyclohexane oxidation

An induction period has been observed for the cyclohexane oxidation reaction. After 8 h, a drastic increase in cyclohexane conversion has been observed. This observation leads us to propose that the reaction proceeds through a radical mechanism. The reaction has been studied in detail by many authors and many have proposed a radical mechanism for the reaction⁴⁰⁻⁴⁶.

Using all the prepared spinels, cyclohexanol is the major product obtained. We are tentatively proposing a mechanism based on early reports, according to which, the formation of observed products can be explained. The active metal cation is first oxidized by decomposition of hydrogen peroxide there by forming hydroxyl radicals. Abstraction of hydrogen from cyclohexane by hydroxyl radicals leads to the formation of cyclohexyl radicals which reacts with molecular oxygen from air to form cyclohexyl hydroperoxy radicals⁴⁰. Some authors have proposed a Russell type termination to be operating using the above cyclohexyl hydroperoxy radicals for the formation of cyclohexanol and cyclohexanone^{40,45}. If Russell termination would have been occurred, cyclohexanol and cyclohexanone would have been obtained in a 1:1 ratio⁴⁰. Since we have obtained cyclohexanol as the major product, Russell termination can be ruled out. The formation of cyclohexanol can be through the formation of cyclohexyl hydroperoxide as proposed by Sakthivel and Selvam⁴⁶. The possible formation of cyclohexyl hydroperoxide is by the abstraction of hydrogen from cyclohexane by cyclohexyl hydroperoxy radicals⁴⁰. Cyclohexyl radical formed in the above mechanism suffers a dehydrogenation to form cyclohexene with a subsequent reduction of metal cation. Cyclohexanol on further oxidation gives cyclohexanone⁴⁵⁻⁴⁷. Schematic

Oxidation Reactions

representation of the above proposed mechanism is shown in Fig.5.1.6.

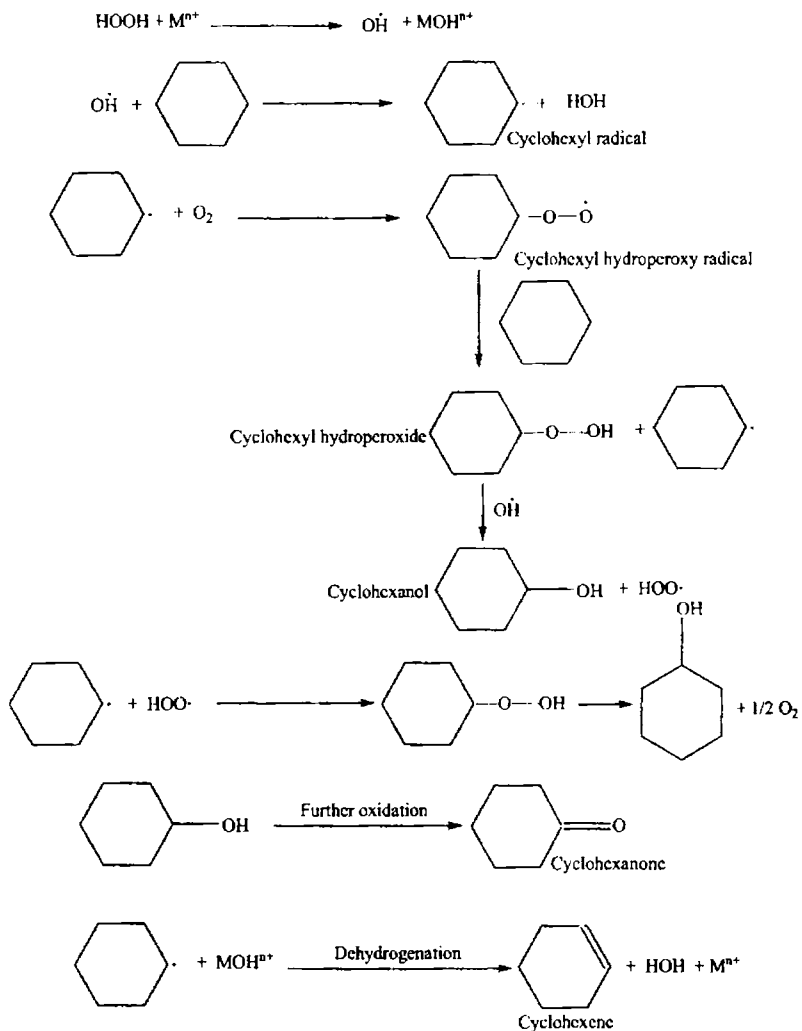


Fig.5.1.6 Reaction mechanism of cyclohexane oxidation.

5.2 Benzyl Alcohol Oxidation

Aromatic aldehydes are important chemicals used in perfumes, foods and other products. Benzaldehyde is an important starting material for the manufacture of odorants, flavours and pharmaceutical intermediates. Many researchers have reported synthesis of benzaldehyde by oxidation of benzyl alcohol using different combinations of H_2O_2 and catalysts¹⁻⁵. Instead of inorganic oxidants, H_2O_2 is preferred as water is formed as the by-product. Inorganic oxidants produce inorganic waste as a by-product. Oxidation of benzyl alcohol with H_2O_2 in acetonitrile using tungstophosphoric acid/aluminium trioxide as a catalyst at 80 °C gave 43 % conversion of benzyl alcohol with 74 % selectivity towards benzaldehyde⁶. Sato et al. reported halide-free oxidation of benzyl alcohol by H_2O_2 in the presence of methyl-tri-*n*-octyl ammonium hydrogen sulphate and tungstate to get 86 % benzaldehyde at 90 °C in 4 h⁷. Barak et al. reported direct oxidation of benzyl alcohol with 30 % H_2O_2 in the presence of didecyl dimethyl ammonium bromide as a phase transfer catalyst and ruthenium trichloride trihydrate as a catalyst⁸. Bortolini et al. obtained 96 % yield of benzaldehyde in the oxidation of benzyl alcohol using anionic molybdenum-peroxo complexes in dichloroethane⁹.

Venturello et al. used methyltrioctylammonium tetrakis (oxodiperoxotungsto) phosphate (III) as a phase transfer catalyst in combination with H_2O_2 for oxidation of benzyl alcohol and obtained 77 % yield of benzaldehyde together with 14 % yield of benzoic acid¹⁰. Dengel et al. reported 40 % yield of benzaldehyde in the oxidation of benzyl alcohol by H_2O_2 with tris-tetrakis-*n*-hexyl ammonium oxodiperoxotungsto phosphate (III) at room temperature in benzene¹¹.

A few studies have been reported on the liquid phase oxidation of benzyl alcohol by oxygen in the presence of non-aqueous solvent using noble metal containing catalysts, such as Pd/C¹², Pd (II) - hydrotalcite¹³, Pd-Ag/Pumice¹⁴, Ru-Co-Al hydrotalcite¹⁵. Recently Choudary et al.¹⁶ reported good activity of Ni-Al hydrotalcite, a noble metal containing catalyst, in the oxidation of benzyl alcohol by oxygen in the presence of toluene as a solvent.

Recently perovskite-type oxides have been extensively studied mainly as catalysts for complete oxidation of hydrocarbons. There has been considerable interest in the use of perovskite and spinel-type mixed oxides for partial oxidation of hydrocarbons and oxygenated compounds. A wide variety of catalysts such as metal oxides and mixed metal oxides are used for the selective oxidation of various organic compounds. Halasz¹⁷ has studied selective oxidation of methanol on YBa₂Cu₃O_{7-x} (x = 0-1) perovskite oxide in the presence as well as in the absence of oxygen, and observed that the catalyst undergoes reduction during the reaction. He concluded from his study that the chemical character of the constructing elements has more influence on the catalytic behaviour of perovskite than their geometrical structure. Dissanayake et al.¹⁸ have studied the partial oxidation of methane on Ba-Pb, Ba-Bi and Ba-Sn perovskite oxides and found that these perovskites also undergo reduction during the reaction. The catalytic activity of these oxides was found to be dependent on the extent of surface reduction. Sumati et al.¹⁹ have studied the effect of nature of B site cation and extent of substitution at B site in ABB¹O₃ (A = Ba, B = Pb, Ce, Ti and B¹ = Bi, Cu, Sb) - type perovskite oxides on the reducibility and catalytic properties. The reaction scheme for benzyl alcohol oxidation is given in Fig.5.2.1.

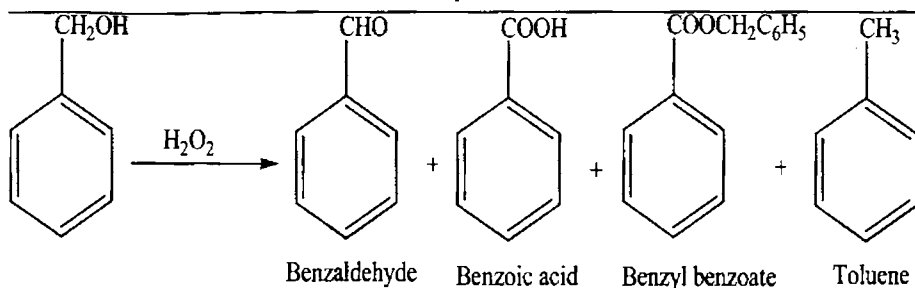


Fig.5.2.1. Reaction scheme for benzyl alcohol oxidation.

In this section a detailed investigation of benzyl alcohol oxidation using different ferrites and cobaltites is presented. Reaction parameters such as time, temperature, reactant molar ratio, effect of solvent etc. were optimized.

5.2.1 Process optimization

5.2.1.1 Effect of reaction temperature

Benzyl alcohol oxidation has been carried out over NF at different temperatures from 30 °C up to 65 °C. The result obtained is shown in Fig.5.2.2.

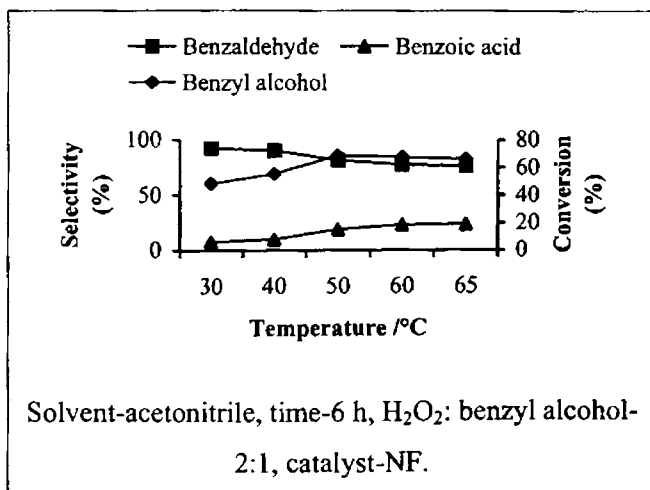


Fig.5.2.2 Effect of reaction temperature on benzyl alcohol oxidation.

Oxidation Reactions

Temperature optimization has been done by using acetonitrile as solvent. The reaction is found to be very much susceptible to the rise in temperature. Benzyl alcohol conversion increased from 48 % to 55 % when the temperature is rised from 30 °C to 40 °C. Maximum conversion has been observed at 50 °C and after that benzyl alcohol conversion decreased by little. Benzaldehyde is the major product obtained. Increase in temperature decreased the selectivity towards benzaldehyde. Benzoic acid is the other product obtained.

5.2.1.2 Effect of solvent

Both protic and aprotic solvents were tried for the reaction. The effect of various solvents on benzyl alcohol oxidation is shown below (Fig.5.2.3.).

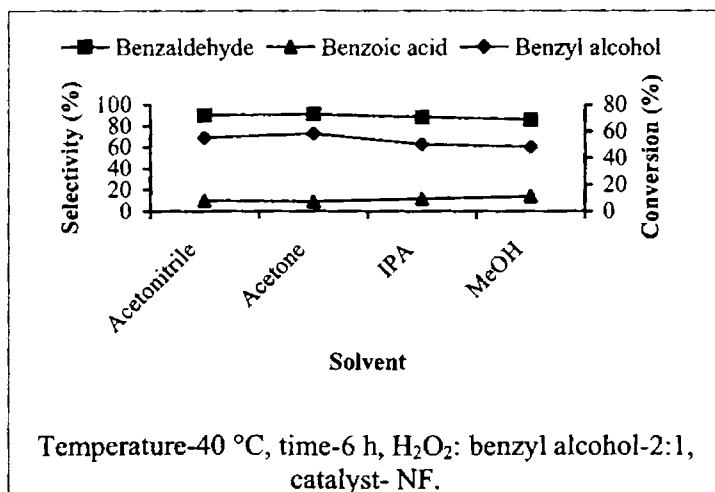


Fig.5.2.3 Effect of solvent on benzyl alcohol oxidation.

Aprotic solvents were found to be more favourable for the reaction. Benzyl alcohol conversion decreased when the reaction has been carried out in

protic solvents. Selectivity towards benzoic acid has improved in protic solvents. Better conversion and selectivity has been observed in acetone. Acetone is selected as solvent for further studies.

5.2.1.3 Effect of reaction time

The reaction was studied for a period of 12 h. The result obtained as a function of time is presented in Fig.5.2.4.

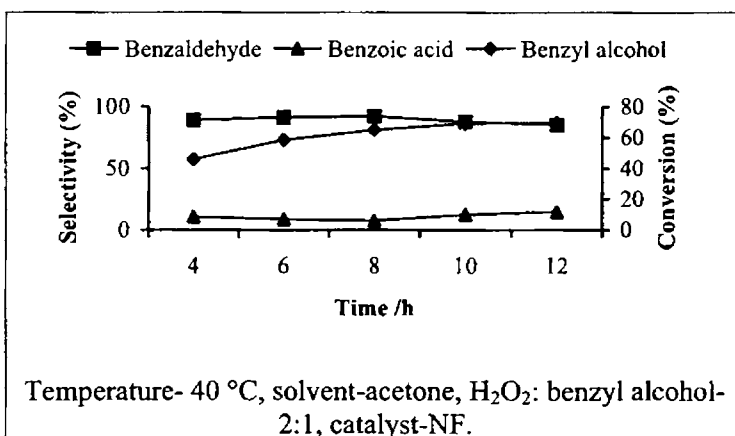


Fig.5.2.4 Effect of reaction time on benzyl alcohol oxidation.

As time proceeds, benzyl alcohol conversion found to be increasing with time. Conversion is observed to be increasing progressively up to a reaction period of 10 h and then remained almost constant. Benzaldehyde formation is the predominant reaction up to 8 h, and at higher reaction time, more benzoic acid formation was noticed. A reaction time of 8 h is selected for further studies.

5.2.1.4 Effect of H₂O₂ to benzyl alcohol molar ratio

Oxidation Reactions

A series of reactions were performed at different H_2O_2 : benzyl alcohol molar ratios. The result obtained is shown in Fig.5.2.5.

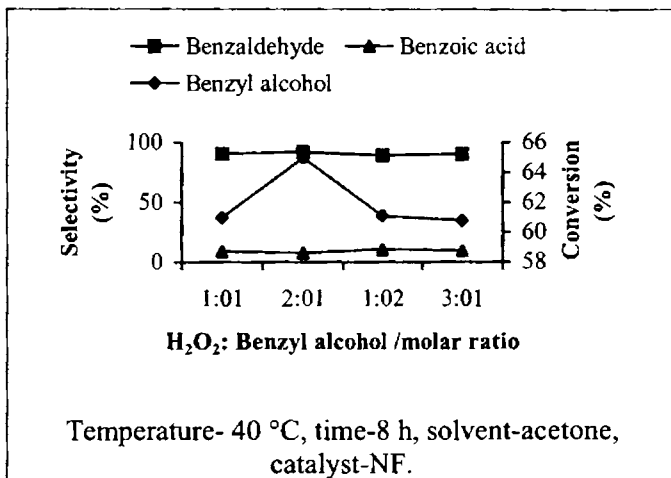


Fig.5.2.5 Effect of reactant molar ratio on benzyl alcohol oxidation.

Increase in H_2O_2 to benzyl alcohol molar ratio increased the benzyl alcohol conversion. But more H_2O_2 in the reaction mixture (beyond the ratio-2:1) decreased the benzyl alcohol conversion. Maximum conversion of 65 % has been observed at a H_2O_2 to benzyl alcohol molar ratio of 2:1.

5.2.2 Effect of catalyst composition

(a) $\text{NiCr}_x\text{Fe}_{2-x}\text{O}_4$ ($x = 0-2$) series

The results obtained for benzyl alcohol oxidation using chromium containing nickel ferrites, carried out under optimized conditions are presented in table 5.2.1.

Both pure and mixed systems are exhibiting good catalytic activity towards benzyl alcohol oxidation. Systems containing both iron and chromium

Table 5.2.1 Benzyl alcohol oxidation over $\text{NiCr}_x\text{Fe}_{2-x}\text{O}_4$ ($x = 0-2$) series.

Catalyst	Benzyl Alcohol Conversion (%)	Selectivity (%)	
		Benzaldehyde	Benzoic acid
NF	65.0	92.2	7.8
NCrF 1	69.3	93.4	6.4
NCrF 2	71.5	93.8	6.2
NCrF 3	72.3	94.0	6.0
NCrF 4	73.5	93.5	6.5
NCr	69.3	94.2	5.8

Temperature- 40 °C, time-8 h, H_2O_2 : benzyl alcohol-2:1, solvent- acetone.

are more active than pure systems. Benzyl alcohol conversion increases with increase in chromium content where as complete replacement of iron by chromium reduces the activity. Even though the activity of nickel chromite is less than compared to mixed systems, it is more active than nickel ferrite. Benzaldehyde is the major product obtained. The trend in variation of benzyl alcohol conversion with chromium incorporation is not observed in benzaldehyde selectivity.

(b) $\text{NiGd}_x\text{Fe}_{2-x}\text{O}_4$ ($x = 0-2$) series

The reaction was studied over gadolinium incorporated nickel ferrites under optimized conditions. The results are presented in table 5.2.2.

Replacing iron by gadolinium is found to increase the activity of the systems towards benzyl alcohol oxidation. Incorporation of gadolinium by 20 % has increased the benzyl alcohol conversion by 5 %. For mixed systems, the activity increases with increase in gadolinium content with NGF4 showing

Oxidation Reactions

Table 5.2.2 Benzyl alcohol oxidation over NiGd_xFe_{2-x}O₄ (x = 0-2) series.

Catalyst	Benzyl Alcohol Conversion (%)	Selectivity (%)	
		Benzaldehyde	Benzoic acid
NF	65.0	92.2	7.8
NGF 1	70.2	93.5	6.5
NGF2	71.4	94.6	5.4
NGF 3	72.7	94.8	5.2
NGF 4	73.0	95.0	5.0
NG	68.2	95.2	4.8

Temperature- 40 °C, time-8 h, H₂O₂ : benzyl alcohol -2:1, solvent- acetone.

maximum activity. Nickel gadolinite is found to be more active than nickel ferrite. Benzaldehyde is the major product obtained for all the systems.

(c) Cobaltite series

The results obtained for cobaltite series is presented in table 5.2.3.

Table 5.2.3 Benzyl alcohol oxidation over cobaltites.

Catalyst	Benzyl Alcohol Conversion (%)	Selectivity (%)	
		Benzaldehyde	Benzoic acid
NC .5	70.2	97.8	2.2
NC 1	72.4	98.2	1.8
NC 1.5	74.6	99.3	0.7
CC .5	73.7	100	--
CC 1	75.5	100	--

Temperature- 40 °C, time-8 h, H₂O₂ : benzyl alcohol -2:1, solvent- acetone.

For nickel cobaltites, the trend in activity is such that increase in nickel content favours the benzyl alcohol oxidation. NC1.5, which is having more nickel, is more active towards benzyl alcohol oxidation. For copper cobaltites, an increase in copper content is found to be favourable for the benzyl alcohol oxidation. As compared to ferrite series, here the selectivity towards benzaldehyde has improved much. Copper cobaltites show 100 % selectivity towards benzaldehyde under optimized conditions.

The activity of spinels depends on the distribution of cations among the octahedral and tetrahedral sites. Many authors have been reported that the octahedral ions present in the spinel crystal lattice were responsible for the activity towards oxidation reactions^{20,21}. According to the cation distribution data, nickel ferrite has maximum concentration of Fe^{3+} ions at the octahedral site. Samples containing both chromium and iron are having less concentration of Fe^{3+} compared to pure nickel ferrite. Chromium preferably occupies octahedral site. Activity studies revealed that incorporation of chromium has improved the activity. So it is supposed that it is the increased concentration of Cr^{3+} ions at the octahedral site which is responsible for the improved activity of chromium containing systems and activity increases with increase in trivalent ion concentration at O_h site. Even though the presence of chromium ions has improved the activity of the systems, it seems that the presence of iron is also desirable for the reaction. The diminished activity of pure nickel chromite (which does not contain iron) compared to mixed systems is the evidence for this. After $x = 0.8$, concentration of Ni^{2+} ions at the octahedral site decreases where as activity has improved with increase in x . These observations leads us to conclude that it is the trivalent ion concentration at the

octahedral site which determines the catalytic activity.

Incorporation of gadolinium has a different effect on the cation distribution. Gadolinium occupies more exposed octahedral site due to its larger size. For mixed systems, incorporation of gadolinium caused more iron to come into the octahedral site and percentage of iron at the octahedral site has increased with incorporation of gadolinium and concentration of Ni^{2+} ions does not change up to $x = 1.2$ which shows that nickel does not seem to play any role in determining the catalytic activity. Total concentration of trivalent ions at the octahedral site increases with increase in gadolinium content and activity increases in the same order. Although incorporation of gadolinium has improved the activity, the presence of iron is found to be favourable for the reaction. Pure nickel gadolinite which does not contain iron is less active than mixed systems containing both iron and gadolinium.

For cobaltite series, a comparison of cation distribution data and activity data show that increase in concentration of divalent ions at the O_h site favours oxidation of benzyl alcohol. Nickel cobaltite has an inverse structure where nickel occupies octahedral site. Increase in concentration of nickel causes more and more nickel to go to the exposed octahedral site and activity increases with increase in concentration of nickel. $\text{Ni}_{1.5}$ is the most active in the studied nickel cobaltites. For copper cobaltites, copper has position both at the tetrahedral and octahedral sites. Here also the increased concentration of divalent ion (copper) at the octahedral site is supposed to be responsible for the increased activity with increase in copper content.

For many oxidation reactions, the activity of the catalyst has been successfully correlated with the reducibility of the catalyst²²⁻²⁴. Namakura et

al.²⁵ have reported that the ease of oxygen desorption, the diffusivity of oxygen molecules and the reducibility of perovskite oxide are closely associated with the catalytic activities for oxidation reactions, and that these properties can be varied by substitution at A or B sites. We have noted the reduction temperature from the H₂-TPR studies and found that the gradation of reduction temperature with substitution or variation of concentration at A or B sites can be very well correlated with catalytic activity. It was observed that systems which show low reduction temperature are showing high activity towards oxidation reaction as compared to those having high reduction temperature. The low reduction temperature in the TPR experiments confirms the availability of lattice oxygen²⁶. Pure nickel ferrite has a high reduction temperature value. Substitution of iron by chromium has reduced the reduction temperature where as complete replacement of iron by chromium has further risen the reduction temperature- NF (510 °C) > NCrF2 (424 °C) > NCrF4 (367 °C) < NCr (509 °C). This variation in reducibility with chromium incorporation is clearly reflected in their activity towards oxidation reaction. Systems containing both chromium and iron are easily reducible as compared to pure systems and accordingly their oxidation behaviour is more as compared to pure systems. For CO oxidation on cuprates, it was reported that the catalytic activity depends on the extent of reduction. Catalytic studies carried out on barium cuprates showed that their activities for selective oxidation of methanol differ significantly, with Ba₂Cu₃O₅ being more active than YBa₂Cu₂O₇. This was attributed to the high reducibility of the former catalysts²⁷. The observed results indicate that oxidation behaviour of chromium incorporated nickel ferrites depends on their reducibility.

Oxidation Reactions

Incorporation of gadolinium also has a similar effect as that of chromium i.e., lowered the reduction temperature of nickel ferrite. Systems having both iron and gadolinium have reduction temperatures lower than pure systems. It follows the order- NF (510 °C) > NGF3 (368 °C) > NGF4 (359 °C) < NG (483 °C) which shows that mixed systems can be easily reduced compared to pure systems. For gadolinium containing systems, the reduction temperature has decreased with increase in gadolinium content and activity towards oxidation reaction increased in the same order.

The observation that systems having low reduction temperature are possessing high oxidation behaviour can also see for cobaltites. For nickel cobaltites, increase in nickel content has lowered the reduction temperature. NC1.5, which is having more nickel, possessing low reduction temperature and has maximum activity in that series. Similar effect has been observed for copper cobaltites. The high oxidation capacity of CC1 as compared to CC.5 may be due to its high reducibility (low reduction temperature).

Even though the trend in oxidation behaviour with in a particular series can be explained with the variation in reducibility, it seems that various other secondary factors also contributing to the reaction. We observed that even though copper cobaltites are having low reducibility as compared to nickel cobaltites, the activity of copper cobaltites is little higher than nickel cobaltites. The presence of other oxide phases (as observed in XRD pattern) is supposed to play some role in deciding the catalytic activity. Omata et al.²⁸, during their study of CO/H₂ oxidation using cobaltites, have reported the involvement of oxide phases other than spinel phase as responsible for the improved catalytic activity for some of the systems.

Catalyst reusability

For checking the reusability, the catalyst was removed from the reaction mixture, washed thoroughly with acetone, dried in an air oven and then activated. The catalyst was then again used for carrying out the same reaction under same conditions. The catalyst was reused up to three cycles. The results obtained were given in table 5.2.4.

Table 5.2.4 Catalyst reusability study for benzyl alcohol oxidation reaction.

Catalyst	1 cycle		2 cycle		3 cycle	
	Benzyl alcohol con. (%)	Benzaldehyde sel. (%)	Benzyl alcohol con. (%)	Benzaldehyde sel. (%)	Benzyl alcohol con. (%)	Benzaldehyde sel. (%)
NCrF4	73.5	94.0	70.1	91.3	67.3	90.2
NGF4	73.5	95.2	71.3	95.0	66.2	93.7
NC1	72.0	98.2	70.8	98.0	66.2	97.5
CC1	77.0	100	75.2	100	70.3	98.5

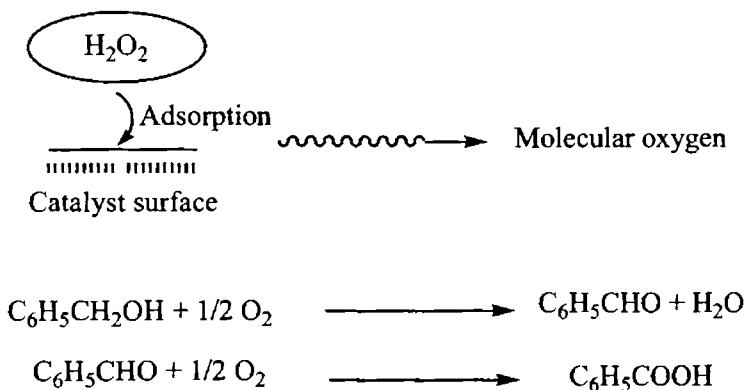
The activity is found to be decreasing considerably in the 3rd cycle. Some of the systems were found to be almost maintaining the benzaldehyde selectivity. The decrease in activity may be due to leaching. Active ions may be leach out from the spinel lattice and there by decreasing the activity.

5.2.3 Mechanism of benzyl alcohol oxidation

Benzyl alcohol oxidation has been studied using hydrogen peroxide as oxidizing agent. The reaction gave little benzoic acid in addition to benzaldehyde. According to Guin et al. who have studied styrene oxidation

Oxidation Reactions

over spinel type catalysts, the oxygen vacancies present in the catalysts will facilitate the adsorption of hydrogen peroxide to form molecular oxygen for the oxidation reaction²⁹. Benzyl alcohol oxidation has been studied by V.R. Choudhary et al.³⁰ on hydrotalcite like materials and they have proposed that the formation of benzaldehyde and benzoic acid occurs through the involvement of molecular oxygen. Wada et al. have studied the reaction over palladium oxide nanoparticles and they also have reported the involvement of molecular oxygen for the oxidation process³¹. We are tentatively proposing a similar mechanism in our case. The molecular oxygen liberated by the adsorption of hydrogen peroxide over the catalyst surface²⁹ may be utilized for the oxidation of benzyl alcohol and benzaldehyde.



5.3 Styrene Oxidation

The development of novel and effective catalysts for the selective oxidation of alkenes is currently of considerable interest. Styrene oxidation is of considerable commercial and academic interest for the synthesis of important products such as benzaldehyde, styrene oxide and phenyl acetaldehyde. Benzaldehyde is an important starting material for the manufacture of odorants, flavours and pharmaceutical intermediates. The use of hydrogen peroxide for oxidizing organic substrates has received much attention in recent years because of its environmental implications, water being the only chemical by-product of oxidation reactions. It is known that the styrene oxidation by hydrogen peroxide at side chain can lead to various reaction products, depending on the catalyst and reaction conditions. Benzaldehyde can be obtained as the main product when the oxidation is carried out in homogeneous manner using metal complexes¹. In the presence of palladium salts, by Wacker process, styrene is mainly converted to acetophenone². On the other side, oxidation reaction can be stopped at the stage of epoxide by the use of $\text{CH}_3\text{ReO}_3\text{-H}_2\text{O}_2$ system in anhydrous CD_3CN , whereas 1,2-diol is obtained in $\text{CH}_3\text{CN}/\text{H}_2\text{O}$ solution³.

In heterogeneous catalysis, over nanosize spinel-type $\text{Mg}_x\text{Fe}_{3-x}\text{O}_4$ or Nb (Co)-MCM-41⁵, the major reaction was oxidative C = C cleavage into benzaldehyde. D.Guin et al.⁶ have studied styrene oxidation using hydrogen peroxide catalyzed by nickel and zinc ferrites and obtained benzaldehyde as the major product (C = C cleavage). By-products such as phenyl acetaldehyde and styrene oxide formation were negligibly low (less than 1%). The use of titanium containing molecular sieves such as TS-1⁷⁻¹⁰, TS-2⁸, BTS-2¹¹ or Ti-

Oxidation Reactions

MCM-41¹² for the styrene oxidation with hydrogen peroxide in organic solvents allow to increase the selectivity towards phenyl acetaldehyde (PhAA). It is considered that PhAA results by an in situ acid catalyzed rearrangement of the styrene oxide, which is the primary product¹³. A considerable increase in styrene oxide was obtained over TS-1 in presence of sodium hydroxide in the reaction medium¹⁴ or using anhydrous urea-H₂O₂ as the oxidizing agent¹⁵. The reaction scheme for styrene oxidation is given in Fig.5.3.1.

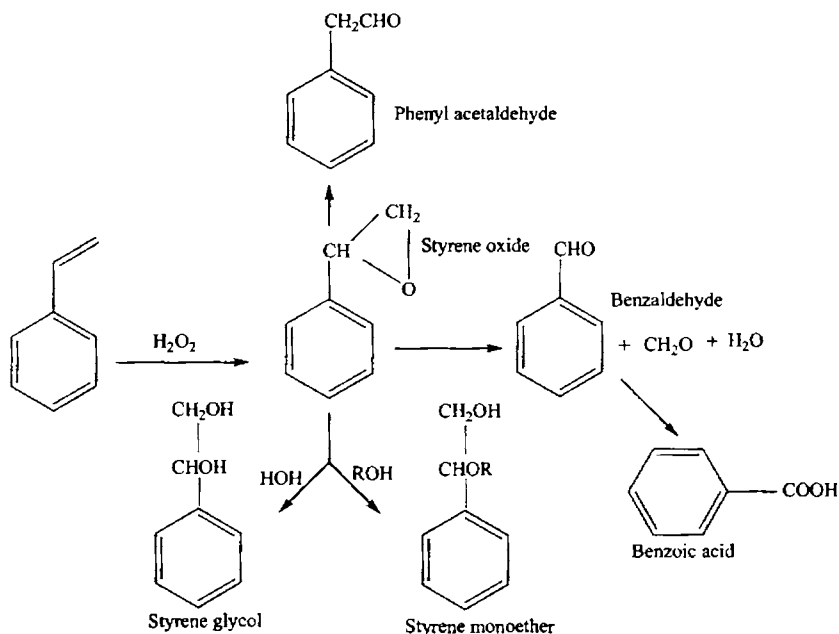


Fig.5.3.1 Reaction scheme for styrene oxidation reaction.

In this section, styrene oxidation using hydrogen peroxide catalyzed by the prepared ferrites and cobaltites is discussed. All the prepared systems were found to be highly active towards styrene oxidation. All the systems formed

exclusively benzaldehyde as the product under optimized conditions.

5.3.1 Process optimization

Process optimization has been done by using NF catalyst. Temperature, time, solvent, reactant molar ratio etc. were optimized. The parameters were optimized such as to improve the selectivity towards benzaldehyde. (Only benzaldehyde selectivity is plotted in the graphs)

5.3.1.1 Effect of reaction temperature

The reaction was studied over a temperature range from 30 °C to 65 °C. Result obtained is depicted in Fig.5.3.2.

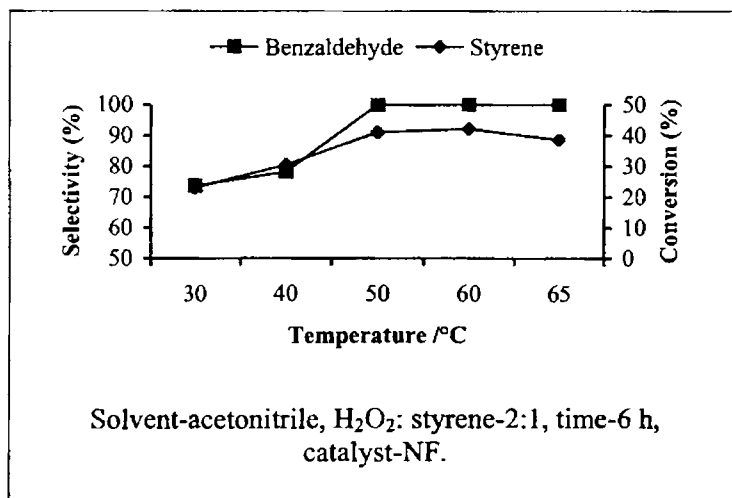


Fig.5.3.2 Effect of temperature on styrene oxidation.

Increase in temperature is found to be favourable for styrene oxidation. Rise in temperature has increased styrene conversion considerably.

Oxidation Reactions

But at higher temperatures, not much increase in styrene conversion was observed and conversion decreased after 60 °C. At lower temperatures, impurities were found to be formed. As temperature increased, selectivity towards benzaldehyde increased and cent percent benzaldehyde was obtained from 50 °C. A temperature of 60 °C was selected for further studies since styrene conversion is maximum at this temperature.

5.3.1.2 Effect of reaction time

Styrene oxidation was studied for a period of 12 h at 60 °C. Styrene conversion and benzaldehyde selectivity as a function of time is presented in Fig.5.3.3.

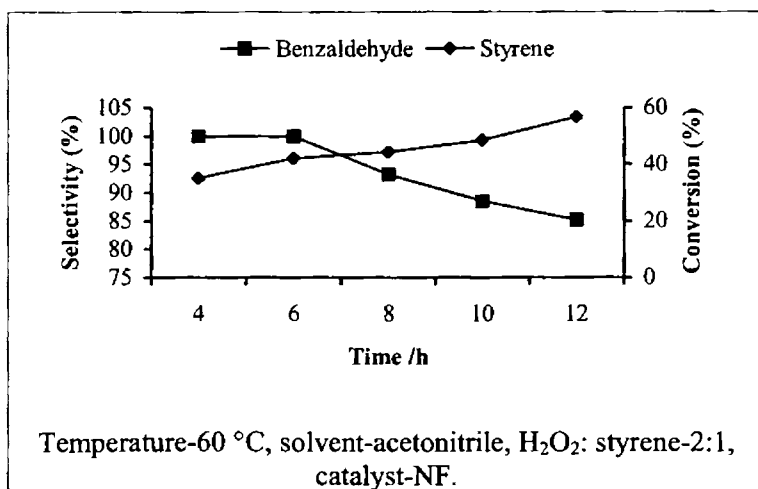


Fig.5.3.3 Effect of reaction time on styrene oxidation.

Running the reaction for a long time is found to be favourable for the oxidation of styrene; styrene conversion increased as time proceeded where as benzaldehyde selectivity decreased with time. Impurities were found to be

formed when the reaction was allowed to run for a long time. Products such as styrene oxide and phenyl acetaldehyde which are the other possible products of styrene oxidation over spinels^{4,6}, were not observed. A reaction time of 6 h is selected for further studies.

5.3.1.3 Effect of solvent

Both protic and aprotic solvents were tried for the styrene oxidation reaction under the above optimized conditions. The results obtained are shown in Fig.5.3.4.

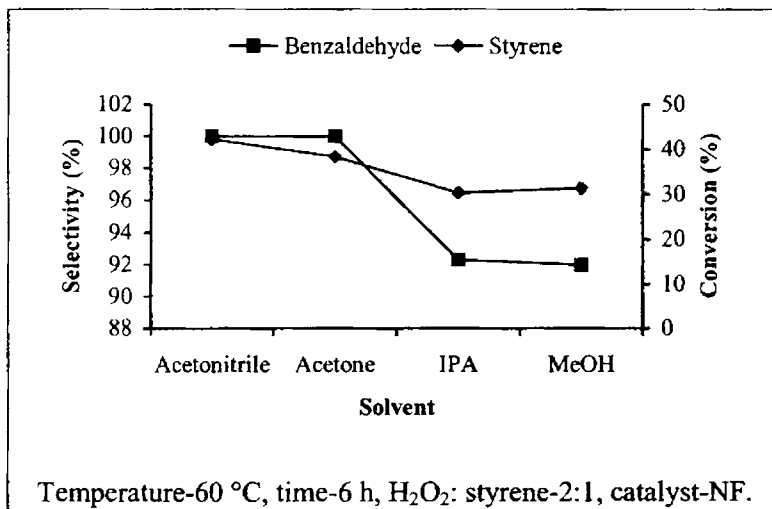


Fig.5.3.4 Effect of solvent on styrene oxidation.

Aprotic solvents were found to be favourable for styrene oxidation both in terms of styrene conversion and benzaldehyde selectivity. In acetonitrile and acetone, benzaldehyde is the exclusive product formed whereas in protic solvents, impurities were formed. Since maximum styrene

conversion was obtained in acetonitrile, it is selected as the solvent for further studies.

5.3.1.4 Effect of H₂O₂ to styrene molar ratio

Styrene oxidation was studied at different reactant molar ratios. The reaction was run for a period of 6 h. The results obtained are presented in Fig.5.3.5.

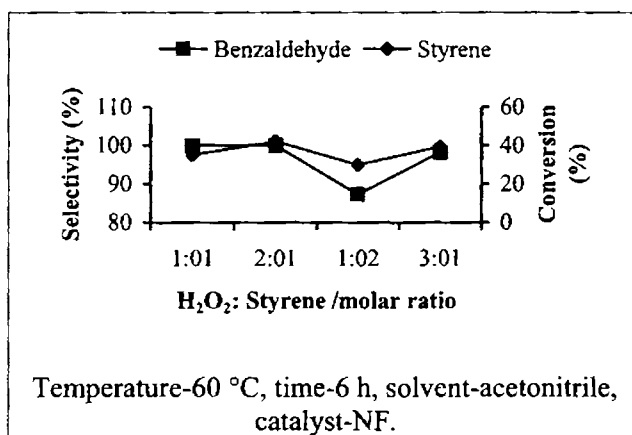


Fig.5.3.5 Effect of reactant molar ratio on styrene oxidation.

Increasing the H₂O₂ to styrene molar ratio from 1:1 to 2:1 is found to increasing styrene conversion where as styrene conversion is lowered when percentage of styrene is increased in the reaction mixture. A reactant molar ratio of 1:2 is found to decrease the styrene conversion. More styrene in the reaction mixture not only decreases the styrene conversion but at the same time lowered the selectivity for benzaldehyde also. Maximum styrene conversion was obtained at a molar ratio of 2:1; it is selected for further studies.

5.3.2 Effect of catalyst composition

(a) $\text{NiCr}_x\text{Fe}_{2-x}\text{O}_4$ ($x = 0-2$) series

Styrene oxidation was studied using chromium incorporated nickel ferrites under optimized conditions. The result obtained is presented in table 5.3.1.

Table 5.3.1 Styrene oxidation over $\text{NiCr}_x\text{Fe}_{2-x}\text{O}_4$ ($x = 0-2$) series.

Catalyst	Styrene conversion (%)	Benzaldehyde sel.(%)
NF	42.2	100
NCrF 1	47.7	100
NCrF 2	50.3	100
NCrF 3	54.6	100
NCrF 4	55.2	100
NCr	43.7	100

Temperature-60 °C, time-6 h, solvent-acetonitrile, H_2O_2 : styrene-2:1.

Under optimized conditions, both pure and mixed systems gave exclusively benzaldehyde as the product. Incorporation of chromium into nickel ferrite has increased the activity of the systems; styrene conversion increased with increase in chromium content. NCrF4 which is the mixed system having maximum chromium content shows a maximum styrene conversion of 55 %. Although the activity of nickel chromite is lower than mixed systems, it is showing improved activity as compared to nickel ferrite.

(b) $\text{NiGd}_x\text{Fe}_{2-x}\text{O}_4$ ($x = 0-2$) series

Result obtained for gadolinium containing nickel ferrites is presented in table 5.3.2.

Oxidation Reactions

Table 5.3.2 Styrene oxidation over $\text{NiGd}_x\text{Fe}_{2-x}\text{O}_4$ ($x = 0-2$) series.

Catalyst	Styrene conversion (%)	Benzaldehyde sel.(%)
NF	42.2	100
NGF 1	46.3	100
NGF2	49.5	100
NGF 3	53.2	100
NGF 4	56.8	100
NG	43.5	100

Temperature-60 °C, time-6 h, solvent-acetonitrile, H_2O_2 : styrene-2:1.

Just as in chromium containing samples, presence of gadolinium has improved the activity of the systems. Pure systems are less active than mixed systems. Styrene conversion increased with increase in gadolinium content. At higher percentages of gadolinium, styrene conversion increased considerably. NGF4 is more active in this series. Even though complete replacement of iron by gadolinium diminished the activity; nickel gadolinite is more active than nickel ferrite. Benzaldehyde is the exclusive product formed under optimized conditions.

(c) Cobaltite series

Result obtained for cobaltite series is presented in table 5.3.3.

Cobaltites are more active towards styrene oxidation as compared to ferrites. Most of the systems showed a styrene conversion of greater than 60 %. For the nickel cobaltite series, styrene conversion increases with increase in nickel content. NC1.5, which contains more nickel, is the most

active among the nickel cobaltites. For copper cobaltites, more copper in the system is found to be favourable for the reaction. CC1 is more active than CC.5. All the cobaltites preferably formed benzaldehyde.

Table 5.3.3. Styrene oxidation over cobaltites.

Catalyst	Styrene conversion (%)	Benzaldehyde sel.(%)
NC .5	58.2	100
NC 1	62.4	100
NC 1.5	66.0	100
CC .5	60.4	100
CC 1	63.8	100

Temperature-60 °C, time-6 h, solvent-acetonitrile, H₂O₂: styrene-2:1.

For spinel type oxides, the distribution of ions at two different crystallographic sites plays a dominant role in determining the catalytic activity. Since the ions present at the octahedral site are preferentially exposed at the spinel surface, they are supposed to be responsible for the catalytic activity as reported by many authors^{16,17}. We can see a correlation between the activity and the distribution of ions at octahedral and tetrahedral sites. For pure and chromium containing nickel ferrites, Fe³⁺ ions occupies tetrahedral and octahedral sites equally as per the Mössbauer data. Chromium preferentially occupies octahedral site due to crystallographic effects. Activity studies revealed that catalytic activity has improved with chromium content (increase in x) and, nickel concentration at octahedral site decreases at higher percentages of chromium. This observation lead us to suggest that nickel ions

Oxidation Reactions

has little or no effect in determining the catalytic activity. The trivalent ions present at the octahedral site determine the catalytic activity. Concentration of trivalent ions at the octahedral site increases with increase in chromium content and activity also increases in the same order. Chromium containing systems are more active than pure nickel ferrite which shows that chromium ions are more active for catalyzing the reaction than iron ions. Even though, nickel chromite is less active than mixed systems which enlightens to the fact that the presence of iron is also required for better catalytic performance.

For gadolinium containing nickel ferrites, percentage of iron at the octahedral site increases with gadolinium content and gadolinium occupies octahedral site. Concentration of nickel at the octahedral site does not change up to NGF3. Activity goes on increasing with increase in percentage of gadolinium. These observations show that it is the concentration of trivalent ions which controls the catalytic activity and neglects the role of nickel ions. We can also conclude that even though the presence of gadolinium is more favourable for the reaction than iron, the presence of iron even in the low concentration is beneficial for better catalytic performance. This conclusion is derived from the observation that systems containing both iron and gadolinium are more active than pure systems and nickel gadolinite (which does not contain iron) is less active than mixed systems.

For cobaltites, an observation different from the above is obtained. i.e., here the divalent ions are found to play the dominant role in determining the activity. Nickel cobaltites have an inverse structure where Ni^{2+} ions occupies octahedral site. Increase in concentration of nickel favours more and more nickel to enter into the more exposed octahedral site. From the cation

distribution data, concentration of Ni^{2+} ions increases where as that of Co^{3+} ions decreases at the octahedral site with increase in concentration of nickel. Comparing this with the activity data it appears that Ni^{2+} ions are involved in catalyzing the reaction since catalytic activity increases with increase in nickel content.

For copper cobaltites, copper ions are found to be involved in catalyzing the reaction. Since copper cobaltites have a partially inverse structure, copper occupies both sites. As copper content increases, concentration of copper at the octahedral site also increases and activity increases in accordance with this.

Activity of the catalysts towards oxidation reaction is related to their reducibility. Reduction behaviour of the catalysts has been studied using H_2 -TPR studies. Temperature programmed reduction studies revealed that incorporation of chromium into nickel ferrite has lowered the reduction temperature, i.e., the systems can be reduced easily. Reduction temperature obtained from TPR studies follows the order- NF ($510\text{ }^\circ\text{C}$) $>$ NCrF_2 ($424\text{ }^\circ\text{C}$) $>$ NCrF_4 ($367\text{ }^\circ\text{C}$) $<$ NCr ($509\text{ }^\circ\text{C}$). This variation in reducibility is clearly reflected in their activity towards the oxidation reaction. Chromium incorporation has increased the oxidation capacity towards styrene oxidation and the activity increased with increase in chromium content. Complete replacement of iron by chromium has diminished the activity as compared to mixed systems. These activity results are in parallel with the gradation in reducibility.

Incorporation of gadolinium also reduced the reduction temperature of pure nickel ferrite. The variation in activity of gadolinium containing nickel

Oxidation Reactions

ferrites is related to their reducibility. Presence of gadolinium minimized the reduction temperature of mixed systems- NF (510 °C) > NGF3 (368 °C) > NGF4 (359 °C) < NG (483 °C) and correspondingly the oxidation capacity of systems having both iron and gadolinium is higher than pure systems. Activity of pure nickel gadolinite is less compared to mixed systems in accordance with its low reducibility.

For cobaltites, increase in percentage of divalent ions has decreased the reduction temperature and correspondingly there observed an increase in activity with incorporation of more and more divalent ions. The reduction temperature obtained from TPR studies for cobaltites follows the order- NC1 (331 °C) > NC1.5 (306 °C), CC.5 (456 °C) > CC1 (434 °C). Comparing these with the activity results, it follows that the high oxidation behaviour of NC1.5 among the nickel cobaltites can be attributed to its high reducibility compared to other systems. Similar behaviour has been observed for copper cobaltites also.

Catalyst reusability

Catalyst reusability was studied by running the reaction using the same catalyst after separating the catalyst from the reaction medium. The reaction mixture was filtered off, washed the catalyst with acetone 3-4 times to make free from the organic contents. The catalyst was then dried, activated and used for the same reaction under the same reaction conditions. The results obtained were shown in table 5.3.4.

After second cycle, there observed a considerable decrease in styrene conversion. For NGF4, a noticeable decrease in benzaldehyde selectivity was

Table 5.3.4 Catalyst reusability study for styrene oxidation reaction.

Catalyst	1 cycle		2 cycle		3 cycle	
	Styr. Con. (%)	Bezaldehyde sel.(%)	Styr. Con. (%)	Bezaldehyde sel.(%)	Styr. Con. (%)	Bezaldehyde sel.(%)
NCrF4	54.0	100	52.2	98.3	48.3	98.0
NGF4	55.5	100	50.3	95.2	46.2	93.3
NC1	62.4	100	60.3	100	56.3	98.1
CC1	63.8	100	62.0	98.3	58.2	98.0

observed even from the second cycle where as for other systems, not much decrease was observed. The loss in activity can be attributed to the leaching effect where by active ions are escaped from the spinel matrix so that they are not available for further catalyzing the reaction.

5.3.3 Mechanism of styrene oxidation

Using all the prepared catalysts, only benzaldehyde formation was observed under optimized conditions. Over spinel type oxides, benzaldehyde formation is the major reaction^{4,6}. According to Guin et al., who had studied styrene oxidation over spinel type catalysts, the oxygen vacancies present in the catalysts will facilitate the adsorption of hydrogen peroxide to form molecular oxygen for the oxidation reaction⁶. Gomez et al. have studied the styrene oxidation over TM-MCM-48 and they obtained benzaldehyde as the major product¹⁸. They obtained styrene oxide and phenyl acetaldehyde as minor products and in some cases with no phenyl acetaldehyde. They have

Oxidation Reactions

proposed that the formation of benzaldehyde from styrene can be of two types: (i) oxidation of side chain, which causes breaking of C = C bond (ii) first epoxide formation to form styrene oxide which further forms benzaldehyde in the presence of peroxide. Formation of benzaldehyde through C = C bond cleavage and through epoxide formation may be occurring in parallel¹⁸. According to Ma et al. and Guin et al., who have studied styrene oxidation over spinel type catalysts, the formation of benzaldehyde occurs through the C = C bond cleavage^{4,6}. The formation of benzaldehyde through the formation of styrene epoxide is acceptable since Guin et al.⁶, who have studied styrene oxidation over nickel and zinc ferrites, have obtained styrene oxide even though in negligible amount (less than 1%). Hulea et al.¹⁹ have studied the oxidation of styrene and they have proposed the formation of benzaldehyde by a nucleophilic attack of hydrogen peroxide to styrene oxide followed by a cleavage of the intermediate- hydroxy hydroperoxystyrene. Guin et al.⁶ have suggested that both H₂O₂ and styrene are getting adsorbed on the active sites of the catalysts followed by the cleavage of the double bond in styrene, forming benzaldehyde. Based on these reports, we are tentatively proposing that styrene oxidation is supposed to be occurring through the following parallel processes (Fig. 5.3.6).

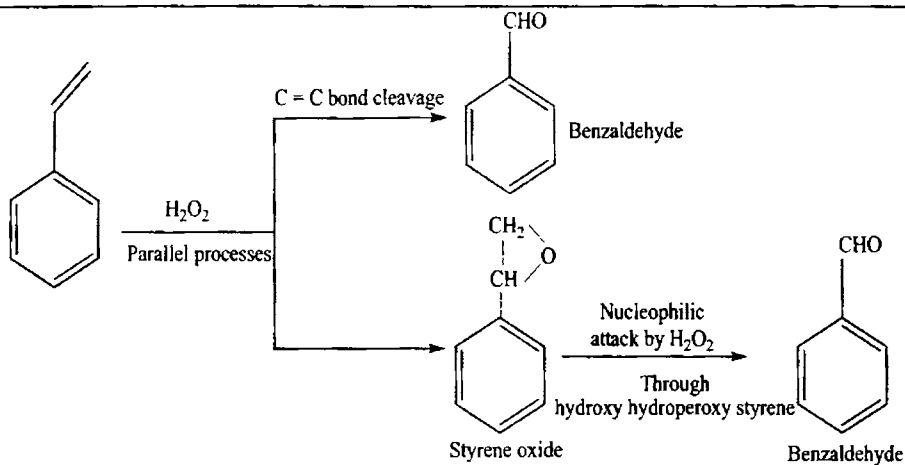


Fig. 5.3.6. Reaction mechanism for styrene oxidation reaction.

References:

Cyclohexane oxidation

- [1] Maschmeyer, J.M.Thoams, G.Sankar, R.D.Olyroyd, I.J.Shannon, J.A.Kleptko, A.F.Masters, J.K.Beattie and C.R.A.Catlow; *Angew. Chem. Int. Ed.*,36 (1997) 1639.
- [2] H.H.Kung., *Adv. Catal.*, 40 (1994) 1.
- [3] E.C.Alyea and M.A.Keane; *J. Catal.*, 164 (1996) 28.
- [4] C.Resini, M.Panizza, F.Raccoli, M.Fadla, M.M.Carnasciali, G.Busca, E.F.Lopez and V.S.Escribano; *Appl. Catal. A. Gen.*, 251 (2003) 29.
- [5] F.Patcas and D.Hönicke; *Catal. Commun.*, 6(1) (2005) 23.
- [6] R.Raja, G.Sankar and J.M.Thomas; *J. Am. Chem. Soc.*, 121 (1999) 11926.
- [7] F.R.Hartly, *Supported Metal complexes*, Reidel, Dordrecht, 1985.
- [8] P.Srinivas and M.Mukhopadhyay; *Ind. Eng. Chem. Res.*,36 (1997) 2066.
- [9] E.Sahle-Demessie, M.A.Gonzalez, J.Enriquez and Q.Zaho; *Ind. Eng. Chem.Res.*, 39 (2000) 4858.
- [10] Z.Hou, B.Han, L.Gao, Z.Liu and G.Yang; *Green Chem.*, 4 (2002) 426.
- [11] T.Hattori, J.Inoko and Y.Murakami; *J. Catal.*, 42 (1976) 60.
- [12] M.P.Rosynk; *Catal. Rev.-Sci. Eng.*, 16 (1977) 111.
- [13] I.Yamanaka, T.Akimoto, K.Nakagaki and K.Otsuka; *J. Mol. Catal. A.* 110 (1996) 119.
- [14] I.Yamanak and K.Otsuka; *J. Mol. Catal. A.*, 95 (1995) 115.
- [15] R.A.Sheldon, in: B.Cornils, W.A.Hermann (Eds.), *Applied Homogeneous Catalysis with Organometallic Compounds*, vol.1,

- VCH.Weinheim, 1996, p.411.
- [16] F.Maspero and U.Romano, European Patent 0,190,609 (1986).
- [17] T.Tatsumi, M.Yako, M.Nakamura, Y.Yahura and H.Tominaga; *J. Mol. Catal. A.*, 78 (1993) L41.
- [18] J.S.Reddy and A.Sayari; *J. Chem. Soc., Chem. Commun.*, 23 (1995).
- [19] (a) H.Arzoumanian, G.Agrifoglio, H.Krentzien and M.Capparelli; *New J.Chem.*, 20 (1996) 699;
(b) H.Arzoumanian, R.Bakthchadjian, G.Agrifoglio, H.Krentzien and J.-C.Daran; *Eur. J. Inorg. Chem.*, (1999) 2255.
- [20] A.Baiker; *Stud. Surf. Sci. Catal.*, 101 (1996) 51.
- [21] R.S.da Cruz, M.M.Dauch, U.Schuchardt and R.Kumar; *Stud. Surf. Sci. Catal.*, 130 (2000) 1037.
- [22] E.L.Pires, U.Arnold and U.Schuchardt; *J. Mol. Catal. A. Chem.*, 169 (1-2) (2001) 157.
- [23] R.S.da Cruz, J.M.S. de Silva, U.Arnold and U.Schuchardt; *J. Mol. Catal. A. Chem.*, 171 (1-2) (2001) 251.
- [24] R.S.da Cruz, J.M.S. de Silva, U.Arnold, M.S.Sercheli and U.Schuchardt; *J. Chem. Soc.*, 13 (2) (2002) 170.
- [25] A.E.Gekhman, I.P.Stolyarov, N.I.Moiseeva, I.I.Moiseev, *C.R.Chimie* 7 (8-9) (2004) 833.
- [26] A.Bellifa, D.Lahcene, Y.N.Tchenar, A.C-Braham, R.Bachir, S.Bedrane and C.Kappenstein; *Appl. Catal. A. Gen.*, 305 (2006) 1.
- [27] A.Sakthivel and P.Selvam; *J. Catal.*, 211 (2002) 134.
- [28] K.Suanta, Mahapatra and P.Selvam; *Chem. Lett.*, 33 (2004) 198.
- [29] R.Zhao, D.Ji, G.Qian, L.Yan, X.Wang and J.Suo; *J. Chem. Soc., Chem.*

- Commun. (2004) 904.
- [30] L.Gaomeng, Z.Rui, Q.Guang, Q.Yanxing, W.Xiaolai and S.Jishuan; Catal. Lett., 97 (2004) 115.
- [31] V.Parvulescu, C.Dascalescu and B.L.Su; Stud. Surf. Sci. Catal., 135 (2001) 4772.
- [32] A.Tuel; Micropor. Mesopor. Mater., 27 (1999) 151.
- [33] S.Biz and M.L.Occelli; Catal. Rev.-Sci. Eng., 40 (1998) 329.
- [34] E.L.Pires, M.Wallau and U.Schuchardt; J. Mol. Catal. A., 136 (1998) 69.
- [35] K.Lazar, T.Mathew, Z.Koppany, J.Megyeri, V.Samuel, S.P.Mirajkar, B.S.Rao and L.Guczzi; Phys. Chem. Chem. Phys., 4 (2002) 3530.
- [36] H.Grabowska, W.Kaczmarczyk and J.Wrzyszcz; Appl. Catal., 47 (1989) 351.
- [37] L.Zanderighi, M.P.Faedda and S.Carra; J. Catal., 35 (1974) 427.
- [38] K.Omata, T.Takado, S.Kasahara and M-Yamada; Appl. Catal. A. Gen., 146 (1996) 255.
- [39] E.C.Buciuman, F.Patcas and T.Hahn; Chemical Engineering and Processing, 38 (1999) 563.
- [40] E.L.Pires, M.Wallau and U.Schuchardt; Appl. Catal. A.Gen., 203 (2000) 231.
- [41] B-Z.Zhan, M.A.White, J.A.Pincock, K.N.Robertson, T.S.Cameron and T-K.Sham; Can. J. Chem., 81 (2003) 764.
- [42] L.Zhou, J.Xu, H.Miao, F.Wang and X.Li; Appl. Catal. A. Gen., 292 (2005) 223.
- [43] U.Schuchardt, R.Pereira and M.Rufo; J. Mol. Catal. A. Chem., 135
-

- (1998) 257.
- [44] O.Lemaire, M.Ribaucour, M.Carlier and R.Minetti; *Combustion and Flame.*, 127 (2001) 1971.
- [45] E.L.Pires, U.Arnold and U.Schuchardt; *J. Mol. Catal. A. Chem.*, 169 (2001) 157.
- [46] A.Sakthivel and P.Selvam; *J. Catal.*, 211 (2002) 134.
- [47] Z.Hou, B.Han, L.Gao, Z.Liu and G.Yang; *Green Chemistry.*, 4 (2002) 426.

Benzyl alcohol oxidation

- [1] T.Nishimura, N.Kakiuchi, M.Inoue and S.Vemura; *Chem. Commun.*, 14 (2000) 1245.
- [2] G.A.Rajkumar, B.Arabindoo and V.Murugesan; *Indian J. Chem. Sect. B.*, 39 (B(1)) (2000) 74.
- [3] A.R.Hajipour, S.E.Mallakpour and H.Adibi; *Chem. Lett.*, 5 (2000) 460.
- [4] N.B.Barhate, M.Sasidharan, A.Sudalai and R.D.Wakharkar; *Tetrahedron Lett.*, 37 (12) (1996) 2067.
- [5] M.M.Hashemi and Y.A.Beni; *J. Chem. Res. Synop.*, 5 (2000) 224.
- [6] S.W.Brown, (Solvay Interlox Ltd.) *PCT. Int. Appl. WO 9421, 5839 Cl.C 45/29, 1994, cf.C.A.122, 33980k.*
- [7] K.Sato, M.Aoki, J.Takagi and R.Noyori; *J. Am. Chem. Soc.*, 119 (50) (1997) 12386.
- [8] G.Barak, J.Dakka and Y.Sasson; *J. Org. Chem.*, 53 (15) (1988) 3553.
- [9] O.Bortolini, S.Campestrini, F.Furia and G.Modena, *J. Org. Chem.*, 53 (24) (1987) 5467.

Oxidation Reactions

- [10] C.Venturello and M.Gambaro; *J. Org. Chem.*, 56 (20) (1991) 5924.
- [11] A.C.Dengel, W.P.Griffith and B.C.Parkin; *J. Chem. Soc. Dalton. Trans.*, 18 (1993) 2683.
- [12] N.S.Bijlani and S.B.Chandalia; *Indian Chem. Eng.*, 23 (1981) 44.
- [13] T.Nishimura, N.Kakiuchi, M.Inoue and S.Uemura; *Chem. Commun.* (2000) 1245; *Bull. Chem. Soc. Jpn.*, 74 (2001) 165.
- [14] L.F.Liotta, A.M.Venezia, G.Deganello, A.Longo, A.Martorana, Z.Schay and L.Guczi; *Catal. Today*, 66 (2001) 271.
- [15] I.Matsushita, K.Ebitani and K.Kaneda; *Chem. Commun.*, (1999) 265.
- [16] B.M.Choudary, M.Lakshmi Kantan, Ateeq Rahman, Ch.Venkat Reddy and K.Koteswara Rao; *Angew. Chem. Int. Ed. Engl.*, 40 (2001) 763.
- [17] I.Halasz; *Appl.Catal.*, 47 (1989) L 17.
- [18] D.Dissanayake, K.C.C.Kharas, J.H.Lunsford and M.P.Rosynek; *J.Catal.*, 129 (1993) 652.
- [19] R.Sumati, K.Johnson, B.Viswanathan and T.K.Varadarajan; *Appl. Catal. A. Gen.*, 172 (1998) 15.
- [20] L.Zanderighi, M.P.Faedda and S.Carra; *J. Catal.*, 35 (1974) 427.
- [21] K.Omata, T.Takado, S.Kasahara and M-Yamada; *Appl. Catal. A. Gen.*, 146 (1996) 255.
- [22] J.J.Carbery, S.Rajadurai, C.D.Alcock and B.Li; *Catal. Lett.*, 4 (1990) 43.
- [23] I.Halasz, A.Brenner, M.Shelef and K.Y.Simon NG; *J. Catal.*, 126 (1990) 349.
- [24] I.Halasz, A.Brenner, M.Shelef and K.Y.Simon NG; *Catal. Lett.*, 6 (1990) 349.

- [25] T.Nakamura, M.Misono and Y.Yoneda; *J. Catal.*, 83 (1983) 151.
- [26] E.C.Buciuman, F.Patcas and T.Hahn; *Chemical Engineering and Processing.*, 38 (1999) 563.
- [27] I.Halasz; *React. Kinet. Catal. Lett.*, 41 (1990) 115.
- [28] K.Omata, T.Takada, S.Kasahara and M.Yamada; *Appl. Catal. A. Gen.*, 146 (1996) 255.
- [29] D.Guin, B.Barawati and S.V.Manorama; *J. Mol. Catal. A. Chem.*, 242 (2005) 26.
- [30] V.R.Choudhari, P.A.Choudhari and V.S.Narkhede; *Catal. Commun.*, 4 (2003) 171.
- [31] K.Wada, K.Yano, T.Kondo and Take-aki Mitsudo; *Catal. Today*, 117 (1-3) (2006) 242.

Styrene oxidation

- [1] G.Barak and Y.Sasson; *J. Chem. Soc., Soc. Commun.* (1987) 126.
- [2] G.Barak and Y.Sasson; *J. Chem. Soc., Soc. Commun.* (1987) 1266.
- [3] A.M.Al-Ajlouni and J.H.Espenson; *J. Am. Chem. Soc.*, 117 (1995) 9243.
- [4] N.Ma, Y.Yue, W.Hua and Z.Gao; *Appl. Catal. A.*, 251 (2003) 39.
- [5] V.PARvulescu, C.constantin and B.L.Su; *J. Mol. Catal. A. Chem.*, 202 (2003) 171.
- [6] D.Guin, B.Barawati and S.V.Manorama; *J. Mol. Catal. A. Chem.*, 242 (2005) 26.
- [7] C.Neri and F.Buonomo; *Eur. Pat.*, 102 097 (1984).
- [8] Q.Xia, G.Wang, G.Chao, L.Zheng, M.Ying and Chin., *J. Mol. Catal.*, 8

- (1994) 313.
- [9] S.B.Kumar, S.P.Mirajkar, G.C.G.Pais, P.Kumar and R.Kumar; *J. Catal.*, 156 (1995) 163.
- [10] M.A.Uguina, D.P.Serrano, R.Sanz, J.L.G.Fierro, M.Lopez-Granados and R.Mariscal; *Catal. Today*, 61 (2000) 263.
- [11] Z.Fu, D.Yin, D.Yin, Q.Li, L.Zang and Y.Zang; *Micropor. Mesopor. Mater.*, 29 (1999) 351.
- [12] W.Zhang, M.Froba, J.Wang, P.T.Tanev, J.Wong and T.J.Pinnavaia; *J. Am. Chem. Soc.*, 118 (1996) 9164.
- [13] J.Zhuang, D.Ma, Z.Yan, X.Liu, X.Han, X.Bao, Y.Zhang, X.Guo and X.Wang; *Appl. Catal. A.*, 258 (2004) 1.
- [14] C.V.Rode, U.N.Nehete and M.K.Dongare; *Catal. Commun.*, 4 (2003) 365.
- [15] S.C.Laha and R.Kumar; *J. Catal.*, 208 (2002) 339.
- [16] L.Zanderighi, M.P.Faedda and S.Carra; *J. Catal.*, 35 (1974) 427.
- [17] K.Omata, T.Takado, S.Kasahara and M-Yamada; *Appl. Catal. A. Gen.*, 146 (1996) 255.
- [18] S.Gomez, L.J.Garces, J.Villegas, R.Ghosh, O.Giraldo and S.L.Suib; *J. Catal.*, 233 (2005) 60.
- [19] V.Hulea and E.Dumtrio; *Appl. Catal. A. Gen.*, 277 (2004) 99.

6.1 Summary of the work

Spinels attracted the attention of physicists and chemists due to their interesting structural, electrical and magnetic properties. These properties depend on the nature of ions, their charge and their distribution among tetrahedral and octahedral sites. Spinels are found to be very efficient catalysts for a number of industrially important reactions. Individual metal oxides lose their catalytic activity rapidly due to ageing and coke formation where as spinel lattice imparts extra stability to the catalysts under various reaction conditions so that these systems have sustained activity for longer periods. Spinels used for studying many industrially important reactions were prepared by co-precipitation method. The spinels used for the present study viz. chromium and gadolinium incorporated nickel ferrites, nickel cobaltites and copper cobaltites were prepared by co-precipitation method using NaOH as the precipitant. Ferrites were prepared by low temperature method where as cobaltites were prepared by high temperature method. The prepared spinels were characterized by various physico-chemical methods. The catalytic activities of these spinels were investigated for liquid phase oxidation of hydrocarbons such as cyclohexane, styrene and benzyl alcohol, and vapour phase alkylation of aromatics such as phenol, *m*-cresol and aniline.

Chapter 1 contains introduction and literature survey on catalysis. A brief description about the spinel structure, preparation of spinels and catalysis by spinels is presented. A detailed description regarding the acid-base properties is also included in this chapter.

Summary and conclusions

Chapter 2 presents a description about the various experimental techniques- both physical and chemical- employed for characterization and principles behind them.

Chapter 3 contains the characterization results of the prepared systems. The spinel phase formation was identified by analyzing the XRD pattern. Crystallite sizes were calculated from the XRD data and all the systems were found to exist in the nanometer range. Crystallite size was found to be varying with substitution and variation in concentration of ions. Existence of spinel phase was again confirmed from DRIFT spectra, which will usually give bands characteristics of spinel phase. Bands at around 500 cm^{-1} and 700 cm^{-1} confirmed the formation of spinel phase. The stoichiometries of the prepared systems were checked by EDAX analysis and the observed results were in good agreement with theoretical values. Surface area of the prepared systems was found to be varying considerably with substitution and variation in concentration of ions. Morphology of the systems was studied by SEM analysis. Replacement of iron by chromium and gadolinium has different effects on the morphology of nickel ferrite. SEM analysis also revealed that copper cobaltite particles are larger in size than nickel cobaltite. Mössbauer spectra were taken for iron containing systems. Systems having chromium lost the magnetic hyperfine splitting where as for gadolinium containing systems, only one site is showing magnetic hyperfine splitting. Acid-base properties of the prepared systems were studied thoroughly. Total acidity was determined by NH_3 -TPD studies. Perylene adsorption studies were employed to find out Lewis acidity. IR studies of pyridine adsorbed samples gave a qualitative idea about acidity. For all the prepared systems, contribution towards total acidity

comes mainly from Lewis type sites. Adsorption studies using electron acceptors such as TCNQ, chloranil and *p*-dinitrobenzene has been used to study electron donating property of the systems. Acid-base properties are varying considerably with substitution and variation in concentration of ions. Two test reactions- cumene cracking and cyclohexanol decomposition- were employed to obtain a qualitative idea about acid-base properties. Ratio of products obtained from cumene cracking reaction gave a qualitative idea about Lewis and Brönsted acid sites. Results obtained from cumene cracking reaction supports pyridine IR results. Results of cyclohexanol decomposition reaction correlates well with the results obtained from NH₃-TPD studies. Since dehydration is an acid catalyzed reaction, the dehydration activities of the systems leading to cyclohexene has been taken as measure of their acid strength.

Chapter 4 contains the results of activity studies towards various alkylation reactions. Effect of change in catalyst composition on activity has been discussed after optimizing the reaction parameters. The parameters were optimized such as to obtain better conversion and product selectivity. Reaction parameters such as flow rate, reactant molar ratio, temperature etc. were optimized. The prepared systems were found to be highly active towards the alkylation reactions. The variation in acid-base properties of the systems with change in composition is found to be influencing their catalytic activity.

Phenol methylation mainly gave two industrially important chemicals – *o*-cresol and 2,6-xylenol. In the NiCr ferrite series, the system having the composition NiCr_{1.2}Fe_{.8}O₄ (which is having maximum acidity in that series) gave a phenol conversion of 94 % and 2,6-xylenol selectivity of 86.3 %. For

Summary and conclusions

all the systems, acidity is the determining factor for the catalytic activity. Nickel gadolinite gave a phenol conversion of 93.5 %. NiGd ferrite series gave *o*-cresol as the main product, with 100 % selectivity for NiGd_{1.6}Fe₄O₄ and NiGd₂O₄. In the case of cobaltites, copper cobaltites are more active and are giving better selectivity for 2,6-xyleneol.

For phenol *tert* butylation, NCrF₃ and NG are giving maximum phenol conversion. In the ferrite series, up to NCrF₂ and NGF₃, 2- *tert* butyl phenol is the preferred product and only after that the selectivity for 4- *tert* butyl phenol increases. All the cobaltite spinels gave 4- *tert* butyl phenol as the preferred product. Copper cobaltite having more copper content gave more selectivity for 4-*tert* butyl phenol. 2-*tert* butyl phenol is the preferred product at shorter contact time. The selectivity for 2,4-ditertiary butyl phenol decreases as temperature increases and this may be due to the dealkylation reaction. Copper cobaltite gave the highest selectivity for 4-*tert* butyl phenol (~ 70 %).

For thymol synthesis, gadolinium containing ferrites are more active than chromium containing ferrites. Both *m*-cresol conversion and thymol selectivity are better for gadolinium containing systems. NiGd₂O₄ gave a maximum *m*-cresol conversion of 88 % with a thymol selectivity of 92 %. All the cobaltite systems gave a thymol selectivity of greater than 80 %.

Ferrites are found to be highly active for the methylation of aniline as compared to cobaltite series. Of these, chromium containing ferrites showed better activity than gadolinium containing series with NiFe₂O₄ showing maximum aniline conversion. N-methyl aniline is the major product formed. Considerable amount of the C-methylated product, *p*-toluidine is formed only in the case of cobaltites. Catalysts having high acidity are found to be forming

benzene and toluene. In the cobaltite series, nickel cobaltites show greater activity than copper cobaltites. Variation in activity of the systems was found to be controlled by the basicity of the systems.

Catalyst stability was studied by running the reactions continuously for long periods. The systems maintained their activity for long periods showing their excellent catalytic stability.

Chapter 5 presents the results of activity studies towards oxidation reactions. Hydrogen peroxide was used as oxidant for all the reactions. The oxidation reactions under study were styrene oxidation, benzyl alcohol oxidation and cyclohexane oxidation. The prepared spinels oxidized styrene and benzyl alcohol to benzaldehyde, where as in the case of benzyl alcohol, little benzoic acid is also formed. The catalysts showed good activity towards cyclohexane oxidation. Cyclohexane oxidation mainly yielded three products-cyclohexene, cyclohexanone and cyclohexanol with greater selectivity towards cyclohexanol. Both ferrites and cobaltites showed almost same selectivity towards cyclohexanol but cobaltites are more active in terms of cyclohexane conversion, which gave a maximum conversion of 73.4 %.

Among the spinels studied for styrene oxidation reaction, cobaltites were found to be more active than ferrites, of which, NC1.5 was found to be more active. Benzaldehyde was the only product obtained in all the cases under optimized conditions. Of the various solvents used for the reaction, aprotic solvents such as acetonitrile and acetone exclusively yielded benzaldehyde where as with solvents such as IPA and methanol, the selectivity for benzaldehyde decreased.

Summary and conclusions

Unlike in the case of styrene oxidation reaction, benzyl alcohol oxidation yielded little benzoic acid. All the catalysts showed high activity for this reaction. Except in the case of copper cobaltites, all the other systems gave a benzaldehyde selectivity of greater than 90 % where as copper cobaltite systems gave exclusively benzaldehyde. Here acetone was found to be good solvent than acetonitrile.

Catalyst reusability study was conducted by running the reactions using the same catalyst after separating from the reaction medium. The activity was found to be decreasing in the third cycle.

6.2 Conclusions

- The spinels were prepared by co-precipitation method using NaOH. Ferrites were prepared at low temperature where as cobaltites were prepared by high temperature method.
- Electronic and surface properties of ferrites were modified by replacing Fe by Cr and Gd where as for cobaltites the properties were modified by changing the stoichiometry of Ni, Co and Cu.
- Spinel phase formation was identified by XRD analysis. Existence of spinel phase was again confirmed by taking DRIFT spectra.
- Modification of spinels increased the acidic character. Incorporation of chromium up to 60 % into nickel ferrite increased the acidity and then decreased where as replacement of Fe by Gd resulted in gradual

increase of acidity. For cobaltites, increase in percentage of Ni and Cu was found to increasing the acidity.

- Total acidity was determined by NH_3 -TPD studies. IR studies of pyridine adsorbed samples showed that the contribution towards total acidity comes mainly from Lewis sites. The strength of Lewis acid sites was determined by conducting adsorption studies using perylene. The variation in Lewis acidity follows the same trend as the total acidity.
- Basic properties were studied by adsorption studies using various electron acceptors. Modification of ferrite by Cr and Gd was found to decreasing the basic character. Increasing the concentration of Ni and Cu in cobaltites also decreased the basic character.
- Test reactions conducted for studying the acid-base properties were cumene cracking and cyclohexanol decomposition reactions. Good correlation has been obtained between the results obtained from these reactions and the results obtained from NH_3 -TPD and perylene adsorption studies.
- The prepared catalysts were found to be highly active towards many alkylation and oxidation reactions, especially phenol methylation, thymol synthesis, oxidation reactions of styrene, cyclohexane etc.

Summary and conclusions

- For alkylation reactions, catalytic activity was found to be controlled by the variation in acid-base properties of the systems. For oxidation reactions, activity varies in accordance with the reducibility of the systems.
- Although all the prepared spinels are highly active towards phenol methylation, gadolinium containing ferrite series gave *o*-cresol as the major product and with 100 % *o*-cresol selectivity by $\text{NiGd}_{1.6}\text{Fe}_{.4}\text{O}_4$ and NiGd_2O_4 .
- The prepared catalysts can be conveniently used for the production of benzaldehyde, which is a fine industrial chemical, by the oxidation of styrene and benzyl alcohol. Also, under optimized conditions, all the systems were found to form exclusively benzaldehyde by the oxidation of styrene.
- Deactivation studies were conducted for vapour phase reactions by running the reactions for a long period. Some of the systems were found to maintain their activity during the time period studied showing their excellent catalytic stability.
- Recycling studies were conducted for liquid phase reactions. The catalysts were recycled up to three cycles. Some of the systems were found to be maintaining the selectivity even in the third cycle.

6.3 Further scope of the work

Chromium and gadolinium containing ferrites and different nickel and copper cobaltites were proved to be excellent catalysts for a number of alkylation and oxidation reactions which are industrially important. The prepared systems were found to be highly active towards alkylation of phenol and substituted phenol such as *m*-cresol. These observations show that the prepared systems can be conveniently tried as catalysts for alkylation of other substituted phenols such as *o* and *p*-cresols; the products of these reactions are important in fine chemical industries. Also it is observed that the studied systems were selectively forming *N*-methyl aniline by the methylation of aniline. The study can be further extended for the alkylation of substituted anilines. Also, the alkylation can be carried out using different alkylating agents. We can modify the properties such as cation distribution, acid-base properties etc. by changing the nature and concentration of ions in the spinel matrix. Since the variation in these properties is found to be very much affecting the catalytic property, we can improve the catalytic activity considerably by incorporating many divalent and trivalent ions. It was observed that the reducibility could be varied considerably by changing the composition of systems. Since reducibility is found to be affecting the oxidation behaviour, we can improve the activity towards oxidation reactions by improving the reducibility by the incorporation of other ions. The excellent catalytic activity towards oxidation reactions shows that the systems can be used for environmentally important reactions such as hydroxylation of phenol, removal of carbon monoxide by oxidation etc.

Papers presented at various National conferences

1. Ramanathan R and S Sugunan, "CYCLOHEXENE OXIDATION BY H₂O₂ USING COBALTITES PREPARED BY CO-PRECIPIATION TECHNIQUE", the National Conference on The Role of Analytical Chemistry In Materials Science and Technology 2006 held at Munnar on May 1, 2006.
2. Ramanathan R and S Sugunan, "BENZYL ALCOHOL OXIDATION USING NiCr FERRITES PREPARED BY LOW TEMPERATURE CO-PRECIPIATION METHOD", UGC sponsored National Seminar on Frontiers In Chemistry (FIC-06) held at the Department of Applied Chemistry, CUSAT, on March 24-25, 2006.
3. Ramanathan R and S Sugunan, "LIQUID PHASE OXIDATION OF STYRENE BY H₂O₂ USING NICKEL CHROMIUM FERRITES PREPARED BY LOW TEMPERATURE CO- PRECIPIATION METHOD", ISCAS symposium- 4th National Symposium & Conference on Solid State Chemistry and Allied Areas held at Goa University during Dec 1-3, 2005.
4. Ramanathan R and S Sugunan, "TERTIARY BUTYLATION OF PHENOL ON NiCr_xFe_{2-x}O₄ PREPARED BY CO-PRECIPIATION METHOD", National seminar on "Emerging Trends & New Vistas in Chemistry organized by the Department of Chemistry, University of Calicut on Nov 29-30 2005.

5. Ramanathan R and S Sugunan, "CHARACTERISATION AND ACTIVITY STUDY OF NICKEL COBALTITES PREPARED BY HIGH TEMPERATURE CO-PRECIPITATION TECHNIQUE", MRSI National Conference "Materials for Automotive Industries" held at NCL, Pune during Feb 2005.

6. Ramanathan R and S Sugunan, "LIQUID PHASE FRIEDEL-CRAFTS ALKYLATION OF TOLUENE USING $\text{NiCr}_x\text{Fe}_{2-x}\text{O}_4$ PREPARED BY LOW TEMPERATURE CO-PRECIPITATION TECHNIQUE", 17th National Symposium on Catalysis held at CSMCRI, Bhavnagar on 18-20 January 2005.